Journal of Drug Delivery

Novel Oncology Therapeutics: Targeted Drug Delivery for Cancer

Guest Editors: Andreas G. Tzakos, Evangelos Briasoulis, Theresia Thalhammer, Walter Jäger, and Vasso Apostolopoulos

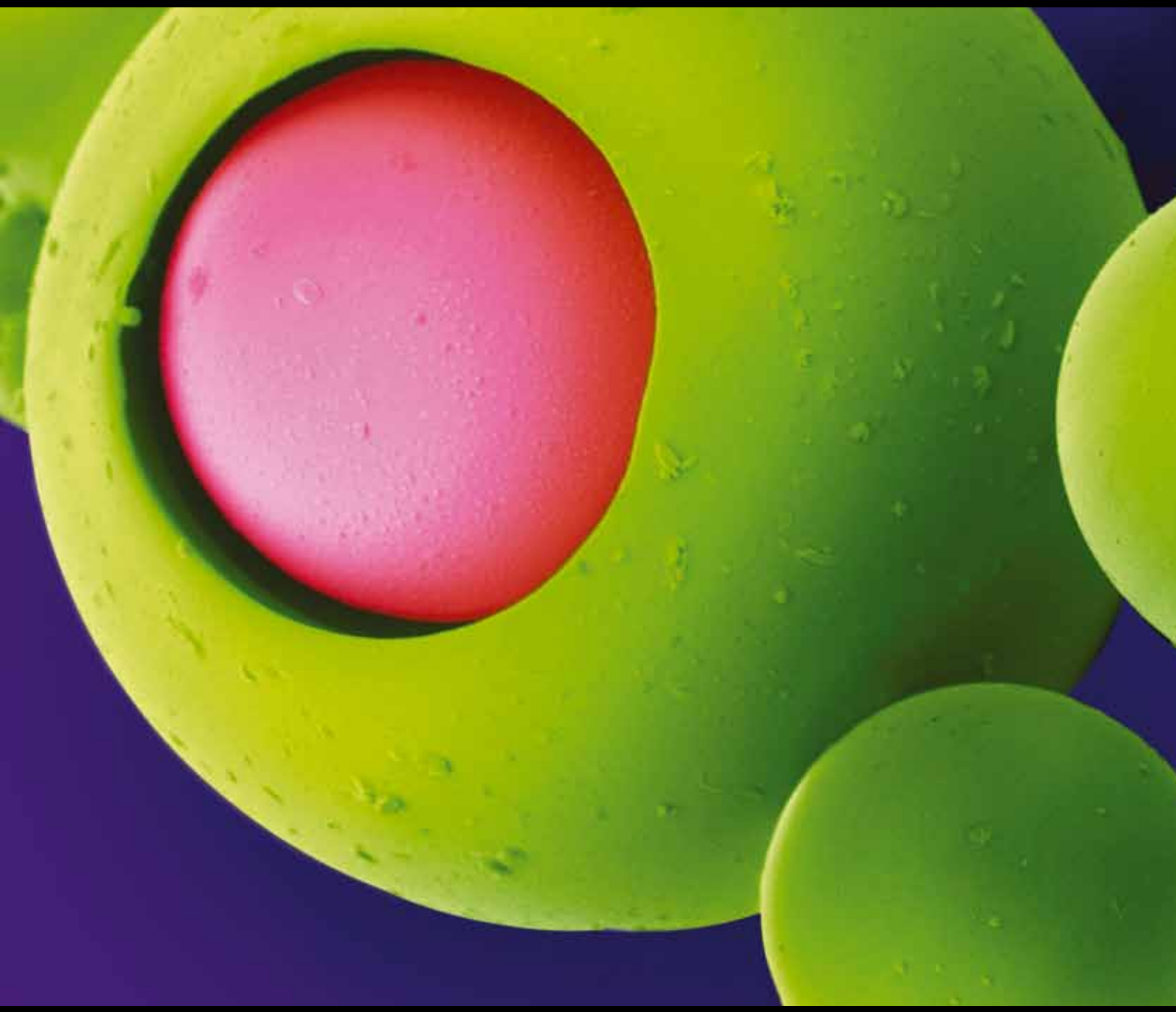

Novel Oncology Therapeutics: Targeted Drug Delivery for Cancer

Journal of Drug Delivery

Novel Oncology Therapeutics: Targeted Drug Delivery for Cancer

Guest Editors: Andreas G. Tzakos, Evangelos Briasoulis, Theresia Thalhammer, Walter Jäger, and Vasso Apostolopoulos

Editorial Board

Contents

Hindawi Publishing Corporation
Journal of Drug Delivery
Volume 2013, Article ID 918304, 5 pages
http://dx.doi.org/10.1155/2013/918304

Editorial

Novel Oncology Therapeutics: Targeted Drug Delivery for Cancer

Andreas G. Tzakos,[1,2] Evangelos Briasoulis,[2] Theresia Thalhammer,[3] Walter Jäger,[4] and Vasso Apostolopoulos[5,6]

[1] *Department of Chemistry, University of Ioannina, GR45110 Ioannina, Greece*
[2] *Cancer Biobank Center, University of Ioannina, GR45110 Ioannina, Greece*
[3] *Institute of Pathophysiology and Allergy Research, Center for Pathophysiology, Immunology and Infectiology, Medical University of Vienna, Vienna, Austria*
[4] *Department of Clinical Pharmacy and Diagnostics, University of Vienna, Vienna, Austria*
[5] *VA Consulting Services, Melbourne, VIC 3030, Australia*
[6] *Victoria University, College of Health and Biomedicine, Melbourne, VIC 3021, Australia*

Correspondence should be addressed to Andreas G. Tzakos; atzakos@cc.uoi.gr

Received 5 September 2013; Accepted 5 September 2013

Despite the progress in techniques for cancer prevention, detection, and treatment, as well as for increasing the public awareness in recent years, this disease is projected to become the leading cause of death worldwide. Advancements in omics, analytical procedures, and high throughput screening in the last five years have led to the realization that human diseases and especially cancer are more complex than were originally conceived. Cancer is not a static entity that can be easily monitored and manipulated. It is characterized by a dynamic and time-dependent network of constantly altered molecular and cellular interactions between players in different pathways. This network is not invariable and rigid but is constantly reshaped and altered conforming to the pliable signaling processes/responses implicated. Its complexity is apparent by the fact that the disease state is not a disruption of a single node or specific nodes in the network organism but is organism-patient dependent, thus requiring personalized perspective approaches.

Numerous challenges hamper effective cancer treatment and development of effective drugs such as ineffective therapeutic drug concentration reaching the tumor site, life-threatening side-effects caused by nonspecific tissue distribution of anticancer agents, and acquired resistance of the cancer cell upon chemotherapy that triggers cross-resistance to a wide range of different drugs.

Such multifactorial states require the development of very delicate approaches in the course of the drug discovery pipeline. The scientific roots of the drug development philosophy should be shifted from the traditional concept of the "magic bullet" drug (i.e., scalped for a single drug target) to the formulation of a navigated vehicle which could spatio-temporally deliver the drug in the correct location and the appropriate time. Thus, the term *targeted drug delivery* should give its place to *navigated drug delivery* since it is not only the cytotoxic drug that targets a specific cellular location but rather a vehicle that navigates the course of the loaded drug to the appropriate site of action. Such drug loaded and navigated vehicles in order to enhance the selective uptake of the cytotoxic agent by the tumor cells and spare the normal cells, should consist of a multidimensional architecture (Figures 1 and 2). The major components of these vehicles are the transporting vehicle (i.e., lipid), the cytotoxic agent that is loaded, the "programmable" navigating/targeting agent (i.e., receptor specific ligand) that enables the appropriate delivery routes to avoid toxicity on healthy proliferating cells as also ineffective concentration of the cytotoxic agent

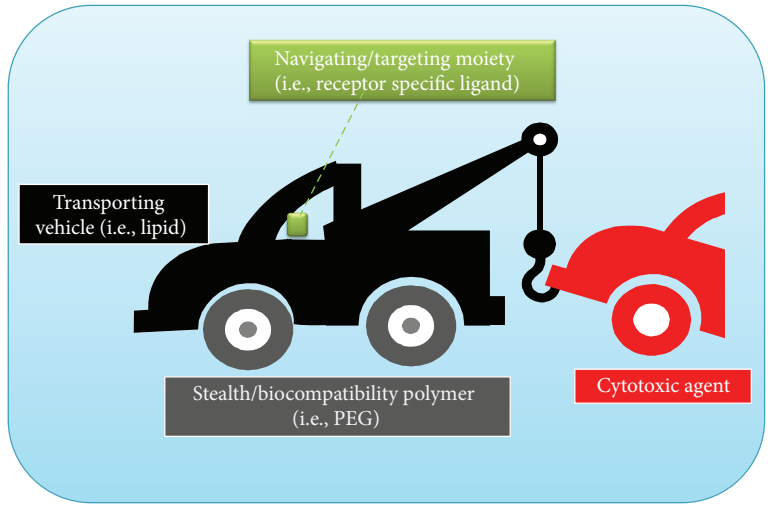

Figure 1: Structural architecture and mechanical analogue of a navigated drug delivery nanoparticle.

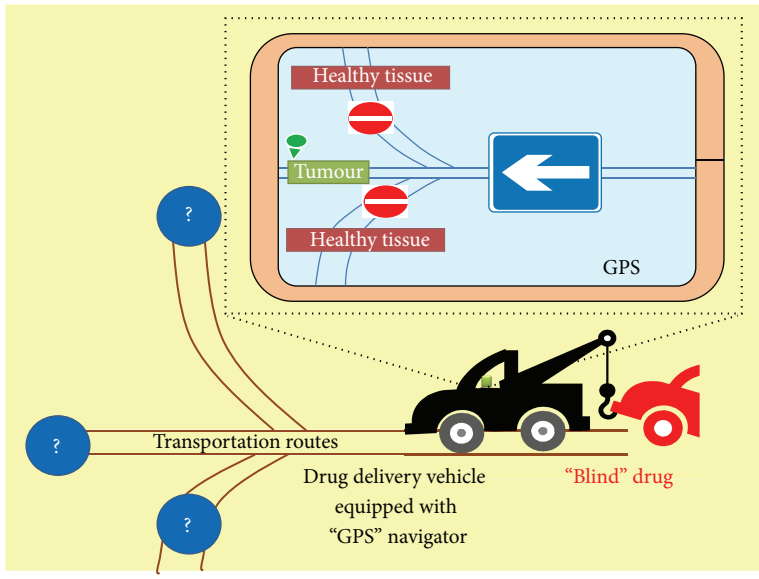

Figure 2: Navigated drug delivery: the drug delivery vehicle is equipped with a "programmable navigation system" that allows the transportation of the "blind" cytotoxic agent in the correct cellular location. In the absence of the drug delivery vehicle that is tagged with navigating delivery routes, toxicity is triggered on healthy proliferating cells against the anticancer agent, and ineffective therapeutic drug concentration reaches the tumor site.

to the tumor site (Figure 2), and the "stealth" nanocarriers (biocompatibility polymers, i.e., PEG) that enhance the short plasma half-life of the drug-loaded transporting vehicle.

In line with the challenges raised by the complexity of cancer, the aim of the present thematic issue is to provide an accumulation of innovative molecularly targeted cancer therapies and entrepreneurial methods of drug delivery in cancer (Table 1). It contains 12 papers embracing most aspects of cancer related to the exploration of active targeted nanoparticles for cancer treatment and diagnosis, including the exploitation of novel cancer drug targets, vaccine design against cancer, innovative methods for drug delivery-based on focused ultrasound or convection enhanced delivery, and mathematical modeling as an indispensable tool to analyze the transport processes and predict the outcome of anticancer treatment.

A constant developmental effort is being conducted for innovative nanoparticles to meet unmet needs in the transportation of imaging and therapeutic agents for cancer diagnosis and therapy. This happens since the nanoscale of these particles allows sculpting of diversity in their capabilities thus, enabling them to respond to a diverse array of functional requirements. Therefore, nanoparticles have been considered as appropriate vehicles to provide an ideal platform for personalized approaches to cancer diagnosis and therapy in cancer disease management. A. D. Miller presents

Table 1: Some of the delivery systems appeared in this issue.

Vehicle	Vehicle description	Navigation device	Target location	Cancer type
Bionanocapsules	A bionanocapsule (BNC) is a hollow nanoparticle consisting of an approximately 100 nm diameter liposome with about 110 molecules of hepatitis B virus (HBV) surface antigen L protein embedded as a transmembrane protein.	Chlorotoxin	MMP-2 protein	Brain tumor
Enzyme-based cancer imaging agents	Dual aromatase-steroid sulfatase inhibitor (DASSI) radiotracers	^{11}C-labelled inhibitors of steroid sulfatase (sulfamate derivatives)	Enzymes of the "sulfatase pathway", particularly steroid sulfatase	Breast, endometrial, ovarian, and colorectal cancer
Cytotoxic drugs coupled to OATP-substrates or OATP-directed antibodies	Substrates of membrane-located OATP isoforms, selectively expressed in cancer cells, for example, microcystins as substrates for OATP1B3	Selective ligands for OATP for example, microcystins or OATP-directed antibodies in cancer cells	Organic anion transporting polypeptides (OATPs)	Gastrointestinal tract, breast, prostate, lung, brain, bladder, kidney, liver, testis
Lipid-based nanoparticles	Genuine particles (approx 100 nm in dimension) assembled from varieties of lipid and other chemical components that act collectively to overcome biological barriers (biobarriers)	*Bona fide* biological receptor specific ligands		
PEGylated Span 80 vesicles PEGylated Span 80 vesicles with immobilized ESA	Span 80 is a heterogeneous mixture of sorbitan mono-, di-, tri-, and tetra-esters	Lectin-sugar binding protein (Eucheuma serra agglutinin)	Sugar chains on the tumor cell-surface	Osteosarcoma
Doxorubicin (DOX)-loaded liposomes	Liposomes composed of DSPG, DSPC, cholesterol, and DSPE-PEG-2000	A triple-helical sequence derived from type IV collagen	CD44/chondroitin sulfate proteoglycan	CD44-overexpressing tumor cells
Mannan	Oxidized or reduced mannan, a poly-mannose, conjugated to cancer antigen	Mannan	Mannose receptor	Adenocarcinoma

a rigorous and descriptive overview on the status of lipid-based nanoparticles (LNPs) in cancer diagnosis and therapy. Special focus is given on LNPs that conform to the ABCD nanoparticle structural paradigm (A: active pharmaceutical ingredient, B: lipids, C: a stealth/biocompatibility polymer layer (like PEG), D: targeting layer-receptor specific ligand) and to triggered, multimodal imaging theranostic drug-nanoparticles for cancer therapy.

Clinical attrition rates are a critical issue in drug development. In oncology, fourfold higher rates of attrition have been determined in respect of other indications. This clearly pinpoints the unmet necessity to steer for novel and traditionally unexplored drug targets to be employed in the drug discovery process towards the development of novel anticancer drugs. In this light, V. Buxhofer-Ausch et al. describe the capacity of members of the organic anion transporter family (OATP) to serve as tumor biomarkers and effective cancer drug targets. The importance of these drug targets is due to their implication on the uptake of clinically important drugs and hormones, thereby affecting drug disposition and cell penetration. An OATP-targeted therapy holds promises to combat cancer efficiently and with lesser side effects due to the tissue specific expression of different OATP members and specifically their differential expression in various cancer and normal tissues.

Enzymes of the sulfatase pathway could offer another appealing cancer drug target. S. Lena et al. provide a comprehensive review about the expression and function of enzymes of the sulfatase pathway, particularly of steroid sulfatase (STS), in breast, endometrial, ovarian, and colorectal cancer. Furthermore, it highlighted the applicability of STS inhibitors to function as enzyme-based cancer imaging agents applied in the biomedical imaging technique positron emission tomography for the diagnosis and therapy of estrogen-sensitive cancers.

Since cancer is considered not only as a genetic but also as an epigenetic disease and tumorigenesis involves multiple genetic and epigenetic alterations that contribute to the transformation of normal cells towards a malignant phenotype, epigenetics should also be the focus of discovering novel

cancer drug targets. E. Hatzimichael and T. Crook reviewed important advances in the field of cancer epigenetics and specifically provide an overview of the clinical use of epigenetics as cancer biomarkers and current progress in the utilization of epigenetic drugs in solid and blood cancers.

Navigated delivery of cytotoxic agents to special sites or organs is a challenging issue that needs to be addressed in order to surpass systematic toxicity. These challenges become even more exigent for drug delivery in brain tumors where intrinsic difficulties are met due to the hurdles faced to cross the brain-tumor and blood-brain barriers. To establish a targeting vehicle for glioblastoma cells, T. Kasai et al. exploited the capability of chlorotoxin to selectively bind to matrix metalloproteinase-2 and other proteins on glioma cell surfaces once it was fused to human IgG-Fcs and displayed on the surface of bionanocapsules. This chlorotoxin loaded bionanocapsule showed specific affinity to the surface of glioma cells and internalized into the cytoplasmic space suggesting that is a promising drug delivery system for targeting glioblastoma.

In order to establish a target-based agent to be specifically delivered to osteosarcomas, K. Hayashi et al. focused on a lectin (Eucheuma serra agglutinin) both as a tumor-targeting agent and as an antitumor agent. Lectins are carbohydrate binding proteins that are highly specific for sugar moieties on the surface of tumor cells. The authors formulated a drug delivery system containing PEGylated Span 80 vesicles which immobilized the specific lectin. They noted that the specific system was not only selectively targeting osteosarcoma cells but was also cytotoxic to the targeted cells emphasizing the dual role adopted by lectins both as navigating and cytotoxic agents.

To achieve an effective approach for enhanced uptake of anticancer drug-loaded vehicles by tumor cells, M. W. Ndinguri et al. explored cell surface proteoglycan CD44 targeting as a way to selectively deliver therapeutic agents encapsulated inside colloidal delivery systems. CD44 has been recognized as a contributor to tumor chemoresistance and as a cancer cell and cancer stem cell biomarker due to its overexpression in cancer compared to normal cells (haematopoietic, epithelial, and neuronal cells). To target CD44, the authors used a triple-helical peptide sequence derived from type IV collagen that was incorporated in doxorubicin-loaded liposomes (composed of DSPG, DSPC, cholesterol, and DSPE-PEG-2000). The CD44-targeted liposomes were found effective in reducing tumor size, highlighting their potential to be used for selective chemotherapeutic treatment of CD44 overexpressing tumor cells.

The immune system has evolved to protect the body against microorganism invasion and thereby prevent diseases. Thus, cancer vaccines could boost the immune system to enable it to combat cancer more effectively. In vaccine development, a major aim is to induce strong, specific T cell responses. This is achieved by targeting antigens to cell surface molecules on dendritic cells (DCs) that efficiently stimulate T cell responses. The paper by V. Apostolopoulos et al. focuses on the most attractive cell surface receptors expressed on DCs to be used as targets for antigen delivery for cancer immunotherapy. The DC cell surface receptors (receptor kinases, Toll-like receptors, and C-type lectin receptors) which induce cellular responses and show promise as targets for vaccine design against cancer are highlighted. Along these lines, K.-C. Sheng et al. investigated the effect of IFN-gamma on DC functional maturation and DC meditated helper T cell activation, in the presence and absence of Toll-like receptor (TLR) ligation. The authors demonstrated an adjuvant effect of IFN-gamma on DC maturation and T cell stimulation and proposed a novel use of IFN-gamma together with Toll-like receptor agonists to enhance antigen-specific T cell responses, for applications in the development of enhanced vaccines and drug targets, against diseases, including cancer.

An alternative to the systemic drug delivery is the convection-enhanced delivery (CED) on the basis of which agents are delivered directly into the tumor and the surrounding infiltrative edges with continuous, positive-pressure infusion, thus allowing direct access to the tumor bed, achieving high local concentrations of the drug with minimal systemic absorption. The paper by J. Yun et al. focuses on the authors preclinical and clinical experience with CED in glioblastoma and highlight the challenges and potency of this methodology. Special emphasis is given onto the translational goals of this work.

M. Thanou and W. Gedroyc provided a comprehensive overview on the utilization of MRI-guided focused ultrasound (MRgFUS) as a new method of drug delivery. This methodology combines a high intensity focused ultrasound beam that can be used as an external stimulus to activate drug delivery in tissues and Magnetic Resonance Imaging system (MRI) which visualizes patient anatomy and controls the treatment by continuously monitoring the tissue effect. The advantages of being noninvasive as well as controlled and focus could establish this methodology as valuable tool in clinic to increase drug targeting and tissue specific drug delivery.

The transport of anticancer drugs and their consequence on tumor cells implicates an array of physical and biochemical processes. Since multiple steps are involved in the drug-transport, drug-release, and drug-uptake pipelines, mathematical models have become an indispensible tool to analyze the transport processes and predict the outcome of anticancer treatment. Mathematical modeling of cancer provides a tool to assist our realization on the interaction and drug-mediated perturbation of such complex processes, thus, fruitfully contributing to the optimization and refinement of drug delivery. W. Zhan and X. Y. Xu present the development of an improved mathematical model that was applied to an idealized geometry consisting of tumor and normal tissues. They predicted the efficacies of direct intravenous administration and thermosensitive liposome-mediated delivery and illustrated that thermo-sensitive liposome-mediated delivery provides a lower drug concentration in normal tissues than direct infusion of non-encapsulated drug as also a significantly higher peak intracellular concentration. These computational results furnish a projection on the effectiveness of two different treatments, within a mathematical framework, and set the basis to develop and corroborate optimized treatments with reduced risk of associated side effects as also

effective tumor cell killing in a short time period of treatment.

Due to the complexity of the disease, efficient cancer therapy can emerge only upon interscience collaboration. This special issue aims to accumulate current knowledge on molecularly targeted cancer therapies and innovative methods of drug delivery in cancer. We believe that this accumulative knowledge will assist to accelerate progress developing more precise navigated drug delivery in cancer based on innovative tools.

Andreas G. Tzakos
Evangelos Briasoulis
Theresia Thalhammer
Walter Jäger
Vasso Apostolopoulos

Hindawi Publishing Corporation
Journal of Drug Delivery
Volume 2013, Article ID 869718, 22 pages
http://dx.doi.org/10.1155/2013/869718

Review Article

Targeting Antigens to Dendritic Cell Receptors for Vaccine Development

Vasso Apostolopoulos,[1,2] Theresia Thalhammer,[3] Andreas G. Tzakos,[4] and Lily Stojanovska[2]

[1] *VA Consulting Services, Melbourne, VIC, Australia*
[2] *College of Health and Biomedicine, Victoria University, VIC, Australia*
[3] *Institute of Pathophysiology and Allergy Research, Centre for Pathophysiology, Immunology and Infectiology, Medical University of Vienna, Vienna, Austria*
[4] *Department of Chemistry, University of Ioannina, Ioannina, Greece*

Correspondence should be addressed to Vasso Apostolopoulos; vasso@scientist.com

Received 12 December 2012; Accepted 11 July 2013

Academic Editor: Ali Nokhodchi

Dendritic cells (DCs) are highly specialized antigen presenting cells of the immune system which play a key role in regulating immune responses. Depending on the method of antigen delivery, DCs stimulate immune responses or induce tolerance. As a consequence of the dual function of DCs, DCs are studied in the context of immunotherapy for both cancer and autoimmune diseases. In vaccine development, a major aim is to induce strong, specific T-cell responses. This is achieved by targeting antigen to cell surface molecules on DCs that efficiently channel the antigen into endocytic compartments for loading onto MHC molecules and stimulation of T-cell responses. The most attractive cell surface receptors, expressed on DCs used as targets for antigen delivery for cancer and other diseases, are discussed.

1. Introduction

The most successful vaccines used to combat infectious disease are the live or live attenuated organisms as used in polio and small pox vaccines. However, with purified proteins or peptides, in most cases adjuvants or suitable danger signals are necessary in order to prime T-cell responses. In the last decade, dendritic cells (DCs), powerful antigen presenting cells, have surfaced as the most important cells, to target antigens for uptake, processing, and presentation to T cells [1]. DCs link the innate immune response to the adaptive immune response in that they bind pathogens and are able to stimulate T-cell responses against antigens. Targeting antigens to DC is therefore an appropriate method to stimulate effective immune responses. Targeting cell surface receptors on DCs represents a more direct and less laborious method and has been the subject of considerable recent investigation. Numerous receptors have been identified to be expressed on DCs, including mannose receptor (MR), DC-SIGN, scavenger receptor (SR), DEC-205, and toll-like receptors. Targeting of these receptors is becoming an efficient strategy of delivering antigens in DC-based anticancer immunotherapy. Furthermore, pattern recognition receptors (PRRs) are expressed by cells of the innate immune system which bind to pathogen associated molecular patterns (PAMPs) on pathogens. PRRs are also known as pathogen recognition receptors or primitive pattern recognition receptors as they evolved before other parts of the immune system, mainly before adaptive immunity. PAMPs bind mannose, lipopolysaccharide, fucose, peptidoglycans, lipoproteins and glucans. PRRs are classified into 2 groups: (i) endocytic PRRs, which phagocytose microorganisms, bind to carbohydrates, and include the mannose receptor (MR), glucan receptor, and scavenger receptor, and (ii) signaling PRRs which include the membrane bound toll-like receptors (TLR) and the cytoplasmic NOD-like receptors. The membrane bound receptors fall into 3 categories: (i) receptor kinases, (ii) TLR, and (iii) C-type lectin receptors. Targeting of these receptors is

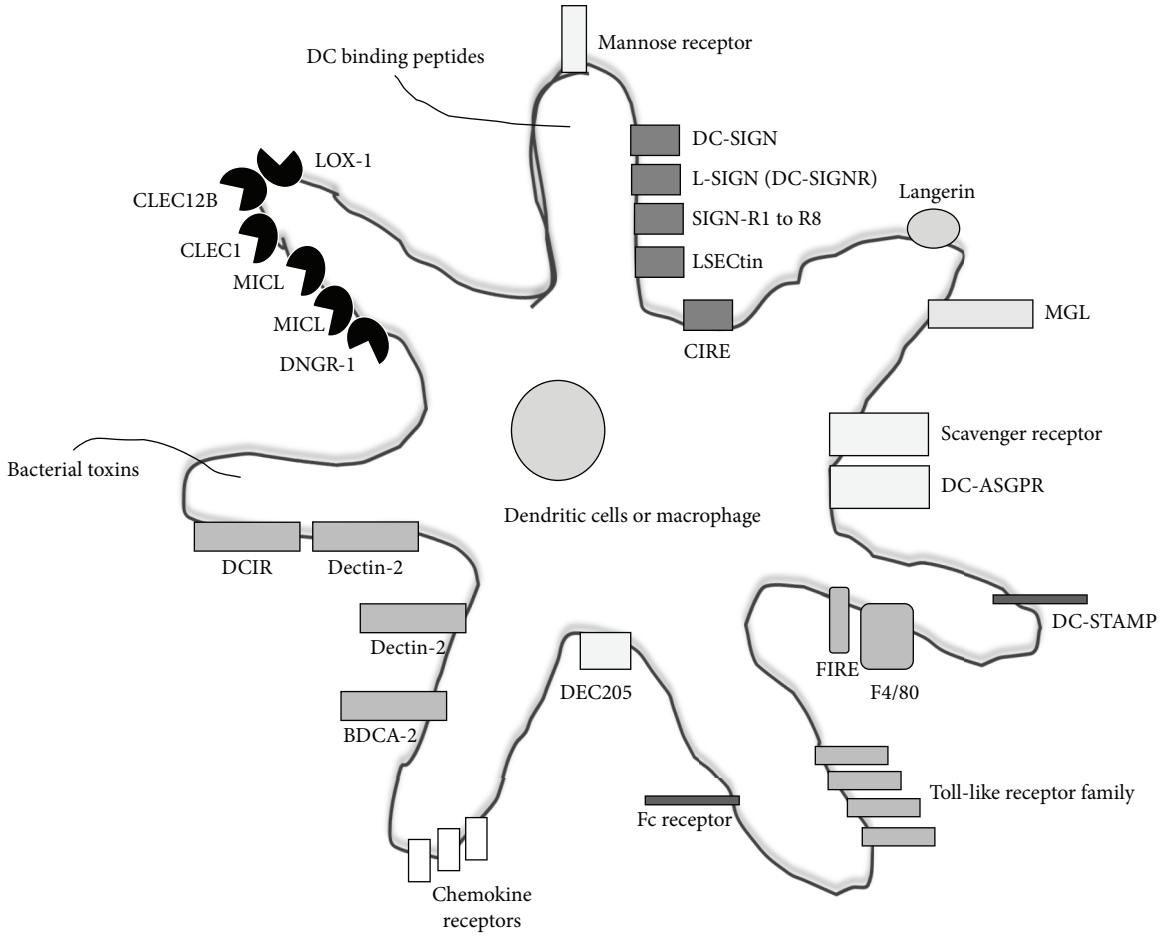

Figure 1: Schematic representation of dendritic cells expressing a number of different cell surface receptors which are targets for antigen targeting therapies.

becoming an efficient strategy of delivering antigens in DC-based anticancer immunotherapy.

2. C-Type Lectin Receptors

Calcium-dependent (C-type) lectins consist of a large family of lectins which consist of carbohydrate recognition domains. The C-type lectin family includes the mannose receptor, mannose binding lectin, and ficolins and are active in immune-system functions such as pathogen recognition. In addition, dendritic cell C-type lectins, DC-SIGN, DC-SIGNR, DCAR, DCIR, Dectins, and DLEC are important in dendritic cell trafficking, formation of the immunological synapse, and inducing cellular and humoral immunity, bringing together both adaptive and innate immunity (Figure 1).

2.1. Group 1 C-Type Lectin Receptors: The Mannose Receptors

2.1.1. Mannose Receptor. The mannose receptor (MR, CD206) is a C-type membrane lectin, carbohydrate (mannose, fucose, glucose, maltose, and GlcNAc) binding protein expressed by DCs and macrophages (Table 1 and Figure 1). MR binds to carbohydrates present on the cell walls of yeast, viruses, and bacteria, leading to endocytosis and phagocytosis [2]. Interestingly, human immunodeficiency virus (HIV) gp120 binds to MR on vaginal epithelial cells and induces the production of matrix metalloproteinases, facilitating transport of HIV across the vaginal epithelium [3]. In addition, HIV binds to the mannose receptor in sperm cells, suggesting that sperm cell-HIV interaction is an important source of infection [4]. The MR is part of the multilectin receptor family and provides a link between innate and adaptive immunity [5]. There are two types of MR in humans each encoded by its own gene, (i) mannose receptor C type 1 (MRC1) and (ii) mannose receptor C type 2 (MRC2).

The MR has been used as a target for vaccines, where DCs take up mannosylated proteins and utilize peptide epitopes for antigen presentation. The high expression of MR on DCs and macrophages suggests that the MR plays a key role in antigen recognition [6, 7]. The uptake of antigens by the MR allows processing and presentation via the MHC class I and II pathways [8–10], hence, suggesting MR a viable target for

Table 1: Summary of dendritic cell receptors targeted for vaccine development: C-type lectin receptors.

Receptor	Designation	Function
1. Group 1 C-type lectin receptors		
1.1. Mannose receptor	CD206	Expressed on macrophages and DCs. Binds to mannan, mannose, fucose, glucose, maltose, GlcNAc, lipoarabinomannan, cell wall of yeast, viruses, and bacteria leading to phagocytosis/endocytosis. Used to target protein, peptides, DNA, dendrimers, liposomes, and anti-MR antibodies for vaccine development with Th1, Th2, CTL, and Ab responses induced. Targeting antigens to MR using mannan has been used in human clinical trials.
2. Group 2 C-type lectin receptors		
2.1. Dendritic cell-specific intercellular adhesion molecule-3-grabbing nonintegrin (DC-SIGN)	CD209 Clec4L	Expressed on immature DCs, macrophages endothelial vascular cells, atherosclerotic plaques, and lymphatic vessels, not on placmacytoid DCs. Binds to mannan, mannose, fucose, GlcNAc, GalNAc, yeast, lewis blood group antigens Le^x, HIV-1 gp120, ebola virus, hepatitis C virus, dengue virus, respiratory syncytial virus, measles virus, *Mycobacterium tuberculosis, Leishmania amastigote, Helicobacter pylori, Leishmania mexicana, Schistosoma mansoni, Porphyromonas gingivalis, Neisseria gonorrhoeae*, *Candida albicans*, house dust mite (Der p1), and dog allergens (Can f1). Interacts with ICAM-3 and ICAM-2. Targeting DC-SIGN using antigen linked to anti-DC-SIGN antibodies, Manalpha-6 Man, lactoside, and Lewis oligosaccharide, stimulates T-cell and/or antibody responses, and has been studied as a potential receptor for vaccine targeting. Eight murine homologues identified, SIGN-R1 (CD209b) to SIGN-R8.
2.1.1. L-SIGN or DC-SIGNR	CD299 CD209L Clec4M	Expressed on liver sinusoidal cells, lymph nodes, and endothelial vascular cells, but not on DCs. Binds to HIV gp120, Man9GlcNAc2, HIV, simian immunodeficiency virus, ebola virus, hepatitis C virus, and respiratory syncytial virus. Targeting L-SIGN with anti-L-SIGN antibodies induces T-cell responses. Targeting L-SIGN shows promise for the development of targeted vaccines.
2.1.2. Liver and lymph node sinusoidal cell type lectin (LSECtin)	Clec4G	Expressed in liver, lymph nodes, sinusoidal endothelial cells, DCs, and Kupffer cells. Binds to N-acetyl-glucosamine, fucose, ebola virus, filovirus glycoproteins, lymphocytic choriomeningitis virus, S-protein of SARS coronavirus, and to CD44, but not to mannose, HIV, and hepatitis C. Coexpressed with DC-SIGNR and CD23. Antibody or ligand-mediated engagement of LSECtin activates rapid internalization, indicating that LSECtin may be a suitable receptor for targeting antiges in the development of vaccination regimes.
2.1.3. C-type lectin immune receptor (CIRE) (murine homologue of DC-SIGN)	CD209	Expressed by immature CD8− splenic DCs (CD8−CD4+ and CD8−CD4−), on some CD4+ DCs, plasmacytoid pre-DCs, and not by, CD8+ DCs, macrophages, or monocytes. It is a ligand for ICAM-3 and binds to HIV. Polyanhydride nanoparticles covalently linked to dimannose and lactose matures DCs and are internalized by DCs. CIRE shows promise as an appropriate target for antigen delivery for improved vaccine development.
2.2. Langerin	CD207 Clec4K	Expressed on Langerhans cells, CD103+ DCs, and splenic CD8+ DCs. Binds to mannose and internalizes mannose residues into Birbeck granules, where Langerin is expressed. Anti-Langerin antibody targeting antigens to Langerin is endocytozed *in vitro* and *in vivo* and induces Th1 and antibody responses.
2.3. MGL (human macrophage galactose- and N-acetylgalactosamine-specific C-type lectin)		Expressed on macrophages, immature DCs galactose, GalNAc, Tn antigen, filoviruses, and gonorrhea. GalNAc modified peptides to target MGL receptor expressed on murine and human DCs, which stimulates T-cell and antibody responses, and this approach could be used to design novel anticancer vaccines.

Table 1: Continued.

Receptor	Designation	Function
2.4. Dectin-1 or beta-glucan receptor (DC-associated C-type lectin-1)	DCAL-1 Clec7A	Expressed on myeloid DCs, CD8−CD8− DCs, dermal DCs, monocytes, macrophages, neutrophils, T cells, B cells, mast cells, eosinophils, and monocytes. Binds to beta-glucan on yeast, mycobacteria, plant cell walls, *Saccharomyces, Candida, Pneumocystis, Coccidioides, Penicillium,* and *Aspergillus*, but not *Cryptococcus* fungal species, and interacts with CD37. Anti-Dectin-1 and anti-Dectin-2 antibodies linked to proteins stimulate CD8+ and CD4+ T cells, and immunization with beta-glycan modified proteins induces CD4+ and Th17 bias responses.
2.4.1. DNGR-1 (NK lectin group receptor-1)	Clec9A	Expressed on murine CD8+ DCs not on CD4+ DCs, on CD11c+ DCs but not by CD11c− cells (B cells, T cells, NK cells, NKT cells, macrophages, and granulocytes), on plasmacytoid DCs, and on human blood DCsBDCA-3+ DCs) and monocytes (CD14+CD16−). Highly expressed on Flt3 ligand bone marrow derived CD8+ DCs. Target for immune response induction.
2.4.2. Myeloid inhibitory C-type lectin receptor (MICL)	Clec12A	Homologous to Dectin-1 and part of Dectin-1 cluster. Also termed as CLL-1, DCAL-2, and KLRL1. Expressed on granulocytes, monocytes, macrophages, B cells, CD8+ T cells in peripheral blood, and DCs.
2.4.3. C-type lectin-like receptor 2 (CLEC2)	Clec1B	Expressed on NK cells, monocytes, granulocytes, platelets, megakaryocytes, and liver sinusoidal epithelial cells. Binds to HIV-1 and facilitates HIV-1 spread to other cells and binds to snake venom rhodocytin. Not much is known regarding stimulating immune responses; however, colocalization with DC-SIGN suggests that it may have an immune stimulatory effect.
2.4.4. CLEC12B (macrophage antigen H)	Clec21B	Part of the NK gene complex/dectin-1 cluster of C-type lectin receptors. Expressed on macrophages, monocytes, and DCs. Not much is known regarding its function.
2.4.5. LOX-1 (Lectin-like receptor for oxidized density lipoprotein-1)	Clec8A	Part of the dectin-1 cluster of C-type lectin receptors and scavenger receptor family. Expressed on endothelial cells, smooth muscle cells, platelets, fibroblasts, and macrophages. Binds to Gram-positive and Gram-negative bacteria, oxidized LDL modified lipoproteins, phospholipids, apoptotic cells, C-reactive protein, and heat shock protein (HSP)-70. Targeting LOX-1 induces immune responses and is a promising target for cancer immunotherapy.
2.5. DC immunoreceptor subfamily		
2.5.1. DC immunoreceptor (DCIR)	Clec4A	Expressed on plasmacytoid DCs, immature and mature monocyte-derived DCs monocytes, macrophages, and B cells. Binds to TLR9. Targeting DCIR stimulates immune responses especially CD8+ T cells.
2.5.2. Dectin-2 (or beta-glucan receptor)	DCAL-2 Clec6A	Expressed on DCs, macrophages neutrophils, and monocytes. Binds to beta1,3 and beta1,6-linked glucans on yeast, mycobacteria, and plant cell walls. Targeting dectin-2 stimulates immune responses in mice.
2.5.3. Blood DC antigen (BDCA-2)	Clec4C	Expressed on human blood DCs. Targeting BDCA-2 suppresses IFN-alpha/beta cytokine secretion.

antigen delivery for vaccine development. Indeed, mannosylated peptides and proteins stimulate MHC class II specific T cells with 200 to 10,000-fold higher efficiency compared to peptides or proteins that are not mannosylated [10]. There is a 100-fold enhanced presentation of soluble antigens to T cells after being internalized by the MR on DCs, as compared to antigens internalized via fluid phase [9]. The MUC1 antigen conjugated to oxidized mannan (polymannose, comprising aldehydes) leads to rapid and 1,000 times more efficient MHC class I presentation to CD8+ T cells with a preferential T1 response, compared to MUC1 antigen conjugated to reduced mannan (no aldehydes) [8]. MUC1 antigen conjugated to reduced mannan results in class II presentation and a T2 immune response [8]. Both conjugate formulations, oxidized and reduced mannan, bind equally to the MR and are taken up into early endosomes [8]. MUC1-oxidized mannan rapidly escapes from the early endosomes into the cytosol for proteasomal processing and transport to the endoplasmic reticulum, Golgi apparatus, and MHC class I on the cell surface. By contrast, MUC1-reduced mannan remains in the early endosomes, to late endosomes, and to lysosomes, resulting in MHC class II presentation of antigens.

Furthermore, both oxidized and reduced mannan stimulated bone marrow derived DCs, showed enhanced allogeneic T-cell proliferation, and enhanced OTI/OTII peptide specific T-cell responses *in vitro*. Mice injected with oxidized or reduced mannan induced a mature phenotype of lymph node and splenic DCs [11]. Oxidized and reduced mannan both stimulated upregulation of inflammatory cytokines interleukin-(IL-) 1beta and tumour necrosis factor-alpha; however, oxidized mannan stimulated IFN-gamma, IL-12p40 cytokines whereas reduced mannan stimulated IL-4, IL-10, and IL-13 [11]. Moreover, the activation of DCs was toll-like receptor-4 (TLR-4) dependent [11]. Thus, the mode of mannan conjugation to antigen is important as the differential immune responses result [12–18]. These studies provided the first demonstration that the MR aided antigens into both the MHC class I or II pathways depending on the chemical modification of mannan. In addition, *ex vivo* targeting of macrophages or DCs with oxidized mannan-MUC1 and reinjection into mice, induces strong CTL responses and protects against MUC1 tumor challenge [6, 19–21]. Humans are injected with oxidized mannan-MUC1 which induce cellular and humoral immune responses and protect against recurrence in breast cancer patients [21–24]. *Ex vivo* culture of human DC and pulsing with oxidized mannan-MUC1 and reinjection into patients with adenocarcinoma result in strong cellular immune responses and clinical responses [25]. Moreover, reduced mannan conjugated to myelin basic protein (MBP) 87–99 or 83–99 altered peptide ligands [26–28] ($R^{91}A^{96}MBP_{87-99}$, $A^{91}A^{96}MBP_{87-99}$, and $Y^{91}MBP_{83-99}$) divert Th1 IFN-gamma responses to Th2 IL-4 responses [29, 30]. Likewise, reduced mannan conjugated to cyclic $A^{91}A^{96}MBP_{87-99}$ and $A^{91}MBP_{83-99}$ peptides significantly altered predominant Th1 responses to predominant Th2 responses [31–33]. Thus, mannan in its oxidized form has been shown to be effective as an anticancer vaccine, and mannan in its reduced form shows promise as a vaccine against autoimmune diseases such as multiple sclerosis.

DNA immunization is an attractive form of vaccination, which has shown promising results only in small animal models. Targeting the MR for DNA vaccines is a viable approach for the rational design of DNA vaccine strategies [34]. Mannosylated liposomes incorporating OVA DNA induced strong CTL responses in mice as compared to nonmannosylated complexes [35]. Complexation of oxidized or reduced mannan to OVA DNA via poly-l-lysine were able to stimulate strong cellular and humoral immune responses in mice [36, 37]. Using MUC1 DNA complexed to oxidized or reduced mannan was more immunogenic (T-cell responses, IFN-gamma secretion, low dose administration, and tumor protection) compared to MUC1 DNA alone [38]. In another approach, cationic amphiphiles containing mannose mimics, quinic acid, and shikimic acid headgroups are able to target the MR on DCs, leading to effective immune responses and tumor protection [39], suggesting that mannosylated DNA is an effective approach in generating immune responses.

Dendrimers are repetitive branched molecules which adopt a spherical 3-dimensional morphology. Dendrimers have 3 major parts, a core, an inner shell, and an outer shell, and attachment of compounds could be added in an attempt to develop novel immunotherapeutics. Mannosylated dendrimer OVA was shown to be taken up, processed, and presented by bone marrow derived DCs and Flt3-L DCs [40]. Mannosylated dendrimer OVA stimulated CD4+ and CD8+ T-cell responses and antibodies and protected mice against a OVA+ tumor challenge. Mannosylated dendrimer OVA induced DC maturation which was largely dependent on TLR-4 [41].

Mannan coated cationic liposomes (nanoparticles) incorporating HIV-1 DNA stimulate cytotoxic T lymphocytes (CTL), IFN-gamma, IgG2a, IgA, and delayed-type hypersensitivity responses [42]. The binding and uptake properties of mannan coated nanoparticles were 50% higher compared to the nonmannan coated nanoparticles, by MR+ cell line, J774E [43]. The binding and uptake were inhibited in the presence of free mannan, suggesting that the uptake was receptor dependent [43]. Anionic liposomes on the other hand, with the bilayer composition of phosphatidylcholine, cholesterol, phosphatidylglycerol, and phosphatidylserine do not bind to DCs. However, mannosylation of anionic liposomes increased their interaction to murine and human DCs, which could be blocked with free mannan [44]. Thus, the type of liposome is important in the development of effective vaccines, although mannan coating could overcome the pitfalls. Mannosylated liposomes incorporating ErbB2 CTL and T helper peptides and synthetic TLR2/1 or TLR2/6 agonists induced higher therapeutic efficacy compared to nonmannosylated liposomes [45]. In addition, mannosylated liposomes bind and are endocytozed by immature DCs; however, only nonspecific endocytosis is observed with nonmannosylated liposomes [46]. Liposomes conatining multibranched mannosylated lipids bind with higher affinity to the MR leading to effective uptake and endocytosis, compared to liposomes containing the monomannosylated analogs [46]. Furthermore, mannan coated poly(D, L-lactide-co-glycolic acid) and PLGA nanoparticles and enhanced CD4+ and CD8+ T-cell responses compared to nonmannan coated nanoparticles [47].

In addition, HER2 protein complexed to cholesteryl group-bearing mannan or pullulan polysaccharides generates CD8+ CTLs which reject HER2+ tumors in mice [48]. Furthermore, mannosylated chitosan microspheres (MCMs) incorporating Bordetella bronchiseptica antigen bound to the MR on murine macrophages (RAW264.7 cells) *in vitro* and induced strong IgA antibody responses *in vivo* [49]. However, mannose coated stealth microspheres, although bound to the MR, were not able to mature DCs *in vitro* [50].

Four lipid-core peptides were synthesized containing a sequence from the human papillomavirus type-16 (HPV-16) E7 protein (E744-62) and d-mannose. Immunization of mice with d-mannose-E7 peptide reduced or cleared tumors more effectively 37/40 compared to 21/30 in mice immunized with nonmannosylated peptides [51]. Numerous vaccines use keyhole limpet hemocyanin (KLH), to aid in antibody and T-cell responses. KLH activates and matures DCs by upregulating CD40, CD80, CD83, CD86, and MHC class II cell surface molecules and stimulating IL-12 and IL-10 cytokines [52].

The interaction of KLH to DCs was noted to be partially mediated by binding to the MR.

Cluster differentiation 1 (CD1) proteins, in particular, CD1b expressed on macrophages and DCs, present lipid antigens (including lipid mycolic acid and lipoarabinomannan) to T cells [53, 54]. The antigen presentation pathway for lipoarabinomannan has been characterized, and the MR is clearly responsible for uptake [55]. Lipoarabinomannan is endocytozed into early endosomes via the MR and from late endosomes is loaded onto CD1b molecules for T-cell presentation [55]. This study linked the MR to presentation of glycolipids via CD1 and suggests that the MR plays a major functional role in processing of carbohydrate antigens.

The melanoma associated antigen pmel17 fused to the heavy chain of an anti-MR antibody (B11-pmel17) and pulsed to DCs results in both MHC class I and class II presentation and CTL generation [56]. Likewise, human chorionic gonadotropin beta protein expressed by cancer cells, coupled to anti-MR antibody (B11-hCGbeta) generated MHC class I and class II T-cell responses and lysed hCGbeta+ cell lines [57]. T helper cells and CTL from cancer patients and healthy subjects were effectively primed with B11-hCGbeta pulsed DCs when a combination of TLR-ligands was used. It was evident that when TLR3 (poly I:C ligand) or TLR7/8 (resiquimod ligand, R-848) were used, concomitant signaling of DCs led to efficient antigen presentation by MR targeting [58]. Thus, MR and TLR together both contribute towards maturation and activation of DCs; in human clinical trials this was well tolerated with strong immune responses in cancer patients, and a phase II study is currently in progress [59, 60]. Similarly, NY-ESO-1, a cancer-testis Ag widely used in clinical cancer vaccine trials, was fused with either anti-MR or anti-DEC205 antibodies [61]. NY-ESO-1-antiMR antibody bound to the MR on DCs and NY-ESO-1-anti-DEC-205 on DCs, leading to stimulation of CD4+ and CD8+ T cells from peripheral blood mononuclear cells of cancer patients [61]. In contrast, nonantibody targeted NY-ESO-1 proteins only activated CD4+ T cells. Thus, targeting either the MR or DEC205 on DCs is a promising vaccination strategy to induce strong cellular immune responses.

In order to retain the characteristics of mannose rich carbohydrates and target the MR on DCs, antigens were expressed in yeast. Several recombinant ovalbumin (OVA) proteins were generated in *Pichia Pastoris* which naturally mannosylated OVA [62]. Mannosylated OVA induced enhanced antigen-specific CD4+ T-cell proliferation compared to non-mannosylated OVA, and, uptake was primarily due to mannose-specific C-type lectin receptors (MR and DC-SIGN) [63]. Further, stronger CTL responses and IFN-gamma, IL-2, IL-4, IL-5 cytokines were induced after vaccination in mice [64]. These studies demonstrate that yeast derived mannosylation of antigens enhances immunogenicity. Therapeutic strategies using tumor-specific immunoglobulin (idiotype, Id) for lymphomas are promising. Id proteins are usually produced via tumor-myeloma hybridomas or recombinant methods in mammalian, bacteria, or insect cells. Using insect cells, the Id produced contain mannose residues which have enhanced immunostimulatory properties (activation of DCs, CD8+ T-cell stimulation, and eradication of lymphomas), compared to Id proteins made in mammalian cells [65]. However, anti-lymphoma antibodies generated by Id insect cell compared to mammalian cells were similar. Thus, insect derived antigens are far more immunostimulatory compared to mammalian derived antigens, primarily due to the expression of mannose which binds to the MR.

Humans with suppressed T cells have high prevalence of *Cryptococcosis*. Soluble Cryptococcus neoformans mannoproteins (MP) are promising vaccine candidates due to their ability to induces delayed-type hypersensitivity and Th1 cytokines. MP binds to the MR and results in CD4+ T-cell stimulation and induce protective responses against *C. neoformans* and *Candida albicans*. The uptake of MP by DCs can be inhibited either by competitive blockade of the MR or by removal of carbohydrate residues critical for recognition [66]. Further, MPs increased the expression of CD40, CD83, CD86, MHC class I and II cell surface moleules, and IL-12 leading to the maturation and activation of DCs [67]. It was clear that the mannose groups on MP provided the immunogenicity of cryptococcal MP and this finding supports vaccination strategies that target the MR.

It is clear that antigen mannosylation is an effective approach to potentiate antigen immunogenicity, due to the enhanced antigen uptake and presentation by DCs and macrophages.

2.2. Group 2 C-Type Lectin Receptors: Asialoglycoprotein Receptor Family

2.2.1. DC-SIGN. Dendritic cell-specific intercellular adhesion molecule-3-grabbing nonintegrin, (DC-SIGN) also known as CD209, Clec4L, is a C-type membrane lectins abundantly expressed on immature DCs, macrophages, endothelial vascular cells, atherosclerotic plaques, and lymphatic vessels, but not on plasmacytoid DCs (Table 1 and Figure 1). Like the MR, DC-SIGN recognizes carbohydrates including mannose, fucose, N-acetylgalactosamine, and N-acetylgiucosamine residues on pathogens mediating endocytosis, thus activating and tailoring the adaptive immune response against pathogens. DC-SIGN also binds yeast derived mannan and Lewis blood group antigens and sialylation or sulfation of Le^x completely abrogated binding to DC-SIGN [68]. DC-SIGN contributes to HIV pathogenesis. HIV-1 gp120, binds to DC-SIGN on monocyte derived DCs more than 80% with residual binding to CD4, as opposed to HIV-1 only binding to CD4 on blood DCs [69]. After binding to DC-SIGN on DCs, HIV-1 is transported by DCs into lymphoid tissues and consequently facilitates HIV-1 infection of target CD4+ T cells [70, 71]. DC-SIGN also has high affinity binding for ebola virus, hepatitis C virus, dengue virus, respiratory syncytial virus, measles virus, *Mycobacterium tuberculosis, Leishmania amastigote, Helicobacter pylori, Leishmania mexicana*, *Schistosoma mansoni*, *Porphyromonas gingivalis*, *Neisseria gonorrhoeae,* and *Candida albicans*, transmitting infection (virus, bacteria, and yeast) to susceptible cells and, inducing Th1 Th2 T cell responses [72–77]. Recently, it was shown that DC-SIGN is the receptor for the major house dust mite (Der p1)

and dog allergens (Can f1) [78]. There is no binding of DC-SIGN with *E. coli*, *Klebsiella pneumoniae*, *Pseudomonas aeruginosa*, and *Staphylococcus aureus* [68]. DC-SIGN was identified through its high affinity interaction with ICAM-3 which facilitates DC interactions with T cells and contributes to the regulation of primary immune responses [70, 71]. DC-SIGN also interacts with ICAM-2 which is responsible for DC migration [79]. In view of these findings, DC-SIGN has implications for antigen targeting and stimulation of T-cell responses and has been studied as a potential receptor for vaccine targeting.

In order to understand the molecular basis of internalization of ligands by DC-SIGN, the putative internalization motif within the cytoplasmic tail was modified resulting in reduced internalization after exposure to antigen [80]. DC-SIGN ligand complexes are internalized by DCs into late endosomes, early lysosomes, and are processed and presented to CD4+ T cells [80]. Further, anti-DC-SIGN monoclonal antibodies are internalized up to 1,000-fold more efficiently compared to control monoclonal antibody and found in intracellular vesicles, indicating that targeting DC-SIGN targets the MHC class II pathway [81]. Anti-DC-SIGN monoclonal antibody conjugated to KLH was rapidly internalized into the lysosomal compartment of DCs and induced up to 100-fold increase stimulation of T cells compared to KLH alone pulsed DCs [82]. In addition, anti-DC-SIGN antibody-KLH-targeted DCs induced proliferation of naive T cells which recognized KLH T-cell epitopes presented by MHC class I and II molecules [82] and inhibited tumor cell growth in mice [83]. These studies use an anti-DC-SIGN monoclonal antibody that binds to the carbohydrate recognition domain. Recently, an anti-DC-SIGN monoclonal antibody which binds to the neck region of DC-SIGN was rapidly internalized into early endosomes by DCs by a clathrin-independent mechanism, unlike anti-DC-SIGN antibodies which target the carbohydrate recognition domain are internalized into late endosomes, via a clathrin dependent mechanism [84]. Further, enhanced (up to 1,000-fold) T-cell stimulation resulted using the antineck region DEC205 antibody [84]. Hence, targeting different regions of DEC205 results in distinct internalization modes, and shows potential for targeted vaccination strategies.

Hamster bone marrow derived DCs, expressing high levels of DEC205 and DC-SIGN, pulsed with tumor lysates of hamster pancreatic cells and injected into tumor bearing hamsters reduced tumor growth significantly [85], further demonstrating that targeting DC-SIGN or DEC205 receptors may be useful for the development of effective vaccines. Liposomes containing calcein are rapidly taken up by immature and mature myeloid DCs [86], and nanoparticles but not microparticles deliver antigen to human DCs via DC-SIGN *in vitro* [87], further demonstrating DC-SIGN as a targeted receptor for vaccine design.

The melanoma antigen, Melan-A/Mart-1 (peptide 16–40, containing the CD8+ HLA-A2 restricted T-cell epitope, amino acids 26–35), was coupled to either Manalpha-6 Man or lactoside, or a Lewis oligosaccharide [88]. The glycoconjugates containing Lewis oligosaccaride bound with high affinity to DC-SIGN were taken up by DCs into acidic vesicles and presented by MHC class I and stimulated CD8+ T-cell responses [88]. However, glycoconjugates containing lactoside were not taken up by DCs. Modification of the melanoma antigen, gp100, with glycans (high mannose) interacted specifically with DCs and induced enhanced CD4+ T-cell responses [89]. Further, Le^x oligosaccharides conjugated to OVA targeted DC-SIGN on DCs effectively and stimulated CTL and IFN-gamma secretion (but not IL-10) by T cells and required 300-fold lower dose to immunize compared to OVA immunization alone [90]. Using human DC-SIGN transgenic DCs, Le^x-OVA was efficiently endocytozed and enhanced OT-I CD8+ and OT-II CD4+ T-cell stimulation resulted, compared to OVA alone [91]. The heparanase tumor antigen is not able to elicit an immune response; however, conjugation of heparanase to Le^x was able to stimulate IFN-gamma cytokine secretion by T cells, CTL responses and delay the growth of established tumors in mice [92]. Liposomes modified to express Le^x and LeB increased binding and internalization by human DCs which was further enhanced, up to 100-fold, and stimulated both CD4+ and CD8+ T-cell responses, in the presence of lipopolysaccharide, compared to nonmodified liposomes. In addition, modified liposome-Le^xLeB encapsulating the melanoma antigen MART-1 in the presence of lipopolysaccharide also enhanced CD8+ T-cell clone activation *in vitro* [93]. Polyamidoamine dendrimers comprising LeB antigen are taken into lysosomes, and dendrimers containing at least 16–32 glycan units are necessary for antigen presentation and cytokine production [94]. Thus, complexes using Le oligosaccharides to target DC-SIGN represent a novel method for vaccination against tumor antigens. Likewise, lentivirus vectors modified with Sindbis virus envelope proteins, when linked to OVA, are taken up by murine bone marrow derived DCs and stimulate OT-I and OT-II T cells, CTL *in vivo* and protects mice against the challenge of OVA expressing tumor cells [95]. The binding of the modified lentivirus vectors with Sindbis virus envelope proteins to DC-SIGN is mannose dependent. Further modification of the vector to include 1-deoxymannojirimycin and to inhibit mannosidases (an enzyme that removes mannose structures during glycosylation) resulted in enhanced antibody responses [96]. These studies demonstrate that glycoconjugates could be designed to target DC-SIGN for developing tumor vaccines. The use of glycans to target DC-SIGN has advantages over anti-DC-SIGN monoclonal antibodies, as they reduce the risk of side effects and their generation relies purely in organic chemistry approaches. However, a recent study demonstrated that receptor-specific antibodies are more effective at inducing immune responses than carbohydrates (glycans) for DC-targeted vaccination strategies [97].

L-SIGN or DC-SIGNR. L-SIGN or DC-SIGNR (also known as CD299, CD209L, and Clec4M) is a type-II transmembrane C-type lectin receptor homologous to DC-SIGN (77% amino acid sequence homology), highly expressed on liver sinusoidal cells, endothelial vascular cells, and in the lymph nodes, but not on DCs, in contrast to DC-SIGN (Table 1 and Figure 1). Like DC-SIGN, L-SIGN has a high affinity binding to ICAM-3, HIV, simian immunodeficiency virus,

Ebola virus, hepatitis C virus and respiratory syncytial virus [72, 73, 75]. L-SIGN also binds with HIV gp120-binding protein and Man9GlcNAc2 oligosaccharide, and binding is enhanced up to 25-fold with Man9GlcNAc2 di-saccharide [98]. Antibodies against L-SIGN, are taken up by human liver sinusoidal endothelial cells and a cross-reactive antibody to L-SIGN/DC-SIGN conjugated to tetanus toxoid induced T-cell responses against tetanus toxoid. Thus, targeting L-SIGN shows promise for the development of targeted vaccines [99].

A further 8-mouse homologs to human DC-SIGN have been documented: SIGN-related gene 1 (SIGN-R1), SIGN-R2, SIGN-R3, SIGN-R4, SIGN-R5, SIGN-R6, SIGN-R7, SIGN-R8 [100]. The carbohydrate specificity of SIGN-R1 (CD209b) and SIGN-R3 is similar to DC-SIGN, in that they bind mannose- and fucose-containing ligands and interact with Lewis blood antigens; however, SIGN-R1 and SIGN-R3 also interact with sialylated Le^x, a ligand for selectins [101, 102]. SIGN-R1 also binds to zymosan, to the capsular polysaccharide of *S. pneumoniae*, and with low affinity to dextran and is highly expressed by macrophages [101, 103–105]. Bovine serum antigen (BSA) consisting, 51 mannoside residues (Man(51)-BSA) binds to SIGN-R1 on lamina propria DCs in the gastrointestinal tract and induces IL-10 cytokine secretion by DCs, but not IL-6 and IL-12p70 [106]. *In vitro* and *in vivo*, Man(51)-BSA stimulates CD4+ type 1 regulatory T-like cells (Tr-1) but not CD4+CD25+Foxp3+ regulatory T cells, suggesting that SIGN-R1 induces tolerance to antigens [106].

LSECtin. LSECtin (liver and lymph node sinusoidal endothelial cell C-type lectin, Clec4G) is a type-II transmembrane C-type lectin protein, similar to the related proteins DC-SIGN and L-SIGN and is expressed in liver, lymph node cells, and sinusoidal endothelial cells but not monocyte derived DCs (Table 1). LSECtin binds to N-acetyl-glucosamine and fucose but does not bind to galactose and may function *in vivo* as a lectin receptor [107]. LSECtin is coexpressed with DC-SIGNR and CD23 and binds to ebola virus, filovirus glycoproteins, lymphocytic choriomeningitis virus, and, to the S-protein of SARS coronavirus but does not interact with HIV-1 and hepatitis C [108]; although a study suggested that LSECtin binds to hepatitis C virus, the interaction was in association DC-SIGNR with [109]. Ligands binding to LSECtin are not inhibited by mannan but by EDTA suggesting that the LSECtin does not bind to mannose [108]. Recently, LSECtin was shown to bind with CD44 [110]. Another study, regarding the expression of LSECtin demonstrated LSECtin, to be expressed on human peripheral blood, thymic DCs, monocyte-derived macrophages and DCs [111], and to human Kupffer cells [112]. Antibody or ligand-mediated engagement of LSECtin activates rapid internalization of LSECtin [111] indicating that LSECtin may be a suitable receptor for targeting antigens in the development of vaccination regimes. Further work is required to determine the viability of LSECtin to be an appropriate target for immunotherapy studies.

CIRE. CIRE (C-type lectin immune receptor, CD209) is a murine type 2 membrane protein which belongs to the C-type lectin receptors and is preferentially expressed by immature CD8− splenic DCs (CD8−CD4+ and CD8−CD4−), on some CD4+ DCs, and on plasmacytoid pre-DCs, with no expression on CD8+ DCs, macrophages, or monocytes (Table 1 and Figure 1) [113]. CIRE that has 57% identity with DC-SIGN is the murine homolog to human DC-SIGN and both bind mannose residues [114]. However, CIRE is downregulated after activation, and incubation with cytokines IL-4 and iL-13 does not enhance expression of CIRE, even though DC-SIGN is enhanced, suggesting differences in gene regulation between the two receptors [113]. CIRE consists of 238 amino acids, and its extracellular domain contains a C-type lectin domain; it is the ligand for ICAM-3 and is a receptor for HIV binding facilitating trans-infection of T cells. Importantly, CIRE does not bind with ebola virus glycoprotein, *Leishmania mexicana*, cytomegalovirus, and lentivirus, which are defined ligands for DC-SIGN [113]. The lack of interaction is due to defect in multimerization of CIRE which is thought to be necessary for pathogen recognition by DC-SIGN [115], suggesting that CIRE and DC-SIGN have functional differences.

Polyanhydride nanoparticles covalently linked to d-mannose and lactose increased the cell surface expression of CD40, CD86, MHC class II, CIRE, and MR on bone marrow derived DCs, compared to nonmodified nanoparticles, although both nanoparticles were similarly internalized [116]. In addition, polyanhydride nanoparticles linked to galactose and d-mannose, increased the cell surface expression (CD40, CD86, MHC class I and II, CIRE, MR and macrphage galactose lectin) and proinflammatory cytokines (IL-1beta, IL-6, and TNF-alpha) on alveolar macrophages [117]. Likewise, polyanhydride microparticles linked to (1,6-bis(pcarboxyphenoxy)hexane (CPH) and sebacic acid) or (1,8-bis(p-carboxyphenoxy)-3,6-dioxaoctane and CPH) were rapidly phagocytosed within 2 hours by bone marrow derived DCs and increased cell surface expression of CD40, CD86, MHC class II and CIRE, and cytokines IL-12p40 and IL-6 [118]. Conjugation of the microparticles to OVA stimulated CD8+ OT-I and CD4+ OT-II T cells [118]. Blocking MR and CIRE inhibited the upregulation of cell surface molecules on DCs, suggesting that CIRE and MR engage together for DC activation [116]. CIRE shows promise as an appropriate target for antigen delivery for improved vaccine development.

2.2.2. Langerin. Langerin (CD207, Clec4K) is a type-II transmembrane cell surface receptor highly expressed on Langerhans cells, CD103+ DCs, and splenic CD8+ DCs (Table 1). Langerin is a C-type lectin which highly binds to mannose residues which are internalized by DCs into Birbeck granules (where Langerin is localized) where there is access to the non-classical antigen processing and presentation pathway.

A comparative study between murine DC-SIGN, SIGN-R1, SIGN-R3, and Langerin demonstrated functional differences amongst the different C-type lectins, despite similarities in the carbohydrate recognition domains. Murine DC-SIGN did not bind dextran, OVA, zymosan, or heat-killed *Candida albicans*, but SIGN-R1, SIGN-R3, and Langerin showed distinct carbohydrate recognition [119]. Only SIGN-R1 bound to *Escherichia coli* and *Salmonella typhimurium* (Gram-negative bacteria), and neither murine DC-SIGN,

SIGN-R1, SIGN-R3 nor Langerin bound to *Staphylococcus aureus* (Gram-positive bacteria) [119]. In addition, SIGN-R1 (but not the other lectin receptors) distinctively bound to zymosan [119]. Langerhans cells (a subset of DCs) are divided into two groups: (i) Langerhans cells that express Langerin and (ii) epidermal Langerhans cells that go to lymph nodes, which function and develop independently [120]. Anti-Langerin monoclonal antibody targeted to Langerin was efficiently endocytozed by Langerhans cells *in vitro* [121] and *in vivo* [122], suggesting further studies in immunizations through the skin for DC-based vaccination therapies. Indeed, anti-Langerin monoclonal antibody conjugated to HIV gag-p24 induced Th1 and CD8+ T-cell responses in mice [123]. Interestingly, anti-DEC-205 monoclonal antibody was recently shown to be taken up by Langerin-positive DCs [124], suggesting there is cross-talk between DEC-205 and Langerin receptors. Further, a noncovalent fusion between anti-Langerin monoclonal antibody and HA1 influenza hemagglutinin elicited antigen-specific T-cell and antibody responses *in vitro* and *in vivo* [125].

2.2.3. MGL. MGL (human macrophage galactose- and N-acetylgalactosamine-specific C-type lectin) is the classical asialoglycoprotein receptor (Figure 1). MGL is highly expressed on macrophages and immature DCs, whose ligand specificity differs from DC-SIGN and L-SIGN, in that it binds to galactose and N-acetylgalactosamine leading to Th2 skewed immunity [126, 127]. In addition, MGL binds the strongest to serine, threonine O-linked glycosylated Tn antigen, a well-known human carcinoma-associated epitope, and not to sialylated Tn antigen [128, 129]. Moreover, hMGL binds to the group of filoviruses and to gonorrhea (via lipooligosaccharides) leading to altered DC cytokine secretion profiles and stimulation of CD4+ Th responses (Table 1) [77, 126, 127].

MUC1 peptide (3 tandem repeats, 60 amino acids enzymatically glycosylated with GalNAc) or short MUC1 or MUC2 peptides containing Tn bound to immature DCs and the MUC1-Tn glycopeptide localized within the MHC class I and class II compartments [130]. MUC1 glycopeptides linked to anti-MGL antibody led to upregulation of human DC cell surface molecules and enhanced CD8+ T stimulation *in vitro* [131]. In mice, MGL+ CD103- dermal DCs bound to glycosylated Tn antigen *in vivo*, stimulating MHC class II CD4+ T-cell responses. Intradermal immunization with Tn-glycopeptides generates antibodies and Th2 cytokine secretion by CD4+ T cells [132]. Recently, a mimic of galactose/N-acetylgalactosamine stimulated blood monocytes and myeloid derived DCs [133], suggesting that glycosylated mimetics could be used to target antigens to MGL expressing DCs. These results demonstrate that the targeting of MGL receptor expressed on murine and human DCs stimulates T-cell and antibody responses, and this approach could be used to design novel anticancer vaccines.

2.2.4. Dectin-1 Subfamily. Dectin-1 (dendritic cell-associated C-type lectin-1, DCAL-1, Clec7A) or beta-glucan receptor is a C-type lectin receptor which is part of the NK gene complex in the Dectin-1 cluster (Table 1 and Figure 1) [134]. It was originally characterized to be DC specific (hence its name), but it is now known to be also expressed on myeloid DCs, CD8−CD4− DCs, dermal DCs, monocytes, macrophages, neutrophils, microglia, T-cell subsets, B cells, mast cells, eosinophils, and monocytes [134–136]. Dectin-1 is a receptor for beta-glucan recognizing beta1,3 and beta1,6-linked glucans on yeast, mycobacterial, and plant cell walls and plays a role in innate immune responses [137, 138]. Zymosan, a beta-glucan and mannan-rich ligand binds to Dectin-1 [139], and Dectin-1 interacts with the tetraspanin molecule CD37. Dectin-1 binds to *Saccharomyces, Candida, Pneumocystis, Coccidiodes, Penicillium,* and *Aspergillus*, but not *Cryptococcus* fungal species, leading to activation of Dectin-1+ cells and elimination of fungal pathogens by activating inflammatory responses, such as TNF-alpha, CDCL1, IL-1beta, GM-CSF, and IL-6, by the presence of an ITAM in its cytoplasmic tail [135]. In fact, Dectin-1 knockout mice are highly susceptible to pathogenic infections due to inflammatory defects and reduced fungal killing [140]. Furthermore, Dectin-1 binds to bacteria resulting in TNF-alpha, IL-6, RANTES, G-CSF, and IL-12 secretion [141]. The stimulation of inflammatory and Th1 cytokines leads to the proposal of Dectin-1 targeting of soluble antigens by appropriate ligands to stimulate cellular immunity.

Anti-Dectin-1 and anti-Dectin-2 monoclonal antibodies conjugated to OVA [142, 143] and induced significant expansion of T cells in the draining lymph nodes of mice and IFN-gamma secretion by T cells [142, 143]. Purified beta1,3-d-glucan from *Saccharomyces cerevisiae* cell wall, free from mannan and other proteins, binds to Dectin-1 receptor on DCs. Beta1,3-d-glucan conjugated to OVA matures bone marrow derived DCs was rapidly phagocytosed and stimulated >100-fold more efficiently CD8+ OT-I and CD4+ OT-II T cells, compared to OVA alone [144]. Immunization of mice with beta1,3-d-glucan stimulated IgG2c antibodies, CD4+ T cells, IFN-gamma, and Th17 biased responses [144]. Thus, robust stimulation of humoral and cellular immune responses results following immunization with vaccine candidates that target Dectin-1 receptor.

DNGR-1. DNGR-1 (NK lectin group receptor-1, Clec9A) is a group V C-type lectin-like type II membrane protein located close to Dectin-1 encoded within the NK gene complex. DNGR-1 is expressed on murine CD8+ DCs not on CD4+ DCs, on CD11c+ DCs but not by CD11c− cells (B cells, T cells, NK cells, NKT cells, macrophages, and granulocytes), on plasmacytoid DCs, and on a small subset of human blood DCs (BDCA-3+ DCs) and monocytes (CD14+CD16−) and induces proinflammatory cytokines [145, 146]. DNGR-1 is also not expressed by interstitial DCs, in skin epidermis, and on GM-CSF derived bone marrow DCs but highly expressed on Flt3 ligand bone marrow derived CD8+ DCs ($CD11b^{low}CD24^{hi}B220-$) [146]. Anti-DNGR-1 monoclonal antibody covalently conjugated to CD8+ peptide from OVA, induced OT-I CD8+ T-cell proliferation and IFN-gamma secretion *in vivo*, and only CD8+ DCs and not plasmacytoid DCs were involved in the presentation of the peptide to CD8+

T cells [146]. In the presence of anti-CD40, CTLs are primed *in vivo* and prevent OVA+ expressing tumor cell growth [146]. Injection of anti-DNGR-1 monoclonal antibody-OVA conjugate into mice was endocytozed by CD8+ DCs, presented antigen to CD4+ T cells, and played a major role in the differentiation of CD4+ T cells into Foxp3+ regulatory T cells [147]. The addition of the adjuvant poly I:C enhanced IL-12 mediated immunity, whereas the adjuvant curdlan primed Th17 cells [147]. In addition, vaccinia virus infected dying cells are endocytozed by DNGR-1 on DCs and mediate cross-priming of antivaccinia virus infected cell CD8+ T-cell responses; loss of DNGR-1 impairs CD8+ CTL responses [148, 149]. Thus, DNGR-1 regulates cross-presentation of viral antigens and could be further assessed as a target for vaccination protocols. Furthermore, a single injection of anti-Clec9A monoclonal antibody induced striking antibody and CD4+ T cells responses in the absence of adjuvant or danger signals in mice and in TLR knockout mice [150, 151]. Targeting antigens to Clec9A shows promise to enhance vaccine efficiency; indeed, anti-Clec9A monoclonal antibody conjugated to HIV gag-p24 induced strong Th1 and CD8+ T-cell responses in mice [123]. DNGR-1/Clec9A could prove useful for developing immunotherapy protocols for cancer and other diseases.

MICL. MICL (myeloid inhibitory C-type lectin-like receptor, Clec12A) is homologous to Dectin-1 and is part of the Dectin-1 cluster [152]. Numerous other groups identified this receptor and named it C-type lectin-like molecule-1 (CLL-1), DC associatedC-type lectin 2 (DCAL-2), and killer cell lectin-like receptor 1 (KLRL1) [153–155]. MICL is expressed on granulocytes, monocytes, macrophages, B cells, CD8+ T cells in peripheral blood, and DCs (Table 1) [156], and, contains a tyrosine based inhibitory motif in its cytoplasmic tail, similar to lectin-like receptor for oxidized density lipoprotein-1 (LOX-1) and Dectin-1, and can inhibit cellular activation. Hence, MICL is a negative regulator of granulocytes and monocytes [152]. MICL has a range of functions including cell adhesion, cell-cell signaling, turnover of glycoproteins, and in inflammation and in immune responses.

CLEC2. CLEC2 (also known as Clec1B), a C-type lectin-like receptor 2, is expressed on NK cells, DCs, monocytes, granulocytes, platelets, megakaryocytes, and liver sinusoidal endothelial cells (Table 1) [157]. CLEC2 is a platelet activation receptor for the endogenous ligand, podoplanin (a mucin-like sialoglycoprotein) expressed on a number of cells including lymphatic endothelial cells and implicated in cancer cell metastasis [158]. CLEC2 on platelets binds to HIV-1 and facilitates HIV-1 spread to other immune cells. The binding of HIV-1 to platelets via CLEC2 is highly dependent on DC-SIGN, suggesting that the two coexist [159]. In addition, the snake venom rhodocytin binds to CLEC2 on platelets and activates cell signaling [160]. Not much is known about CLEC2 and stimulation of immune responses, but its expression on DCs and its colocalization with DC-SIGN suggest it may have immune stimulatory effects.

CLEC12B. CLEC12B (macrophage antigen H) is part of the NK gene complex/Dectin-1 cluster of C-type lectin receptors, highly expressed on macrophages, monocytes, and DCs and contains immunoinhibitory sequences in its cytoplasmic tail [161, 162]. There not much known regarding CLEC12B and its function on DCs and macrophages. It is possible that CLEC12B could be used as a receptor to target antigens for immunotherapy studies for diseases, including cancer; however, this is still to be determined.

LOX-1. LOX-1 (lectin-like receptor for oxidized density lipoprotein-1, Clec8A) is part of the Dectin-1 cluster of C-type lectin receptors. LOX-1 is also considered to be a member of the scavenger receptor family. LOX-1 is expressed on endothelial cells, smooth muscle cells, platelets, fibroblasts, and macrophages and binds to Gram-positive and gram-negative bacteria, oxidized-LDL modified lipoproteins, phospholipids, apoptotic cells, C-reactive protein, and heat shock protein (HSP)-70 [163]. LOX-1 does not contain the classical signaling motifs in its cytoplasmic tail but is involved in endocytosis, phagocytosis, cytokine production, and in the production of reactive oxygen species [164, 165]. As a consequence of the binding of LOX-1 to HSP-70, DC-mediated antigen cross-presentation results [166]. An anti-LOX-1 monoclonal antibody which inhibits the binding of HSP-70 to DCs also inhibits HSP-70 induced cross-presentation of antigens. Anti-LOX-1 monoclonal antibody linked to OVA protein specifically stimulated CD4+ OVA T-cell hybridoma *in vitro* as measured by IL-2 production [166]. Injection of anti-LOX-1-OVA conjugated into mice prevented the growth of OVA expressing tumor cells [166]. Hence, targeting LOX-1 is a promising target for cancer immunotherapy studies.

2.2.5. DC Immunoreceptor (DCIR) Subfamily

DCIR. DCIR (DC immunoreceptor) is a C-type lectin receptor, with tyrosine based immune-inhibitory functions, Clec4A). DCIR is primarily expressed on plasmacytoid DCs (pDCs), on immature and mature monocyte-derived DCs, on monocytes, macrophages, and B cells, and after maturation of pDCs, DCIR is reduced (Table 1). Binding to TLR9 on pDCs induces IFN-alpha, which is inhibited by DCIR activations whilst costimulatory molecules are not affected [167]. DCIR has a range of functions including cell adhesion, cell-cell signaling, turnover of glycoproteins, and in inflammation and in immune responses. Targeting DCIR is rapidly internalized into clathrin pits and processed and presented to T cells [167]. An anti-DCIR monoclonal antibody is rapidly internalized by human monocyte derived DCs into endolysosomal vesicles and does not unregulate TLR4 nor TLR8 mediated upregulation of costimulatory molecules, CD80 and CD86, but does inhibit TLR8 mediated IL-12 and TNF-alpha production [168]. Thus, targeting DCIR activates T cells but also inhibits TLR8-induced (IL-12 and TNF-alpha production) and TLR9-induced (IFN-alpha production), which may be applied in vaccine development for disease prevention and treatment. Targeting antigens to DCIR were evaluated for their potential to stimulate CD8+ T-cell responses. Anti-DCIR monoclonal antibody linked to influenza matrix protein, melanoma antigen MART-1, or to HIV gag antigens resulted in expansion of CD8+ T cells *in vitro* [169] and stimulation of Th1 and

CD8+ T cells *in vivo* [123]. The addition of TLR-7/8 agonists enhanced T expansion of primed CD8+ T cells and induced the production of IFN-gamma and TNF-alpha and reduced the levels of Th2 cytokines [169]. It is clear that, antigen targeting via the DCIR activates specific CD8+ T-cell immune responses.

Dectin-2. Dectin-2 (or DCAL-2, Clec6A) or beta-glucan receptor is a C-type lectin receptor expressed on DCs, macrophages, neutrophils, and monocytes (Table 1) [170]. Dectin-2 is a receptor for beta-glucan recognizing beta1,3 and beta1,6-linked glucans on yeast, mycobacterial, and plant cell walls and plays a role in innate immune responses [137, 138]. Anti-Dectin-2 monoclonal antibody conjugated to antigen stimulate, CD8+ T cells in mice [142]. In addition, a lentivector using the mouse Dectin-2 gene promoter, was taken up by bone marrow derived DCs, Langerhans cells, and dermal DCs *in vitro* [171]. The Dectin-2 lentivector encoding the human melanoma antigen, NY-ESO-1, stimulated CD4+ and CD8+ T cells in mice [171]. Thus, Dectin-2 expressed on DCs is a potential targeting protein for vaccinations.

BDCA-2. Blood DC antigen 2 (BDCA-2, Clec4C) is a type II C-type lectin expressed on human blood DCs, which has 57% homology with its murine homolog Dectin-2. Anti-BDCA-2 monoclonal antibody is rapidly internalized by plasmacytoid DCs and presented to T cells and suppresses the induction of IFN-alpha/beta cytokine secretion [172].

3. DEC205

DEC-205 (CD205 or lymphocyte antigen Ly 75) is a type-I integral membrane protein homologous to the macrophage MR family of C-type lectins, which binds carbohydrates and mediates endocytosis (Figure 1) [173]. DEC-205 is primarily expressed on DCs and thymic epithelial cells. DEC205 mediates a number of different biological functions, such as binding and internalization of ligands for processing and presentation by DCs (Table 2). Although the ligands which bind to DEC205 are not clear, following ligand binding, DEC-205 is rapidly internalized by means of coated pits and vesicles and is delivered to multivesicular endosomal compartments that resemble the MHC class II-containing vesicles implicated in antigen presentation. Due to the endocytic properties of DEC205, it is a promising receptor for antigen delivery for vaccines and targeted immunotherapies [174]. Upon DC maturation, DEC205 is upregulated, unlike other members of the macrophage MR family.

In an attempt to design vaccines that target DEC205, the cytosolic tail of DEC-205 was fused to the external domain of the CD16 Fc gamma receptor and was studied in stable L cell transfectants [175]. The DEC-205 tail recycled CD16 through MHC II-positive late endosomal/lysosomal vacuoles and also mediated a 100-fold increase in antigen presentation to CD4+ T cells. An anti-DEC-205 monoclonal antibody conjugated to OVA was shown to stimulate OVA-specific CD4+ and CD8+ T cells by CD11+ lymph node DCs, but not by CD11c− DCs [176]. Injection of anti-DEC-205-OVA conjugate in mice was taken up by draining lymph node DCs and stimulated CD8+ T (OT-I) cells 400 times more efficiently compared to OVA alone; this response was further enhanced *in vivo* (as measured by IL-2, IFN-gamma, CTL, and tumor protection), with the addition of anti-CD40 antibody (a DC maturation stimulus) [176]. Further, anti-DEC-205 antibody-OVA intradermally injected in mice was rapidly taken up by Langerhans cells and stimulated both CD4+ and CD8+ T-cell responses [122]. Langerin positive skin DCs play a major role in transport of anti-DEC-205-OVA complex, although Langerin negative dermal DCs and CD8+ DCs were responsible for the T-cell stimulation [124]. Hence, there is cross-talk between DC subsets.

Conjugation of the anti-DEC-205 monoclonal antibody to the melanoma antigen tyrosinase-related protein TRP-2, induced CD4+ and CD8+ T-cell responses which protected mice against B16 tumor cell growth and slowed growth of established B16 tumors [177]. In addition, anti-DEC205 monoclonal antibody linked to survivin (a survival protein overexpressed on carcinoma cells) together with anti-CD40 and poly I:C stimulated surviving-specific CD4+ T-cell responses (IFN-gamma, TNF-alpha, IL-2 secretion), lytic MHC class II+ T cells but not CD8+ T cells. Depletion of CD25+foxp3+ cell prior to immunization led to further enhanced immune responses [178]. Interestingly, HER2/neu protein expressed on breast cancer cells was genetically engineered into anti-DEC205 monoclonal antibody, and in combination with poly I:C and CD40 antibody, elicited robust CD4+ and CD8+ T-cell responses and antibody responses which protected mice against Her2+ breast tumor challenge [179]. Further, HIV p24 gag protein conjugated to anti-DEC205 monoclonal antibody, or HIV gag p24-single chain DEC-205 Fv DNA vaccines, was taken up by DCs and stimulated proliferation and IFN-gamma secretion by CD8+ T cells that had been isolated from HIV-infected donors [180, 181]. Similarly, in mice, immunization led to Th1 (IFN-gamma, IL-2), CD4+ and CD8+ T-cell responses, and 10-fold higher antibody levels [123, 181–183]. Likewise, priming with the DNA vaccine and boosting with adenoviral vector (comprising anti-DEC205 monoclonal antibody conjugated to OVA or HIV-1 gag together with anti-CD40) induced strong CD8+ T-cell responses; no enhanced effect was seen with the addition of TLR-9 ligand CpG and TLR-3 ligand poly I:C or CD40 ligand [184]. Recombinant Newcastle disease virus vaccine vector (rNDV) on its own induces IFN-alpha and IFN-beta production and DC maturation. Immunization with rNDV encoding anti-DEC205 and HIV-1 gag antigen enhanced CD8+ gag specific T-cell responses and increased the number of CD4+ and CD8+ T cells in the spleen compared to rNDV encoding gag antigen alone [185]. Furthermore, mice were protected against challenge of recombinant vaccinia virus expressing HIV gag protein [185]. Conjugation of anti-NLDC-145 monoclonal antibody (monoclonal antibody against murine DEC205) to a model antigen stimulated both antibody and T-cell responses in animal models [186]. Conversely, using a self antigen, proteolipid protein ($PLP_{139–151}$) conjugated to anti-DEC205 monoclonal antibody tolerized T cells *in vivo* and reduced the secretion of IL-17 by CD4+ T cells and *in vitro* CD4+Vbeta6+ T-cell receptor T cells specific for $PLP_{139–151}$ became anergic [187]. Hence,

Table 2: Summary of dendritic cell receptors targeted for vaccine development: other receptors.

Receptor	Designation	Function
3. Type-1 integral membrane proteins		
3.1. DEC205	CD205 Ly 75	Homologous to the mannose receptor. Expressed on DCs and thymic epithelial cells. Targeting DEC205 induces an array of immune responses.
4. Scavenger receptors		
4.1. Scavenger receptor		Expressed on macrophages. Bind to modified low density lipoproteins (LDL) by oxidation (oxLDL) or acetylation (acLDL). Bind to CD68, macrosialin, mucins, and LOX-1. Targeting of scavenger receptors induces immune responses in mice.
4.1.1. Scavenger receptor class A	SR-A1 SR-A2	Expressed on macrophages as a trimer. Members include SCARA1 (MSR1), SCARA2 (MARCO), SCARA3, SCARA4 (COLEC12), and SCARA5.
4.1.2. Scavenger receptor class B	SR-B1	Consists of 2 transmembrane units. Members include SCARB1, SCARB2, and SCARB3 (CD36).
4.1.3. Scavenger receptor class C	SR-B1	Consists of a transmembrane region in which the N-terminus is located extracellularly.
4.2. DC-asialoglycoprotein receptor (DC-ASGPR)		A lectin-like scavenger receptor. Expressed on monocyte derived DCs (CD14+CD34+), tonsillar interstitial-type DCs, and granulocytes. Targeting DC-ASGPR induces suppressive responses.
5. F4/80 receptor		Expression restricted to macrophages. Murine homolog of the epidermal growth factor-like module containing mucin-like hormone receptor-1 protein encoded by the EMR1 gene.
5.1. FIRE		Expressed on CD8−CD4+ and CD8−CD4− immature DCs, and weakly on monocytes and macrophages. Targeting FIRE stimulates immune responses in mice.
6. DC-specific transmembrane protein (DC-STAMP)		Expressed on DCs and activated blood DCs. Targeting DC-STAMP results in immunosuppressive responses in some studies and in other studies stimulates strong cellular responses.
7. FcR		Links humoral and cellular immune (Fc Receptor) responses, links innate and adaptive immune responses by binding pathogens and immune complexes, and stimulates T cells. Targeting FcR is a novel vaccine strategy for stimulating immune responses.

targeting self-antigens to DEC-205 induces tolerance. It is clear that, targeting DCs using DEC-205 directed antibody-antigen conjugates represents a novel method of inducing tolerance to self-antigens and antitumor immunity *in vivo*.

4. Scavenger Receptor

The scavenger receptors (SRs) are a group of receptors that recognize modified low density lipoprotein (LDL) by oxidation (oxLDL) or acetylation (acLDL) (Figure 1). Scavenger receptor was given its name based on its "scavenging" function. SR is primarily present on macrophages internalize endotoxins, oxLDL, and other negatively charged proteins. SR, are grouped into classes A, B, and C according to their structural features. (i) Scavenger receptor class A (SR-A1, SR-A2) is mainly expressed on macrophages as a trimer and has 6 domains (cytosol, transmembrane, spacer, alpha-helical coiled-coil, collagen-like, and cystein-rich domains) (Table 2). Members include SCARA1 (MSR1), SCARA2 (MARCO), SCARA3, SCARA4 (COLEC12), and SCARA5. (ii) Class B (SR-B1) has 2 transmembrane regions and are identified as as ocLDL receptors. Members include SCARB1, SCARB2, and SCARB3 (CD36). (iii) Class C has a transmembrane region in which the N-terminus is located extracellularly. There are other receptors that have been reported to bind to oxLDL which include CD68 and its murine homolog macrosialin, mucins, and LOX-1.

Despite the scavenging functions of SR, SRs have been shown to endocytoze antigens and present antigens to MHC class I and II and stimulate effective CD4+ and CD8+ T-cell responses. Using 200 nm particles coated with oligonucleotide polyguanylic acid (SR-targeting agent) showed specific binding to SR, and particles were localized in intracellular vesicles and processing via the endocytotic pathway [188]. An early example demonstrating immune responses generation was with maleylated OVA which bound to SR, enhancing its presentation and stimulation of CTLs by macrophages

and B cells [189]. Maleylated diphtheria toxoid was also more immunogenic than nonmaleylated diphtheria toxoid, generating enhanced antibody and T-cell proliferative responses [190]. Likewise, in chickens, immunization with maleylated bovine serum albumin yielded Th1 immune response via antibodies. In addition, high levels of IFN-gamma mRNA were detected in splenocytes compared to nonmaleylated bovine serum antigen that stimulated Th2 immune responses [191]. Tropomyosin from shrimp causes allergic responses in some individuals inducing a dominant Th2 cytokine profile and IgE antibody responses. Modifying tropomyosin to maleylated tropomyosin, diverted responses from IL-4 Th2 dominant proallergic phenotype to an IFN-gamma Th1 antiallergic phenotype. Thus, modification of proteins to target the SR on macrophages elicits Th1 IFN-gamma responses [192]. SRs recognize malondialdehyde and acetaldehyde adducted proteins [193] and when linked to hen egg lysozyme protein, stable adducts (oxidative products) are formed. Immunization in mice results in strong T-cell proliferative and antibody responses [193]. MARCO, a SR class A family member expressed on murine macrophages and human monocyte-derived DCs, plays an influential role in mediating immune responses. Anti-MARCO antibody linked to tumor lysate-pulsed DCs enhance, tumor-reactive IFN-gamma producing T cells and reduced tumor growth in mice [194]. These studies demonstrate the implications of targeting antigens to MARCO and other SRs for use in human clinical DC vaccine trials.

4.1. DC-ASGPR. DC-asialoglycoprotein receptor (DC-ASGPR) is a lectin-like scavenger receptor. It is expressed on monocyte derived DCs (CD14+CD34+), on tonsillar interstitial-type DCs and granulocytes, but not on T cells, B cells, NK cells, monocytes, Langerhans cells, and CD1a derived DCs (Table 2) [195]. Anti-DC-ASGPR monoclonal antibody is rapidly internalized into early endosomes, indicating that DC-ASGPR is involved in antigen capture and processing [195]. Targeting DC-ASGPR induces a suppressive CD4+ T-cell response that secretes IL-10 *in vitro* and *in vivo* [196]. Hence, targeting antigens to DC-ASGPR induces antigen specific IL-10-producing suppressive T cells, and DC-ASGPR could be utilized to induce a suppressive immunotherapeutic effect to self- or non-self-antigens.

5. F4/80 Receptor

F4/80 is restricted to macrophages, and for over 40 years F4/80 has been used to identify and characterize macrophages in tissues and its functional role in macrophage biology [197]. F4/80 is the murine homolog of the epidermal growth factor-like module containing mucin-like hormone receptor-1 protein encoded by the EMR1 gene. F4/80 although highly expressed on macrophages does not play a role in macrophage development (Table 2 and Figure 1). However, F4/80 receptor was found to be necessary for the induction of CD8+ T regulatory cells responsible for peripheral immune tolerance [197]. No ligands to F4/80 are known, and much work is still required to understand the role of F4/80 in the immune response and could be a novel antigen targeting receptor.

5.1. FIRE. FIRE is an F4/80-like receptor expressed specifically on CD8−CD4+ and CD8−CD4− immature DCs and weakly on monocytes and macrophages (Table 2) [198]. Rat anti-FIRE (6F12) and rat anti-CIRE (5H10) antibodies (targeting the FIRE and CIRE receptors on CD8− DCs) were injected into mice, and anti-rat Ig titres were measured and compared to control rat antibody [198]. Anti-FIRE and anti-CIRE IgG1 antibody responses were 100–1,000-fold greater to non-targeted control rat antibody. The magnitude of the responses was equivalent to that seen when CpG was included as an adjuvant [198]. Conversely targeting the DEC205 receptor, expressed on CD8+ DCs with rat anti-DEC-205 antibody (NLDC-145), did not induce humoral immune responses unless CpG was added [198]. This study demonstrated the differences in the ability of CD8+ and CD8− DC subsets to stimulate immune responses *in vivo*.

6. DC-STAMP

DC-specific transmembrane protein (DC-STAMP) contains 7 transmembrane regions and has no sequence homology with other multimembrane cell surface receptors and has an intracellular C-terminus. DC-STAMP resides in the endoplasmic reticulum, where it interacts with LUMAN (also known as CREB3 or LZIP) of immature DCs and upon stimulation DC-STAMP translocates to the Golgi apparatus and is expressed on the cell surface upon maturation [199]. DC-STAMP is specifically expressed by DC, on activated but not resting blood DCs, and not in a panel of other leukocytes or nonhematopoietic cells (Table 2) [200]. DC-STAMP lentiviral vector-OVA in mice tolerize OT-I CD8+ and OT-II CD4+ T-cell responses, leading to elimination and functional inactivation of CD4 and CD8 T cells in peripheral organs and in the thymus [201]. Binuclear and multinuclear DCs express low levels of MHC class II and IL-12p70 with high levels of IL-10 which suppress T-cell proliferative responses [202]. Blocking of DC-STAMP decreased the number of binuclear cells, suggesting that the DC-STAMP is responsible for the immunosuppresive effects of binucleated DCs [202]. Thus, targeting antigens to DC-STAMP tolerize antigen specific T-cell responses *in vivo*. Conversely, using DC-STAMP promoter driven construct linked to OVA, resulted in strong OVA-specific CD4+ and CD8+ T-cell responses *in vitro* and *in vivo* and protected mice against OVA+ tumor challenge [203]. Thus, DC-STAMP shows promise as a target for cancer vaccine antigen targeting approach.

7. Fc Receptor

Fc receptors (FcR) for immunoglobulins link humoral and cellular immune responses [204]. They also link the innate immune response to the adaptive immune response by binding to pathogens and immune complexes and stimulating T cells. There is a different FcR for each class of immunoglobulin FcαlphaR (IgA), FcεpsilonR (IgE), FcγammaR (IgG),

and Fcαlpha/μegaR (IgA and IgM). There are 4 types of FcγammaR: FcγammaRI (CD64), FcγammaRII (CD32), FcγammaRIII (CD16), and FcγammaRIV. It is becoming evident that antibody-antigen complexes present antigen more efficiently than antigen alone via the FcγammaR. OVA antigen complexed with anti-OVA antibody injected into mice is presented 10 times more efficiently to T cells compared to OVA alone [205]. An interesting study demonstrated that γamma-chain knockout mice which lack FcγammaRI/FcγammaRIII/FcγammaRIV induced similar CD8+ T-cell responses in mice compared to the wild-type mice. However, CD8+ T-cell proliferative responses were reduced in FcγammaRI/FcγammaRII/FcγammaRIII knockout mice compared to wild type mice, suggesting that all FcR other than FcγammaRIV take up immune complexes and stimulate CD8+ T-cell responses [205]. In a comparative study between FcR and MR targeting of prostate serum antigen (PSA), PSA antigen/anti PSA antibody complex induced both CD4+ and CD8+ T-cell responses however, mannose-PSA stimulated only CD4+ T cells [206]. However, given that the antigen is mannosylated in the appropriate form, CD8+ T cells could be generated, as seen with oxidized versus reduced mannan-MUC1 conjugates (Table 2) [6, 8, 12, 13, 21].

7.1. FcγammaRIII (CD16). FcγammaRIII is also known as CD16. Conjugation of tetanus toxoid 14 amino acid peptide or a hepatitis C virus peptide to anti-CD16 antibody activated CD4+ T-cell clones 500 times more effectively compared to peptide alone [207]. Hence, FcγammaRIII has properties of antigen uptake, processing, and presentation to T cells for effective immune response generation.

7.2. FcαlphaRI (CD89). FcαlphaRI is expressed on myeloid cells, interstitial-type DCs, CD34+ DCs, and monocyte derived DCs [208]. FcαlphaR1 binds to *Porphyromonas gingivalis*, *Bordetella pertussis,* and *Candida albicans* stimulating efficient immune responses for their elimination [209–213]. Cross-linking of FcαlphaRI induced internalization of receptor and activation of DCs; however, there was very minimal antigen presentation [214, 215]. Therefore, it is unlikely that targeting antigen to human FcalphaRI will result in generating increased immune responses.

7.3. FcεpsilonRII (CD23). FcεpsilonRII (CD23) is a type 2 transmembrane C-type lectin that binds with low affinity to IgE. CD23 also interacts with CD21, CD11b, and CD11c. Unlike other Fc receptors, CD23 is a C-type lectin. Its main function is in allergic responses, and it is expressed on activated B cells, activated macrophages, eosinophils, platelets, and follicular DCs. CD23 is noncovalently associated with DC-SIGN and MHC class II on the surface of human B cells. Following endocytosis of anti-CD23 antibodies, CD23 is lost from the cells; however, endocytosis anti-MHC class II antibody leads to recycling of HLA-DR-CD23 complex to the cell surface, consistent with the recycling of MHC class II in antigen presentation; CD23 is internalized into cytoplasmic organelles that resembled the compartments for peptide loading (MHC class II vesicles) [216]. This may lead to peptide presentation, and the return of CD23 with MHC class II to the cell surface may aid in the stabilization of B-cell-T-cell interactions, leading to T-cell responses [216]. It is apparent that human and murine B cells take up IgE-antigen complexes via CD23 and present antigenic peptides via MHC class II stimulating CD4+ T cells. TNP-(trinitrophenyl-) specific IgE linked to BSA or OVA and injected into mice results in 100-fold enhanced IgG antibody responses as compared to either IgE or BSA or OVA injected alone; the enhanced antibody effects are completely dependent on CD23 [217, 218]. In addition, the coexpression of CD23 with DC-SIGN further suggests that antigen presentation and stimulation of antigens is possible between the cross-talk of these two receptors. Hence, targeting CD23 is a novel vaccine strategy for stimulating CD4+ T-cell immune responses.

8. Conclusions

A promising strategy to improve the immunogenicity of antigens is "antigen targeting." DCs are unique in their ability to present antigen to naive T cells and, hence, play a major role in initiating immune responses. Characterization of DC receptors aid in the understanding of the mechanism underlying their potent antigen presenting capacity. A major challenge for vaccine design is targeting antigens to DCs *in vivo*, facilitating cross-presentation, and conditioning the microenvironment for Th1- and Th2-type immune responses. We have analysed numerous DC cell surface receptors, which function in inducing cellular responses and individually each shows promise as targets for vaccine design against cancer. More recently there has been an upsurge of information regarding toll-like receptor (TLR) targeting and stimulation of DCs via TLR. It is clear that in mice, use of TLR ligands to activate DCs stimulates effective cellular immune responses and activation of DCs. However, no substantial TLR-targeting vaccine trials have been completed in humans and it remains to be determined whether TLR targeted approach will result in significant benefits in humans as those seen in mice. Furthermore, targeting antigens to chemokine receptors [1] on DCs (CCR1, CCR2, CXCR4, CCR5, CCR6, and CXCR1) generates enhanced immune responses *in vitro* and *in vivo.* Furthermore, bacterial toxins, DC binding peptides and internalization peptide (Int) also target antigens to DCs; however, the targeting does not involve receptor targeting. It is clear that receptor targeting of antigens is a promising new approach for cancer immunotherapy studies.

References

[1] N. S. Wilson and J. A. Villadangos, "Regulation of antigen presentation and cross-presentation in the dendritic cell network: acts, hypothesis, and immunological implications," *Advances in Immunology*, vol. 86, pp. 241–305, 2005.

[2] R. A. B. Ezekowitz, K. Sastry, P. Bailly, and A. Warner, "Molecular characterization of the human macrophage mannose receptor: demonstration of multiple carbohydrate recognition-like domains and phagocytosis of yeasts in Cos-1 cells," *Journal of Experimental Medicine*, vol. 172, no. 6, pp. 1785–1794, 1990.

[3] S. E. Fanibunda, D. N. Modi, J. S. Gokral, and A. H. Bandivdekar, "HIV gp120 binds to mannose receptor on vaginal epithelial cells and induces production of matrix metalloproteinases," *PLoS ONE*, vol. 6, no. 11, Article ID e28014, 2011.

[4] W. Cardona-Maya, P. A. Velilla, C. J. Montoya, Á. Cadavid, and M. T. Rugeles, "In vitro human immunodeficiency virus and sperm cell interaction mediated by the mannose receptor," *Journal of Reproductive Immunology*, vol. 92, no. 1-2, pp. 1–7, 2011.

[5] V. Apostolopoulos and I. F. McKenzie, "Role of the mannose receptor in the immune response," *Current Molecular Medicine*, vol. 1, no. 4, pp. 469–474, 2001.

[6] V. Apostolopoulos, N. Barnes, G. A. Pietersz, and I. F. C. McKenzie, "Ex vivo targeting of the macrophage mannose receptor generates anti-tumor CTL responses," *Vaccine*, vol. 18, no. 27, pp. 3174–3184, 2000.

[7] A. Avraméas, D. McIlroy, A. Hosmalin et al., "Expression of a mannose/fucose membrane lectin on human dendritic cells," *European Journal of Immunology*, vol. 26, no. 2, pp. 394–400, 1996.

[8] V. Apostolopoulos, G. A. Pietersz, S. Gordon, L. Martinez-Pomares, and I. F. McKenzie, "Aldehyde-mannan antigen complexes target the MHC class I antigen-presentation pathway," *European Journal of Immunology*, vol. 30, pp. 1714–1723, 2000.

[9] A. J. Engering, M. Cella, D. Fluitsma et al., "The mannose receptor functions as a high capacity and broad specificity antigen receptor in human dendritic cells," *European Journal of Immunology*, vol. 27, no. 9, pp. 2417–2425, 1997.

[10] M. C. A. A. Tan, A. M. Mommaas, J. W. Drijfhout et al., "Mannose receptor-mediated uptake of antigens strongly enhances HLA class II-restricted antigen presentation by cultured dendritic cells," *European Journal of Immunology*, vol. 27, no. 9, pp. 2426–2435, 1997.

[11] K. C. Sheng, D. S. Pouniotis, M. D. Wright et al., "Mannan derivatives induce phenotypic and functional maturation of mouse dendritic cells," *Immunology*, vol. 118, no. 3, pp. 372–383, 2006.

[12] V. Apostolopoulos, G. A. Pietersz, B. E. Loveland, M. S. Sandrin, and I. F. C. Mckenzie, "Oxidative/reductive conjugation of mannan to antigen selects for T1 or T2 immune responses," *Proceedings of the National Academy of Sciences of the United States of America*, vol. 92, no. 22, pp. 10128–10132, 1995.

[13] V. Apostolopoulos, G. A. Pietersz, and I. F. C. McKenzie, "Cell-mediated immune responses to MUC1 fusion protein coupled to mannan," *Vaccine*, vol. 14, no. 9, pp. 930–938, 1996.

[14] C. J. Lees, V. Apostolopoulos, B. Acres, C. S. Ong, V. Popovski, and I. F. C. McKenzie, "The effect of T1 and T2 cytokines on the cytotoxic T cell response to mannan-MUC1," *Cancer Immunology Immunotherapy*, vol. 48, no. 11, pp. 644–652, 2000.

[15] C. J. Lees, V. Apostolopoulos, and I. F. C. McKenzie, "Cytokine production from murine CD4 and CD8 cells after mannan-MUC1 immunization," *Journal of Interferon and Cytokine Research*, vol. 19, no. 12, pp. 1373–1379, 1999.

[16] S. A. Lofthouse, V. Apostolopoulos, G. A. Pietersz, W. Li, and I. F. C. McKenzie, "Induction of T1 (cytotoxic lymphocyte) and/or T2 (antibody) responses to a mucin-1 tumour antigen," *Vaccine*, vol. 15, no. 14, pp. 1586–1593, 1997.

[17] I. F. C. McKenzie, V. Apostolopoulos, C. Lees et al., "Oxidised mannan antigen conjugates preferentially stimulate T1 type immune responses," *Veterinary Immunology and Immunopathology*, vol. 63, no. 1-2, pp. 185–190, 1998.

[18] G. A. Pietersz, W. Li, V. Popovski, J. A. Caruana, V. Apostolopoulos, and I. F. C. McKenzie, "Parameters for using mannan-MUC1 fusion protein to induce cellular immunity," *Cancer Immunology Immunotherapy*, vol. 45, no. 6, pp. 321–326, 1998.

[19] V. Apostolopoulos, S. A. Lofthouse, V. Popovski, G. Chelvanayagam, M. S. Sandrin, and I. F. C. McKenzie, "Peptide mimics of a tumor antigen induce functional cytotoxic T cells," *Nature Biotechnology*, vol. 16, no. 3, pp. 276–280, 1998.

[20] V. Apostolopoulos, C. Osinski, and I. F. C. Mckenzie, "MUC1 cross-reactive Galα(1,3)Gal antibodies in humans switch immune responses from cellular to humoral," *Nature Medicine*, vol. 4, no. 3, pp. 315–320, 1998.

[21] V. Apostolopoulos, D. S. Pouniotis, P. J. van Maanen et al., "Delivery of tumor associated antigens to antigen presenting cells using penetratin induces potent immune responses," *Vaccine*, vol. 24, no. 16, pp. 3191–3202, 2006.

[22] V. Karanikas, L. A. Hwang, J. Pearson et al., "Antibody and T cell responses of patients with adenocarcinoma immunized with mannan-MUC1 fusion protein," *Journal of Clinical Investigation*, vol. 100, no. 11, pp. 2783–2792, 1997.

[23] V. Karanikas, J. Lodding, V. C. Maino, and I. F. C. McKenzie, "Flow cytometric measurement of intracellular cytokines detects immune responses in MUC1 immunotherapy," *Clinical Cancer Research*, vol. 6, no. 3, pp. 829–837, 2000.

[24] V. Karanikas, G. Thynne, P. Mitchell et al., "Mannan mucin-1 peptide immunization: influence of cyclophosphamide and the route of injection," *Journal of Immunotherapy*, vol. 24, no. 2, pp. 172–183, 2001.

[25] B. E. Loveland, A. Zhao, S. White et al., "Mannan-MUC1-pulsed dendritic cell immunotherapy: a phase I trial in patients with adenocarcinoma," *Clinical Cancer Research*, vol. 12, no. 3, pp. 869–877, 2006.

[26] M. Katsara, J. Matsoukas, G. Deraos, and V. Apostolopoulos, "Towards immunotherapeutic drugs and vaccines against multiple sclerosis," *Acta Biochimica et Biophysica Sinica*, vol. 40, no. 7, pp. 636–642, 2008.

[27] M. Katsara, G. Minigo, M. Plebanski, and V. Apostolopoulos, "The good, the bad and the ugly: how altered peptide ligands modulate immunity," *Expert Opinion on Biological Therapy*, vol. 8, no. 12, pp. 1873–1884, 2008.

[28] T. V. Tselios, F. N. Lamari, I. Karathanasopoulou et al., "Synthesis and study of the electrophoretic behavior of mannan conjugates with cyclic peptide analogue of myelin basic protein using lysine-glycine linker," *Analytical Biochemistry*, vol. 347, no. 1, pp. 121–128, 2005.

[29] M. Katsara, E. Yuriev, P. A. Ramsland et al., "Mannosylation of mutated MBP83-99 peptides diverts immune responses from Th1 to Th2," *Molecular Immunology*, vol. 45, no. 13, pp. 3661–3670, 2008.

[30] M. Katsara, E. Yuriev, P. A. Ramsland et al., "Altered peptide ligands of myelin basic protein (MBP87-99) conjugated to reduced mannan modulate immune responses in mice," *Immunology*, vol. 128, no. 4, pp. 521–533, 2009.

[31] M. Katsara, G. Deraos, T. Tselios, J. Matsoukas, and V. Apostolopoulos, "Design of novel cyclic altered peptide ligands of myelin basic protein MBP83-99 that modulate immune responses in SJL/J mice," *Journal of Medicinal Chemistry*, vol. 51, no. 13, pp. 3971–3978, 2008.

[32] M. Katsara, G. Deraos, T. Tselios et al., "Design and synthesis of a cyclic double mutant peptide (cyclo(87-99)[A 91,A96]MBP87-99) induces altered responses in mice after conjugation to mannan: implications in the immunotherapy of multiple sclerosis," *Journal of Medicinal Chemistry*, vol. 52, no. 1, pp. 214–218, 2009.

[33] M. Katsara, E. Yuriev, P. A. Ramsland et al., "A double mutation of MBP83-99 peptide induces IL-4 responses and antagonizes IFN-γ responses," *Journal of Neuroimmunology*, vol. 200, no. 1-2, pp. 77–89, 2008.

[34] C. K. Tang, K. C. Sheng, V. Apostolopoulos, and G. A. Pietersz, "Protein/peptide and DNA vaccine delivery by targeting C-type lectin receptors," *Expert Review of Vaccines*, vol. 7, no. 7, pp. 1005–1018, 2008.

[35] Y. Hattori, S. Kawakami, Y. Lu, K. Nakamura, F. Yamashita, and M. Hashida, "Enhanced DNA vaccine potency by mannosylated lipoplex after intraperitoneal administration," *Journal of Gene Medicine*, vol. 8, no. 7, pp. 824–834, 2006.

[36] C. K. Tang, J. Lodding, G. Minigo et al., "Mannan-mediated gene delivery for cancer immunotherapy," *Immunology*, vol. 120, no. 3, pp. 325–335, 2007.

[37] G. Minigo, A. Scholzen, C. K. Tang et al., "Poly-l-lysine-coated nanoparticles: a potent delivery system to enhance DNA vaccine efficacy," *Vaccine*, vol. 25, no. 7, pp. 1316–1327, 2007.

[38] C. K. Tang, K. C. Sheng, D. Pouniotis et al., "Oxidized and reduced mannan mediated MUC1 DNA immunization induce effective anti-tumor responses," *Vaccine*, vol. 26, no. 31, pp. 3827–3834, 2008.

[39] R. Srinivas, P. P. Karmali, D. Pramanik et al., "Cationic amphiphile with shikimic acid headgroup shows more systemic promise than its mannosyl analogue as DNA vaccine carrier in dendritic cell based genetic immunization," *Journal of Medicinal Chemistry*, vol. 53, no. 3, pp. 1387–1391, 2010.

[40] K. C. Sheng, M. Kalkanidis, D. S. Pouniotis, M. D. Wright, G. A. Pietersz, and V. Apostolopoulos, "The adjuvanticity of a mannosylated antigen reveals TLR4 functionality essential for subset specialization and functional maturation of mouse dendritic cells," *Journal of Immunology*, vol. 181, no. 4, pp. 2455–2464, 2008.

[41] K. C. Sheng, M. Kalkanidis, D. S. Pouniotis et al., "Delivery of antigen using a novel mannosylated dendrimer potentiates immunogenicity in vitro and in vivo," *European Journal of Immunology*, vol. 38, no. 2, pp. 424–436, 2008.

[42] S. Toda, N. Ishii, E. Okada et al., "HIV-1-specific cell-mediated immune responses induced by DNA vaccination were enhanced by mannan-coated liposomes and inhibited by anti-interferon-γ antibody," *Immunology*, vol. 92, no. 1, pp. 111–117, 1997.

[43] Z. Cui, C. H. Hsu, and R. J. Mumper, "Physical characterization and macrophage cell uptake of mannan-coated nanoparticles," *Drug Development and Industrial Pharmacy*, vol. 29, no. 6, pp. 689–700, 2003.

[44] C. Foged, C. Arigita, A. Sundblad, W. Jiskoot, G. Storm, and S. Frokjaer, "Interaction of dendritic cells with antigen-containing liposomes: effect of bilayer composition," *Vaccine*, vol. 22, no. 15-16, pp. 1903–1913, 2004.

[45] J. S. Thomann, B. Heurtault, S. Weidner et al., "Antitumor activity of liposomal ErbB2/HER2 epitope peptide-based vaccine constructs incorporating TLR agonists and mannose receptor targeting," *Biomaterials*, vol. 32, no. 20, pp. 4574–4583, 2011.

[46] S. Espuelas, C. Thumann, B. Heurtault, F. Schuber, and B. Frisch, "Influence of ligand valency on the targeting of immature human dendritic cells by mannosylated liposomes," *Bioconjugate Chemistry*, vol. 19, no. 12, pp. 2385–2393, 2008.

[47] S. Hamdy, A. Haddadi, A. Shayeganpour, J. Samuel, and A. Lavasanifar, "Activation of antigen-specific T cell-responses by mannan-decorated PLGA nanoparticles," *Pharmaceutical Research*, vol. 28, no. 9, pp. 2288–2301, 2011.

[48] H. Shiku, L. Wang, Y. Ikuta et al., "Development of a cancer vaccine: peptides, proteins, and DNA," *Cancer Chemotherapy and Pharmacology*, vol. 46, pp. S77–S82, 2000.

[49] H. L. Jiang, M. L. Kang, J. S. Quan et al., "The potential of mannosylated chitosan microspheres to target macrophage mannose receptors in an adjuvant-delivery system for intranasal immunization," *Biomaterials*, vol. 29, no. 12, pp. 1931–1939, 2008.

[50] U. Wattendorf, G. Coullerez, J. Vörös, M. Textor, and H. P. Merkle, "Mannose-based molecular patterns on stealth microspheres for receptor-specific targeting of human antigen-presenting cells," *Langmuir*, vol. 24, no. 20, pp. 11790–11802, 2008.

[51] P. M. Moyle, C. Olive, M. F. Ho et al., "Toward the development of prophylactic and therapeutic human papillomavirus type-16 lipopeptide vaccines," *Journal of Medicinal Chemistry*, vol. 50, no. 19, pp. 4721–4727, 2007.

[52] P. Presicce, A. Taddeo, A. Conti, M. L. Villa, and S. Della Bella, "Keyhole limpet hemocyanin induces the activation and maturation of human dendritic cells through the involvement of mannose receptor," *Molecular Immunology*, vol. 45, no. 4, pp. 1136–1145, 2008.

[53] S. A. Porcelli, "The CD1 family: a third lineage of antigen-presenting molecules," *Advances in Immunology*, vol. 59, pp. 1–98, 1995.

[54] S. A. Porcelli and R. L. Modlin, "CD1 and the expanding universe of T cell antigens," *Journal of Immunology*, vol. 155, no. 8, pp. 3709–3710, 1995.

[55] T. I. Prigozy, P. A. Sieling, D. Clemens et al., "The mannose receptor delivers lipoglycan antigens to endosomes for presentation to T cells by CD1b molecules," *Immunity*, vol. 6, no. 2, pp. 187–197, 1997.

[56] V. Ramakrishna, J. F. Treml, L. Vitale et al., "Mannose receptor targeting of tumor antigen pmel17 to human dendritic cells directs anti-melanoma T cell responses via multiple HLA molecules," *Journal of Immunology*, vol. 172, no. 5, pp. 2845–2852, 2004.

[57] L. Z. He, V. Ramakrishna, J. E. Connolly et al., "A novel human cancer vaccine elicits cellular responses to the tumor-associated antigen, human chorionic gonadotropin β," *Clinical Cancer Research*, vol. 10, no. 6, pp. 1920–1927, 2004.

[58] V. Ramakrishna, J. P. Vasilakos, J. D. Tario Jr., M. A. Berger, P. K. Wallace, and T. Keler, "Toll-like receptor activation enhances cell-mediated immunity induced by an antibody vaccine targeting human dendritic cells," *Journal of Translational Medicine*, vol. 5, article 5, 2007.

[59] M. A. Morse, D. A. Bradley, T. Keler et al., "CDX-1307: a novel vaccine under study as treatment for muscle-invasive bladder cancer," *Expert Review of Vaccines*, vol. 10, no. 6, pp. 733–742, 2011.

[60] M. A. Morse, R. Chapman, J. Powderly et al., "Phase I study utilizing a novel antigen-presenting cell-targeted vaccine with toll-like receptor stimulation to induce immunity to self-antigens in cancer patients," *Clinical Cancer Research*, vol. 17, no. 14, pp. 4844–4853, 2011.

[61] T. Tsuji, J. Matsuzaki, M. P. Kelly et al., "Antibody-targeted NY-ESO-1 to mannose receptor or DEC-205 in vitro elicits dual human CD8+ and CD4+ T cell responses with broad antigen

specificity," *Journal of Immunology*, vol. 186, no. 2, pp. 1218–1227, 2011.

[62] J. S. Lam, M. K. Mansour, C. A. Specht, and S. M. Levitz, "A model vaccine exploiting fungal mannosylation to increase antigen immunogenicity," *Journal of Immunology*, vol. 175, no. 11, pp. 7496–7503, 2005.

[63] J. S. Lam, H. Huang, and S. M. Levitz, "Effect of differential N-linked and O-linked mannosylation on recognition of fungal antigens by dendritic cells," *PLoS ONE*, vol. 2, no. 10, Article ID e1009, 2007.

[64] G. Ahlen, L. Strindelius, T. Johansson et al., "Mannosylated mucin-type immunoglobulin fusion proteins enhance antigen-specific antibody and T lymphocyte responses," *PloS One*, vol. 7, no. 10, Article ID e46959, 2012.

[65] D. J. Betting, X. Y. Mu, K. Kafi et al., "Enhanced immune stimulation by a therapeutic lymphoma tumor antigen vaccine produced in insect cells involves mannose receptor targeting to antigen presenting cells," *Vaccine*, vol. 27, no. 2, pp. 250–259, 2009.

[66] M. K. Mansour, L. S. Schlesinger, and S. M. Levitz, "Optimal T cell responses to Cryptococcus neoformans mannoprotein are dependent on recognition of conjugated carbohydrates by mannose receptors," *Journal of Immunology*, vol. 168, no. 6, pp. 2872–2879, 2002.

[67] D. Pietrella, C. Corbucci, S. Perito, G. Bistoni, and A. Vecchiarelli, "Mannoproteins from Cryptococcus neoformans promote dendritic cell maturation and activation," *Infection and Immunity*, vol. 73, no. 2, pp. 820–827, 2005.

[68] B. J. Appelmelk, I. van Die, S. J. van Vliet, C. M. J. E. Vandenbroucke-Grauls, T. B. H. Geijtenbeek, and Y. van Kooyk, "Cutting edge: carbohydrate profiling identifies new pathogens that interact with dendritic cell-specific ICAM-3-grabbing non-integrin on dendritic cells," *Journal of Immunology*, vol. 170, no. 4, pp. 1635–1639, 2003.

[69] S. G. Turville, J. Arthos, K. MacDonald et al., "HIV gp120 receptors on human dendritic cells," *Blood*, vol. 98, no. 8, pp. 2482–2488, 2001.

[70] T. B. H. Geijtenbeek, D. S. Kwon, R. Torensma et al., "DC-SIGN, a dendritic cell-specific HIV-1-binding protein that enhances trans-infection of T cells," *Cell*, vol. 100, no. 5, pp. 587–597, 2000.

[71] T. B. H. Geijtenbeek, R. Torensma, S. J. van Vliet et al., "Identification of DC-SIGN, a novel dendritic cell-specific ICAM-3 receptor that supports primary immune responses," *Cell*, vol. 100, no. 5, pp. 575–585, 2000.

[72] C. P. Alvarez, F. Lasala, J. Carrillo, O. Muñiz, A. L. Corbí, and R. Delgado, "C-type lectins DC-SIGN and L-SIGN mediate cellular entry by Ebola Virus in cis and in trans," *Journal of Virology*, vol. 76, no. 13, pp. 6841–6844, 2002.

[73] A. A. Bashirova, T. B. H. Geijtenbeek, G. C. F. van Duijnhoven et al., "A dendritic cell-specific intercellular adhesion molecule 3-grabbing nonintegrin (DC-SIGN)-related protein is highly expressed on human liver sinusoidal endothelial cells and promotes HIV-1 infection," *Journal of Experimental Medicine*, vol. 193, no. 6, pp. 671–678, 2001.

[74] A. Cambi, K. Gijzen, I. J. M. de Vries et al., "The C-type lectin DC-SIGN (CD209) is an antigen-uptake receptor for Candida albicans on dendritic cells," *European Journal of Immunology*, vol. 33, no. 2, pp. 532–538, 2003.

[75] P. Y. Lozach, H. Lortat-Jacob, A. de Lacroix de Lavalette et al., "DC-SIGN and L-SIGN are high affinity binding receptors for hepatitis C virus glycoprotein E2," *Journal of Biological Chemistry*, vol. 278, no. 22, pp. 20358–20366, 2003.

[76] B. Tassaneetrithep, T. H. Burgess, A. Granelli-Piperno et al., "DC-SIGN (CD209) mediates dengue virus infection of human dendritic cells," *Journal of Experimental Medicine*, vol. 197, no. 7, pp. 823–829, 2003.

[77] S. J. van Vliet, L. Steeghs, S. C. M. Bruijns et al., "Variation of Neisseria gonorrhoeae lipooligosaccharide directs dendritic cell-induced T helper responses," *PLoS Pathogens*, vol. 5, no. 10, Article ID e1000625, 2009.

[78] M. Emara, P. J. Royer, J. Mahdavi, F. Shakib, and A. M. Ghaemmaghami, "Retagging identifies dendritic cell-specific intercellular adhesion molecule-3 (ICAM3)-grabbing non-integrin (DC-SIGN) protein as a novel receptor for a major allergen from house dust mite," *Journal of Biological Chemistry*, vol. 287, no. 8, pp. 5756–5763, 2012.

[79] T. B. H. Geijtenbeek, D. J. E. B. Krooshoop, D. A. Bleijs et al., "DC-SIGN-1CAM-2 interaction mediates dendritic cell trafficking," *Nature Immunology*, vol. 1, no. 4, pp. 353–357, 2000.

[80] A. Engering, T. B. H. Geijtenbeek, S. J. van Vliet et al., "The dendritic cell-specific adhesion receptor DC-SIGN internalizes antigen for presentation to T cells," *Journal of Immunology*, vol. 168, no. 5, pp. 2118–2126, 2002.

[81] K. W. Schjetne, K. M. Thompson, T. Aarvak, B. Fleckenstein, L. M. Sollid, and B. Bogen, "A mouse Cκ-specific T cell clone indicates that DC-SIGN is an efficient target for antibody-mediated delivery of T cell epitopes for MHC class II presentation," *International Immunology*, vol. 14, no. 12, pp. 1423–1430, 2002.

[82] P. J. Tacken, I. J. M. de Vries, K. Gijzen et al., "Effective induction of naive and recall T-cell responses by targeting antigen to human dendritic cells via a humanized anti-DC-SIGN antibody," *Blood*, vol. 106, no. 4, pp. 1278–1285, 2005.

[83] A. Kretz-Rommel, F. Qin, N. Dakappagari et al., "In vivo targeting of antigens to human dendritic cells through DC-SIGN elicits stimulatory immune responses and inhibits tumor growth in grafted mouse models," *Journal of Immunotherapy*, vol. 30, no. 7, pp. 715–726, 2007.

[84] P. J. Tacken, W. Ginter, L. Berod et al., "Targeting DC-SIGN via its neck region leads to prolonged antigen residence in early endosomes, delayed lysosomal degradation, and cross-presentation," *Blood*, vol. 118, no. 15, pp. 4111–4119, 2011.

[85] Y. Akiyama, K. Maruyama, N. Nara et al., "Antitumor effects induced by dendritic cell-based immunotherapy against established pancreatic cancer in hamsters," *Cancer Letters*, vol. 184, no. 1, pp. 37–47, 2002.

[86] R. K. Gieseler, G. Marquitan, M. J. Hahn et al., "DC-SIGN-specific liposomal targeting and selective intracellular compound delivery to human myeloid dendritic cells: implications for HIV disease," *Scandinavian Journal of Immunology*, vol. 59, no. 5, pp. 415–424, 2004.

[87] L. J. Cruz, P. J. Tacken, R. Fokkink et al., "Targeted PLGA nano- but not microparticles specifically deliver antigen to human dendritic cells via DC-SIGN in vitro," *Journal of Controlled Release*, vol. 144, no. 2, pp. 118–126, 2010.

[88] O. Srinivas, P. Larrieu, E. Duverger et al., "Synthesis of glycocluster—tumor antigenic peptide conjugates for dendritic cell targeting," *Bioconjugate Chemistry*, vol. 18, no. 5, pp. 1547–1554, 2007.

[89] C. A. Aarnoudse, M. Bax, M. Sánchez-Hernández, J. J. García-Vallejo, and Y. van Kooyk, "Glycan modification of the tumor antigen gp100 targets DC-SIGN to enhance dendritic cell induced antigen presentation to T cells," *International Journal of Cancer*, vol. 122, no. 4, pp. 839–846, 2008.

[90] J. Wang, Y. Zhang, J. Wei et al., "Lewis X oligosaccharides targeting to DC-SIGN enhanced antigen-specific immune response," *Immunology*, vol. 121, no. 2, pp. 174–182, 2007.

[91] S. K. Singh, J. Stephani, M. Schaefer et al., "Targeting glycan modified OVA to murine DC-SIGN transgenic dendritic cells enhances MHC class I and II presentation," *Molecular Immunology*, vol. 47, no. 2-3, pp. 164–174, 2009.

[92] H. Chen, B. Yuan, Z. Zheng, Z. Liu, and S. Wang, "Lewis X oligosaccharides-heparanase complex targeting to DCs enhance antitumor response in mice," *Cellular Immunology*, vol. 269, no. 2, pp. 144–148, 2011.

[93] W. W. J. Unger, A. J. van Beelen, S. C. Bruijns et al., "Glycan-modified liposomes boost CD4+ and CD8+ T-cell responses by targeting DC-SIGN on dendritic cells," *Journal of Controlled Release*, vol. 160, no. 1, pp. 88–95, 2012.

[94] J. J. Garcia-Vallejo, M. Ambrosini, A. Overbeek et al., "Multivalent glycopeptide dendrimers for the targeted delivery of antigens to dendritic cells," *Molecular Immunology*, vol. 53, pp. 387–397, 2012.

[95] L. Yang, H. Yang, K. Rideout et al., "Engineered lentivector targeting of dendritic cells for in vivo immunization," *Nature Biotechnology*, vol. 26, no. 3, pp. 326–334, 2008.

[96] A. Tai, S. Froelich, K. I. Joo, and P. Wang, "Production of lentiviral vectors with enhanced efficiency to target dendritic cells by attenuating mannosidase activity of mammalian cells," *Journal of Biological Engineering*, vol. 5, article 1, 2011.

[97] L. J. Cruz, P. J. Tacken, J. M. Pots, R. Torensma, S. I. Buschow, and C. G. Figdor, "Comparison of antibodies and carbohydrates to target vaccines to human dendritic cells via DC-SIGN," *Biomaterials*, vol. 33, no. 16, pp. 4229–4239, 2012.

[98] D. A. Mitchell, A. J. Fadden, and K. Drickamer, "A novel mechanism of carbohydrate recognition by the C-type lectins DC-SIGN and DC-SIGNR. Subunit organization and binding to multivalent ligands," *Journal of Biological Chemistry*, vol. 276, no. 31, pp. 28939–28945, 2001.

[99] N. Dakappagari, T. Maruyama, M. Renshaw et al., "Internalizing antibodies to the C-type lectins, L-SIGN and DC-SIGN, inhibit viral glycoprotein binding and deliver antigen to human dendritic cells for the induction of T cell responses," *Journal of Immunology*, vol. 176, no. 1, pp. 426–440, 2006.

[100] C. G. Park, K. Takahara, E. Umemoto et al., "Five mouse homologues of the human dendritic cell C-type lectin, DC-SIGN," *International Immunology*, vol. 13, no. 10, pp. 1283–1290, 2001.

[101] C. Galustian, C. G. Park, W. Chai et al., "High and low affinity carbohydrate ligands revealed for murine SIGN-R1 by carbohydrate array and cell binding approaches, and differing specificities for SIGN-R3 and langerin," *International Immunology*, vol. 16, no. 6, pp. 853–866, 2004.

[102] E. A. Koppel, I. S. Ludwig, B. J. Appelmelk, Y. van Kooyk, and T. B. H. Geijtenbeek, "Carbohydrate specificities of the murine DC-SIGN homologue mSIGNR1," *Immunobiology*, vol. 210, no. 2–4, pp. 195–201, 2005.

[103] Y. S. Kang, J. Y. Kim, S. A. Bruening et al., "The C-type lectin SIGN-R1 mediates uptake of the capsular polysaccharide of Streptococcus pneumoniae in the marginal zone of mouse spleen," *Proceedings of the National Academy of Sciences of the United States of America*, vol. 101, no. 1, pp. 215–220, 2004.

[104] Y. S. Kang, S. Yamazaki, T. Iyoda et al., "SIGN-R1, a novel C-type lectin expressed by marginal zone macrophages in spleen, mediates uptake of the polysaccharide dextran," *International Immunology*, vol. 15, no. 2, pp. 177–186, 2003.

[105] P. R. Taylor, G. D. Brown, J. Herre, D. L. Williams, J. A. Willment, and S. Gordon, "The role of SIGNR1 and the β-glucan receptor (Dectin-1) in the nonopsonic recognition of yeast by specific macrophages," *Journal of Immunology*, vol. 172, no. 2, pp. 1157–1162, 2004.

[106] Y. Zhou, H. Kawasaki, S. C. Hsu et al., "Oral tolerance to food-induced systemic anaphylaxis mediated by the C-type lectin SIGNR1," *Nature Medicine*, vol. 16, no. 10, pp. 1128–1133, 2010.

[107] W. Liu, L. Tang, G. Zhang et al., "Characterization of a novel C-type lectin-like gene, LSECtin: demonstration of carbohydrate binding and expression in sinusoidal endothelial cells of liver and lymph node," *Journal of Biological Chemistry*, vol. 279, no. 18, pp. 18748–18758, 2004.

[108] T. Gramberg, H. Hofmann, P. Möller et al., "LSECtin interacts with filovirus glycoproteins and the spike protein of SARS coronavirus," *Virology*, vol. 340, no. 2, pp. 224–236, 2005.

[109] Y. Li, B. Hao, X. Kuai et al., "C-type lectin LSECtin interacts with DC-SIGNR and is involved in hepatitis C virus binding," *Molecular and Cellular Biochemistry*, vol. 327, no. 1-2, pp. 183–190, 2009.

[110] L. Tang, J. Yang, X. Tang, W. Ying, X. Qian, and F. He, "The DC-SIGN family member LSECtin is a novel ligand of CD44 on activated T cells," *European Journal of Immunology*, vol. 40, no. 4, pp. 1185–1191, 2010.

[111] A. Dominguez-Soto, L. Aragoneses-Fenoll, E. Martin-Gayo et al., "The DC-SIGN-related lectin LSECtin mediates antigen capture and pathogen binding by human myeloid cells," *Blood*, vol. 109, no. 12, pp. 5337–5345, 2007.

[112] Á. Domínguez-Soto, L. Aragoneses-Fenoll, F. Gómez-Aguado et al., "The pathogen receptor liver and lymph node sinusoidal endotelial cell C-type lectin is expressed in human Kupffer cells and regulated by PU.1," *Hepatology*, vol. 49, no. 1, pp. 287–296, 2009.

[113] I. Caminschi, A. J. Corbett, C. Zahra et al., "Functional comparison of mouse CIRE/mouse DC-SIGN and human DC-SIGN," *International Immunology*, vol. 18, no. 5, pp. 741–753, 2006.

[114] I. Caminschi, K. M. Lucas, M. A. O'Keeffe et al., "Molecular cloning of a C-type lectin superfamily protein differentially expressed by CD8α-splenic dendritic cells," *Molecular Immunology*, vol. 38, no. 5, pp. 365–373, 2001.

[115] T. Gramberg, I. Caminschi, A. Wegele, H. Hofmann, and S. Pöhlmann, "Evidence that multiple defects in murine DC-SIGN inhibit a functional interaction with pathogens," *Virology*, vol. 345, no. 2, pp. 482–491, 2006.

[116] B. Carrillo-Conde, E. H. Song, A. Chavez-Santoscoy et al., "Mannose-functionalized "pathogen-like" polyanhydride nanoparticles target C-type lectin receptors on dendritic cells," *Molecular Pharmaceutics*, vol. 8, no. 5, pp. 1877–1886, 2011.

[117] A. V. Chavez-Santoscoy, R. Roychoudhury, N. L. B. Pohl, M. J. Wannemuehler, B. Narasimhan, and A. E. Ramer-Tait, "Tailoring the immune response by targeting C-type lectin receptors on alveolar macrophages using "pathogen-like" amphiphilic polyanhydride nanoparticles," *Biomaterials*, vol. 33, no. 18, pp. 4762–4772, 2012.

[118] M. P. Torres, J. H. Wilson-Welder, S. K. Lopac et al., "Polyanhydride microparticles enhance dendritic cell antigen presentation and activation," *Acta Biomaterialia*, vol. 7, no. 7, pp. 2857–2864, 2011.

[119] K. Takahara, Y. Yashima, Y. Omatsu et al., "Functional comparison of the mouse DC-SIGN, SIGNR1, SIGNR3 and Langerin, C-type lectins," *International Immunology*, vol. 16, no. 6, pp. 819–829, 2004.

[120] L. F. Poulin, S. Henri, B. de Bovis, E. Devilard, A. Kissenpfennig, and B. Malissen, "The dermis contains langerin+ dendritic cells that develop and function independently of epidermal Langerhans cells," *Journal of Experimental Medicine*, vol. 204, no. 13, pp. 3119–3131, 2007.

[121] V. Flacher, F. Sparber, C. H. Tripp, N. Romani, and P. Stoitzner, "Targeting of epidermal Langerhans cells with antigenic proteins: attempts to harness their properties for immunotherapy," *Cancer Immunology, Immunotherapy*, vol. 58, no. 7, pp. 1137–1147, 2009.

[122] V. Flacher, C. H. Tripp, P. Stoitzner et al., "Epidermal langerhans cells rapidly capture and present antigens from C-type lectin-targeting antibodies deposited in the dermis," *Journal of Investigative Dermatology*, vol. 130, no. 3, pp. 755–762, 2010.

[123] J. Idoyaga, A. Lubkin, C. Fiorese et al., "Comparable T helper 1 (Th1) and CD8 T-cell immunity by targeting HIV gag p24 to CD8 dendritic cells within antibodies to Langerin, DEC205, and Clec9A," *Proceedings of the National Academy of Sciences of the United States of America*, vol. 108, no. 6, pp. 2384–2389, 2011.

[124] V. Flacher, C. H. Tripp, B. Haid et al., "Skin langerin+ dendritic cells transport intradermally injected anti-DEC-205 antibodies but are not essential for subsequent cytotoxic CD8+ T cell responses," *Journal of Immunology*, vol. 188, no. 5, pp. 2146–2155, 2012.

[125] A. L. Flamar, S. Zurawski, F. Scholz et al., "Noncovalent assembly of anti-dendritic cell antibodies and antigens for evoking immune responses in vitro and in vivo," *Journal of Immunology*, vol. 189, pp. 2645–2655, 2012.

[126] S. de Koker, B. G. de Geest, S. K. Singh et al., "Polyelectrolyte microcapsules as antigen delivery vehicles to dendritic cells: uptake, processing, and cross-presentation of encapsulated antigens," *Angewandte Chemie*, vol. 48, no. 45, pp. 8485–8489, 2009.

[127] A. Takada, K. Fujioka, M. Tsuiji et al., "Human macrophage C-type lectin specific for galactose and N-acetylgalactosamine promotes filovirus entry," *Journal of Virology*, vol. 78, no. 6, pp. 2943–2947, 2004.

[128] N. Suzuki, K. Yamamoto, S. Toyoshima, T. Osawa, and T. Irimura, "Molecular cloning and expression of cDNA encoding human macrophage C-type lectin: its unique carbohydrate binding specificity for Tn antigen," *Journal of Immunology*, vol. 156, no. 1, pp. 128–135, 1996.

[129] K. Yamamoto, C. Ishida, Y. Shinohara et al., "Interaction of immobilized recombinant mouse C-type macrophage lectin with glycopeptides and oligosaccharides," *Biochemistry*, vol. 33, no. 26, pp. 8159–8166, 1994.

[130] C. Napoletano, A. Rughetti, M. P. Agervig Tarp et al., "Tumor-associated Tn-MUC1 glycoform is internalized through the macrophage galactose-type C-type lectin and delivered to the HLA class I and II compartments in dendritic cells," *Cancer Research*, vol. 67, no. 17, pp. 8358–8367, 2007.

[131] C. Napoletano, I. G. Zizzari, A. Rughetti et al., "Targeting of macrophage galactose-type C-type lectin (MGL) induces DC signaling and activation," *European Journal of Immunology*, vol. 42, no. 4, pp. 936–945, 2012.

[132] T. Freire, X. Zhang, E. Dériaud et al., "Glycosidic Tn-based vaccines targeting dermal dendritic cells favor germinal center B-cell development and potent antibody response in the absence of adjuvant," *Blood*, vol. 116, no. 18, pp. 3526–3536, 2010.

[133] S. V. Kushchayev, T. Sankar, L. L. Eggink et al., "Monocyte galactose/N-acetylgalactosamine-specific C-type lectin receptor stimulant immunotherapy of an experimental glioma. Part 1: stimulatory effects on blood monocytes and monocyte-derived cells of the brain," *Cancer Management and Research*, vol. 4, pp. 309–323, 2012.

[134] K. Ariizumi, G. L. Shen, S. Shikano et al., "Identification of a novel, dendritic cell-associated molecule, dectin-1, by subtractive cDNA cloning," *Journal of Biological Chemistry*, vol. 275, no. 26, pp. 20157–20167, 2000.

[135] G. D. Brown, "Dectin-1: a signalling non-TLR pattern-recognition receptor," *Nature Reviews Immunology*, vol. 6, no. 1, pp. 33–43, 2006.

[136] P. R. Taylor, G. D. Brown, D. M. Reid et al., "The β-glucan receptor, dectin-1, is predominantly expressed on the surface of cells of the monocyte/macrophage and neutrophil lineages," *Journal of Immunology*, vol. 169, no. 7, pp. 3876–3882, 2002.

[137] E. P. McGreal, M. Rosas, G. D. Brown et al., "The carbohydrate-recognition domain of Dectin-2 is a C-type lectin with specificity for high mannose," *Glycobiology*, vol. 16, no. 5, pp. 422–430, 2006.

[138] E. J. Ryan, A. J. Marshall, D. Magaletti et al., "Dendritic cell-associated lectin-1: a novel dendritic cell-associated, C-type lectin-like molecule enhances T cell secretion of IL-4," *Journal of Immunology*, vol. 169, no. 10, pp. 5638–5648, 2002.

[139] G. D. Brown, P. R. Taylor, D. M. Reid et al., "Dectin-1 is a major β-glucan receptor on macrophages," *Journal of Experimental Medicine*, vol. 196, no. 3, pp. 407–412, 2002.

[140] P. R. Taylor, S. V. Tsoni, J. A. Willment et al., "Dectin-1 is required for β-glucan recognition and control of fungal infection," *Nature Immunology*, vol. 8, no. 1, pp. 31–38, 2007.

[141] A. G. Rothfuchs, A. Bafica, C. G. Feng et al., "Dectin-1 interaction with Mycobacterium tuberculosis leads to enhanced IL-12p40 production by splenic dendritic cells," *Journal of Immunology*, vol. 179, no. 6, pp. 3463–3471, 2007.

[142] R. W. Carter, C. Thompson, D. M. Reid, S. Y. C. Wong, and D. F. Tough, "Induction of CD8+ T cell responses through targeting of antigen to Dectin-2," *Cellular Immunology*, vol. 239, no. 2, pp. 87–91, 2006.

[143] R. W. Carter, C. Thompson, D. M. Reid, S. Y. C. Wong, and D. F. Tough, "Preferential induction of CD4+ T cell responses through in vivo targeting of antigen to dendritic cell-associated C-type lectin-1," *Journal of Immunology*, vol. 177, no. 4, pp. 2276–2284, 2006.

[144] H. Huang, G. R. Ostroff, C. K. Lee, C. A. Specht, and S. M. Levitz, "Robust stimulation of humoral and cellular immune responses following vaccination with antigen-loaded β-Glucan particles," *mBio*, vol. 1, no. 3, 2010.

[145] C. Huysamen, J. A. Willment, K. M. Dennehy, and G. D. Brown, "CLEC9A is a novel activation C-type lectin-like receptor expressed on BDCA3+ dendritic cells and a subset of monocytes," *Journal of Biological Chemistry*, vol. 283, no. 24, pp. 16693–16701, 2008.

[146] D. Sancho, D. Mourão-Sá, O. P. Joffre et al., "Tumor therapy in mice via antigen targeting to a novel, DC-restricted C-type lectin," *Journal of Clinical Investigation*, vol. 118, no. 6, pp. 2098–2110, 2008.

[147] O. P. Joffre, D. Sancho, S. Zelenay, A. M. Keller, and C. Reis E Sousa, "Efficient and versatile manipulation of the peripheral CD4+ T-cell compartment by antigen targeting to DNGR-1/CLEC9A," *European Journal of Immunology*, vol. 40, no. 5, pp. 1255–1265, 2010.

[148] S. Iborra, H. M. Izquierdo, M. Martínez-López, N. Blanco-Menéndez, C. Reis E Sousa, and D. Sancho, "The DC receptor

DNGR-1 mediates cross-priming of CTLs during vaccinia virus infection in mice," *Journal of Clinical Investigation*, vol. 122, no. 5, pp. 1628–1643, 2012.

[149] S. Zelenay, A. M. Keller, P. G. Whitney et al., "The dendritic cell receptor DNGR-1 controls endocytic handling of necrotic cell antigens to favor cross-priming of CTLs in virus-infected mice," *Journal of Clinical Investigation*, vol. 122, no. 5, pp. 1615–1627, 2012.

[150] I. Caminschi, A. I. Proietto, F. Ahmet et al., "The dendritic cell subtype-restricted C-type lectin Clec9A is a target for vaccine enhancement," *Blood*, vol. 112, no. 8, pp. 3264–3273, 2008.

[151] M. H. Lahoud, F. Ahmet, S. Kitsoulis et al., "Targeting antigen to mouse dendritic cells via Clec9A induces potent CD4 T cell responses biased toward a follicular helper phenotype," *Journal of Immunology*, vol. 187, no. 2, pp. 842–850, 2011.

[152] A. S. J. Marshall, J. A. Willmen, H. H. Lin, D. L. Williams, S. Gordon, and G. D. Brown, "Identification and characterization of a novel human myeloid inhibitory C-type lectin-like receptor (MICL) that is predominantly expressed on granulocytes and monocytes," *Journal of Biological Chemistry*, vol. 279, no. 15, pp. 14792–14802, 2004.

[153] A. B. H. Bakker, S. van den Oudenrijn, A. Q. Bakker et al., "C-type lectin-like molecule-1: a novel myeloid cell surface marker associated with acute myeloid leukemia," *Cancer Research*, vol. 64, no. 22, pp. 8443–8450, 2004.

[154] C. H. Chen, H. Floyd, N. E. Olson et al., "Dendritic-cell-associated C-type lectin 2 (DCAL-2) alters dendritic-cell maturation and cytokine production," *Blood*, vol. 107, no. 4, pp. 1459–1467, 2006.

[155] Y. Han, M. Zhang, N. Li et al., "KLRL1, a novel killer cell lectin-like receptor, inhibits natural killer cell cytotoxicity," *Blood*, vol. 104, no. 9, pp. 2858–2866, 2004.

[156] E. Pyz, C. Huysamen, A. S. J. Marshall, S. Gordon, P. R. Taylor, and G. D. Brown, "Characterisation of murine MICL (CLEC12A) and evidence for an endogenous ligand," *European Journal of Immunology*, vol. 38, no. 4, pp. 1157–1163, 2008.

[157] M. Colonna, J. Samaridis, and L. Angman, "Molecular characterization of two novel C-type lectin-like receptors, one of which is selectively expressed in human dendritic cells," *European Journal of Immunology*, vol. 30, no. 2, pp. 697–704, 2000.

[158] K. Suzuki-Inoue, Y. Kato, O. Inoue et al., "Involvement of the snake toxin receptor CLEC-2, in podoplanin-mediated platelet activation, by cancer cells," *Journal of Biological Chemistry*, vol. 282, no. 36, pp. 25993–26001, 2007.

[159] C. Chaipan, E. J. Soilleux, P. Simpson et al., "DC-SIGN and CLEC-2 mediate human immunodeficiency virus type 1 capture by platelets," *Journal of Virology*, vol. 80, no. 18, pp. 8951–8960, 2006.

[160] K. Suzuki-Inoue, G. L. J. Fuller, Á. García et al., "Anovel Syk-dependent mechanism of platelet activation by the C-type lectin receptor CLEC-2," *Blood*, vol. 107, no. 2, pp. 542–549, 2006.

[161] S. C. Hoffmann, C. Schellack, S. Textor et al., "Identification of CLEC12B, an inhibitory receptor on myeloid cells," *Journal of Biological Chemistry*, vol. 282, no. 31, pp. 22370–22375, 2007.

[162] Y. Sobanov, A. Bernreiter, S. Derdak et al., "A novel cluster of lectin-like receptor genes expressed in monocytic, dendritic and endothelial cells maps close to the NK receptor genes in the human NK gene complex," *European Journal of Immunology*, vol. 31, pp. 3493–3503, 2001.

[163] T. Sawamura, N. Kume, T. Aoyama et al., "An endothelial receptor for oxidized low-density lipoprotein," *Nature*, vol. 386, no. 6620, pp. 73–77, 1997.

[164] S. Dunn, R. S. Vohra, J. E. Murphy, S. Homer-Vanniasinkam, J. H. Walker, and S. Ponnambalam, "The lectin-like oxidized low-density-lipoprotein receptor: a pro-inflammatory factor in vascular disease," *Biochemical Journal*, vol. 409, no. 2, pp. 349–355, 2008.

[165] J. L. Mehta, J. Chen, P. L. Hermonat, F. Romeo, and G. Novelli, "Lectin-like, oxidized low-density lipoprotein receptor-1 (LOX-1): a critical player in the development of atherosclerosis and related disorders," *Cardiovascular Research*, vol. 69, no. 1, pp. 36–45, 2006.

[166] Y. Delneste, G. Magistrelli, J. F. Gauchat et al., "Involvement of LOX-1 in dendritic cell-mediated antigen cross-presentation," *Immunity*, vol. 17, no. 3, pp. 353–362, 2002.

[167] F. Meyer-Wentrup, D. Benitez-Ribas, P. J. Tacken et al., "Targeting DCIR on human plasmacytoid dendritic cells results in antigen presentation and inhibits IFN-alpha production," *Blood*, vol. 111, no. 8, pp. 4245–4253, 2008.

[168] F. Meyer-Wentrup, A. Cambi, B. J. Joosten et al., "DCIR is endocytosed into human dendritic cells and inhibits TLR8-mediated cytokine production," *Journal of Leukocyte Biology*, vol. 85, no. 3, pp. 518–525, 2009.

[169] E. Klechevsky, A. L. Flamar, Y. Cao et al., "Cross-priming CD8+ T cells by targeting antigens to human dendritic cells through DCIR," *Blood*, vol. 116, no. 10, pp. 1685–1697, 2010.

[170] K. Ariizumi, G. L. Shen, S. Shikano et al., "Cloning of a second dendritic cell-associated C-type lectin (dectin-2) and its alternatively spliced isoforms," *Journal of Biological Chemistry*, vol. 275, no. 16, pp. 11957–11963, 2000.

[171] L. Lopes, M. Dewannieux, U. Gileadi et al., "Immunization with a lentivector that targets tumor antigen expression to dendritic cells induces potent CD8+ and CD4+ T-cell responses," *Journal of Virology*, vol. 82, no. 1, pp. 86–95, 2008.

[172] A. Dzionek, Y. Sohma, J. Nagafune et al., "BDCA-2, a novel plasmacytoid dendritic cell-specific type II C-type lectin, mediates antigen capture and is a potent inhibitor of interferon α/β induction," *Journal of Experimental Medicine*, vol. 194, no. 12, pp. 1823–1834, 2001.

[173] W. Jian, W. J. Swiggard, C. Heufler et al., "The receptor DEC-205 expressed by dendritic cells and thymic epithelial cells is involved in antigen processing," *Nature*, vol. 375, no. 6527, pp. 151–155, 1995.

[174] M. Butler, A. S. Morel, W. J. Jordan et al., "Altered expression and endocytic function of CD205 in human dendritic cells, and detection of a CD205-DCL-1 fusion protein upon dendritic cell maturation," *Immunology*, vol. 120, no. 3, pp. 362–371, 2007.

[175] K. Mahnke, M. Guo, S. Lee et al., "The dendritic cell receptor for endocytosis, DEC-205, can recycle and enhance antigen presentation via major histocompatibility complex class II-positive lysosomal compartments," *Journal of Cell Biology*, vol. 151, no. 3, pp. 673–683, 2000.

[176] L. Bonifaz, D. Bonnyay, K. Mahnke, M. Rivera, M. C. Nussenzweig, and R. M. Steinman, "Efficient targeting of protein antigen to the dendritic cell receptor DEC-205 in the steady state leads to antigen presentation on major histocompatibility complex class I products and peripheral CD8+ T cell tolerance," *Journal of Experimental Medicine*, vol. 196, no. 12, pp. 1627–1638, 2002.

[177] K. Mahnke, Y. Qian, S. Fondel, J. Brueck, C. Becker, and A. H. Enk, "Targeting of antigens to activated dendritic cells in vivo cures metastatic melanoma in mice," *Cancer Research*, vol. 65, no. 15, pp. 7007–7012, 2005.

[178] A. Charalambous, M. Oks, G. Nchinda, S. Yamazaki, and R. M. Steinman, "Dendritic cell targeting of survivin protein in a xenogeneic form elicits strong CD4+ T cell immunity to mouse survivin," *Journal of Immunology*, vol. 177, no. 12, pp. 8410–8421, 2006.

[179] B. Wang, N. Zaidi, L. Z. He et al., "Targeting of the non-mutated tumor antigen HER2/neu to mature dendritic cells induces an integrated immune response that protects against breast cancer in mice," *Breast Cancer Research*, vol. 14, no. 2, article R39, 2012.

[180] L. Bozzacco, C. Trumpfheller, F. P. Siegal et al., "DEC-205 receptor on dendritic cells mediates presentation of HIV gag protein to CD8+ T cells in a spectrum of human MHC I haplotypes," *Proceedings of the National Academy of Sciences of the United States of America*, vol. 104, no. 4, pp. 1289–1294, 2007.

[181] G. Nchinda, J. Kuroiwa, M. Oks et al., "The efficacy of DNA vaccination is enhanced in mice by targeting the encoded protein to dendritic cells," *Journal of Clinical Investigation*, vol. 118, no. 4, pp. 1427–1436, 2008.

[182] C. Cheong, J. H. Choi, L. Vitale et al., "Improved cellular and humoral immune responses in vivo following targeting of HIV Gag to dendritic cells within human anti-human DEC205 monoclonal antibody," *Blood*, vol. 116, no. 19, pp. 3828–3838, 2010.

[183] M. Tenbusch, G. Nchinda, M. Storcksdieck genannt Bonsmann, V. Temchura, and K. Überla, "Targeting the antigen encoded by adenoviral vectors to the DEC205 receptor modulates the cellular and humoral immune response," *International Immunology*, vol. 25, no. 4, pp. 247–258, 2013.

[184] C. Grossmann, M. Tenbusch, G. Nchinda et al., "Enhancement of the priming efficacy of DNA vaccines encoding dendritic cell-targeted antigens by synergistic toll-like receptor ligands," *BMC Immunology*, vol. 10, article 43, 2009.

[185] J. Maamary, F. Array, Q. Gao et al., "Newcastle disease virus expressing a dendritic cell-targeted HIV Gag protein induces a potent Gag-specific immune response in mice," *Journal of Virology*, vol. 85, no. 5, pp. 2235–2246, 2011.

[186] C. Demangel, J. Zhou, A. B. H. Choo, G. Shoebridge, G. M. Halliday, and W. J. Britton, "Single chain antibody fragments for the selective targeting of antigens to dendritic cells," *Molecular Immunology*, vol. 42, no. 8, pp. 979–985, 2005.

[187] J. N. H. Stern, D. B. Keskin, Z. Kato et al., "Promoting tolerance to proteolipid protein-induced experimental autoimmune encephalomyelitis through targeting dendritic cells," *Proceedings of the National Academy of Sciences of the United States of America*, vol. 107, no. 40, pp. 17280–17285, 2010.

[188] P. Brož, S. M. Benito, C. Saw et al., "Cell targeting by a generic receptor-targeted polymer nanocontainer platform," *Journal of Controlled Release*, vol. 102, no. 2, pp. 475–488, 2005.

[189] P. Bansal, P. Mukherjee, S. K. Basu, A. George, V. Bal, and S. Rath, "MHC class I-restricted presentation of maleylated protein binding to scavenger receptors," *Journal of Immunology*, vol. 162, no. 8, pp. 4430–4437, 1999.

[190] R. Abraham, N. Singh, A. Mukhopadhyay, S. K. Basu, V. Bal, and S. Rath, "Modulation of immunogenicity and antigenicity of proteins by maleylation to target scavenger receptors on macrophages," *Journal of Immunology*, vol. 154, no. 1, pp. 1–8, 1995.

[191] S. S. Vandaveer, G. F. Erf, and J. M. Durdik, "Avian T helper one/two immune response balance can be shifted toward inflammation by antigen delivery to scavenger receptors," *Poultry Science*, vol. 80, no. 2, pp. 172–181, 2001.

[192] D. Rajagopal, K. A. Ganesh, and P. V. Subba Rao, "Modulation of allergen-specific immune responses to the major shrimp allergen, tropomyosin, by specific targeting to scavenger receptors on macrophages," *International Archives of Allergy and Immunology*, vol. 121, no. 4, pp. 308–316, 2000.

[193] M. S. Willis, L. W. Klassen, D. J. Tuma, M. F. Sorrell, and G. M. Thiele, "Adduction of soluble proteins with malondialdehyde-acetaldehyde (MAA) induces antibody production and enhances T-cell proliferation," *Alcoholism*, vol. 26, no. 1, pp. 94–106, 2002.

[194] N. Matsushita, H. Komine, A. Grolleau-Julius, S. Pilon-Thomas, and J. J. Mulé, "Targeting MARCO can lead to enhanced dendritic cell motility and anti-melanoma activity," *Cancer Immunology, Immunotherapy*, vol. 59, no. 6, pp. 875–884, 2010.

[195] J. Valladeau, V. Duvert-Frances, J. J. Pin et al., "Immature human dendritic cells express asialoglycoprotein receptor isoforms for efficient receptor-mediated endocytosis," *Journal of Immunology*, vol. 167, no. 10, pp. 5767–5774, 2001.

[196] D. Li, G. Romain, A. L. Flamar et al., "Targeting self- and foreign antigens to dendritic cells via DC-ASGPR generates IL-10-producing suppressive CD4+ T cells," *Journal of Experimental Medicine*, vol. 209, no. 1, pp. 109–121, 2012.

[197] H. H. Lin, M. Stacey, J. Stein-Streilein, and S. Gordon, "F4/80: the macrophage-specific adhesion-GPCR and its role in immunoregulation," *Advances in Experimental Medicine and Biology*, vol. 706, pp. 149–156, 2010.

[198] A. J. Corbett, I. Caminschi, B. S. McKenzie et al., "Antigen delivery via two molecules on the CD8- dendritic cell subset induces humoral immunity in the absence of conventional "danger"," *European Journal of Immunology*, vol. 35, no. 10, pp. 2815–2825, 2005.

[199] D. Eleveld-Trancikova, A. Sanecka, M. A. van Hout-Kuijer et al., "DC-STAMP interacts with ER-resident transcription factor LUMAN which becomes activated during DC maturation," *Molecular Immunology*, vol. 47, no. 11-12, pp. 1963–1973, 2010.

[200] F. C. Hartgers, J. L. Vissers, M. W. Looman et al., "DC-STAMP, a novel multimembrane-spanning molecule preferentially expressed by dendritic cells," *European Journal of Immunology*, vol. 30, pp. 3585–3590, 2000.

[201] C. Dresch, S. L. Edelmann, P. Marconi, and T. Brocker, "Lentiviral-mediated transcriptional targeting of dendritic cells for induction of T cell tolerance in vivo," *Journal of Immunology*, vol. 181, no. 7, pp. 4495–4506, 2008.

[202] R. Dong, D. Moulding, N. Himoudi et al., "Cells with dendritic cell morphology and immunophenotype, binuclear morphology, and immunosuppressive function in dendritic cell cultures," *Cellular Immunology*, vol. 272, no. 1, pp. 1–10, 2011.

[203] V. Moulin, M. E. Morgan, D. Eleveld-Trancikova et al., "Targeting dendritic cells with antigen via dendritic cell-associated promoters," *Cancer Gene Therapy*, vol. 19, no. 5, pp. 303–311, 2012.

[204] F. Nimmerjahn and J. V. Ravetch, "Fcγ receptors: old friends and new family members," *Immunity*, vol. 24, no. 1, pp. 19–28, 2006.

[205] J. M. H. de Jong, D. H. Schuurhuis, A. Ioan-Facsinay et al., "Murine Fc receptors for IgG are redundant in facilitating presentation of immune complex derived antigen to CD8+ T cells in vivo," *Molecular Immunology*, vol. 43, no. 13, pp. 2045–2050, 2006.

[206] K. A. Berlyn, B. Schultes, B. Leveugle, A. A. Noujaim, R. B. Alexander, and D. L. Mann, "Generation of CD4+ and CD8+ T

lymphocyte responses by dendritic cells armed with PSA/anti-PSA (antigen/antibody) complexes," *Clinical Immunology*, vol. 101, no. 3, pp. 276–283, 2001.

[207] I. Mende, P. Hoffmann, A. Wolf et al., "Highly efficient antigen targeting to M-DC8+ dendritic cells via FcγRIII/CD16-specific antibody conjugates," *International Immunology*, vol. 17, no. 5, pp. 539–547, 2005.

[208] M. A. Otten and M. van Egmond, "The Fc receptor for IgA (FcαRI, CD89)," *Immunology Letters*, vol. 92, no. 1-2, pp. 23–31, 2004.

[209] S. M. M. Hellwig, A. B. van Spriel, J. F. P. Schellekens, F. R. Mooi, and J. G. J. van de Winkel, "Immunoglobulin A-mediated protection against Bordetella pertussis infection," *Infection and Immunity*, vol. 69, no. 8, pp. 4846–4850, 2001.

[210] T. Kobayashi, A. Takauchi, A. B. V. Spriel et al., "Targeting of Porphyromonas gingivalis with a bispecific antibody directed to FcαRI (CD89) improves in vitro clearance by gingival crevicular neutrophils," *Vaccine*, vol. 23, no. 5, pp. 585–594, 2004.

[211] M. E. Rodriguez, S. M. M. Hellwig, D. F. Hozbor, J. Leusen, W. L. van der Pol, and J. G. J. van de Winkel, "Fc receptor-mediated immunity against Bordetella pertussis," *Journal of Immunology*, vol. 167, no. 11, pp. 6545–6551, 2001.

[212] M. van Egmond, A. J. H. van Vuuren, H. C. Morion et al., "Human immunoglobulin A receptor (FcαRI, CD89) function in transgenic mice requires both FCR γ chain and CR3 (CD11b/CD18)," *Blood*, vol. 93, no. 12, pp. 4387–4394, 1999.

[213] A. B. van Spriel, I. E. van den Herik-Oudijk, N. M. van Sorge, H. A. Vilé, J. A. G. van Strijp, and J. G. J. van de Winkel, "Effective phagocytosis and killing of Candida albicans via targeting Fcγ/RI (CD64) or FcαRI (CD89) on neutrophils," *Journal of Infectious Diseases*, vol. 179, no. 3, pp. 661–669, 1999.

[214] M. A. Otten, I. Groenveld, J. G. J. van de Winkel, and M. van Egmond, "Inefficient antigen presentation via the IgA Fc receptor (FcαRI) on dendritic cells," *Immunobiology*, vol. 211, no. 6–8, pp. 503–510, 2006.

[215] B. Pasquier, Y. Lepelletier, C. Baude, O. Hermine, and R. C. Monteiro, "Differential expression and function of IgA receptors (CD89 and CD71) during maturation of dendritic cells," *Journal of Leukocyte Biology*, vol. 76, no. 6, pp. 1134–1141, 2004.

[216] S. N. Karagiannis, J. K. Warrack, K. H. Jennings et al., "Endocytosis and recycling of the complex between CD23 and HLA-DR in human B cells," *Immunology*, vol. 103, no. 3, pp. 319–331, 2001.

[217] A. Getahun, F. Hjelm, and B. Heyman, "IgE enhances antibody and T cell responses in vivo via CD23+ B cells," *Journal of Immunology*, vol. 175, no. 3, pp. 1473–1482, 2005.

[218] B. Heyman, L. Tianmin, and S. Gustavsson, "In vivo enhancement of the specific antibody response via the low-affinity receptor for IgE," *European Journal of Immunology*, vol. 23, no. 7, pp. 1739–1742, 1993.

Hindawi Publishing Corporation
Journal of Drug Delivery
Volume 2013, Article ID 165981, 9 pages
http://dx.doi.org/10.1155/2013/165981

Review Article

Lipid-Based Nanoparticles in Cancer Diagnosis and Therapy

Andrew D. Miller[1,2]

[1] *Institute of Pharmaceutical Science, King's College London, Franklin-Wilkins Building, Waterloo Campus, 150 Stamford Street, London SE1 9NH, UK*
[2] *GlobalAcorn Ltd., London, UK*

Correspondence should be addressed to Andrew D. Miller; a.miller07@btinternet.com

Received 7 December 2012; Revised 7 May 2013; Accepted 24 May 2013

Academic Editor: Vasso Apostolopoulos

Today, researchers are constantly developing new nanomaterials, nanodevices, and nanoparticles to meet unmet needs in the delivery of therapeutic agents and imaging agents for cancer therapy and diagnosis, respectively. Of particular interest here are lipid-based nanoparticles (LNPs) that are genuine particles (approximately 100 nm in dimension) assembled from varieties of lipid and other chemical components that act collectively to overcome biological barriers (biobarriers), in order for LNPs to preferentially accumulate in or around disease-target cells for the functional delivery of therapeutic agents for treatment or of imaging agents for diagnosis. The capabilities of these LNPs will clearly vary depending on functional requirements, but the nanoscale allows for an impressive level of diversity in capabilities to enable corresponding LNPs to address an equally diverse range of functional requirements. Accordingly, LNPs should be considered appropriate vehicles to provide an integrated, personalized approach to cancer diagnosis and therapy in future cancer disease management.

1. Introduction

Unmet medical needs in cancer diagnosis and therapy remain substantial in spite of decades of research. On the other hand, there are substantial numbers of potentially potent therapeutic agents available (both biopharmaceutical and small molecule drug related) that are either too large in size, too highly charged, too metabolically unstable, and/or too insoluble to reach cancer target cells without the assistance of delivery "vehicles." Nowadays, this situation is seen to be an opportunity for cancer nanotechnology, a field that seeks to take a multidisciplinary, problem-driven approach to research that cuts across the traditional boundaries of biology, chemistry, engineering, and medicine with the aim of using nanotechnology to bring about major advances in cancer detection, diagnosis, and treatment [1–4]. In particular cancer nanotechnology could leverage an opening up of 1000s of new potential disease targets for therapeutic intervention by enabling the functional delivery of new classes of therapeutic agents to target cells. Following this there is the eventual likelihood that cancer nanotechnology could also open up opportunities for personalised cancer diagnosis and treatment regimes [3], by means of multifunctional nanoparticles for (a) the detection of cancer disease-specific biomarkers, (b) the imaging of tumours and their metastases, (c) the functional delivery of therapeutic agents to target cells, and (d) the real-time monitoring of treatment in progression. If this is the potential, how close are we really?

Where nanoparticles are to be created for the functional delivery of imaging and/or therapeutic agents, many factors have to be taken into consideration. This fact can be illustrated with reference to the fields of gene therapy and RNA interference (RNAi) therapeutics where lipid-based nanoparticles (LNPs) have been devised for functional delivery of therapeutic nucleic acids with some success. When LNPs have been designed successfully and used to mediate the functional delivery of therapeutic nucleic acids *in vivo*, these LNPs conform typically to the ABCD nanoparticle paradigm (Figure 1). According to this general paradigm, functional delivery nanoparticles consist of active pharmaceutical ingredients (APIs) (A-component) surrounded initially by compaction/association agents (B-components—lipids in this case) designed to help sequester, carry, and promote functional delivery of the A-component. Such AB-core nanoparticles may have some utility *in vivo* but more

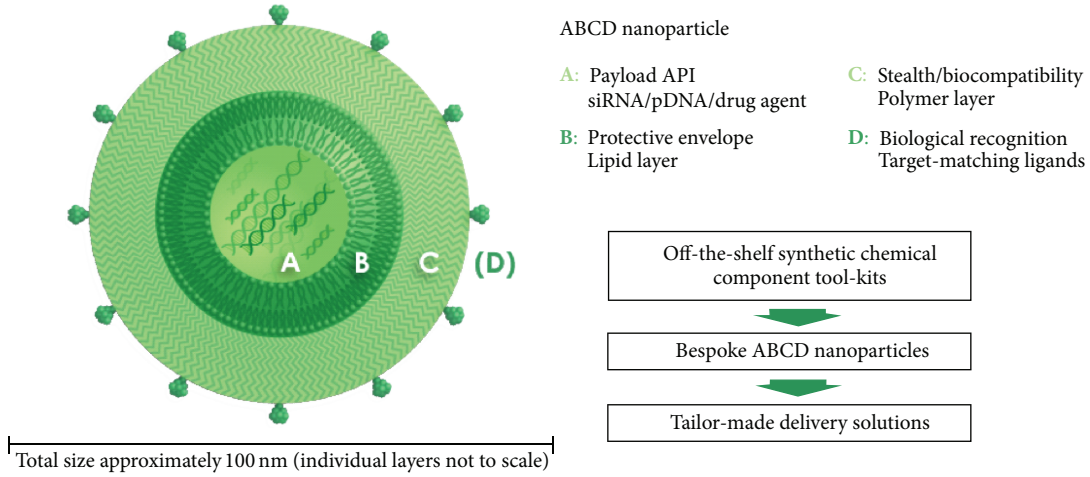

Figure 1: Active pharmaceutical ingredient (API; therapeutic bioactive or intractable drug) condensed within functional concentric layers of chemical components making up nanoparticle structure designed to enable efficient delivery (trafficking) of active therapeutic agent to target cells (used with permission of GlobalAcorn Limited).

typically require coating with a stealth/biocompatibility polymer layer (C-component—most often polyethylene glycol (PEG)) designed to render resulting ABC nanoparticles with colloidal stability in biological fluids and immunoprotection from the reticuloendothelial system (RES) plus other immune system responses. Finally, an optional biological targeting layer (D-components—*bona fide* biological receptor-specific ligands) might be added to confer the resulting ABCD nanoparticle with target cell specificity. A key design principle here is that tailor-made LNPs can self-assemble reliably from tool-kits of purpose designed chemical components [5–15]. Accordingly, the concept of a personalized LNP formulation, assembled in the pharmacy for an individual patient does not seem so far removed from reality.

The ABCD nanoparticle paradigm represents a set of well-found principles of design that are being implemented in the real world with the formation of actual LNPs leading to actual demonstrated functional properties at least in preclinical studies. As such, the design principles laid out in the ABCD nanoparticle paradigm are widely corroborated in the literature [1, 16–24]. Clearly functional nanoparticles need to be constructed from a range of chemical components designed to promote functional delivery of different diagnostic and/or therapeutic agents *in vivo*. In practise this means that nanoparticles need to be equipped to overcome relevant "bio-barriers" in accordance with the pharmacological requirements of API use such as site, time, and duration of action. Importantly too, with clinical goals in mind, nanoparticles have to be considered differently to small and large molecular drugs. For instance, regulations from the FDA state that Absorption, Distribution, Metabolism and Excretion (ADME) studies need to be redesigned in the case of nanoparticles to take into consideration their aggregation and surface chemical characteristics [25].

In terms of cancer diagnosis and therapy, there is one factor that is very much in favour of multifunctional LNP use. LNPs administered in the blood stream (i.v. administration) frequently accumulate in tumours anyway due to the enhanced permeability and retention (EPR) effect, a behaviour that was identified by Matsumura and Maeda as a means to target anticancer therapeutic agents to tumours [26]. LNP accumulation in tumours takes place due to the presence of highly permeable blood vessels in tumours with large fenestrations (>100 nm in size), a result of rapid, defective angiogenesis. In addition tumours are characterised by dysfunctional lymphatic drainage that helps the retention of LNPs in tumour for long enough to enable local nanoparticle disintegration in the vicinity of tumour cells. The phenomenon has been used widely to explain the efficiency of nanoparticle and macromolecular drug accumulation in tumours [27]. Unfortunately, knowledge of LNP biokinetics, metabolism, and clearance is otherwise poor since too few LNP products have been clinically tested. This is a major limitation in the growth of the field of cancer nanotechnology. Nevertheless, cancer nanotechnology is a fast developing field and new data is arriving all the time. In the following sections, the status of LNP use in cancer diagnosis and therapy will be surveyed.

2. Prototype Drug Nanoparticles for Cancer Therapy

The capacity of LNPs to be prepared by reliable, spontaneous self-assembly from purpose designed chemical components (most of which are lipids either natural or synthetic) is due to the unrivalled capacity of structural lipids in aqueous solution to undergo association and controlled assembly into potentially vast three-dimensional macromolecular assemblies. Selected structural lipids self-assemble into liposomes that are typically approximately 100 nm in diameter and consist of a lipid bilayer surrounding an aqueous cavity [28–30]. This cavity can be used to entrap water-soluble drugs in an enclosed volume resulting in a drug-AB nanoparticle [31, 32].

The first drug-AB nanoparticles reported were designed to improve the pharmacokinetics and biodistribution of

the anthracycline drug doxorubicin. Doxorubicin is a potent anticancer agent but is cardiotoxic. In order to minimize cardiotoxicity, doxorubicin was initially encapsulated in anionic liposomes giving anionic doxorubicin-AB nanoparticles that enabled improved drug accumulation in tumours and increased antitumour activity while diminishing side effects of cardiotoxicity [33, 34]. Such drug formulations have been used efficiently in clinic for the treatment of ovarian and breast cancer [35, 36]. Thereafter, Doxil was devised corresponding to a drug-ABC nanoparticle system (PEGylated drug nanoparticle system), comprising PEGylated liposomes with encapsulated doxorubicin. These Doxil drug nanoparticles were designed to improve drug pharmacokinetics and reduce toxicity further by maximizing RES avoidance [37–39], making use of the PEG layer to reduce uptake by RES macrophages of the mononuclear phagocyte system (MPS) [40, 41].

In more recent times, prototype nucleic acid-AB, -ABC, or -ABCD nanoparticles have been tested for functional delivery of therapeutic nucleic acids to target cells in animal models of human disease (to liver for treatment of hepatitis B and C virus infection, to ovarian cancer lesions for cancer therapy) and to target cells in murine lungs [42–47]. Rules for enhancing efficient delivery through receptor-mediated uptake of nucleic acid-ABCD nanoparticles into target cells are also being studied and appreciated [48–50] (Wang, M. et al., J. Drug Del., 2013, paper in submission).

3. Prototype Imaging Nanoparticles for Cancer Imaging

From the point of view of using LNPs for the imaging of cancer, the ability to combine imaging agents appropriately is central. In terms of the ABCD nanoparticle paradigm, the A-component now becomes an imaging agent(s) instead of a therapeutic agent. Potentially important preclinical studies have been carried out recently with imaging LNPs set up for positive contrast magnetic resonance imaging (MRI) [51, 52]. The first described LNPs of this class were formulated by trapping water-soluble, paramagnetic, positive contrast imaging agents (such as $MnCl_2$, gadolinium (III) diethylenetriamine pentaacetic acid (Gd.DTPA), and the manganese (II) equivalent (Mn.DTPA)) in the enclosed volume of a liposome resulting in prototype lipid-based, positive contrast imaging LNPs [53, 54]. Disadvantages were quickly reported such as poor encapsulation efficiency, poor stability, and clear toxicities due to importune contrast agent leakage and poor relaxivity [55]. These problems were obviated when hydrophobic lipidic chains were "grafted" on to contrast agents, thereby enabling these agents to be hosted by a lipid bilayer [56]. Such lipidic contrast agents formulated in association with the bilayer of a liposome exhibit improved ionic relaxivity and therefore could be used for dynamic MRI experiments in mice *in vivo* [57].

A potentially significant variation on this theme involves gadolinium (III) ions complexed with 1,4,7,10-tetraazacyclododecane-1,4,7,10-tetraacetic acid (DOTA) to which hydrophobic lipidic chains are attached. In particular, gadolinium (III) 2-(4,7-bis-carboxymethyl-10-[(*N*,*N*-distearylamidomethyl-*N*′-amidomethyl]-1,4,7,10-tetraazacyclododec-1-yl)-acetic acid (Gd.DOTA.DSA) was prepared and formulated into passively targeted Gd-ABC (no biological targeting layer) and folate-receptor targeted Gd-ABCD nanoparticles in conjunction with a number of other naturally available and synthetic lipid components such as (ω-methoxy-polyethylene glycol 2000)-*N*-carboxy-distearoyl-L-α-phosphatidylethanolamine (DSPE-PEG^{2000}) or its folate variant (DSPE-PEG^{2000}-folate), and fluorescent lipid dioleoyl-L-α-phosphatidylethanolamine-*N*-(lissamine rhodamine B sulphonyl) (DOPE-Rhodamine) (Figure 2). These bimodal imaging LNP systems demonstrated excellent tumour tissue penetration and tumour MRI contrast imaging in both instances [58–60]. Interestingly, the folate-receptor targeted Gd-ABCD nanoparticles exhibited a 4-fold decrease in tumor T_1 value in just 2 h after-injection, a level of tissue relaxation change that was observed only 24 h after administration of passively targeted Gd-ABC nanoparticles [58, 59]. Preparations for clinical trial are now underway beginning with cGMP manufacturing and preclinical toxicology testing. These Gd-ABC/ABCD nanoparticles are potentially excellent nanotechnology tools for the early detection and diagnosis of primary and metastatic cancer lesions. How effective remains to be seen when clinical trials can be performed.

On the other hand, Müller et al. have described solid lipid nanoparticle (SLN) systems that represent genuinely alternative LNP systems [61–63]. Under optimised conditions, SLNs can carry MRI contrast agents [64], and SLNs containing $[Gd\text{-}DTPA(H_2O)]^{2-}$ and $[Gd\text{-}DOTA(H_2O)]^{-}$ have even been prepared for preclinical studies.

Very recently, a multimodal imaging theranostic siRNA-ABC nanoparticle system (PEGylated siRNA-nanoparticle system) was described that had been assembled by the stepwise formulation of PEGylated cationic liposomes (prepared using Gd.DOTA.DSA and DOPE-Rhodamine amongst other lipids), followed by the entrapment of Alexa fluor 488-labelled antisurvivin siRNA. These nanoparticles were found able to mediate functional delivery of siRNA to tumours giving rise to a significant phenotypic (pharmacodynamic) reductions in tumour sizes relative to controls, while at the same time nanoparticle biodistribution (DOPE-Rhodamine fluorescence plus MRI) and siRNA pharmacokinetic behaviour (Alexa fluor 488 fluorescence) could be observed by means of simultaneous real-time imaging [45]. This concept of multimodal imaging theranostic nanoparticles for cancer imaging and therapy is certain to grow in importance in preclinical cancer nanotechnology studies and maybe too in the clinic.

4. Next Generation LNPs for Cancer Imaging and Therapy

Multimodal imaging theranostic nanoparticles may offer substantial benefits for cancer diagnosis and therapy going forward but only in combination with further advances in nanoparticle platform delivery technologies. What might

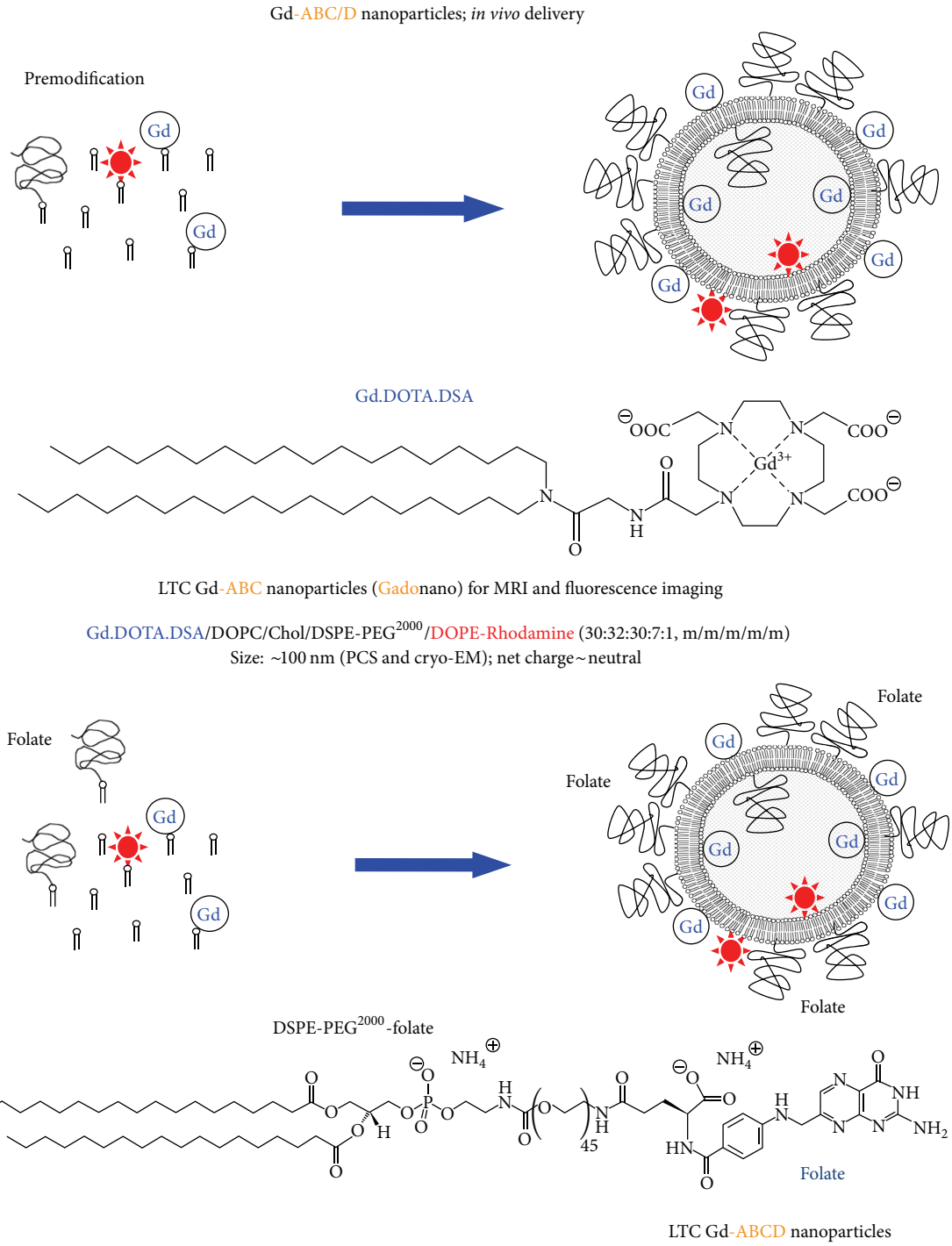

FIGURE 2: Schematic diagrams showing self-assembly of passively targeted Gd-ABC (top) and folate-receptor targeted Gd-ABCD nanoparticles (bottom) for IGROV-1 tumour imaging from combinations of structural lipids, PEG-lipids and imaging lipids [58, 59]. LTC: long-term circulation enabled by virtue of the use of bilayer stabilizing lipids and 7 mol% PEG-lipid in the outer leaflet membranes of nanoparticle structures.

these advances be and how might they be implemented? As far as imaging LNPs are concerned for detection of cancer, providing that all that is required for diagnosis is LNP accumulation within cancer lesions then current imaging nanoparticle technologies may well be sufficient. However, for personalized medicine to really take off, the detection of cancer disease specific biomarkers *in vivo* is really required. In order to achieve this, considerable attention may well have to be paid to the appropriate design and selection of ligands for the biological targeting layer (D-layer).

As far as LNPs for cancer therapy are concerned, the opportunities for delivery are relatively limited at this point in time, primarily due to the facile partition of current LNPs postadministration to liver and to solid tumours *in vivo* and in clinic. In order to enable partition to other organs of interest and even to diseased target cell populations within, there is now an imperative to introduce new design features involving new tool-kits of chemical components. Clearly the design of these new tool-kits of chemical components should be informed by rules for the control of nanoparticle biodistribution and API pharmacokinetics. Such rule sets are emerging but may take several years yet to become fully or even sufficiently understood. In addition, there are other issues. For instance, the central ABCD nanoparticle paradigm has a primary design weakness in that the stealth biocompatibility polymer layer (typically PEG-based) (C-layer) does not prevent nanoparticle entry into cells but may substantially inhibit functional intracellular delivery of the therapeutic agent, unless sufficiently removed by the time of target cell-entry or else during the process of cell-entry. Hence, overcoming the C-layer paradox should be a primary focus for ABCD nanoparticle development over the next few years. In this respect, there has been a growing interest in the concept of nanoparticles that possess the property of triggerability. Such nanoparticles are designed for high levels of stability in biological fluid from points of administration to target cells whereupon they become triggered for the controlled release of therapeutic agent payload(s) by changes in local endogenous conditions (such as in pH, $t_{1/2}$, enzyme, redox state, and temperature status), [42–46, 65] or through application of an external/exogenous stimulus (Wright M. et al., 2013, papers in preparation and submission). While much of previous work on this topic has revolved around change(s) in local endogenous conditions [42–46, 65], the development of appropriate exogenous stimuli looks to be a real growth area for the future. In principle, all ABC/ABCD nanoparticles could be triggered to exhibit physical property change(s) through interaction with light, ultrasound, radiofrequency, and thermal radiation from defined sources. So how might this be harnessed?

Today, the journey to triggered, multimodal imaging theranostic drug nanoparticles for cancer therapy appears well underway. A few years ago, a thermally triggered drug-ABC nanoparticle system (thermally triggered PEGylated drug nanoparticle system, now known as ThermoDox, Celsion) was described based upon Doxil. ThermoDox nanoparticles were formulated using lipid compositions that included lyso-phospholipids in order to encapsulate doxorubicin within thermosensitive lipid bilayer membranes [66, 67]. At induced temperatures above 37°C, these membranes were observed to become porous allowing for substantial controlled local drug release. Needham et al. were first to demonstrate the use of such thermally triggered drug-ABC nanoparticles for the controlled local release of drug into target tissues *in vivo* [68], thus allowing for the treatment of tumours more efficiently than was achieved following administration of the thermally insensitive, Doxil parent system [69]. ThermoDox is currently the subject of phase III HEAT studies and phase II ABLATE studies. In the latter studies, ThermoDox was administered intravenously in combination with radio frequency ablation (RFA) of tumour tissue. In this case, the RFA acts as an exogenous source of local tissue hyperthermia (39.5–42°C) that simultaneously acts as a thermal trigger for controlled release of ThermoDox encapsulated doxorubicin. The company's pipeline going forward focuses on the use of Thermodox nanoparticles under thermal triggered release conditions for the treatment of breast, colorectal, and primary liver cancer lesions [70, 71]. This is the first time that thermally triggered drug-ABC nanoparticles have been devised and used in clinical trials.

A further evolution of this concept has now been more recently reported with the simultaneous entrapment of both doxorubicin and an MRI positive contrast agent, $Gd(HPDO_3A)(H_2O)$, into thermally triggered drug-ABC nanoparticles [72]. High frequency ultrasound (HIFU) was used as an alternative thermal trigger for the controlled release of encapsulated drug at 42°C. The simultaneous release of MRI contrast agent enabled the observation of release in real time and led to an estimation of doxorubicin release kinetics. Researchers involved in ThermoDox have similarly reported on the development of a thermally triggered drug-ABC nanoparticle system with doxorubicin co-encapsulated with the MRI contrast agent Prohance [73]. Using HIFU as a thermal trigger once more, they were able to promote controlled release of drug in rabbits with Vx2 tumours and monitor drug release in real time by MRI [74]. The same researchers also developed an algorithm to simulate the thermal trigger effects of HIFU [75]. Simulation data were in agreement with the HIFU-induced mean tissue temperature increasing from 37°C to between 40.4°C and 41.3°C, leading to quite heterogeneous kinetic drug release behaviour [75]. On the other hand, we have striven to draw inspiration from the Gd-ABC and Gd-ABCD imaging nanoparticle systems described above [58–60, 76, 77] and ThermoDox data, in order to derive alternative thermally triggered theranostic drug-ABC nanoparticles. These could also be described as thermal trig-anostic drug-ABC nanoparticles shortened to the acronym thermal TNPs (Figure 3).

By description, these nanoparticles are enabled for thermally triggered release of encapsulated drug in tumours by means of ultrasound, together with real-time, diagnostic imaging of nanoparticle biodistribution with drug pharmacokinetics. Critical to this proposition is the use of Gd.DOTA.DSA once again. Going forward, MRI agent use could be supplemented with other substantive clinical imaging agents leading to new families of triggered multimodal imaging theranostic drug-ABC nanoparticles. An alternative description for such nanoparticles might be trig-anostic^n drug-ABC nanoparticles where n is number of clinical imaging modes employed, a description that could then be shortened to the acronym ^{n}TNPs.

Following this, the ultimate would be the realization of targeted trig-anostic^n therapeutically multifunctional drug-ABCD nanoparticles. These might be described alternatively as targeted trig-anostic^n drug^m-ABCD nanoparticles where m is the number of active therapeutic agents encapsulated/entrapped, a description that reduces to the simple

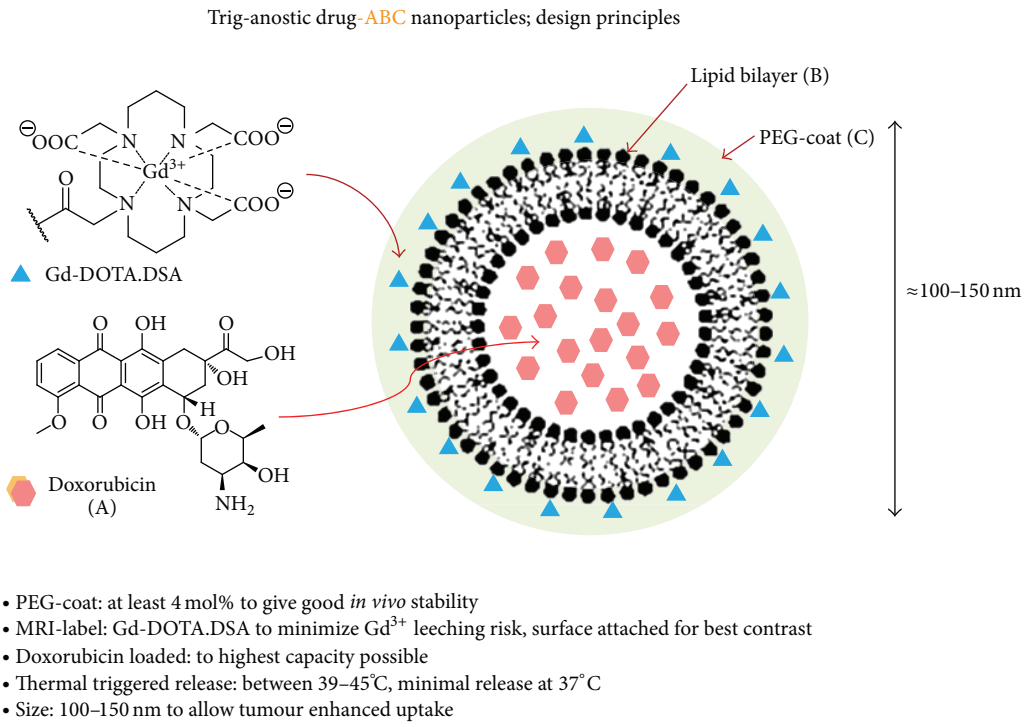

Figure 3: Schematic of thermal trig-anostic drug-ABC nanoparticles (thermal TNPs) enabled for thermally triggered release of encapsulated drug in tumours by means of ultrasound, together with real-time, diagnostic imaging of nanoparticle biodistribution by MRI with drug pharmacokinetics.

acronym of targeted $^{n}T_{m}$NPs. Indeed some nanoshell structures have recently been reported predoped with MRI probes (by introduction of a 10 nm iron oxide layer over the silica core) and/or NIR probes (indocyanine green dye), then set up (with streptavidin) for surface conjugation of anticancer antibodies (biotin labelled) plus the surface postcoupling (disulphide bond formation) of a PEG biocompatibility layer. The result could be described directly as a targeted trig-anostic^{2} drug^{2}-ABCD nanoparticle system (i.e., targeted $^{2}T_{2}$NP system) created with the capability for real time MRI and NIR contrast imaging in combination with the capacity for anti-HER-2 chemotherapy and photothermal ablation therapy (post illumination with 808 nm wavelength NIR laser) both *in vitro* and *in vivo* [78, 79]. The LNP equivalent is now awaited.

5. Conclusions and Future Perspective

Nanotechnology is revolutionising research and development in healthcare. Currently, the most advanced clinical grade nanotechnologies in cancer are LNPs. Unfortunately there remains scepticism from the big pharma industry and from clinicians themselves regarding the efficacy and safety of such nanoparticle technologies. Such scepticism will only be solved with the advent of reliable cGMP-grade manufacturing processes and reliable preclinical ADME/toxicology data, followed by a range of successful first-in-man studies. While these data are being acquired, nanoparticle technologies continue to be innovated in the laboratory. The ultimate push will be for targeted trig-anostic^{n} drug^{m}-ABCD nanoparticles (targeted $^{n}T_{m}$NPs) that are enabled for targeted delivery then triggered release of m active therapeutic agents (or drug entities), all monitored by simultaneous, real-time diagnostic imaging using n different imaging agent probes integrated into the nanoparticle. Of the latter, both NIR and ^{19}F-NMR spectroscopy probes [80] could have real clinical potential alongside MRI. Such multiplicity of functions offers the very real opportunity for highly personalized drug nanoparticles assembly from selected tool-kits of chemical components, highly refined for specific, personalized delivery applications. As this vision begins to take shape, so we will be looking on a very different world of innovative, interactive healthcare products with vastly more potential to treat and even to cure cancer than has ever been seen before.

Inevitably, words of balance and caution need to be expressed as well. This review has focused on LNPs and particularly on those that conform to the ABCD nanoparticle structural paradigm. There is plenty enough good reason for this focus given prospects for LNPs that conform to this paradigm *in vivo*, in pre-clinical studies and even in clinic. However, nanoparticles now come in many shapes and sizes ranging from polymer-based nanoparticles (PNPs) to hard, inorganic nanoparticle structures, such as the highly novel and advanced targeted $^{2}T_{2}$NP system mentioned above. However, in general, although many such systems are showing promise *in vivo*, few PNPs or inorganic nanoparticle structures have advanced significantly towards clinical applications. My own view is that many of these technologies may induce significant toxicologies in humans, not seen with LNP systems; therefore, substantial preclinical evaluation would

be essential and clinical trials would need to be performed with extreme caution in these cases. Accordingly, my expectation is that LNPs should be the first nanoparticle systems to make a substantial impact on cancer nanotechnology going forward and on the management of cancers in general. Therefore, Doxil nanoparticles should be seen as just the first of a wave of exciting new LNP-mediated drug delivery products that could have a truly transformational impact on anticancer therapeutics and diagnostics in the years to come.

Conflict of Interests

Professor Andrew D. Miller is chief executive and chief science officer of GlobalAcorn Ltd. and is also a shareholder in this company.

References

[1] M. Ferrari, "Cancer nanotechnology: opportunities and challenges," *Nature Reviews Cancer*, vol. 5, no. 3, pp. 161–171, 2005.

[2] P. R. Srinivas, P. Barker, and S. Srivastava, "Nanotechnology in early detection of cancer," *Laboratory Investigation*, vol. 82, no. 5, pp. 657–662, 2002.

[3] S. Nie, Y. Xing, G. J. Kim, and J. W. Simons, "Nanotechnology applications in cancer," *Annual Review of Biomedical Engineering*, vol. 9, pp. 257–288, 2007.

[4] M. D. Wang, D. M. Shin, J. W. Simons, and S. Nie, "Nanotechnology for targeted cancer therapy," *Expert Review of Anticancer Therapy*, vol. 7, no. 6, pp. 833–837, 2007.

[5] A. D. Miller, "Towards safe nanoparticle technologies for nucleic acid therapeutics," *Tumori*, vol. 94, no. 2, pp. 234–245, 2008.

[6] K. Kostarelos and A. D. Miller, "Synthetic, self-assembly ABCD nanoparticles; a structural paradigm for viable synthetic non-viral vectors," *Chemical Society Reviews*, vol. 34, no. 11, pp. 970–994, 2005.

[7] S. Fletcher, A. Ahmad, E. Perouzel, A. Heron, A. D. Miller, and M. R. Jorgensen, "In vivo studies of dialkynoyl analogues of DOTAP demonstrate improved gene transfer efficiency of cationic liposomes in mouse lung," *Journal of Medicinal Chemistry*, vol. 49, no. 1, pp. 349–357, 2006.

[8] S. Fletcher, A. Ahmad, E. Perouzel, M. R. Jorgensen, and A. D. Miller, "A dialkynoyl analogue of DOPE improves gene transfer of lower-charged, cationic lipoplexes," *Organic and Biomolecular Chemistry*, vol. 4, no. 2, pp. 196–199, 2006.

[9] S. Fletcher, A. Ahmad, W. S. Price, M. R. Jorgensen, and A. D. Miller, "Biophysical properties of CDAN/DOPE-analogue lipoplexes account for enhanced gene delivery," *ChemBioChem*, vol. 9, no. 3, pp. 455–463, 2008.

[10] A. D. Miller, "The problem with cationic liposome/micelle-based non-viral vector systems for gene therapy," *Current Medicinal Chemistry*, vol. 10, no. 14, pp. 1195–1211, 2003.

[11] A. D. Miller, "Gene therapy needs robust synthetic nonviral platform technologies," *ChemBioChem*, vol. 5, no. 1, pp. 53–54, 2004.

[12] A. D. Miller, "Nonviral liposomes," in *Suicide Gene Therapy*, C. J. Springer, Ed., Methods in Molecular Medicine, pp. 107–137, Humana Press, Totowa, NJ, USA, 2004.

[13] M. Oliver, M. R. Jorgensen, and A. D. Miller, "The facile solid-phase synthesis of cholesterol-based polyamine lipids," *Tetrahedron Letters*, vol. 45, no. 15, pp. 3105–3107, 2004.

[14] S. Spagnou, A. D. Miller, and M. Keller, "Lipidic carriers of siRNA: differences in the formulation, cellular uptake, and delivery with plasmid DNA," *Biochemistry*, vol. 43, no. 42, pp. 13348–13356, 2004.

[15] T. Tagawa, M. Manvell, N. Brown et al., "Characterisation of LMD virus-like nanoparticles self-assembled from cationic liposomes, adenovirus core peptide μ (mu) and plasmid DNA," *Gene Therapy*, vol. 9, no. 9, pp. 564–576, 2002.

[16] D. J. Bharali, M. Khalil, M. Gurbuz, T. M. Simone, and S. A. Mousa, "Nanoparticles and cancer therapy: a concise review with emphasis on dendrimers," *International Journal of Nanomedicine*, vol. 4, no. 1, pp. 1–7, 2009.

[17] K. Cho, X. Wang, S. Nie, Z. G. Chen, and D. M. Shin, "Therapeutic nanoparticles for drug delivery in cancer," *Clinical Cancer Research*, vol. 14, no. 5, pp. 1310–1316, 2008.

[18] M. E. Davis, Z. G. Chen, and D. M. Shin, "Nanoparticle therapeutics: an emerging treatment modality for cancer," *Nature Reviews Drug Discovery*, vol. 7, no. 9, pp. 771–782, 2008.

[19] O. C. Farokhzad and R. Langer, "Impact of nanotechnology on drug delivery," *ACS Nano*, vol. 3, no. 1, pp. 16–20, 2009.

[20] T. Lammers, W. E. Hennink, and G. Storm, "Tumour-targeted nanomedicines: principles and practice," *British Journal of Cancer*, vol. 99, no. 3, pp. 392–397, 2008.

[21] D. Peer, J. M. Karp, S. Hong, O. C. Farokhzad, R. Margalit, and R. Langer, "Nanocarriers as an emerging platform for cancer therapy," *Nature Nanotechnology*, vol. 2, no. 12, pp. 751–760, 2007.

[22] T. Tanaka, P. Decuzzi, M. Cristofanilli et al., "Nanotechnology for breast cancer therapy," *Biomedical Microdevices*, vol. 11, no. 1, pp. 49–63, 2009.

[23] B.-B. C. Youan, "Impact of nanoscience and nanotechnology on controlled drug delivery," *Nanomedicine*, vol. 3, no. 4, pp. 401–406, 2008.

[24] J. D. Byrne, T. Betancourt, and L. Brannon-Peppas, "Active targeting schemes for nanoparticle systems in cancer therapeutics," *Advanced Drug Delivery Reviews*, vol. 60, no. 15, pp. 1615–1626, 2008.

[25] B. S. Zolnik and N. Sadrieh, "Regulatory perspective on the importance of ADME assessment of nanoscale material containing drugs," *Advanced Drug Delivery Reviews*, vol. 61, no. 6, pp. 422–427, 2009.

[26] Y. Matsumura and H. Maeda, "A new concept for macromolecular therapeutics in cancer chemotherapy: mechanism of tumoritropic accumulation of proteins and the antitumor agent smancs," *Cancer Research*, vol. 46, no. 12, pp. 6387–6392, 1986.

[27] M. Thanou and R. Duncan, "Polymer-protein and polymer-drug conjugates in cancer therapy," *Current Opinion in Investigational Drugs*, vol. 4, no. 6, pp. 701–709, 2003.

[28] B. E. Cohen and A. D. Bangham, "Diffusion of small non-electrolytes across liposome membranes," *Nature*, vol. 236, no. 5343, pp. 173–174, 1972.

[29] S. M. Johnson and A. D. Bangham, "Potassium permeability of single compartment liposomes with and without valinomycin," *Biomembranes*, vol. 193, no. 1, pp. 82–91, 1969.

[30] D. Lasic, Ed., *Medical Applications of Liposomes*, Elsevier, Amsterdam, The Netherlands, 1998.

[31] T. M. Allen and P. R. Cullis, "Drug delivery systems: entering the mainstream," *Science*, vol. 303, no. 5665, pp. 1818–1822, 2004.

[32] V. P. Torchilin, "Recent advances with liposomes as pharmaceutical carriers," *Nature Reviews Drug Discovery*, vol. 4, no. 2, pp. 145–160, 2005.

[33] E. A. Forssen and Z. A. Tokes, "Improved therapeutic benefits of doxorubicin by entrapment in anionic liposomes," *Cancer Research*, vol. 43, no. 2, pp. 546–550, 1983.

[34] J. Treat, A. Greenspan, D. Forst et al., "Antitumor activity of liposome-encapsulated doxorubicin in advanced breast cancer: phase II study," *Journal of the National Cancer Institute*, vol. 82, no. 21, pp. 1706–1710, 1990.

[35] N. J. Robert, C. L. Vogel, I. C. Henderson et al., "The role of the liposomal anthracyclines and other systemic therapies in the management of advanced breast cancer," *Seminars in Oncology*, vol. 31, supplement 13, pp. 106–146, 2004.

[36] R. M. Straubinger, N. G. Lopez, R. J. Debs, K. Hong, and D. Papahadjopoulos, "Liposome-based therapy of human ovarian cancer: parameters determining potency of negatively charged and antibody-targeted liposomes," *Cancer Research*, vol. 48, no. 18, pp. 5237–5245, 1988.

[37] T. M. Allen and F. J. Martin, "Advantages of liposomal delivery systems for anthracyclines," *Seminars in Oncology*, vol. 31, supplement 13, pp. 5–15, 2004.

[38] A. Gabizon and F. Martin, "Polyethylene glycol-coated (pegylated) liposomal doxorubicin. Rationale for use in solid tumours," *Drugs*, vol. 54, supplement 4, pp. 15–21, 1997.

[39] A. Gabizon, H. Shmeeda, and Y. Barenholz, "Pharmacokinetics of pegylated liposomal doxorubicin: review of animal and human studies," *Clinical Pharmacokinetics*, vol. 42, no. 5, pp. 419–436, 2003.

[40] D. Papahadjopoulos, T. M. Allen, A. Gabizon et al., "Sterically stabilized liposomes: improvements in pharmacokinetics and antitumor therapeutic efficacy," *Proceedings of the National Academy of Sciences of the United States of America*, vol. 88, no. 24, pp. 11460–11464, 1991.

[41] M. C. Woodle and D. D. Lasic, "Sterically stabilized liposomes," *Biochimica et Biophysica Acta*, vol. 1113, no. 2, pp. 171–199, 1992.

[42] A. Aissaoui, M. Chami, M. Hussein, and A. D. Miller, "Efficient topical delivery of plasmid DNA to lung in vivo mediated by putative triggered, PEGylated pDNA nanoparticles," *Journal of Controlled Release*, vol. 154, no. 3, pp. 275–284, 2011.

[43] S. Carmona, M. R. Jorgensen, S. Kolli et al., "Controlling HBV replication in vivo by intravenous administration of triggered PEGylated siRNA-nanoparticles," *Molecular Pharmaceutics*, vol. 6, no. 3, pp. 706–717, 2009.

[44] C. R. Drake, A. Aissaoui, O. Argyros et al., "Bioresponsive small molecule polyamines as noncytotoxic alternative to polyethylenimine," *Molecular Pharmaceutics*, vol. 7, no. 6, pp. 2040–2055, 2010.

[45] G. D. Kenny, N. Kamaly, T. L. Kalber et al., "Novel multifunctional nanoparticle mediates siRNA tumour delivery, visualisation and therapeutic tumour reduction in vivo," *Journal of Controlled Release*, vol. 149, no. 2, pp. 111–116, 2011.

[46] S. Kolli, S.-P. Wong, R. P. Harbottle, B. Johnson, M. Thanou, and A. D. Miller, "pH-Triggered nanoparticle mediated delivery of siRNA to liver cells in vitro and in vivo," *Bioconjugate Chemistry*, vol. 24, pp. 314–332, 2013.

[47] M. Mével, N. Kamaly, S. Carmona et al., "DODAG; a versatile new cationic lipid that mediates efficient delivery of pDNA and siRNA," *Journal of Controlled Release*, vol. 143, no. 2, pp. 222–232, 2010.

[48] A. Andreu, N. Fairweather, and A. D. Miller, "Clostridium neurotoxin fragments as potential targeting moieties for liposomal gene delivery to the CNS," *ChemBioChem*, vol. 9, no. 2, pp. 219–231, 2008.

[49] J. Chen, M. R. Jorgensen, M. Thanou, and A. D. Miller, "Post-coupling strategy enables true receptor-targeted nanoparticles," *Journal of RNAi and Gene Silencing*, vol. 7, no. 1, pp. 449–455, 2011.

[50] M. Wang, D. W. P. M. Löwik, A. D. Miller, and M. Thanou, "Targeting the urokinase plasminogen activator receptor with synthetic self-assembly nanoparticles," *Bioconjugate Chemistry*, vol. 20, no. 1, pp. 32–40, 2009.

[51] S. Erdogan, "Liposomal nanocarriers for tumor imaging," *Journal of Biomedical Nanotechnology*, vol. 5, no. 2, pp. 141–150, 2009.

[52] W. J. M. Mulder, G. J. Strijkers, G. A. F. van Tilborg, A. W. Griffioen, and K. Nicolay, "Lipid-based nanoparticles for contrast-enhanced MRI and molecular imaging," *NMR in Biomedicine*, vol. 19, no. 1, pp. 142–164, 2006.

[53] J. M. Devoisselle, J. Vion-Dury, J. P. Galons et al., "Entrapment of Gadolinium-DTPA in liposomes. Characterization of vesicles by P-31 NMR spectroscopy," *Investigative Radiology*, vol. 23, no. 10, pp. 719–724, 1988.

[54] E. Unger, T. Fritz, D. K. S. de Kang Shen, and G. Wu, "Manganese-based liposomes: comparative approaches," *Investigative Radiology*, vol. 28, no. 10, pp. 933–938, 1993.

[55] D. Kozlowska, P. Foran, P. MacMahon, M. J. Shelly, S. Eustace, and R. O'Kennedy, "Molecular and magnetic resonance imaging: the value of immunoliposomes," *Advanced Drug Delivery Reviews*, vol. 61, no. 15, pp. 1402–1411, 2009.

[56] G. W. Kabalka, M. A. Davis, E. Buonocore, K. Hubner, E. Holmberg, and L. Huang, "Gd-labeled liposomes containing amphipathic agents for magnetic resonance imaging," *Investigative Radiology*, vol. 25, supplement 1, pp. S63–S64, 1990.

[57] G. A. F. van Tilborg, G. J. Strijkers, E. M. Pouget et al., "Kinetics of avidin-induced clearance of biotinylated bimodal liposomes for improved MR molecular imaging," *Magnetic Resonance in Medicine*, vol. 60, no. 6, pp. 1444–1456, 2008.

[58] N. Kamaly, T. Kalber, G. Kenny, J. Bell, M. Jorgensen, and A. Miller, "A novel bimodal lipidic contrast agent for cellular labelling and tumour MRI," *Organic and Biomolecular Chemistry*, vol. 8, no. 1, pp. 201–211, 2010.

[59] N. Kamaly, T. Kalber, M. Thanou, J. D. Bell, and A. D. Miller, "Folate receptor targeted bimodal liposomes for tumor magnetic resonance imaging," *Bioconjugate Chemistry*, vol. 20, no. 4, pp. 648–655, 2009.

[60] N. Kamaly, T. Kalber, A. Ahmad et al., "Bimodal paramagnetic and fluorescent liposomes for cellular and tumor magnetic resonance imaging," *Bioconjugate Chemistry*, vol. 19, no. 1, pp. 118–129, 2008.

[61] A. J. Almeida and E. Souto, "Solid lipid nanoparticles as a drug delivery system for peptides and proteins," *Advanced Drug Delivery Reviews*, vol. 59, no. 6, pp. 478–490, 2007.

[62] R. Cavalli, O. Caputo, M. E. Carlotti, M. Trotta, C. Scarnecchia, and M. R. Gasco, "Sterilization and freeze-drying of drug-free and drug-loaded solid lipid nanoparticles," *International Journal of Pharmaceutics*, vol. 148, no. 1, pp. 47–54, 1997.

[63] R. H. Muller, W. Mehnert, J.-S. Lucks et al., "Solid lipid nanoparticles (SLN)—an alternative colloidal carrier system for controlled drug delivery," *European Journal of Pharmaceutics and Biopharmaceutics*, vol. 41, no. 1, pp. 62–69, 1995.

[64] S. Morel, E. Terreno, E. Ugazio, S. Aime, and M. R. Gasco, "NMR relaxometric investigations of solid lipid nanoparticles (SLN) containing gadolinium(III) complexes," *European Journal of Pharmaceutics and Biopharmaceutics*, vol. 45, no. 2, pp. 157–163, 1998.

[65] P. Yingyuad, M. Mével, C. Prata et al., "Enzyme-triggered PEGylated pDNA-nanoparticles for controlled release of pDNA in tumours," *Bioconjugate Chemistry*, vol. 24, pp. 343–362, 2013.

[66] G. Kong, G. Anyarambhatla, W. P. Petros et al., "Efficacy of liposomes and hyperthermia in a human tumor xenograft model: importance of triggered drug release," *Cancer Research*, vol. 60, no. 24, pp. 6950–6957, 2000.

[67] R. T. P. Poon and N. Borys, "Lyso-thermosensitive liposomal doxorubicin: a novel approach to enhance efficacy of thermal ablation of liver cancer," *Expert Opinion on Pharmacotherapy*, vol. 10, no. 2, pp. 333–343, 2009.

[68] D. Needham, G. Anyarambhatla, G. Kong, and M. W. Dewhirst, "A new temperature-sensitive liposome for use with mild hyperthermia: characterization and testing in a human tumor xenograft model," *Cancer Research*, vol. 60, no. 5, pp. 1197–1201, 2000.

[69] D. Needham and M. W. Dewhirst, "The development and testing of a new temperature-sensitive drug delivery system for the treatment of solid tumors," *Advanced Drug Delivery Reviews*, vol. 53, no. 3, pp. 285–305, 2001.

[70] M. B. Thomas, D. Jaffe, M. M. Choti et al., "Hepatocellular carcinoma: consensus recommendations of the National Cancer Institute Clinical Trials Planning Meeting," *Journal of Clinical Oncology*, vol. 28, no. 25, pp. 3994–4005, 2010.

[71] B. J. Wood, R. T. Poon, J. K. Locklin et al., "Phase i study of heat-deployed liposomal doxorubicin during radiofrequency ablation for hepatic malignancies," *Journal of Vascular and Interventional Radiology*, vol. 23, no. 2, pp. 248–255, 2012.

[72] M. de Smet, S. Langereis, S. van den Bosch, and H. Grüll, "Temperature-sensitive liposomes for doxorubicin delivery under MRI guidance," *Journal of Controlled Release*, vol. 143, no. 1, pp. 120–127, 2010.

[73] A. H. Negussie, P. S. Yarmolenko, A. Partanen et al., "Formulation and characterisation of magnetic resonance imageable thermally sensitive liposomes for use with magnetic resonance-guided high intensity focused ultrasound," *International Journal of Hyperthermia*, vol. 27, no. 2, pp. 140–155, 2011.

[74] A. Ranjan, G. C. Jacobs, D. L. Woods et al., "Image-guided drug delivery with magnetic resonance guided high intensity focused ultrasound and temperature sensitive liposomes in a rabbit Vx2 tumor model," *Journal of Controlled Release*, vol. 158, no. 3, pp. 487–494, 2012.

[75] A. Partanen, P. S. Yarmolenko, A. Viitala et al., "Mild hyperthermia with magnetic resonance-guided high-intensity focused ultrasound for applications in drug delivery," *International Journal of Hyperthermia*, vol. 28, pp. 320–336, 2012.

[76] N. Kamaly and A. D. Miller, "Paramagnetic liposome nanoparticles for cellular and tumour imaging," *International Journal of Molecular Sciences*, vol. 11, no. 4, pp. 1759–1776, 2010.

[77] N. Kamaly, A. D. Miller, and J. D. Bell, "Chemistry of tumour targeted T1 based MRI contrast agents," *Current Topics in Medicinal Chemistry*, vol. 10, no. 12, pp. 1158–1183, 2010.

[78] R. Bardhan, W. Chen, M. Bartels et al., "Tracking of multimodal therapeutic nanocomplexes targeting breast cancer in vivo," *Nano Letters*, vol. 10, no. 12, pp. 4920–4928, 2010.

[79] R. Bardhan, S. Lal, A. Joshi, and N. J. Halas, "Theranostic nanoshells: from probe design to imaging and treatment of cancer," *Accounts of Chemical Research*, vol. 44, no. 10, pp. 936–946, 2011.

[80] J. Chen, G. M. Lanza, and S. A. Wickline, "Quantitative magnetic resonance fluorine imaging: today and tomorrow," *Wiley Interdisciplinary Reviews*, vol. 2, no. 4, pp. 431–440, 2010.

Hindawi Publishing Corporation
Journal of Drug Delivery
Volume 2013, Article ID 516749, 9 pages
http://dx.doi.org/10.1155/2013/516749

Research Article

Enhanced Dendritic Cell-Mediated Antigen-Specific CD4+ T Cell Responses: IFN-Gamma Aids TLR Stimulation

Kuo-Ching Sheng,[1,2] Stephanie Day,[1,3] Mark D. Wright,[3] Lily Stojanovska,[4] and Vasso Apostolopoulos[1,5]

[1] *Immunology and Vaccine Laboratory, Burnet Institute, Melbourne, VIC 3004, Australia*
[2] *Institute for Glycomics, Griffith University, Gold Coast, QLD 4215, Australia*
[3] *Department of Immunology, Monash University, Melbourne, VIC 3004, Australia*
[4] *College of Health and Biomedicine, Victoria University, VIC 3021, Australia*
[5] *VA Consulting Services, Melbourne, VIC 3030, Australia*

Correspondence should be addressed to Mark D. Wright; mark.wright@monash.edu and Vasso Apostolopoulos; vasso@scientist.com

Received 12 December 2012; Accepted 18 February 2013

Academic Editor: Theresia Thalhammer

Phenotypic maturation and T cell stimulation are two functional attributes of DCs critical for immune induction. The combination of antigens, including those from cancer, with Toll-like receptor (TLR) ligands induces far superior cellular immune responses compared to antigen alone. In this study, IFN-gamma treatment of bone marrow-derived DC, followed by incubation with the TLR2, TLR4, or TLR9 agonists, enhanced DC activation compared to TLR ligation alone. Most notably, the upregulation of CD40 with LPS stimulation and CD86 with CpG stimulation was observed in *in vitro* cultures. Similarly, IFN-gamma coinjected with TLR ligands was able to promote DC activation *in vivo*, with DCs migrating from the site of immunization to the popliteal lymph nodes demonstrating increased expression of CD80 and CD86. The heightened DC activation translated to a drastic increase in T cell stimulatory capacity in both antigen independent and antigen dependent fashions. This is the first time that IFN-gamma has been shown to have a combined effect with TLR ligation to enhance DC activation and function. The results demonstrate the novel use of IFN-gamma together with TLR agonists to enhance antigen-specific T cell responses, for applications in the development of enhanced vaccines and drug targets against diseases including cancer.

1. Introduction

Vaccination requires highly purified proteins or synthetic peptides usually in combination with immune stimulating adjuvants or danger signals, to successfully prime T cells. In the last 10 years, there has been an upsurge of data suggesting that dendritic cells (DCs) are the most important cells to stimulate immune responses against antigens [1]. DCs link the innate and adaptive immune responses by (i) binding a vast array of pathogens through their cell surface receptors, including C-type lectins, Toll-like receptors (TLRs), and scavenger receptors and inducing inflammatory responses for their elimination and (ii) are able to stimulate CD4+ T cell responses and cross present antigens for CD8+ T cell stimulation against antigens. Numerous strategies have been utilized to target antigens to DCs, following the abundance of information becoming available regarding cell surface expression of receptors and their role in stimulating immune responses [2]. The mannose receptor, DC-SIGN, scavenger receptor, DEC-205, and Toll-like receptors (TLRs) are amongst the most thoroughly studied DC receptors [2]. Targeting of these receptors is becoming an effective strategy of delivering antigens in DC-based anticancer immunotherapy studies.

TLRs are a class of proteins (pathogen recognition receptors, PRRs) that play a key role in the innate immune system and recognize molecules derived from pathogens (bacteria, fungi, virus, parasitic protozoa, mycoplasma), leading to

stimulation of immune responses. Toll was first identified, almost 20 years ago, when it was found to have an essential role in the fly's immunity to fungal infections [3] and the first human TLR (TLR1) to be identified immediately followed [4]. Three years later, it was demonstrated that TLR4 initiated an adaptive immune response following ligation of the receptor with antibody [5], and lipopolysaccharide (LPS) was found to be the main ligand for TLR4 [6]. Using a series of gene ablations in mice, identification of other TLRs followed, mainly by Akira and colleagues [7–9], and to date 13, TLRs (TLR1-TLR13) have been identified. In brief, the ligands for each TLR are lipopeptides (TLR1), glycolipids, lipoproteins, heat shock protein (HSP)-70, zymosan (TLR2), double stranded RNA, poly I : C (TLR3), LPS, several HSPs (TLR4), flagellin (TLR5), multiple diacyl lipopeptides (TLR6), imidazoquinoline, loxoribine, bropirimine, imiquimod, resiquimod (TLR7), small synthetic compounds, imiquimod, resiquimod (TLR8), unmethylated CpG oligodeoxynucleotide DNA (TLR9), profilin (TLR11), and a bacterial ribosomal RNA sequence (TLR13). No ligands are known for TLR10 and TLR12. TLRs are expressed on different cells; however, all (except TLR12 which is exclusively expressed on neurons) are expressed on the key antigen presenting cells, monocytes, macrophages, DCs, and B cells. An exponential amount of papers are being published emphasizing the enhanced potency of vaccines by incorporating ligands that target TLRs on DCs with antigens, in animal models. TLR2 [10–12], TLR4 [13–18], TLR7 [19], TLR8 [20], and TLR9 [21] have been targeted with adjuvants which demonstrated significant antigen-specific enhancement in immune responses as compared to vaccinations without TLR agonists.

IFN-gamma is a type II interferon produced by a variety of leukocyte populations including type I helper T (Th1) cells, natural killer (NK) cells, cytotoxic T lymphocytes (CTLs), antigen-presenting cells (APCs) including macrophages and DCs, and B cells. IFN-gamma is a potent immunomodulatory cytokine which exerts multiple biological effects on a range of cell types. Whilst typically known as an antiviral cytokine due to its capacity to block viral replication [22, 23], IFN-gamma has a broad range of functions on several arms of the immune system, including skewing T cell responses towards the type I helper T (Th1) cell phenotype [24, 25]. As a result, cellular immunity mediated by innate NK cells, adaptive CTLs, and macrophages [26]. IFN-gamma induces IL-12 and IFN-gamma production and inhibits IL-4 secretion and functions, resulting in suppression of the Th2 response [27–32]. These functional characteristics correspond evidently to its role in antimicrobial and antitumor immunity [33].

IFN-gamma priming has been shown to enhance macrophage activation through TLR ligation [34–37]. IFN-gamma promotes TLR ligand stimulation resulting in enhanced production of microbicidal nitric oxide and proinflammatory cytokines like IL-12. In addition to the synergy with TLRs, IFN-gamma alone enhances antigen processing and presentation in macrophages by upregulating subunits essential for the MHC-class I and II antigen presentation pathways [27–32]. Whilst the effect of IFN-gamma with or without TLR ligands on macrophages has been extensively studied, its adjuvanticity in DCs and its role in DC-mediated T cell proliferative responses have not been thoroughly clarified. In the current study, we investigate the effect of IFN-gamma on DC functional maturation and DC-meditated helper T cell activation, in the presence and absence of TLR ligation (TLR4 (LPS), TLR2/6 (zymosan) and TLR9 (CpG)).

2. Material and Methods

2.1. Animals. C57BL/6 and OT-II mice (aged 6–10 weeks) used throughout this study were purchased from the animal facilities of the Walter and Eliza Hall Institute (Melbourne, Australia) or PAC in Alfred Medical Research and Education Precinct (AMREP), Melbourne, Australia. C57BL/6 mice were used as wild-type mice to evaluate IFN-gamma adjuvanticity. OT-II mice were donors of OVA helper peptide-specific CD4+ T cells. All mice were bred and maintained under specific pathogen-free conditions and were used in accordance with animal ethics guidelines. Ethics approval was granted by AMREP Ethics Committee, and all mice were treated and handled in accordance to the guidelines of the National Health and Medical Research Council (NHMRC) of Australia.

2.2. DC Generation and Purification. Bone marrow cells from femurs and tibias of C57BL/6 mice were collected by flushing with complete media (RPMI supplemented with 2% HEPES, 0.1 mM 2-ME, 100 U/mL penicillin, 100 μg/mL streptomycin, 2 mM glutamine, and 10% FCS) through 70 μM cell strainers and then were treated with red blood cell lysis buffer (0.15 M NH_4Cl, 1 mM $KHCO_3$, and 0.1 mM Na_2EDTA) for 5 mins at room temperature. Washed cells were cultured in 24-well plates in complete media supplemented with 10 ng/mL GM-CSF and 10 ng/mL IL-4 (BD BioSciences, USA), at 5×10^5 cells/well for 4-5 days. Cells were harvested by gently pipetting and were either used as is for proliferation assays (approximately 70% CD11c+) or were purified by magnetic cell sorting. Briefly, cells were pelleted and incubated with anti-CD11c MAC beads (400 μL/10^8 cells) (Miltenyi Biotec, Auburn, CA, USA) in the presence of 0.5% FCS and 2 mM EDTA in PBS at 4°C for 15 min. Cells were washed, resuspended, and purified using the autoMACS system (Miltenyi Biotec) following manufacturer's instructions. The percentage of CD11c+ cells purified in this manner was above 94% as measured by FACS analysis.

2.3. DC Maturation. To precondition DC for IFN-gamma studies, DC monolayers were incubated in complete media containing 10 ng/mL IFN-gamma for 2 hours. Cells were then washed and stimulated with either 1 μg/mL LPS (derived from *Escherichia coli* (0111 : B4) Sigma, San Diego, USA), 20 μg/mL zymosan A (from *Saccharomyces cerevisiae*, Sigma) or 10 μg/mL CpG1668 (GeneWorks, Adelaide, Australia) for 16 h at 37°C. This procedure was previously optimized using the DC2.4 cell line (data not shown). Cells (5×10^5) were washed and resuspended with FITC-conjugated anti-CD40

(FGK-45.5), anti-CD80 (16.10.A1), anti-CD86 (GL1), anti-MHC-class II (IA^b) (M5/114.15.2), all constructed in house, or PE-conjugated anti-MHC-class I (BD BioSciences), together with APC-conjugated anti-CD11c (BD Biosciences) at 4°C for 30 min. Cells were then analyzed for expression of surface maturation markers by gating on live CD11c+ cells.

2.4. T Cell Purification. Splenocytes from C57BL/6 or OT-II mice were collected, washed, and incubated in red blood cell lysis buffer at room temperature for 5 min. Cells were incubated with antibody mix which contained in-house produced rat anti-mouse Gr-1 (RB6-8C5), anti-CD11b (M1/70.15), anti-erythrocyte (TER-119), and anti-MHC-class II (M5/114.15.2) monoclonal antibodies at 4°C for 30 min. To purify CD4+ and CD8+ T cells, rat anti-mouse CD8-alpha (YTS169.4) and anti-CD4 (GK1.5) were included in the antibody mix, respectively. Labeled cells were depleted with 2 rounds of bead separation. In each round, cells were incubated with goat anti-rat Ig magnetic beads (8 beads/cell) (Qiagen, Melbourne, Australia) at 4°C for 25 min. Cells were washed and those that bound to the beads were removed by magnets. The purity of T cells was at least 94%.

2.5. Antigen-Specific T Cell Proliferation. Purified DCs were preconditioned with IFN-gamma (10 ng/mL) for 2 h and subsequently treated with endotoxin-depleted OVA (40 μg/mL) and LPS (1 μg/mL) or zymosan (20 μg/mL) for 3 h. To evaluate the capacity of treated DCs to stimulate OVA-specific helper T cells, titrated DCs ($1–4 \times 10^3$) were seeded with 2×10^4 purified OT-II CD4+ T cells in quadruplicates in 96-well plates. Proliferation of T cells was monitored by the addition of 1 μCi ^{3}H-thymidine from day 1 to day 5. The radioactivity was measured in counts per minute (CPM). Peak proliferation of OT-II T cells on day 3 was compared.

2.6. T Cell Costimulation Assay. C57BL/6 DCs ($1–4 \times 10^3$) pretreated with IFN-gamma and/or TLR ligands were seeded with 2×10^4 C57BL/6 CD4+ T cells in quadruplicates in the 96-well plates precoated with 5 g/mL anti-CD3 (KT3-1.1). T cell proliferation was monitored by ^{3}H-thymidine incorporation from day 2 to 7. Peak proliferation on day 5 was compared.

2.7. In Vivo DC Maturation. C57BL/6 mice were injected with LPS (2 μg) or CpG intradermally into each footpad, with or without IFN-gamma (2 ng). After 18 h, popliteal lymph node cells were collected. All mice were treated and handled as approved by the AMREP animal ethics committee, Melbourne Australia and in accordance to the ethics guidelines by NHMRC Australia. The maturation state of live CD11c+ DCs was determined by labelling with FITC-conjugated anti-CD80 and anti-CD86 and analyzed by flow cytometry.

2.8. Statistical Analysis. All data are shown as the mean ± standard error of the mean (SEM). The data generated in this study were analyzed by student's *t*-test. Significance of difference was determined by the *P* value (≤ 0.05).

3. Results

3.1. IFN-Gamma Enhances DC Maturation with or without TLR Ligands. The ability of IFN-gamma to promote DC maturation *in vitro* was assessed using day 5 bone marrow-derived DC in the presence or absence of TLR ligands, LPS (TLR4), and CpG (TLR9), by measuring cell surface expression of CD40, CD80, CD86, and MHC class II (Figure 1). IFN-gamma alone had a moderate effect on the upregulation of the activation markers, compared to untreated cells, most notably causing an enhancement in the levels of CD86 and MHC II expression. Likewise, CpG alone induced low levels of expression of the four surface markers compared to untreated cells; however, this was augmented in the presence of IFN-gamma, most notably, C40 and CD86. LPS strongly induced DC maturation as measured by the expression of the activation markers, and in the presence of IFN-gamma, only CD40 expression was further upregulated, albeit weak.

The ability of IFN-gamma to promote DC maturation *in vivo* was similarly assessed, following hock injection of mice with IFN-gamma in the presence or absence of TLR ligands (Figure 2). CD11c+ DCs from the popliteal lymph nodes showed increased CD80 and CD86 expression following IFN-gamma injection, compared to PBS-injected mice. Again, LPS alone strongly induced the expression of both activation markers which was not further augmented in the presence of IFN-gamma. CpG alone had minimal effect on CD86 expression, but increased CD80 expression; however, the inclusion of IFN-gamma further upregulated the expression of both markers, indicating enhancement of bone marrow-derived DC maturation.

3.2. IFN-Gamma Promotes DC Costimulation to CD4+ T Cells Only in the Presence of TLR Ligands. CD80 and CD86 which both bind CD28 and CTLA-4 on the surface of T cells providing regulatory signals leading to T cell activation are two of several cell surface molecules involved in T cell costimulation. Given the ability of IFN-gamma to upregulate surface expression of CD80 and CD86 on DC, we next investigated the capacity of these cells to promote T cell costimulation resulting in proliferation. Day 5 bone marrow-derived DCs were pretreated with IFN-gamma and TLR ligands, LPS, or zymosan and then assessed for their ability to co-stimulate proliferation of CD4+ T cells in the presence of immobilized anti-CD3 antibody (Figure 3). IFN-gamma-treated DCs alone were unable to induce CD4+ T cell proliferation, in line with the low levels of CD80 and CD86 expression observed on these cells (Figures 1 and 3). However, in the presence of TLR ligands, IFN-gamma-treated DC promoted a high level of CD4+ T cell proliferation, peaking at day 5. At this time point, the correlation between DC number and CD4+ T cell proliferation was assessed, with a positive trend between DC number and CD4+ T cell proliferation observed (Figure 3).

3.3. IFN-Gamma Enhances Antigen-Specific CD4+ T Cell Response Only in the Presence of TLR Ligands. The ability of IFN-gamma to potentiate antigen specific CD4+ T cell proliferation was investigated. DCs were incubated with

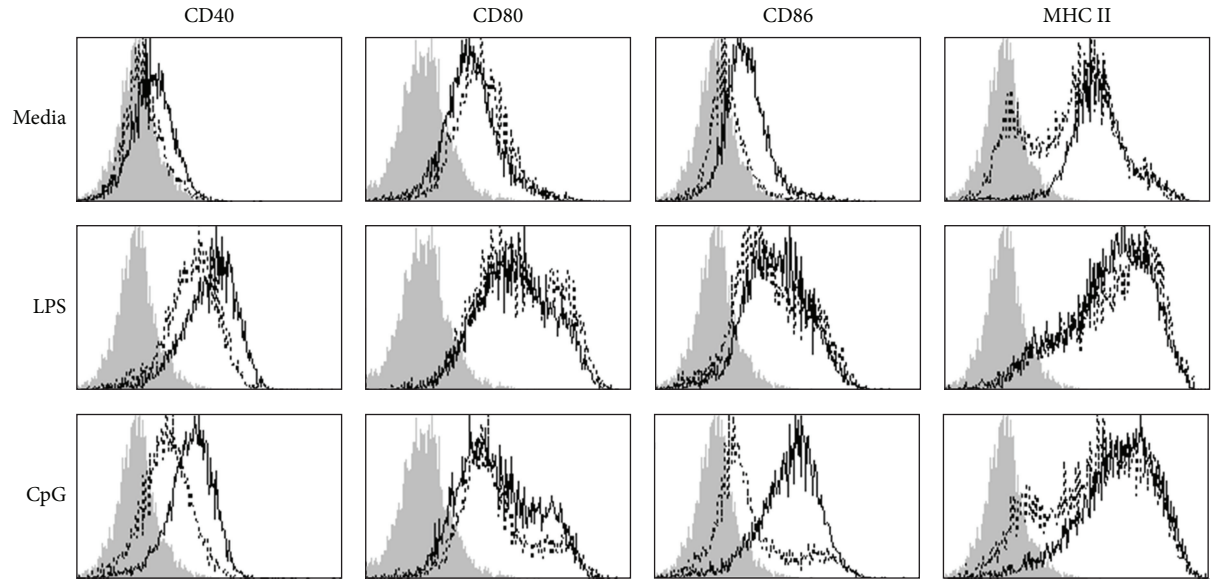

Figure 1: IFN-gamma enhances DC maturation with or without TLR ligands *in vitro*. C57BL/6 bone marrow cells were cultured with GM-CSF to generate bone marrow derived DCs. At days 4-5, cells were preconditioned with IFN-gamma for 2 h (solid line) or no IFN-gamma (dotted line), followed by LPS (TLR4 ligand) or CpG (TLR9 ligand) stimulation for 16 h. Cells were harvested and labelled with fluorescent antibodies. Live CD11c+ cells were gated and analyzed for CD40, CD80, CD86, and MHC-class II expression. Data shown are representative of at least two experiments. The shaded area represents cells stained with the respective secondary antibody.

IFN-gamma and pulsed with the model antigen ovalbumin (OVA) and then incubated with CD4+ transgenic T cells from OT-II mice which carry a transgenic CD4 T cell receptor specific for the MHC class II restricted OVA peptide, $OVA_{323–339}$ [38]. The ability of the DC to induce proliferation of the OT-II CD4+ T cells in the presence and absence of TLR ligation was monitored from days 1–5 (Figure 4). Interestingly, the presence of TLR ligands alone induced CD4+ T cell proliferation to OVA very poorly. However, IFN-gamma pre-treatment dramatically enhanced antigen presentation by DCs, as evident with the high levels of CD4+ T cell proliferation. At the peak day of proliferation, day 3, the effect of DC number on proliferative responses was examined, with results again demonstrating a positive correlation between DC number and the magnitude of CD4+ T cell proliferation.

4. Discussion

TLRs are essential receptors of the innate immune system which stimulate a vast array of inflammatory responses and eliminate invading pathogens. In addition, stimulation of TLR by binding to their respective ligands has been shown to lead to Th1, Th2, CD4+, and CD8+ T cell immune responses [39]. Antigens in combination with TLR ligand induce far superior immune responses compared to using antigen alone in animal models. Agonists to TLR7 activate plasmacytoid DCs (IFN-gamma, IFN-inducible protein, and IFN-inducible T cell alpha chemoattractant secretion), and TLR8 agonists activate myeloid DCs and monocyte-derived DCs (TNFalpha, IL-12, and MIP-1alpha, IFN-gamma) and upregulated CD40, CD80, and CD86 cell surface expression [40]. TLR7/8 agonists conjugated to HIV-1 Gag protein induce strong Th1/CD8+ T cell responses. Targeting TLR7 and TLR8 is effective in stimulating immune responses *in vivo* [41]. In TLR9 knockout mice, DCs stimulated with CpG have defective IL-12 and type-1 IFN secretion, even though Th1 and IFN-gamma responses were induced in TLR9 knockout mice following DNA immunizations [42]. TLR4 targeting has been shown to upregulate cell surface co-stimulatory markers (CD40, CD80, CD86), MHC molecules, and Th1 and Th2 cytokines on bone marrow-derived DCs [14–18]. Further, totally synthetic vaccines which target TLR2 (Pam3CysSer) carrying different antigens stimulate CD4+ and CD8+ T cell and/or antibody responses [10–12]. Targeting TLR5 using flagellin linked to antigens (ovalbumin (OVA), *Listeria monocytogenes* antigen p60 peptides or listeriolysin) induced IgG1, IgG2a antibodies, and protective CD8+ T cells responses in mice [43].

Phenotypic maturation and T cell stimulation are two functional attributes of DCs critical for immune induction, and their effective maturation into potent professional antigen presenting cells has been shown to be dependent on a number of critical cellular interactions, as well as by cytokine and TLR signalling. IFN-gamma is a key player in the development of T cell-mediated immunity and in mounting an adaptive immune response against infection or disease. In this study, we determined the ability of IFN-gamma to augment DC maturation and antigen presentation induced by TLR signalling. Data demonstrate that whilst IFN-gamma alone has a minor effect on DC functionality, however, when used to treat DC before subsequent TLR ligation, it significantly enhanced DC activation and T cell stimulatory capacity.

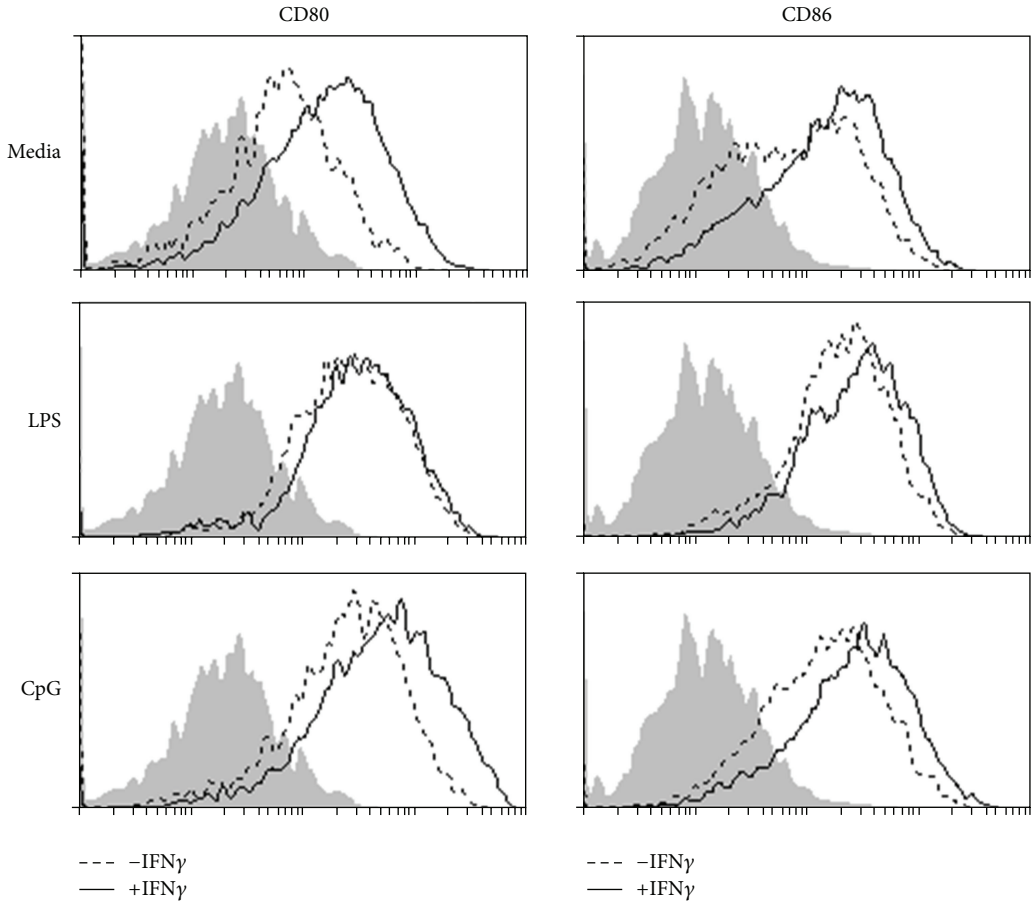

Figure 2: IFN-gamma enhances DC maturation with or without TLR ligands *in vivo*. C57BL/6 mice were injected with LPS (TLR4 ligand) or CpG (TLR9 ligand) with (solid line) or without (dotted line) IFN-gamma intradermally using the Hock immunization protocol. At 18 h, popliteal lymph cells were isolated. Live CD11c-high cells were analyzed for CD80 and CD86 expression. Data shown are representative of at least two experiments. The shaded area represents cells stained with the respective secondary antibody.

In the present study, it is clear that IFN-gamma treatment of bone marrow-derived DC followed by incubation with the TLR4 (LPS) or TLR9 (CpG) agonists greatly enhanced DC activation compared to TLR ligation alone. Most notably, the upregulation of CD40 with LPS stimulation and CD86 with CpG stimulation was observed in *in vitro* cultures. Similarly, IFN-gamma coinjected with TLR ligands was able to promote DC activation *in vivo*, with DCs migrated from the site of immunization to the popliteal lymph nodes demonstrating increased expression of CD80 and CD86. The heightened DC activation translated to a drastic increase in T cell stimulatory capacity in both antigen independent and dependent fashions. This is the first time that IFN-gamma has been shown to have a combined effect with TLR ligation to enhance DC activation and function. In contrast, the effect of IFN-gamma on other APC populations has been well characterized.

Much work has been done to study the effects of IFN-gamma treatment on macrophages, with the consensus of studies concluding that IFN-gamma primes macrophages into a semiactive state which is highly receptive to activation by a subsequent signal such as TLR ligation (for review see [44]). For example, upregulation of CD40 and CD80 on monocytes has been noted by IFN-gamma. Human acute myeloid leukemia blasts express low levels of both co-stimulatory molecules, demonstrating poor antigen presenting capacity. Incubation with IFN-gamma was found to upregulate CD40 and CD80 expression, and this was found to be dependent on IRF-1 activation [45]. In addition, pretreatment of macrophages with IFN-gamma induced pro-inflammatory cytokines, inducing an accumulation of IL-12 p40 and p35 mRNA, but only with subsequent TLR ligation by LPS was IL-12 protein produced [46]. However, more recent studies have demonstrated a cross talk between IFN-gamma and TLR signalling pathways, with multiple elements of the signalling pathways synergizing to induce expression of proinflammatory factors [47]. In DC, TLR engagement is an important factor in inducing DC maturation; however, as with macrophages, it is likely that a combination of TLR engagement and IFN-gamma signalling, thus mimicking the inflammatory conditions *in vivo*, is necessary to produce optimal DC activation. Indeed, the current studies show that the combination of both signals not only promotes the expression of activation markers but also corresponds with

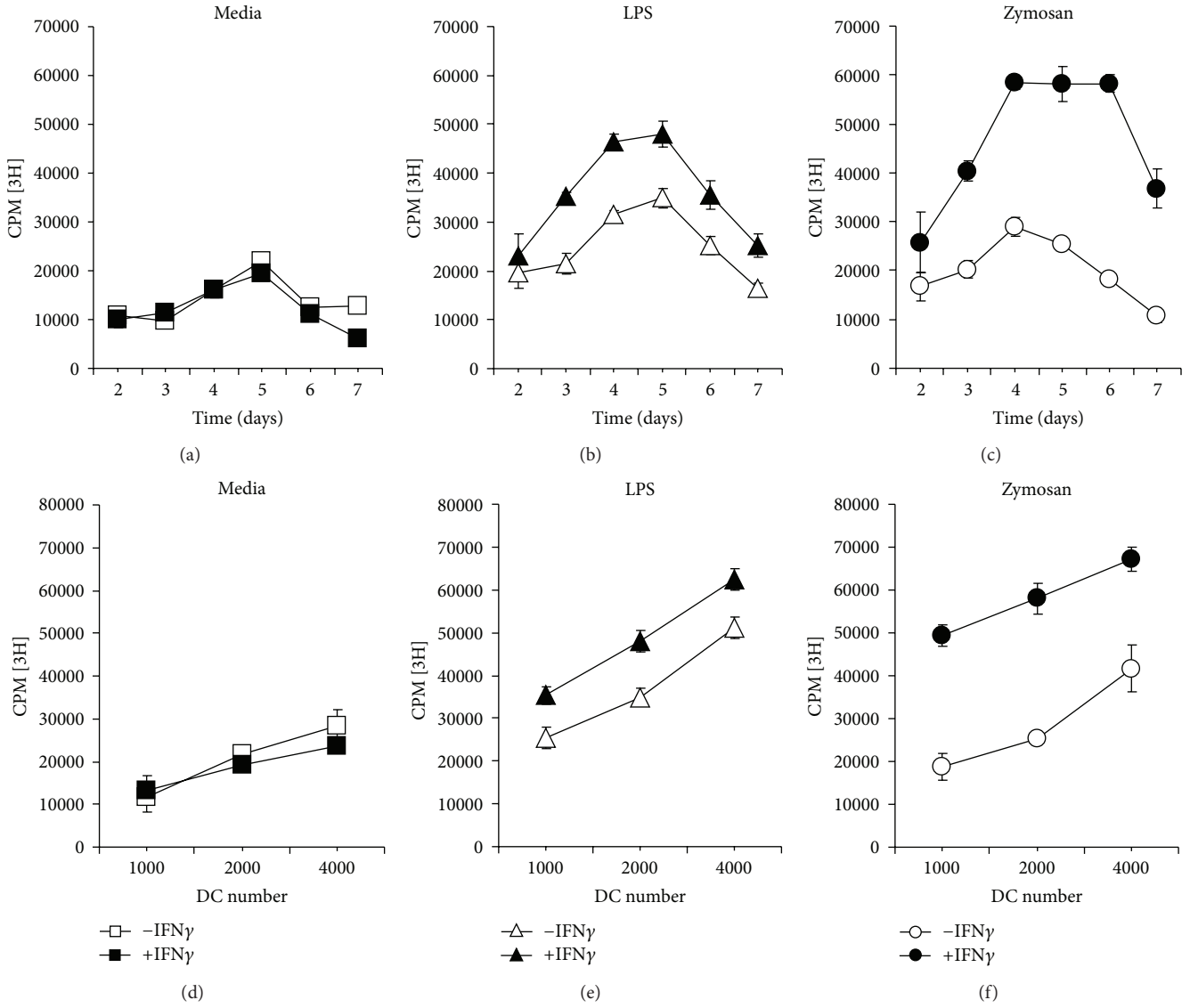

FIGURE 3: IFN-gamma enhances DC costimulation only when the TLR ligand is present. Days 4-5 bone marrow cultures preconditioned with IFN-gamma (black symbols) or no IFN-gamma (open symbols) for 2 h was stimulated with LPS (TLR4 ligand) or zymosan (TLR2 ligand) for 16 h. DCs were purified via the AutoMacs system as described in Section 2. Titrated bone marrow-derived DCs (1×10^3–4×10^3) were incubated with 2×10^3 CD4 T cells in quadruplicates in 96-well plates that were precoated with anti-CD3. Cell proliferation was monitored from day 2 to day 7. Proliferation kinetics was exemplified when DCs were seeded at 2×10^3 (a, b, c). As proliferation in general peaked at day 5, it was compared across DC titrations (d, e, f). Data shown are representative of two separate experiments. $P < 0.05$ in LPS and zymosan groups at all points except time point 2 days, based on quadruplicate values.

increased signalling to CD4+ T cells, in both nonspecific and antigen-specific fashions.

Various signals can promote DC maturation, including direct cell-to-cell contact, cytokine signalling, and TLR signalling from microbial stimuli. Reports investigating the bidirectional cross talk between NK cells and DC have indicated that DC can activate NK cells which in turn enhance DC maturation [48]. In the presence of direct cell-to-cell contact, strong DC maturation was observed as indicated by CD86 expression; however, both IFN-gamma and TNF-alpha produced by the activated NK cells were found to enhance the levels of CD86 expression, although on their own the cytokines had little effect [48]. Likewise, in the current studies, IFN-gamma alone had little effect on the induction of DC maturation markers CD40, CD80, CD86, and MHC class II. In the presence of a secondary stimuli via TLR ligation, however, the upregulation of the cell surface markers was enhanced following IFN-gamma priming.

In other studies, cultures of splenic DC with IFN-gamma upregulated expression of CTLA-4 counter receptor (however any counter receptor they measured in these studies is unclear), but not ICAM-1, heat stable antigen or MHC

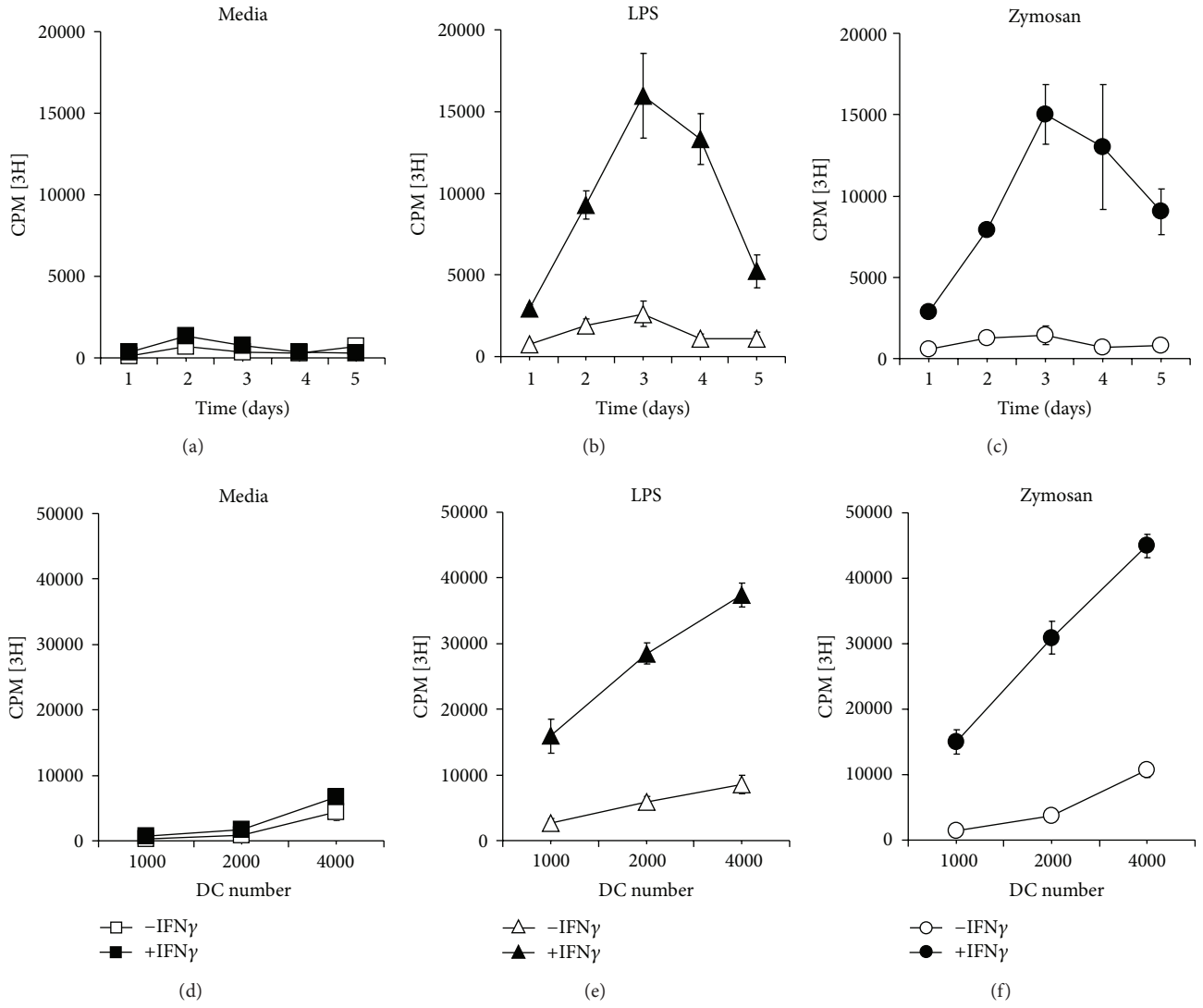

Figure 4: IFN-gamma enhances DC antigen presentation via MHC-class II, only in the presence of a TLR stimulus. Day 4 bone marrow cultures preconditioned with IFN-gamma for 2 h were pulsed with OVA in the presence of LPS (TLR4 ligand) or zymosan (TLR2 ligand) for 3 h. DCs were purified as described in Section 2. Titrated bone marrow-derived DCs (1×10^3–4×10^3) were incubated with 2×10^3 CD4 T cells in quadruplicates in 96-well plates. Cell proliferation was monitored from day 1 to day 5. Proliferation kinetics was exemplified when DCs were seeded at 2×10^3 (a, b, c). Peak proliferation at day 3 was compared across DC titrations (d, e, f). Data shown are representative of two separate experiments. $P < 0.05$ in all LPS and zymosan groups at all points, based on quadruplicate values.

class I or class II [49]. However, despite the upregulation of this T cell receptor co-stimulatory signal, the ability of IFN-gamma treated DC to induce T cell proliferation was not enhanced. Similarly, another study investigating the effects of cytokine pre-treatment on DC function demonstrated that when DCs were cultured overnight with IFN-gamma and used in mixed lymphocyte reactions, the T cell proliferation was in fact lower than using untreated DC [50]. While the DC populations studied in these reports were different to the bone marrow-derived DC used in the current studies, the results clearly substantiate the current findings that additional costimulation (in the form of TLR ligation) is necessary to promote the adjuvanticity of IFN-gamma.

The synergy between IFN-gamma and TLR ligands suggest that such combination is likely to be more highly beneficial to boost immune responses than IFN-gamma or TLR ligand alone in therapeutic settings for diseases, including cancer. Here, we unravel the adjuvant effect of IFN-gamma on DC maturation and T cell stimulation which are two important steps to achieve adaptive immunity for diseases, including cancer.

Authors' Contribution

Kuo-Ching Sheng and Stephaine Day contributed equally to the work.

References

[1] N. S. Wilson and J. A. Villadangos, "Regulation of antigen presentation and cross-presentation in the dendritic cell network: facts, hypothesis, and immunological implications," *Advances in Immunology*, vol. 86, pp. 241–305, 2005.

[2] O. Proudfoot, V. Apostolopoulos, and G. A. Pietersz, "Receptor-mediated delivery of antigens to dendritic cells: anticancer applications," *Molecular Pharmaceutics*, vol. 4, no. 1, pp. 58–72, 2007.

[3] B. Lemaitre, E. Nicolas, L. Michaut, J. M. Reichhart, and J. A. Hoffmann, "The dorsoventral regulatory gene cassette spatzle/Toll/Cactus controls the potent antifungal response in Drosophila adults," *Cell*, vol. 86, no. 6, pp. 973–983, 1996.

[4] N. Nomura, N. Miyajima, T. Sazuka et al., "Prediction of the coding sequences of unidentified human genes. I. The coding sequences of 40 new genes (KIAA0001-KIAA0040) deduced by analysis of randomly sampled cDNA clones from human immature myeloid cell line KG-1," *DNA Research*, vol. 1, no. 1, pp. 27–35, 1994.

[5] R. Medzhitov, P. Preston-Hurlburt, and C. A. Janeway Jr., "A human homologue of the Drosophila toll protein signals activation of adaptive immunity," *Nature*, vol. 388, no. 6640, pp. 394–397, 1997.

[6] A. Poltorak, I. Smirnova, X. He et al., "Genetic and physical mapping of the Lps locus: identification of the toll-4 receptor as a candidate gene in the critical region," *Blood Cells, Molecules, and Diseases*, vol. 24, no. 3, pp. 340–355, 1998.

[7] T. Kawai and S. Akira, "The role of pattern-recognition receptors in innate immunity: update on toll-like receptors," *Nature Immunology*, vol. 11, no. 5, pp. 373–384, 2010.

[8] T. Kawai and S. Akira, "Toll-like receptors and their crosstalk with other innate receptors in infection and immunity," *Immunity*, vol. 34, no. 5, pp. 637–650, 2011.

[9] H. Kumar, T. Kawai, and S. Akira, "Toll-like receptors and innate immunity," *Biochemical and Biophysical Research Communications*, vol. 388, no. 4, pp. 621–625, 2009.

[10] D. C. Jackson, F. L. Yuk, T. Le et al., "A totally synthetic vaccine of generic structure that targets Toll-like receptor 2 on dendritic cells and promotes antibody or cytotoxic T cell responses," *Proceedings of the National Academy of Sciences of the United States of America*, vol. 101, no. 43, pp. 15440–15445, 2004.

[11] B. L. Wilkinson, S. Day, R. Chapman, S. Perrier, V. Apostolopoulos, and R. J. Payne, "Synthesis and immunological evaluation of self-assembling and self-adjuvanting tricomponent glycopeptide cancer-vaccine candidates," *Chemistry*, vol. 18, pp. 16540–16548, 2012.

[12] B. L. Wilkinson, S. Day, L. R. Malins, V. Apostolopoulos, and R. J. Payne, "Self-adjuvanting multicomponent cancer vaccine candidates combining per-glycosylated muc1 glycopeptides and the toll-like receptor 2 agonist pam3CysSer," *Angewandte Chemie*, vol. 50, no. 7, pp. 1635–1639, 2011.

[13] S. U. Ahmed, M. Okamoto, T. Oshikawa et al., "Anti-tumor effect of an intratumoral administration of dendritic cells in combination with TS-1, an oral fluoropyrimidine anticancer drug, and OK-432, a streptococcal immunopotentiator: involvement of toll-like receptor 4," *Journal of Immunotherapy*, vol. 27, no. 6, pp. 432–441, 2004.

[14] K. C. Sheng, M. Kalkanidis, D. S. Pouniotis et al., "Delivery of antigen using a novel mannosylated dendrimer potentiates immunogenicity in vitro and in vivo," *European Journal of Immunology*, vol. 38, no. 2, pp. 424–436, 2008.

[15] K. C. Sheng, M. Kalkanidis, D. S. Pouniotis, M. D. Wright, G. A. Pietersz, and V. Apostolopoulos, "The adjuvanticity of a mannosylated antigen reveals TLR4 functionality essential for subset specialization and functional maturation of mouse dendritic cells," *Journal of Immunology*, vol. 181, no. 4, pp. 2455–2464, 2008.

[16] K. C. Sheng, G. A. Pietersz, M. D. Wright, and V. Apostolopoulos, "Dendritic cells: activation and maturation—applications for cancer immunotherapy," *Current Medicinal Chemistry*, vol. 12, no. 15, pp. 1783–1800, 2005.

[17] K. C. Sheng, D. S. Pouniotis, M. D. Wright et al., "Mannan derivatives induce phenotypic and functional maturation of mouse dendritic cells," *Immunology*, vol. 118, no. 3, pp. 372–383, 2006.

[18] C. K. Tang, K. C. Sheng, S. E. Esparon, O. Proudfoot, V. Apostolopoulos, and G. A. Pietersz, "Molecular basis of improved immunogenicity in DNA vaccination mediated by a mannan based carrier," *Biomaterials*, vol. 30, no. 7, pp. 1389–1400, 2009.

[19] N. Craft, K. W. Bruhn, B. D. Nguyen et al., "The TLR7 agonist imiquimod enhances the anti-melanoma effects of a recombinant Listeria monocytogenes vaccine," *Journal of Immunology*, vol. 175, no. 3, pp. 1983–1990, 2005.

[20] S. Xu, U. Koldovsky, M. Xu et al., "High-avidity antitumor T-cell generation by toll receptor 8-primed, myeloid- derived dendritic cells is mediated by IL-12 production," *Surgery*, vol. 140, no. 2, pp. 170–178, 2006.

[21] M. H. M. G. M. Den Brok, R. P. M. Sutmuller, S. Nierkens et al., "Synergy between in situ cryoablation and TLR9 stimulation results in a highly effective in vivo dendritic cell vaccine," *Cancer Research*, vol. 66, no. 14, pp. 7285–7292, 2006.

[22] E. Frederick Wheelock, "Interferon-like virus-inhibitor induced in human leukocytes by phytohemagglutinin," *Science*, vol. 149, no. 3681, pp. 310–311, 1965.

[23] E. F. Wheelock and W. A. Sibley, "Circulating virus, interferon and antibody after vaccination with the 17-D strain of yellow-fever virus," *The New England Journal of Medicine*, vol. 273, pp. 194–198, 1965.

[24] P. Parronchi, M. De Carli, R. Manetti et al., "IL-4 and IFN (α and γ) exert opposite regulatory effects on the development of cytolytic potential by Th1 or Th2 human T cell clones," *Journal of Immunology*, vol. 149, no. 9, pp. 2977–2983, 1992.

[25] P. Scott, "IFN-γ modulates the early development of Th1 and Th2 responses in a murine model of cutaneous leishmaniasis," *Journal of Immunology*, vol. 147, no. 9, pp. 3149–3155, 1991.

[26] A. Thakur, L. E. Pedersen, and G. Jungersen, "Immune markers and correlates of protection for vaccine induced immune responses," *Vaccine*, vol. 30, pp. 4907–4920, 2012.

[27] P. Di Marzio, P. Puddu, L. Conti, F. Belardelli, and S. Gessani, "Interferon γ upregulates its own gene expression in mouse peritoneal macrophages," *Journal of Experimental Medicine*, vol. 179, no. 5, pp. 1731–1736, 1994.

[28] W. P. Lafuse, D. Brown, L. Castle, and B. S. Zwilling, "IFN-γ increases cathepsin H mRNA levels in mouse macrophages," *Journal of Leukocyte Biology*, vol. 57, no. 4, pp. 663–669, 1995.

[29] N. Li, R. C. Salter, and D. P. Ramji, "Molecular mechanisms underlying the inhibition of IFN-γ-induced, STAT1-mediated gene transcription in human macrophages by simvastatin and agonists of PPARs and LXRs," *Journal of Cellular Biochemistry*, vol. 112, no. 2, pp. 675–683, 2011.

[30] L. Marodi and R. B. Johnston Jr., "Enhancement of macrophage candidacidal activity by interferon-gamma," *Immunodeficiency*, vol. 4, no. 1–4, pp. 181–185, 1993.

[31] L. Marodi, S. Schreiber, D. C. Anderson, R. P. MacDermott, H. M. Korchak, and R. B. Johnston Jr., "Enhancement of macrophage candidacidal activity by interferon-γ. Increased phagocytosis, killing, and calcium signal mediated by a decreased number of mannose receptors," *Journal of Clinical Investigation*, vol. 91, no. 6, pp. 2596–2601, 1993.

[32] I. J. Molina and B. T. Huber, "Regulation of macrophage activation markers by IL-4 and IFN-γ is subpopulation-specific," *Cellular Immunology*, vol. 134, no. 1, pp. 241–248, 1991.

[33] G. Perona-Wright, K. Mohrs, and M. Mohrs, "Sustained signaling by canonical helper T cell cytokines throughout the reactive lymph node," *Nature Immunology*, vol. 11, no. 6, pp. 520–526, 2010.

[34] J. Chen and L. B. Ivashkiv, "IFN-γ abrogates endotoxin tolerance by facilitating Toll-like receptor-induced chromatin remodeling," *Proceedings of the National Academy of Sciences of the United States of America*, vol. 107, no. 45, pp. 19438–19443, 2010.

[35] A. Dragičević, T. Džopalić, S. Vasilijić et al., "The influence of CD40 ligation and interferon-γ on functional properties of human monocyte-derived dendritic cells activated with polyinosinic-polycytidylic acid," *Vojnosanitetski Pregled*, vol. 68, no. 4, pp. 301–308, 2011.

[36] X. Hu, P. K. Paik, J. Chen et al., "IFN-γ suppresses IL-10 production and synergizes with TLR2 by regulating GSK3 and CREB/AP-1 proteins," *Immunity*, vol. 24, no. 5, pp. 563–574, 2006.

[37] T. Southworth, A. Metryka, S. Lea, S. Farrow, J. Plumb, and D. Singh, "IFN-gamma synergistically enhances LPS signalling in alveolar macrophages from COPD patients and controls by corticosteroid-resistant STAT1 activation," *British Journal of Pharmacology*, vol. 166, pp. 2070–2083, 2012.

[38] M. J. Barnden, J. Allison, W. R. Heath, and F. R. Carbone, "Defective TCR expression in transgenic mice constructed using cDNA- based α- and β-chain genes under the control of heterologous regulatory elements," *Immunology and Cell Biology*, vol. 76, no. 1, pp. 34–40, 1998.

[39] A. Abdelsadik and A. Trad, "Toll-like receptors on the fork roads between innate and adaptive immunity," *Human Immunology*, vol. 72, pp. 1188–1193, 2011.

[40] K. B. Corden, K. S. Gorski, S. J. Gibson et al., "Synthetic TLR agonists reveal functional differences between human TLR7 and TLR8," *Journal of Immunology*, vol. 174, no. 3, pp. 1259–1268, 2005.

[41] U. Wille-Reece, C. Y. Wu, B. J. Flynn, R. M. Kedl, and R. A. Seder, "Immunization with HIV-1 gag protein conjugated to a TLR7/8 agonist results in the generation of HIV-1 gag-specific Th1 and CD8+ T cell responses," *Journal of Immunology*, vol. 174, no. 12, pp. 7676–7683, 2005.

[42] D. Tudor, C. Dubuquoy, V. Gaboriau, F. Lefèvre, B. Charley, and S. Riffault, "TLR9 pathway is involved in adjuvant effects of plasmid DNA-based vaccines," *Vaccine*, vol. 23, no. 10, pp. 1258–1264, 2005.

[43] J. W. Huleatt, A. R. Jacobs, J. Tang et al., "Vaccination with recombinant fusion proteins incorporating Toll-like receptor ligands induces rapid cellular and humoral immunity," *Vaccine*, vol. 25, no. 4, pp. 763–775, 2007.

[44] K. Schroder, M. J. Sweet, and D. A. Hume, "Signal integration between IFNγ and TLR signalling pathways in macrophages," *Immunobiology*, vol. 211, no. 6–8, pp. 511–524, 2006.

[45] B. Bauvois, J. Nguyen, R. Tang, C. Billard, and J. P. Kolb, "Types I and II interferons upregulate the costimulatory CD80 molecule in monocytes via interferon regulatory factor-1," *Biochemical Pharmacology*, vol. 78, no. 5, pp. 514–522, 2009.

[46] M. P. Hayes, J. Wang, and M. A. Norcross, "Regulation of interleukin-12 expression in human monocytes: selective priming by interferon-γ of lipopolysaccharide-inducible p35 and p40 genes," *Blood*, vol. 86, no. 2, pp. 646–650, 1995.

[47] C. Zhao, M. W. Wood, E. E. Galyov et al., "Salmonella typhimurium infection triggers dendritic cells and macrophages to adopt distinct migration patterns in vivo," *European Journal of Immunology*, vol. 36, no. 11, pp. 2939–2950, 2006.

[48] F. Gerosa, B. Baldani-Guerra, C. Nisii, V. Marchesini, G. Carra, and G. Trinchieri, "Reciprocal activating interaction between natural killer cells and dendritic cells," *Journal of Experimental Medicine*, vol. 195, no. 3, pp. 327–333, 2002.

[49] C. P. Larsen, S. C. Ritchie, R. Hendrix et al., "Regulation of immunostimulatory function and costimulatory molecule (B7-1 and B7-2) expression on murine dendritic cells," *Journal of Immunology*, vol. 152, no. 11, pp. 5208–5219, 1994.

[50] S. L. Koide, K. Inaba, and R. M. Steinman, "Interleukin 1 enhances T-dependent immune responses by amplifying the function of dendritic cells," *Journal of Experimental Medicine*, vol. 165, no. 2, pp. 515–530, 1987.

Hindawi Publishing Corporation
Journal of Drug Delivery
Volume 2013, Article ID 616197, 12 pages
http://dx.doi.org/10.1155/2013/616197

Review Article

MRI-Guided Focused Ultrasound as a New Method of Drug Delivery

M. Thanou[1] and W. Gedroyc[2]

[1] *Institute of Pharmaceutical Science, King's College London, Franklin-Wilkins Building, Stamford Street, London SE1 9NH, UK*
[2] *Department of Experimental Medicine, Imperial College, St. Mary's Hospital, Praed Street, London W2 1NY, UK*

Correspondence should be addressed to M. Thanou; maya.thanou@kcl.ac.uk

Received 18 November 2012; Accepted 5 February 2013

Academic Editor: Andreas G. Tzakos

Ultrasound-mediated drug delivery under the guidance of an imaging modality can improve drug disposition and achieve site-specific drug delivery. The term focal drug delivery has been introduced to describe the focal targeting of drugs in tissues with the help of imaging and focused ultrasound. Focal drug delivery aims to improve the therapeutic profile of drugs by improving their specificity and their permeation in defined areas. Focused-ultrasound- (FUS-) mediated drug delivery has been applied with various molecules to improve their local distribution in tissues. FUS is applied with the aid of microbubbles to enhance the permeability of bioactive molecules across BBB and improve drug distribution in the brain. Recently, FUS has been utilised in combination with MRI-labelled liposomes that respond to temperature increase. This strategy aims to "activate" nanoparticles to release their cargo locally when triggered by hyperthermia induced by FUS. MRI-guided FUS drug delivery provides the opportunity to improve drug bioavailability locally and therefore improve the therapeutic profiles of drugs. This drug delivery strategy can be directly translated to clinic as MRg FUS is a promising clinically therapeutic approach. However, more basic research is required to understand the physiological mechanism of FUS-enhanced drug delivery.

1. Introduction

Therapeutic high intensity focused ultrasound (HIFU) or Focused Ultrasound (FUS) is a noninvasive medical treatment that allows the deposition of energy inside the human body. Frequencies of 0.8–3.5 MHz are generally used during the clinical applications of FUS. The energy levels carried in the ultrasound beam are several orders of magnitude greater than those of a standard diagnostic ultrasound beam. In the case of focused ultrasound, the ultrasound waves can be focused at a given point. The high energy levels carried in a HIFU beam can therefore be magnified further and delivered with precision to a small volume, while sparing surrounding tissues. FUS energy can be deposited in small areas providing a substantial advantage for drug targeting. The volume of energy deposition following a single HIFU exposure is small and will vary according to transducer characteristics but is typically cigar shaped with dimensions in the order of 1–3 mm (transverse) 8–15 mm (along beam axis) [1]. HIFU transducers deliver ultrasound with intensities in the range of 100–10,000 W/cm^2 to the focal region, with peak compression pressures of up to 30 MPa peak and rarefaction pressures up to 10 MPa [2]. The ultrasound wave propagates through tissues, causing alternating cycles of increased and reduced pressure (compression and rarefaction, resp.). In the case of tissue ablation during HIFU treatments, the temperature at the focus can rise rapidly (up to 80°C) which can cause cell damage. "Inertial cavitation" occurs simultaneously with tissue heating. Ultrasound affects the molecular structure of the tissues during the alternating cycles of compression and rarefaction. During rarefaction, gas can be drawn out of the solution to form bubbles, which can collapse rapidly. In this case injury is induced through a combination of mechanical stresses and thermal effects at a microscopic level. When Ultrasound is applied in biological systems it can induce local tissue heating, cavitation, and radiation force, which

can be used to initiate local (focal) drug delivery, increase permeation through membranes, and enhance diffusivity of drugs, respectively, only at the site of sonication therefore allowing control of local drug release [3].

The ability of FUS to induce thermal or mechanical effects at very defined (focal) locations in living tissue has been first described in 1942, when Lynn et al. tested FUS [4] in the brain. In the 1950s Fry brothers developed a clinical FUS device for treating patients with Parkinson disease. They used a sonication system in combination with X-rays to determine the target location relative to skull and to focus the ultrasound beam through a craniotomy into deep brain for effective functional neurosurgery [5]. Later on, in the 1980s the first FDA-approved FUS system, Sonocare CST-100, was developed to treat ocular disorders such as glaucoma and many patients were successfully treated with this system [6]. More recently substantial technological developments have led to new FUS equipment for a number of different applications. Current research and development aims to explore transducer technology and array design to achieve faster delivery of focal sonications, to improve transducer accessibility (smaller devices) or fit them to certain parts of the body such as a helmet of arrays for brain focal treatment.

Several FUS devices are investigated currently in clinical trials. These devices can operate under image guidance to provide real-time monitoring of the treatment.

Guidance and monitoring of acoustic therapy controls the treatment region and minimizes damage to adjacent structures. Monitoring using real-time imaging, such as with sonography (diagnostic ultrasound), ensures that the targeting of the FUS beam is maintained on the correct area throughout the procedure. MRI and sonography are the two imaging modalities currently being used for guidance and monitoring FUS therapy. MRI has the advantage of providing temperature data during FUS treatment. However, MRI guidance is expensive, labor-intensive, and of lower spatial resolution in some cases. Sonographic (ultrasound) guidance provides the benefit of imaging using the same form of energy that is being used for therapy. The advantage of this is that the acoustic window can be verified with sonography. Therefore, if the target cannot be well visualised with sonography, then it is unlikely that FUS therapy will be effective. Temperature monitoring using sonography is not yet available [2]. InSightec manufactures the ExAblate2000 which uses MRI for extracorporeal treatment of uterine fibroids (FDA-approved) with significant success, and extensive current research focuses on investigating its application in other parts of the body [7, 8]. ExAblate technologies are used for prostate cancer or bone metastasis (ExAblate 2100 Conformal Bone System); these applications are currently under development by InSightec. The Ablatherm HIFU/US consists of a transrectal probe for prostate treatment and has CE mark approval [9]. The Sonablate 500, an ultrasound guided system uses a transrectal probe to carry out prostate cancer focal ablation [10]. The Sonalleve HIFU/MR is an MR compatible device developed to examine a series of applications as fibroids and other body sites [11]. A recently introduced device is the transcranial MR-guided focused ultrasound. This is a hemispheric phased-array transducer (ExAblate Neuro; InSightec Ltd., Tirat Carmel, Israel) with each element driven separately, providing individual correction of skull distortion as well as electronic steering. The device received CE Mark for neurological disorders recently (December 2012). The device has been used for the treatment of neuropathic pain essential tremor and there is also evidence of possible application for brain tumours [12, 13]. Essential tremor noninterventional functional neurosurgery treatment has shown an immense potential of transcranial MRgFUS application to induce lesions focally and treat patients nonsurgically [14].

2. Fundamentals of Focused Ultrasound Treatments

Ultrasound propagates as mechanical vibrations that induce molecules within the medium to oscillate around their positions in the direction of the wave propagation. The molecules form compressions and rarefactions that propagate the wave. The ultrasound energy is decreased exponentially through the tissue. The decrease in acoustic energy per unit distance travelled is called "attenuation." The rate of energy flow through a unit area, normal to the direction of the wave propagation, is called acoustic intensity. At 1 MHz the ultrasound wave is attenuated about 50% while it propagates through 7 cm of tissue. The attenuated energy is transformed into temperature elevation in the tissue [15, 16].

Ultrasound is transmitted from one soft tissue layer to another. Usually in soft tissues a small amount of wave is reflected back except at the soft tissue-bone interface where approximately one-third of the incident energy is reflected back. In addition, the amplitude attenuation coefficient of ultrasound is about 10–20 times higher in bone than in soft tissues. This causes the transmitted beam to be absorbed rapidly within the bone [17]. Ultrasound induces mechanical vibration of the particles or molecules of a material. Each particle moves small distances from its rest position but the vibrational energy is propagated as a wave traveling from particle to particle through the material. Ultrasound is attenuated as it travels through a tissue due to beam divergence, absorption, and deflection of the acoustic energy. Deflection consists of the processes of reflection, refraction, and scattering. The energy required for a sound wave to travel through a tissue must overcome the internal friction intrinsic to any material. As a sound wave travels through tissue, it continually loses a proportion of its energy to the tissue (attenuation). The reasons of attenuation are divergence, deflection, and absorption. Divergence of the sound beam spreads the acoustic energy over a larger beam area and reduces the intensity along the beam axis. Deflection of acoustic energy out of the beam also reduces the intensity. The greatest cause of attenuation in the body is absorption, in which energy is transferred from the sound beam to the tissue and ultimately is degraded to heat. The amount of absorption depends on the frequency of the ultrasound beam. Whenever a sound beam encounters a boundary between two materials, some of the energy is reflected and the remainder is transmitted through the boundary. The direction of the reflected wave, or the echo, depends on the

orientation of the boundary surface to the sound wave. The major physical effects of ultrasound are heat, mechanical effects, cavitation, and chemical effects. Acoustic impedance is a measure of the resistance that a material offers to the passage of an ultrasound wave and is expressed in units of rayls (kg/m^2/sec). Acoustic impedance of water is 1.5×10^{-6} Mrayls whereas that of bone is 8×10^{-6} Mrayls. The greater the difference in acoustic impedance between two materials, the stronger the echo (reflected wave) arising from their interface. Heat is the most common physical effect generated by sound waves in the body. When the rate of heat generation is higher than the rate of heat dissipation in the body, the body temperature will rise significantly. Temperatures above 43°C if maintained for extended period can be damaging. Mechanical effects, such as the breaking of bonds, can occur if the amplitude of the ultrasound wave is significantly large. Cavitation occurs when an ultrasound beam of sufficient intensity travels through a liquid in which gas bubbles have been generated. The alternating high- and low-pressure periods of the ultrasound wave forces the bubbles to contract and expand. The amplitude of the bubble oscillation increases with increasing ultrasonic intensity. During the bubble contraction, the internal pressure can increase and the temperature can reach 10,000°C. A sonic explosion can occur, releasing a large amount of energy, although for very short (μm) distances. Tissues and cells in the vicinity can be damaged. Cavitation is the responsible mechanism for the disintegrations of stones in lithotripsy. Chemical effects, such as the acceleration of chemical reactions, can occur due to an increase in the temperature and pressure. These effects would be expected in high-intensity ultrasound fields [18]. When ultrasound beams are focused a focal diameter of 1 mm can be achieved at 1.5 MHz. The length of the focus is 5–20 times larger than the diameter. If the ultrasound beam is transmitted from an applicator 2–3 cm in diameter, the ultrasound intensity at the millimeter-sized focal spot can be several hundred times higher than in the overlying tissues. Typical diagnostic ultrasound transducers deliver ultrasound with time-averaged intensities of approximately 0.1–100 mW/cm^2 or compression and rarefaction pressures of 0.001–0.003 MPa, depending on the mode of imaging. In contrast, HIFU transducers deliver ultrasound with intensities in the range of 100–10,000 W/cm^2 to the focal region, with peak compression pressures of up to 30 MPa and peak rarefaction pressures up to 10 MPa [2]. The ultrasound exposure drops off rapidly across the area within the sonication path and therefore focusing provides a method to overcome attenuation losses and to concentrate energy deep in the body while avoiding the surrounding tissues [19].

Focusing is dramatically improved with the use of transducer arrays that are driven with signals having the necessary phase difference to obtain a common focal point. The main advantage of these phased arrays is that the focal spot can be controlled. In addition, the electronically focussed beam allows multiple focal points to be induced simultaneously or fast electronic scanning of the focal spot which increases the size of the focal region. This feature allows shorter treatment time [20, 21].

3. Image Guided Focused Ultrasound Mediated Drug Delivery

3.1. Using Clinical Imaging and Drug Delivery Systems. The combination of high-intensity focused ultrasound together with high-resolution MR guidance has created a system that can produce tissue destruction deep within solid organs without any invasion. Accurate targeting and detailed accurate thermal mapping are provided by MRI [22].

In recent years imaging has been combined with FUS to provide real-time manipulation of drug guidance within the targeted area. Ultrasound and magnetic resonance (MR) imaging are widely used clinical imaging modalities that can be combined with FUS for image guided FUS treatments. In the area of drug delivery ultrasound microbubbles or nanocarriers providing contrast enhancement can be used.

When using nanocarriers sensitive to mechanical forces (the oscillating ultrasound pressure waves) and/or sensitive to temperature, the content of the nanocarriers can be released locally. Thermosensitive liposomes have been suggested for local drug release in combination with local hyperthermia more than 25 years ago. Microbubbles may be designed specifically to enhance cavitation effects. Real-time imaging methods, such as magnetic resonance, optical and ultrasound imaging, have led to novel insights and methods for ultrasound triggered drug delivery. Image guidance of ultrasound can be used for: (1) target identification and characterization; (2) spatiotemporal guidance of actions to release or activate the drugs and/or permeabilize membranes; (3) evaluation of biodistribution, pharmacokinetics and pharmacodynamics; and (4) physiological read-outs to evaluate the therapeutic efficacy.

3.2. FUS Induced Increase in Temperature for Tissue Specific Drug Release from Thermosensitive Carriers. Liposomes show significant advantages for drug delivery in tumours. The enhanced permeability and retention effect has served as a basic rationale for using liposomes and other nanoparticles to treat solid tumors. However, it has been recently noticed that the enhanced permeation and retention effect does not guarantee a uniform delivery. This heterogeneous distribution of therapeutics is a result of physiological barriers presented by the abnormal tumor vasculature and interstitial matrix. In a recent review by Jain and Stylianopoulos, the barriers of tumour nanoparticle delivery were summarised. First, the abnormal structure of tumor vessels results in heterogeneous tumor perfusion and extravasation, and a hostile tumor microenvironment that supports drug resistance and tumor progression. Second, in highly fibrotic tumors, the extracellular matrix blocks penetration of large nanoparticles leaving them concentrated in perivascular region. To overcome these barriers the authors suggest normalization of the vascular network and the extracellular matrix as well as development of nanoparticles that release therapeutic agents in response to the tumor microenvironment or an external stimulus (such as heat light and HIFU) [23].

Thermosensitive carriers have a long presence in research and development. Yatvin et al. first described the effect of hyperthermia on liposomal carriers in 1978 [24]. However,

development of thermosensitive liposomal carriers for cancer was only introduced as recently as 1999 when Needham's group evaluated phase transition enhanced liposomal permeability [25]. *In vivo* data using cancer models were presented one year later when the authors described a new lipid formulation containing doxorubicin optimized for mild hyperthermic temperatures (39°C to 40°C) that are readily achievable in the clinic leading to very rapid release times of the drugs. This new liposome, in combination with mild hyperthermia, was found to be significantly more effective than free drug or current liposome formulations at reducing tumour growth in a human squamous cell carcinoma xenograft [26]. These low temperature-sensitive liposomes (LTSL) were further developed in dogs having canine tumours to show a superior efficiency [27, 28]. A formulation based on these thermosensitive liposomes took the brand name Thermodox and was further developed by Celsion corporation. Thermodox liposomes can be triggered to release their payload by any heat-based treatment such as radiofrequency thermal ablation (RFA), microwave hyperthermia, and high intensity focused ultrasound (HIFU). Results from a Phase I study that used Thermodox was recently published [29]. In a Phase I study researchers used escalating dose of Thermodox with radiofrequency (RF) ablation and concluded that Thermodox can be safely administered at 50 mg/m^2 in combination with RF ablation. Currently Thermodox in combination with RF ablation is being tested in a large Phase I study to treat hepatocellular carcinoma [30].

The concept of using liposomes and HIFU was introduced recently, in 2006 when Frenkel et al. used liposomal doxorubicin (Doxil) in combination with pulsed high-intensity focused ultrasound (HIFU) exposures in a murine breast cancer tumor model. Doxil is a stable liposomal preparation that has no response to increased temperature [31] and was developed to minimise doxorubicin's cardiotoxicity, by encapsulating doxorubicin within stealth liposomes. Although Doxil achieves long circulation of doxorubicin with minimum cardiotoxicity it does not rapidly release the drug within the tumour. Pulsed-HIFU exposures were not found to enhance the therapeutic delivery of doxorubicin and did not induce tumour regression. However, a fluorescent dextran showed blood vessels to be dilated as a result of the exposures. Experiments with polystyrene nanoparticles of similar size to the liposomes showed a greater abundance to be present in the treated tumours [32]. Although this study did not achieve or prove a therapeutic advantage of the use of HIFU with temperature stable liposomes it showed clearly that pulsed HIFU induces a substantial increase of permeation of macromolecules and nanoparticles in tumours.

In 2007 Dromi et al. presented the first study on thermosensitive liposomes (Low Temperature Sensitive Liposomes (LTSL)) and HIFU. The authors investigated pulsed-high intensity focused ultrasound as a source of hyperthermia with thermosensitive liposomes to enhance delivery and efficacy of doxorubicin in murine adenocarcinoma tumours. *In vitro* treatments simulating the pulsed-HIFU thermal dose (42°C for 2 min) triggered release of 50% of doxorubicin from the thermosensitive liposomes; however, no detectable release from the nontemperature sensitive liposomes (similar to Doxil) was observed. Similarly, *in vivo* experiments showed that pulsed-HIFU exposures combined with the LTSL resulted in more rapid delivery of doxorubicin as well as significantly higher concentration within the tumour when compared with LTSLs alone or nonthermosensitive liposomes, with or without exposures [33].

In a later study the same team developed MR imageable thermosensitive liposomes (iLTSL), with the objective to characterise drug release in phantoms and *in vivo*. An MRI contrast agent (ProHance® Gd-HP-DO3A) and doxorubicin were loaded and drug release was quantified by spectroscopic and fluorescence techniques, respectively. Release with HIFU under MR guidance was examined in tissue-mimicking phantoms containing iLTSL and in a VX2 rabbit tumour model. iLTSLs demonstrated consistent size and doxorubicin release kinetics. Release of doxorubicin and ProHance® from iLTSL was minimal at 37°C but fast when heated to 41.3°C. Relaxivity of iLTSL increased significantly from 1.95 ± 0.05 to 4.01 ± 0.1 mMs^{-1} when liposomes were heated above the phase transition temperature indicating the release of ProHance® from liposomes and its exposure to the aqueous surroundings. Importantly, the signal increase corresponded spatially and temporally to MR-HIFU-heated locations in phantoms. *In vivo*, the investigators confirmed MRI signal after i.v. iLTSL injection and after each 10-min heating, with greatest increase in the heated tumour region. The authors concluded that MR-HIFU combined with iLTSL may enable real-time monitoring and spatial control of drug release from liposomes [34].

In a follow-up study the authors investigated the effect of iLTSL in rabbits bearing VX2 tumours. In that study image-guided noninvasive hyperthermia was applied for a total of 30 min, completed within 1 h after LTSL infusion and quantified doxorubicin release in tumours with HPLC and fluorescence microscopy. Sonication of VX2 tumours resulted in accurate and spatially homogenous temperature control in the target region. LTSL+MR-HIFU resulted in significantly higher tumour doxorubicin concentrations (3.4-fold greater compared LTSL resp.). The authors observed that free doxorubicin and LTSL treatments appeared to deliver more drug in the tumour periphery as compared to the tumour core indicating that HIFU induced hyperthermia and LTSL increases doxorubicin's permeability as doxorubicin was found in both the tumour periphery and core [35]. The group further developed a heating algorithm using the same rabbit tumour model proving that the use of the binary feedback algorithm results in accurate and homogenous heating within the targeted area [36]. A computational model that simulated the tissue heating with HIFU treatment and the resulting hyperthermia that leads to drug release was developed by Haemmerich. In this model a spatiotemporal multicompartmental pharmacokinetic model simulated the drug release in the blood vessels and its transport into the interstitium as well as cell uptake. Two heating schedules were simulated each lasting 30 min, the first corresponding to hyperthermia, (HT; 43°C) and the second corresponding to hyperthermia followed by a high temperature (50°C) for

20s pulse, (HT+). Using the computational model (validated in rabbit VX2 tumours) the authors found that cellular drug uptake is directly related to hyperthermia duration. HT+ enhanced drug delivery by 40% compared to HT [37]. The study indicates the importance of simulations in the application of drug delivery mechanisms to tumours.

In addition to the progress in the understanding of the physical mechanism of drug delivery from well validated thermosensitive liposomes carrying doxorubicin, researchers further investigated the chemical composition of such liposomes in response to HIFU induced hyperthermia.

De Smet et al. compared thermosensitive liposomes carrying doxorubicin and ProHance®. Two temperature-sensitive systems composed of the following lipids DPPC:MPPC: DPPE-PEG2000 (low temperature-sensitive liposomes; LTSL) and DPPC: HSPC:cholesterol:DPPE-PEG2000 (traditional temperature-sensitive liposomes; TTSL) were investigated for their stability and release profile at 37°C and 42°C in phantoms using MRI 1,2-Dipalmitoyl-*sn*-glycero-3-phosphocholine (DPPC), 1-palmitoyl-*sn*-glycero-3-phosphocholine (MPPC), 1,2-dipalmitoyl-*sn*-glycero-3-phosphoethanolamine-N[methoxy(polyethyleneglycol)-2000] (DPPE-PEG2000), hydrogenated-L-α-phosphatidylcholine (HSPC). The LTSL system showed a higher leakage of doxorubicin at 37°C, but a faster release of doxorubicin at 42°C compared to the TTSL system indicating that lipid composition plays an important role on stability and release profile [38]. The authors further investigated the more stable traditional temperature sensitive liposomes carrying doxorubicin and ProHance® *in vivo* in rats bearing 9L gliosarcoma tumours. A clinical MRI-HIFU system was applied in a proof-of-concept study to induce local hyperthermia for 30 min. The local temperature-triggered release of ProHance® was monitored with interleaved T_1 mapping of the tumour. A good correlation between the ΔR_1 (change in longitudinal relaxation rate $\Delta R_1 = \Delta(1/T_1)$) and the intratumour doxorubicin and gadolinium concentration was found, implying that the *in vivo* release of doxorubicin from the thermosensitive liposomes can be probed in situ with the longitudinal relaxation time of the coreleased MRI contrast agent (dose painting).

Temperature sensitive liposomes release their encapsulated drugs at the melting phase transition temperature (T_m) of the lipid bilayer. At this T_m the lipid membrane changes its structure as it transfers from a gel to the liquid crystalline phase [39]. When the liposomal membranes are in the gel phase they show less permeability to molecules and water compared to the liquid crystalline phase.

The liposomes' transition to the liquid crystalline phase can be achieved with the incorporation of a lysophospholipid such as MSPC (R = $-C_{17}H_{35}$). This lipid is also the lipid used in the thermodox® formulation [40]. A potential disadvantage of MSPC containing liposomal formulations is their rapid doxorubicin leakage at 37°C [37]. Tagami et al. prepared temperature sensitive liposomes using nonionic surfactants Brij which are PEG-ylated lysolipids resembling the chemical structures of MSPC and DSPE-PEG(2000). Results indicated that the optimal acyl chain length of the surfactant was between C(16) and C(18) with a saturated carbon chain and a PEG repeating unit ranging between 10 and 100 with a molecule weight above 600 Da. In the panel of surfactants tested, Brij78 was optimal and could be incorporated into the liposomes by the thin film hydration or the postinsertion method with an optimal range of 1 to 8 mol% [41]. The authors continued with *in vivo* experiments in mice bearing mammary carcinoma cells EMT-6, investigating Gd^{3+}DTPA (diethylene triamine pentaacetic acid) release with relaxometry. The authors observed a good correlation between relaxation enhancement in the heated tumour and the inhibition of tumour growth at day 21 after treatment [42].

Kono et al. investigated the effect of poly [2-ethoxy(ethoxyethyl)vinyl ether] chains (having a lower critical solution temperatures) and polyamidoamine G3 dendron-based lipids having Gd^{3+} chelate residues into PEGylated liposomes. These designed liposomes exhibited excellent ability to shorten the longitudinal proton relaxation time. When administered intravenously into tumour-bearing mice, accumulated liposomes in tumours increased with time, reaching a constant level 8 h after administration by following T_1-weighted MRI signal intensity in tumours. Liposome size affected the liposome accumulation efficiency in tumours: liposomes of about 100 nm diameter were accumulated more efficiently than those with about 50 nm diameter. Tumour growth was strongly suppressed when liposomes loaded with doxorubicin were administered intravenously into tumour-bearing mice and the tumour was heated mildly at 44°C for 10 min at 8 h after administration [43].

In our group we have investigated the potential of an MRI labelled phospholipid/lysolipid containing liposome to accumulate in tumours and release the drug under conditions of mild hyperthermia induced by FUS.

We label the liposome nanoparticles with a lipid that consists of a DOTA [1,4,7,10-tetraazacyclododecane-1,4,7,10-tetraacetic acid] headgroup (Figure 1) [44, 45]. Introducing the imaging lipid in the lipid bilayer provides a better and clearer monitoring of liposomal particle kinetics and a better knowledge of the time required for maximum nanoparticles accumulation in tumours (monitored by MRI).

Although most research studies have focused mainly in thermoresponsive liposomes and FUS activation of drug release, there is limited work on the use of polymers (thermoresponsive or not) and their application in FUS triggered drug delivery. The effect of ultrasound on drug release from polymers was studied in 1989 by Kost et al. and indeed the authors found that ultrasound can increase the polymer degradation rate leading to 20 times higher release rate. Interestingly the authors observed that the release rate increased in proportion to the intensity of ultrasound proposing that cavitation appeared to play a significant role [46].

3.3. Ultrasound and Microbubbles to Increase Drug Permeability in Tissues. Triggered drug delivery using an external physical force provides the required control of drug deposition in certain tissues avoiding exposure of healthy tissues

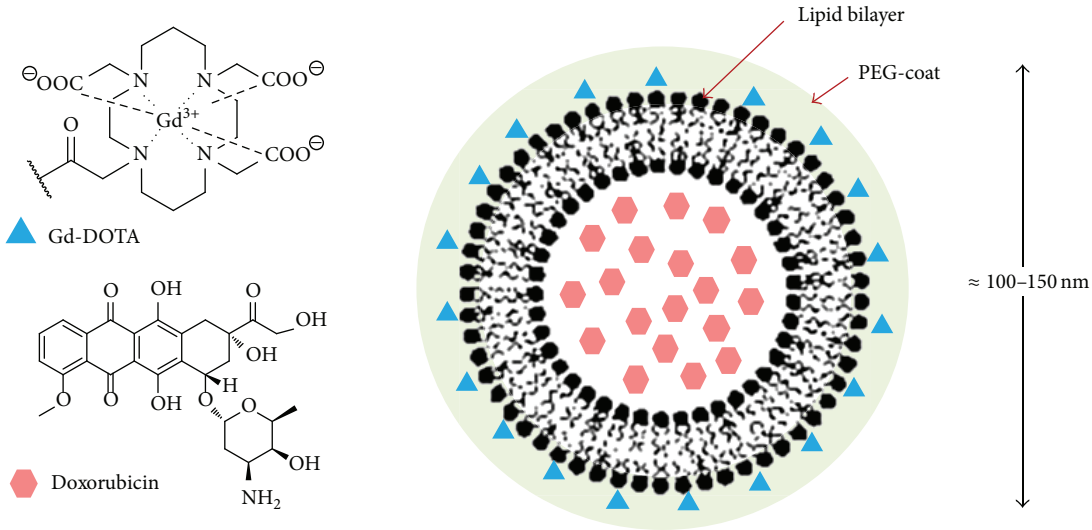

Figure 1: Thermosensitive liposome for real-time monitoring of nanoparticle accumulation in tumours.

to high (toxic) concentrations. The trigger induced delivery should be acute and the effect induced on nontargeted tissues nondamaging and reversible. Hyperthermia induced by a means like ultrasound can be exploited as an external trigger in drug delivery [3, 47].

Mild hyperthermia can be induced by pulsed FUS that can reduce extreme tissue heating by allowing the tissue to cool down between US exposures [48]. The increase in temperature can be 3–5°C (hyperthermia) despite the high energy deposited in the tissue. Hyperthermia applied in tumours can increase blood flow and enhance vascular permeability. Studies with canine soft tissue sarcoma and human tumour clinical studies have also demonstrated that hyperthermia improves tumour oxygenation and enhances response of such tumours to radiotherapy or chemoradiotherapy. The increased blood flow and vascular permeability caused by temperatures such as 42°C may also improve the delivery of chemotherapy drugs, immunotherapeutic agents and genes to tumour cells [49]. FUS exposures in pulsed mode lower the rates of energy deposition and generate primarily mechanical effects for enhancing tissue permeability to improve local drug delivery. These pulsed exposures can be modified for low-level hyperthermia as an enhancement of drug delivery that would lead to better drug deposition and better therapeutic effect [50]. Mild hyperthermia of 42°C can improve the degree of nanocarrier extravasation as shown by Kong et al. [51]. The reason that this leads to increased extravasation maybe due to downregulation of VE-cadherin that contributes to vascular integrity as it was shown in HUVEC endothelial cells [52]. It is clear that hyperthermia can provide a boost to extravasation and drug deposition in tumours. This should provide an adjuvant effect when nanocarriers are used and accumulate in tumours due to enhanced permeation and retention effect. It would be interesting to investigate the effect of hyperthermia on tumour/tissue drug clearance.

FUS can also induce nonthermal effects on tissues. Acoustic cavitation can be induced using microbubbles exposed to US [53]. Acoustic cavitation can be defined as the growth, oscillation, and collapse of gas containing bubbles under the influence of the varying pressure field of sound waves in a fluid and can have an effect on the permeability of a biological tissue [53–55]. There are two types of acoustic cavitation: noninertial and inertial cavitation. The noninertial (stable) cavitation occurs when bubbles persist for a number of acoustic cycles. In this case the bubble's radius increases and decreases (expands and contracts) according to the applied US frequency. Inertial (transient cavitation) occurs when bubbles grow faster expanding 2- or 3-fold their resonant size, oscillate unstably, and collapse in a single compression half cycle [54]. It has been considered that the primary mechanism to affect the structure of intact cells is inertial cavitation that can induce irreversible damage as well as increase cell membrane permeability [56, 57].

An important application of HIFU and microbubbles lies in the area of altering the permeability of the blood brain barrier (BBB). In a study in 2002, Mesiwala et al. observed that HIFU could alter BBB permeability. HIFU induced reversible, nondestructive, BBB disruption in a targeted area and this opening reversed after 72 h. The authors showed with microscopy that HIFU either entirely preserved brain architecture while opening the BBB, or generated tissue damage in a small volume within the region of BBB opening. Further electron microscopy suggested that HIFU disrupted the BBB by opening capillary endothelial cell tight junctions, a mechanism that was not observed in other methods used to open BBB [58].

The effect of FUS on tight junctions' integrity was later confirmed in a study investigating rat brain microvessels

after this BBB disruption. The authors used immunoelectron microscopy to identify tight junctional proteins such as occludin, claudin-1, claudin-5, and submembranous ZO-1 after sonication. They found substantial redistribution and loss of occludin, claudin-5 and ZO-1. However, claudin-1 seemed less involved. Monitoring the leakage of horseradish peroxidase (MW 40 KDa) the authors observed that the BBB disruption appears to last up to 4 h after sonication [59]. In a later study the role of caveolin in the mechanism of FUS-BBB enhanced permeation was suggested. In a study investigating caveolae density it was found that caveolae and caveolin-1 were primarily localized in the brain microvascular endothelial cells of all the animals tested (rats) regardless of treatment, and that caveolin-1 expression was the highest in the rats treated with both FUS and microbubbles. The authors concluded that caveolin-1-mediated transcellular transport pathway may cooperate with other transport pathways (e.g., tight junctional disruption) to induce opening of the BBB [60].

Hynynen and colleagues investigated the BBB FUS enhanced permeability in rabbits. Rabbit brains were exposed to pulsed focused ultrasound while microbubbles were intravenously administered. The BBB opening was measured by an MRI contrast agent evaluating the local enhancement in the brain. The authors found that low ultrasound powers and pressure amplitudes were found to cause focal enhancement of BBB permeability. Trypan blue injected before animals were sacrificed indicated blue spots in the areas of the sonicated locations [61]. The authors concluded that HIFU disruption of BBB could be used enhancing drug delivery to the brain [62].

McDannold et al. tested the safety of this method by searching for ischemia and apoptosis in areas with BBB disruption induced by pulsed ultrasound in the presence of gas bubbles and by looking for posttreatment effects up to one month after sonication. Pulsed ultrasound exposures (sonications) were performed in the brains of rabbits under monitoring by MRI. BBB disruption was confirmed with contrast-enhanced MR images. Whole brain histologic examination was performed using staining for ischemic neurons and TUNEL staining for apoptosis. Tiny regions of extravasated red blood cells scattered around the sonicated locations, indicated capillaries. Despite these vasculature effects, only a few cells in some of the sonicated areas showed evidence of apoptosis or ischemia. The authors found that ultrasound-induced BBB disruption is possible without inducing substantial vascular damage that would result in ischemic or apoptotic death to neurons [63].

The method could find application in the delivery of large therapeutic molecules that do not normally permeate the BBB. Herceptin (trastuzumab), a humanized anti-human epidermal growth factor receptor 2 (HER2/c-erbB2) monoclonal antibody, was delivered locally and noninvasively into the mouse central nervous system through the blood-brain barrier under image guidance by using an MRI-guided focused ultrasound. The amount of herceptin delivered to the target tissue was correlated with the extent of the MRI-monitored barrier opening, making it possible to estimate indirectly the amount of Herceptin delivered. The method could be used to treat breast cancer metastases to the brain [64]. It was further shown that dopamine D(4) receptor-targeting antibody could also be delivered using the same technique in the brain [65, 66].

Delivery of small molecules can also be enhanced with the use of HIFU cavitation disruption of the BBB. Treat et al. demonstrated relatively high concentrations of doxorubicin in the brain with minimal healthy tissue damage effects. The authors observed that doxorubicin accumulation in nontargeted contralateral brain tissue remained significantly lower. MRI signal enhancement in the sonicated region correlated strongly with tissue doxorubicin concentration, suggesting that contrast-enhanced MRI could perhaps indicate drug penetration during image-guided interventions [67].

Konofagou and coworkers assessed the spatial permeability of the BBB-opened region using dynamic contrast-enhanced MRI (DCE-MRI) in mice. The authors processed DCE-MR images using the general kinetic model and the reference region model. Permeability maps were generated and the K_{trans} (the transfer rate constant from the intravascular system to the extracellular extravascular space) values were calculated for a predefined volume of interest in the sonicated and the control area for each mouse. The results demonstrated that K_{trans} in the BBB-opened region was at least two orders of magnitude higher when compared to the contralateral (control) side [68].

There are several parameters to affect the level of BBB enhanced permeability and the endothelial tight junctions disruption; the pulse sequence comprising short bursts, the spacing between bursts or the rate of infusion of the microbubbles, and the size of microbubbles were found to affect the effect on BBB disruption [69, 70].

The method could be applied for a number of therapeutic applications. The brain-derived neurotrophic factor (BDNF) was delivered to the left hippocampus in mice through the noninvasively disrupted blood-brain barrier (BBB) using focused ultrasound. The BDNF bioactivity was found to be preserved following delivery as assessed quantitatively by immunohistochemical detection of the pTrkB receptor and activated pAkt, pMAPK, and pCREB in the hippocampal neurons. It was shown that BDNF delivered this way induced signalling effects in a highly localized region in the brain [71].

However it is the area of targeting brain tumours that have attracted most interest in the FUS disrupted BBB [72]. Mei and colleagues investigated the effects of targeted and reversible disruption of the blood-brain barrier by MRI-guided focused ultrasound and delivery of methotrexate to the rabbit brain. The authors recorded that the methotrexate concentration in the sonicated group was notably higher than that in both the control group (intravenous administration) and the internal carotid artery administered group. They observed a greater than 10-fold increase in the drug level compared to internal carotid administration without FUS [73].

Liu et al. investigated the delivery of 1,3-bis(2-chloroethyl)-1-nitrosourea (BCNU) to glioblastomas in rats with induced tumours with the help of FUS. The authors found that FUS significantly enhanced the penetration of BCNU through the BBB in normal and tumour-implanted brains

without causing bleeding. Surprisingly, treatment of tumour-implanted rats with focused ultrasound alone had no beneficial effect on tumour progression. However, treatment with focused ultrasound before BCNU administration controlled tumour progression and improved animal survival relative to untreated controls [74].

Liu and colleagues recently assessed FUS-mediated delivery of an iron oxide magnetic nanoparticle (MNPs) conjugated to an antineoplastic agent, epirubicin. They used MNPs because of the favourable MR imaging characteristics, which could facilitate imaging. They demonstrated a substantial accumulation of MNPs, as well as epirubicin, up to 15 times the therapeutic range in the brain when delivered with FUS. They further showed decreased tumour progression in animals with brain tumours that received MNP with epirubicin via FUS [75].

Receptors targeting liposomal nanocarriers have been combined with MRgFUS to treat brain tumours. In a recently presented study it was shown that pulsed HIFU and human atherosclerotic plaque-specific peptide-1- (AP-1-) conjugated liposomes containing doxorubicin (AP-1 Lipo-Dox) acted synergistically in an experimental brain tumour model. Prior to each sonication, AP-1 Lipo-Dox or unconjugated Lipo-Dox were administered intravenously, and the concentration in the brain was quantified. Drug injection with sonication increased the tumour-to-normal brain doxorubicin ratio of the target tumours by about twofold compared with the control tumours. Moreover, the tumour-to-normal brain ratio was the highest after the injection of AP-1 Lipo-Dox with sonication. The results of this study indicate that combining targeting strategies can substantially enhance delivery of chemotherapy in the brain [76]. In a separate study the authors investigated the pharmacokinetics of ^{111}I-labeled AP1-Lipo-dox using microSPECT. The authors confirmed that sonication increased liposomal doxorubicin concentrations in tumour areas (murine glioblastoma) and that molecular targeting acts synergistically with FUS [77].

Targeted gene transfer into central nervous system was investigated using MRI-guided focused ultrasound-induced blood-brain barrier disruption. The results of this study showed that MRI-guided FUS achieved plasmid DNA transfer across the opened BBB furthermore plasmid ware internalized into the neurons presenting heterogeneous distribution and numerous transparent vesicles were observed in the cytoplasm of the neurons in the sonicated region, suggesting vesicle-mediated endocytosis. BDNF (and BDNF-EGFP) expressions were markedly enhanced by the combination of ultrasound and pBDNF-EGFP-loaded microbubbles about 20-fold than that of the control group. The method by using MRI-guided FUS to induce the local BBB disruption could accomplish effective targeted exogenous gene transfer in the CNS. In this study the microbubbles were used as the plasmid carrier. The investigators conjugated plasmid onto the surface of microbubbles and they coated these carriers using polymers in a layer by layer technique [78].

An exciting application is the delivery of therapeutic stem cells to the brain using FUS to potentially treat neurodegenerative diseases, traumatic brain injury, and stroke. MRI guidance was used to target the ultrasound beam thereby delivering iron-labeled, green fluorescent protein (GFP) expressing neural stem cells specifically to the striatum and the hippocampus of the rat brain. Immunohistochemical analysis confirmed the presence of GFP-positive cells in the targeted brain regions suggesting that MRIgFUS may be an effective alternative to invasive intracranial surgery for stem cell transplantation [79].

Although a very efficient approach, the use of microbubbles to enhance drug permeation through tissues, it may require significant safety consideration. In a key study in 2005 Prentice et al. presented clearly in a well-designed experimental setup that there are important interactions between individual cells and violently cavitating microbubbles leading to large pores in the cell membrane (sonoporation) [80]. These effects on cell membrane will need to be thoroughly investigated at microscopical and molecular level to design efficient and safe FUS regimes.

3.4. Drug Delivery Dosage Forms and FUS Future Perspective. During the last few years there has been an expansion in research in MRgFUS drug delivery. The main dosage forms tested in MRgFUS drug delivery strategy are the thermosensitive liposomes and the lipid based microbubbles that can be conjugated with drugs or other liposomes on their surface [78, 81].

There is limited research in the area of using other responsive materials or nanocarriers. Rapoport discussed recently the potential of using micelles and FUS [82] for enhanced tissue permeation. Micelles are nanosized carriers able to carry hydrophobic drugs; their combination with FUS could substantially enhance their delivery in tissues. Kostarelos and colleagues suggested the incorporation of thermosensitive peptides onto liposome bilayers to enhance thermoresponsiveness [83], and the group of Lammers designed polymer-based microbubbles for ultrasound drug release [84].

It is clear that already established delivery systems such as different structurally nanocarriers have not been investigated in combination with image guided FUS. It would be interesting to see the effect of FUS on the enhanced permeability of micelles, polymers (dendrimers cyclodextrins), or metal nanoparticles (gold-iron) to tissues. Thermosensitive materials have been hardly explored in this field. Polymers or proteins that respond to small change of temperature could form suitable image guided FUS triggered platforms.

The effects of FUS in biological tissues with or without carriers will require a more thorough investigation to understand the short- and long-term effects of ultrasound in the body and the complex environments such as tumours, blood vessels, and bone. The mechanism of FUS induced hyperthermia and/or the FUS tissue permeability increase is not well understood at cellular and molecular levels. There is limited knowledge on the effects of FUS on genomic DNA and if certain proteins are overexpressed after FUS treatment.

In addition to the above, the frequency of FUS drug delivery treatments (or dosing) and the long-term effects in the body will have to be investigated in preclinical studies in order to design a FUS drug treatment regime.

An imaging modality will have to be used for accurate image guided FUS therapy. In the case of MRI clinically approved contrast enhancing agents will have to be added to the delivery system to monitor carriers' distribution in the treatment area as well as efficient and rapid release.

Considering the approval in clinical applications, such treatments will require the control of several factors such as drug and drug carrier, MRI contrast enhancing agents, and MRgFUS parameters, and this could mean several regulatory hurdles. However, the fact that most of the components (FUS, liposomes) have been tested in clinical trials is encouraging for such approach to move forward.

Most of the current strategies to increase tumour specificity of nanocarriers include the use of tumour biomarkers for either targeting (receptors) or for triggered release (internal stimuli; pH proteases) and/or the use of external stimuli such as light and ultrasound. Biomarkers and internal stimuli may vary in different tumours indicating that such nanocarriers for cancer treatments should be "individualised." External stimuli can be used independent the tumours characteristics and therefore guarantee a more uniform effect. FUS can be used as an external stimulus to activate drug delivery in tissues. It also shows the significant advantages of being noninvasive as well as controlled and focused.

Overall MRgFUS drug delivery is a novel and valuable tool to increase drug targeting and tissue specific drug delivery. It is expected that future studies will prove the clinical efficacy of MRgFUS drug delivery applications.

Conflict of Interests

The authors of the paper do not have a direct financial relation with any commercial identity mentioned in this manuscript that might lead to a conflict of interests.

References

[1] J. E. Kennedy, "High-intensity focused ultrasound in the treatment of solid tumours," *Nature Reviews Cancer*, vol. 5, no. 4, pp. 321–327, 2005.

[2] T. J. Dubinsky, C. Cuevas, M. K. Dighe, O. Kolokythas, and H. H. Joo, "High-intensity focused ultrasound: current potential and oncologic applications," *American Journal of Roentgenology*, vol. 190, no. 1, pp. 191–199, 2008.

[3] R. Deckers and C. T. W. Moonen, "Ultrasound triggered, image guided, local drug delivery," *Journal of Controlled Release*, vol. 148, no. 1, pp. 25–33, 2010.

[4] J. G. Lynn, R. L. Zwemer, A. J. Chick, and A. E. Miller, "A new method for the generation and use of focused ultrasound in experimental biology," *The Journal of General Physiology*, vol. 26, pp. 179–193, 1942.

[5] W. J. Fry and F. J. Fry, "Fundamental neurological research and human neurosurgery using intense ultrasound," *IRE Transactions on Medical Electronics*, vol. 7, pp. 166–181, 1960.

[6] J. Haut, J. P. Colliac, L. Falque, and Y. Renard, "Indications and results of Sonocare (ultrasound) in the treatment of ocular hypertension. A preliminary study of 395 cases," *Ophtalmologie*, vol. 4, no. 2, pp. 138–141, 1990.

[7] E. A. Dick and W. M. W. Gedroyc, "ExAblate magnetic resonance-guided focused ultrasound system in multiple body applications," *Expert Review of Medical Devices*, vol. 7, no. 5, pp. 589–597, 2010.

[8] E. M. Weeks, M. W. Platt, and W. Gedroyc, "MRI-guided focused ultrasound (MRgFUS) to treat facet joint osteoarthritis low back pain-case series of an innovative new technique," *European Radiology*, vol. 22, no. 12, pp. 2822–2835, 2012.

[9] D. Pfeiffer, J. Berger, and A. J. Gross, "Single application of high-intensity focused ultrasound as a first-line therapy for clinically localized prostate cancer: 5-year outcomes," *BJU International*, vol. 110, no. 11, pp. 1702–1707, 2012.

[10] H. U. Ahmed, R. G. Hindley, L. Dickinson et al., "Focal therapy for localised unifocal and multifocal prostate cancer: a prospective development study," *The Lancet Oncology*, vol. 13, pp. 622–632, 2012.

[11] A. M. Venkatesan, A. Partanen, T. K. Pulanic et al., "Magnetic resonance imaging-guided volumetric ablation of symptomatic leiomyomata: correlation of imaging with histology," *Journal of Vascular and Interventional Radiology*, vol. 23, pp. 786–794, 2012.

[12] D. Jeanmonod, B. Werner, A. Morel et al., "Transcranial magnetic resonance imaging-guided focused ultrasound: noninvasive central lateral thalamotomy for chronic neuropathic pain," *Neurosurg Focus*, vol. 32, no. 1, p. E1, 2012.

[13] N. McDannold, G. T. Clement, P. Black, F. Jolesz, and K. Hynynen, "Transcranial magnetic resonance imaging- guided focused ultrasound surgery of brain tumors: initial findings in 3 patients," *Neurosurgery*, vol. 66, no. 2, pp. 323–332, 2010.

[14] R. Medel, S. J. Monteith, W. J. Elias et al., "Magnetic resonance-guided focused ultrasound surgery: part 2: a review of current and future applications," *Neurosurgery*, vol. 71, pp. 755–763, 2012.

[15] P. Wells, *Biomedical Ultrasound*, Academic Press, 1977.

[16] W. D. O'Brien Jr., "Ultrasound-biophysics mechanisms," *Progress in Biophysics and Molecular Biology*, vol. 93, pp. 212–255, 2007.

[17] K. Hynynen and D. DeYoung, "Temperature elevation at muscle-bone interface during scanned, focused ultrasound hyperthermia," *International Journal of Hyperthermia*, vol. 4, no. 3, pp. 267–279, 1988.

[18] M. C. Ziskin, "Fundamental physics of ultrasound and its propagation in tissue," *Radiographics*, vol. 13, no. 3, pp. 705–709, 1993.

[19] C. M. C. Tempany, N. J. McDannold, K. Hynynen, and F. A. Jolesz, "Focused ultrasound surgery in oncology: overview and principles," *Radiology*, vol. 259, no. 1, pp. 39–56, 2011.

[20] X. Fan and K. Hynynen, "A study of various parameters of spherically curved phased arrays for noninvasive ultrasound surgery," *Physics in Medicine and Biology*, vol. 41, no. 4, pp. 591–608, 1996.

[21] E. B. Hutchinson and K. Hynynen, "Intracavitary ultrasound phased arrays for prostate thermal therapies: MRI compatibility and in vivo testing," *Medical Physics*, vol. 25, no. 12, pp. 2392–2399, 1998.

[22] W. M. W. Gedroyc and A. Anstee, "MR-guided focused ultrasound," *Expert Review of Medical Devices*, vol. 4, no. 4, pp. 539–547, 2007.

[23] R. K. Jain and T. Stylianopoulos, "Delivering nanomedicine to solid tumors," *Nature Reviews Clinical Oncology*, vol. 7, no. 11, pp. 653–664, 2010.

[24] M. B. Yatvin, J. N. Weinstein, W. H. Dennis, and R. Blumenthal, "Design of liposomes for enhanced local release of drugs by hyperthermia," *Science*, vol. 202, no. 4374, pp. 1290–1293, 1978.

[25] G. R. Anyarambhatla and D. Needham, "Enhancement of the phase transition permeability of DPPC liposomes by incorporation of MPPC: a new temperature-sensitive liposome for use with mild hyperthermia," *Journal of Liposome Research*, vol. 9, no. 4, pp. 491–506, 1999.

[26] D. Needham, G. Anyarambhatla, G. Kong, and M. W. Dewhirst, "A new temperature-sensitive liposome for use with mild hyperthermia: characterization and testing in a human tumor xenograft model," *Cancer Research*, vol. 60, no. 5, pp. 1197–1201, 2000.

[27] M. L. Hauck, S. M. La Rue, W. P. Petros et al., "Phase I trial of doxorubicin-containing low temperature sensitive liposomes in spontaneous canine tumors," *Clinical Cancer Research*, vol. 12, no. 13, pp. 4004–4010, 2006.

[28] D. Needham and M. W. Dewhirst, "The development and testing of a new temperature-sensitive drug delivery system for the treatment of solid tumors," *Advanced Drug Delivery Reviews*, vol. 53, no. 3, pp. 285–305, 2001.

[29] B. J. Wood, R. T. Poon, J. K. Locklin et al., "Phase I study of heat-deployed liposomal doxorubicin during radiofrequency ablation for hepatic malignancies," *Journal of Vascular and Interventional Radiology*, vol. 23, pp. 248–255, 2012.

[30] R. T. Poon and N. Borys, "Lyso-thermosensitive liposomal doxorubicin: an adjuvant to increase the cure rate of radiofrequency ablation in liver cancer," *Future Oncology*, vol. 7, pp. 937–945, 2011.

[31] R. Solomon and A. A. Gabizon, "Clinical pharmacology of liposomal anthracyclines: focus on pegylated liposomal doxorubicin," *Clinical Lymphoma and Myeloma*, vol. 8, no. 1, pp. 21–32, 2008.

[32] V. Frenkel, A. Etherington, M. Greene et al., "Delivery of liposomal doxorubicin (Doxil) in a breast cancer tumor model: investigation of potential enhancement by pulsed-high intensity focused ultrasound exposure," *Academic Radiology*, vol. 13, no. 4, pp. 469–479, 2006.

[33] S. Dromi, V. Frenkel, A. Luk et al., "Pulsed-high intensity focused ultrasound and low temperature—sensitive liposomes for enhanced targeted drug delivery and antitumor effect," *Clinical Cancer Research*, vol. 13, no. 9, pp. 2722–2727, 2007.

[34] A. H. Negussie, P. S. Yarmolenko, A. Partanen et al., "Formulation and characterisation of magnetic resonance imageable thermally sensitive liposomes for use with magnetic resonance-guided high intensity focused ultrasound," *International Journal of Hyperthermia*, vol. 27, pp. 140–155, 2011.

[35] A. Ranjan, G. C. Jacobs, D. L. Woods et al., "Image-guided drug delivery with magnetic resonance guided high intensity focused ultrasound and temperature sensitive liposomes in a rabbit Vx2 tumor model," *Journal of Controlled Release*, vol. 158, no. 3, pp. 487–494, 2012.

[36] A. Partanen, P. S. Yarmolenko, A. Viitala et al., "Mild hyperthermia with magnetic resonance-guided high-intensity focused ultrasound for applications in drug delivery," *International Journal of Hyperthermia*, vol. 28, pp. 320–336, 2012.

[37] A. Gasselhuber, M. R. Dreher, A. Partanen et al., "Targeted drug delivery by high intensity focused ultrasound mediated hyperthermia combined with temperature-sensitive liposomes: computational modelling and preliminary in vivovalidation," *International Journal of Hyperthermia*, vol. 28, pp. 337–348, 2012.

[38] M. de Smet, S. Langereis, S. V. den Bosch, and H. Grüll, "Temperature-sensitive liposomes for doxorubicin delivery under MRI guidance," *Journal of Controlled Release*, vol. 143, no. 1, pp. 120–127, 2010.

[39] E. Evans and D. Needham, "Physical properties of surfactant bilayer membranes: thermal transitions, elasticity, rigidity, cohesion, and colloidal interactions," *Journal of Physical Chemistry*, vol. 91, no. 16, pp. 4219–4228, 1987.

[40] G. Kong, G. Anyarambhatla, W. P. Petros et al., "Efficacy of liposomes and hyperthermia in a human tumor xenograft model: importance of triggered drug release," *Cancer Research*, vol. 60, no. 24, pp. 6950–6957, 2000.

[41] T. Tagami, M. J. Ernsting, and S. D. Li, "Optimization of a novel and improved thermosensitive liposome formulated with DPPC and a Brij surfactant using a robust in vitro system," *Journal of Controlled Release*, vol. 154, pp. 290–297, 2011.

[42] T. Tagami, W. D. Foltz, M. J. Ernsting et al., "MRI monitoring of intratumoral drug delivery and prediction of the therapeutic effect with a multifunctional thermosensitive liposome," *Biomaterials*, vol. 32, no. 27, pp. 6570–6578, 2011.

[43] K. Kono, S. Nakashima, D. Kokuryo et al., "Multi-functional liposomes having temperature-triggered release and magnetic resonance imaging for tumor-specific chemotherapy," *Biomaterials*, vol. 32, no. 5, pp. 1387–1395, 2011.

[44] N. Kamaly, J. A. Pugh, T. L. Kalber et al., "Imaging of gadolinium spatial distribution in tumor tissue by laser ablation inductively coupled plasma mass spectrometry," *Molecular Imaging and Biology*, vol. 12, no. 4, pp. 361–366, 2010.

[45] N. Kamaly, T. Kalber, M. Thanou, J. D. Bell, and A. D. Miller, "Folate receptor targeted bimodal liposomes for tumor magnetic resonance imaging," *Bioconjugate Chemistry*, vol. 20, no. 4, pp. 648–655, 2009.

[46] J. Kost, K. Leong, and R. Langer, "Ultrasound-enhanced polymer degradation and release of incorporated substances," *Proceedings of the National Academy of Sciences of the United States of America*, vol. 86, no. 20, pp. 7663–7666, 1989.

[47] A. Yudina and C. Moonen, "Ultrasound-induced cell permeabilisation and hyperthermia: strategies for local delivery of compounds with intracellular mode of action," *International Journal of Hyperthermia*, vol. 28, pp. 311–319, 2012.

[48] V. Frenkel and K. C. P. Li, "Potential role of pulsed-high intensity focused ultrasound in gene therapy," *Future Oncology*, vol. 2, no. 1, pp. 111–119, 2006.

[49] C. W. Song, H. J. Park, C. K. Lee, and R. Griffin, "Implications of increased tumor blood flow and oxygenation caused by mild temperature hyperthermia in tumor treatment," *International Journal of Hyperthermia*, vol. 21, no. 8, pp. 761–767, 2005.

[50] S. Wang, V. Zderic, and V. Frenkel, "Extracorporeal, low-energy focused ultrasound for noninvasive and nondestructive targeted hyperthermia," *Future Oncology*, vol. 6, no. 9, pp. 1497–1511, 2010.

[51] G. Kong, R. D. Braun, and M. W. Dewhirst, "Characterization of the effect of hyperthermia on nanoparticle extravasation from tumor vasculature," *Cancer Research*, vol. 61, no. 7, pp. 3027–3032, 2001.

[52] J. Friedl, E. Turner, and H. R. Alexander Jr., "Augmentation of endothelial cell monolayer permeability by hyperthermia but not tumor necrosis factor: evidence for disruption of vascular integrity via VE-cadherin down-regulation," *International Journal of Oncology*, vol. 23, pp. 611–616, 2003.

[53] J. Wu and W. L. Nyborg, "Ultrasound, cavitation bubbles and their interaction with cells," *Advanced Drug Delivery Reviews*, vol. 60, no. 10, pp. 1103–1116, 2008.

[54] V. Frenkel, "Ultrasound mediated delivery of drugs and genes to solid tumors," *Advanced Drug Delivery Reviews*, vol. 60, no. 10, pp. 1193–1208, 2008.

[55] R. E. Apfel, "Acoustic cavitation: a possible consequence of biomedical uses of ultrasound," *British Journal of Cancer*, vol. 45, supplement 5, pp. 140–146, 1982.

[56] M. W. Miller, T. A. Sherman, and A. A. Brayman, "Comparative sensitivity of human and bovine erythrocytes to sonolysis by 1-MHz ultrasound," *Ultrasound in Medicine and Biology*, vol. 26, no. 8, pp. 1317–1326, 2000.

[57] C. Y. Lai, C. H. Wu, C. C. Chen, and P. C. Li, "Quantitative relations of acoustic inertial cavitation with sonoporation and cell viability," *Ultrasound in Medicine and Biology*, vol. 32, no. 12, pp. 1931–1941, 2006.

[58] A. H. Mesiwala, L. Farrell, H. J. Wenzel et al., "High-intensity focused ultrasound selectively disrupts the blood-brain barrier in vivo," *Ultrasound in Medicine and Biology*, vol. 28, no. 3, pp. 389–400, 2002.

[59] N. Sheikov, N. McDannold, S. Sharma, and K. Hynynen, "Effect of focused ultrasound applied with an ultrasound contrast agent on the tight junctional integrity of the brain microvascular endothelium," *Ultrasound in Medicine and Biology*, vol. 34, no. 7, pp. 1093–1104, 2008.

[60] J. Deng, Q. Huang, F. Wang et al., "The role of caveolin-1 in blood-brain barrier disruption induced by focused ultrasound combined with microbubbles," *Journal of Molecular Neuroscience*, vol. 46, pp. 677–687, 2012.

[61] K. Hynynen, N. McDannold, N. Vykhodtseva, and F. A. Jolesz, "Non-invasive opening of BBB by focused ultrasound," *Acta Neurochirurgica, Supplementum*, no. 86, pp. 555–558, 2003.

[62] F. A. Jolesz, K. Hynynen, N. McDannold, and C. Tempany, "MR imaging-controlled focused ultrasound ablation: a noninvasive image-guided surgery," *Magnetic Resonance Imaging Clinics of North America*, vol. 13, no. 3, pp. 545–560, 2005.

[63] N. McDannold, N. Vykhodtseva, S. Raymond, F. A. Jolesz, and K. Hynynen, "MRI-guided targeted blood-brain barrier disruption with focused ultrasound: histological findings in rabbits," *Ultrasound in Medicine and Biology*, vol. 31, no. 11, pp. 1527–1537, 2005.

[64] M. Kinoshita, N. McDannold, F. A. Jolesz, and K. Hynynen, "Noninvasive localized delivery of Herceptin to the mouse brain by MRI-guided focused ultrasound-induced blood-brain barrier disruption," *Proceedings of the National Academy of Sciences of the United States of America*, vol. 103, no. 31, pp. 11719–11723, 2006.

[65] K. Hynynen, "Focused ultrasound for blood-brain disruption and delivery of therapeutic molecules into the brain," *Expert Opinion on Drug Delivery*, vol. 4, no. 1, pp. 27–35, 2007.

[66] M. Kinoshita, N. McDannold, F. A. Jolesz, and K. Hynynen, "Targeted delivery of antibodies through the blood-brain barrier by MRI-guided focused ultrasound," *Biochemical and Biophysical Research Communications*, vol. 340, no. 4, pp. 1085–1090, 2006.

[67] L. H. Treat, N. McDannold, N. Vykhodtseva, Y. Zhang, K. Tam, and K. Hynynen, "Targeted delivery of doxorubicin to the rat brain at therapeutic levels using MRI-guided focused ultrasound," *International Journal of Cancer*, vol. 121, no. 4, pp. 901–907, 2007.

[68] F. Vlachos, Y. S. Tung, and E. E. Konofagou, "Permeability assessment of the focused ultrasound-induced blood-brain barrier opening using dynamic contrast-enhanced MRI," *Physics in Medicine and Biology*, vol. 55, no. 18, pp. 5451–5466, 2010.

[69] J. J. Choi, J. A. Feshitan, B. Baseri et al., "Microbubble-size dependence of focused ultrasound-induced bloodBrain barrier opening in mice in vivo," *IEEE Transactions on Biomedical Engineering*, vol. 57, no. 1, pp. 145–154, 2010.

[70] M. A. O'Reilly, A. C. Waspe, M. Ganguly, and K. Hynynen, "Focused-ultrasound disruption of the blood-brain barrier using closely-timed short pulses: influence of sonication parameters and injection rate," *Ultrasound in Medicine and Biology*, vol. 37, no. 4, pp. 587–594, 2011.

[71] B. Baseri, J. J. Choi, T. Deffieux et al., "Activation of signaling pathways following localized delivery of systemically administered neurotrophic factors across the blood-brain barrier using focused ultrasound and microbubbles," *Physics in Medicine and Biology*, vol. 57, no. 7, pp. N65–N81, 2012.

[72] A. B. Etame, R. J. Diaz, C. A. Smith, T. G. Mainprize, K. Hynynen, and J. T. Rutka, "Focused ultrasound disruption of the blood-brain barrier: a new frontier for therapeutic delivery in molecular neurooncology," *Neurosurgical Focus*, vol. 32, no. 1, p. E3, 2012.

[73] J. Mei, Y. Cheng, Y. Song et al., "Experimental study on targeted methotrexate delivery to the rabbit brain via magnetic resonance imaging-guided focused ultrasound," *Journal of Ultrasound in Medicine*, vol. 28, no. 7, pp. 871–880, 2009.

[74] H. L. Liu, M. Y. Hua, P. Y. Chen et al., "Blood-brain barrier disruption with focused ultrasound enhances delivery of chemotherapeutic drugs for glioblastoma treatment," *Radiology*, vol. 255, no. 2, pp. 415–425, 2010.

[75] H. L. Liu, M. Y. Hua, H. W. Yang et al., "Magnetic resonance monitoring of focused ultrasound/magnetic nanoparticle targeting delivery of therapeutic agents to the brain," *Proceedings of the National Academy of Sciences of the United States of America*, vol. 107, no. 34, pp. 15205–15210, 2010.

[76] F. Y. Yang, T. T. Wong, M. C. Teng et al., "Focused ultrasound and interleukin-4 receptor-targeted liposomal doxorubicin for enhanced targeted drug delivery and antitumor effect in glioblastoma multiforme," *Journal of Controlled Release*, vol. 160, pp. 652–658, 2012.

[77] F. Y. Yang, H. E. Wang, R. S. Liu et al., "Pharmacokinetic analysis of (111)in-labeled liposomal Doxorubicin in murine glioblastoma after blood-brain barrier disruption by focused ultrasound," *PLoS One*, vol. 7, Article ID e45468, 2012.

[78] Q. Huang, J. Deng, F. Wang et al., "Targeted gene delivery to the mouse brain by MRI-guided focused ultrasound-induced blood-brain barrier disruption," *Experimental Neurology*, vol. 233, pp. 350–356, 2012.

[79] A. Burgess, C. A. Ayala-Grosso, M. Ganguly, J. F. Jordao, I. Aubert, and K. Hynynen, "Targeted delivery of neural stem cells to the brain using MRI-guided focused ultrasound to disrupt the blood-brain barrier," *PLoS One*, vol. 6, Article ID e27877, 2011.

[80] P. Prentice, A. Cuschierp, K. Dholakia, M. Prausnitz, and P. Campbell, "Membrane disruption by optically controlled microbubble cavitation," *Nature Physics*, vol. 1, pp. 107–110, 2005.

[81] I. Lentacker, B. Geers, J. Demeester, S. C. De Smedt, and N. N. Sanders, "Design and evaluation of doxorubicin-containing microbubbles for ultrasound-triggered doxorubicin delivery: cytotoxicity and mechanisms involved," *Molecular Therapy*, vol. 18, no. 1, pp. 101–108, 2010.

[82] N. Rapoport, "Ultrasound-mediated micellar drug delivery," *International Journal of Hyperthermia*, vol. 28, pp. 374–385, 2012.

[83] Z. S. Al-Ahmady, W. T. Al-Jamal, J. V. Bossche et al., "Lipid-Peptide vesicle nanoscale hybrids for triggered drug release by mild hyperthermia in vitro and in vivo," *ACS Nano*, vol. 6, pp. 9335–9346, 2012.

[84] S. Fokong, B. Theek, Z. Wu et al., "Image-guided, targeted and triggered drug delivery to tumors using polymer-based microbubbles," *Journal of Controlled Release*, vol. 163, pp. 75–81, 2012.

Hindawi Publishing Corporation
Journal of Drug Delivery
Volume 2013, Article ID 529312, 9 pages
http://dx.doi.org/10.1155/2013/529312

Review Article

Cancer Epigenetics: New Therapies and New Challenges

Eleftheria Hatzimichael[1,2] and Tim Crook[3]

[1] *Department of Haematology, University Hospital of Ioannina, St. Niarchou Avenue, 45110 Ioannina, Greece*
[2] *Computational Medicine Center, Jefferson Medical College, Thomas Jefferson University, Philadelphia, PA 19107, USA*
[3] *Division of Cancer Research, Medical Research Institute, University of Dundee, Hospital and Medical School, Dundee DD1 9SY, UK*

Correspondence should be addressed to Eleftheria Hatzimichael; ehatzim@cc.uoi.gr

Received 3 December 2012; Accepted 20 January 2013

Academic Editor: Evangelos Briasoulis

Cancer is nowadays considered to be both a genetic and an epigenetic disease. The most well studied epigenetic modification in humans is DNA methylation; however it becomes increasingly acknowledged that DNA methylation does not work alone, but rather is linked to other modifications, such as histone modifications. Epigenetic abnormalities are reversible and as a result novel therapies that work by reversing epigenetic effects are being increasingly explored. The biggest clinical impact of epigenetic modifying agents in neoplastic disorders thus far has been in haematological malignancies, and the efficacy of DNMT inhibitors and HDAC inhibitors in blood cancers clearly attests to the principle that therapeutic modification of the cancer cell epigenome can produce clinical benefit. This paper will discuss the most well studied epigenetic modifications and how these are linked to cancer, will give a brief overview of the clinical use of epigenetics as biomarkers, and will focus in more detail on epigenetic drugs and their use in solid and blood cancers.

1. Introduction

It has been thirty years since the "war on cancer" was declared, yet in 2008, the most recent year for which incidence and mortality rates are available, almost 12.7 million people were diagnosed with cancer and more than 7.5 million died of the disease [1]. Enormous progress has been made in the understanding of the molecular basis of carcinogenesis and the complete sequencing of the human genome represents a milestone in this quest [2]. The situation though is far more complex than a simple catalogue of genes and despite this progress the discovery of anticancer drugs remains a highly challenging endeavor and cancer a hard-to-cure disease.

Traditionally, the development of cancer is thought to be largely due to the accumulation of genetic defects such as mutations, amplifications, deletions, and translocations affecting the cancer cell machinery and providing the cancer cell with the advantage to survive and metastasize. In addition, interactions between cancer cells and their microenvironment further support these processes [3]. Of equal importance is a second system that cells use to determine when and where a particular gene will be expressed during development. This system is overlaid on DNA in the form of epigenetic marks that are heritable during cell division but do not alter the DNA sequence [4]. The pattern of these chemical tags is called the epigenome of the cell, whereas epigenetics is the study of these marks that lead to changes in gene expression in the absence of corresponding structural changes in the genome. It is now well recognized that tumorigenesis is a multistep process involving multiple genetic and epigenetic alterations, with the latter often termed epimutations that contribute to the progressive transformation of normal cells towards a malignant phenotype, so that cancer is nowadays consider to be both a *genetic* and an *epigenetic* disease [5, 6]. Epigenetic abnormalities are reversible and as a result novel therapies that work by reversing epigenetic effects are being increasingly explored. More recently, increasing evidence suggests that genetic and epigenetic mechanisms intertwine and take advantage of each other during malignant transformation.

There are many chemical modifications that affect not only DNA, but also RNA and proteins, and create different epigenetic layers. The most well studied epigenetic modification in humans is DNA methylation; however, it becomes increasingly acknowledged that DNA methylation does not work alone, but rather is linked to other modifications, such

as histone modifications. This paper will discuss the most well studied epigenetic modifications and how these are linked to cancer, give a brief overview of the clinical use of epigenetics as biomarkers, and focus in more detail on epigenetic drugs and their use in solid and blood cancers.

2. DNA Methylation

DNA methylation consists of the addition of a methyl group to carbon 5 of the cytosine within the dinucleotide CpG. Regions of DNA in the human genome, ranging from 0.5 to 5 kb, that are CG rich are called CpG islands and are usually found in the promoters of genes. Approximately half of all gene promoters have CpG islands that when methylated lead to transcriptional silencing. *De nov*o DNA methylation is brought about by DNA methyltransferases (DNMT) 3A and 3B that convert cytosine residues of CpG dinucleotides into 5-methylcytosine, whereas DNA methylation is maintained by DNMT1. 5-methylcytosine can be further converted into 5-hydroxymethyl-2′-deoxycytidine by the Ten-Eleven-Translocation (TET) family enzymes [7]. The function and significance of 5-hydroxymethylation are still unclear and under investigation. Although methylation of DNA in 5′ promoters has been well studied and has been shown to suppress gene expression, recently DNA methylation was described downstream of the promoters in intra- and intergenic regions [8] as well in CpG shores, that is regions with lower CpG density neighboring CpG islands [9].

3. Histone Modifications

Histones are proteins around which DNA winds to form nucleosomes. A nucleosome is the basic unit of DNA packaging within the nucleus and consists of 147 base pairs of genomic DNA wrapped twice around a highly conserved histone octamer, consisting of 2 copies each of the core histones H2A, H2B, H3, and H4. Histones, however, are not only packaging elements, but also critical regulators of gene expression. Histone tails may undergo many posttranslational chemical modifications, such as acetylation, methylation, phosphorylation, ubiquitylation, and sumoylation that constitute a code, named the "histone code." These modifications can alter the chromatin structure, from an open to a closed, condensed form and vice versa. Histone modifications act, except for chromatin packaging, on various other biological processes including transcriptional repression, gene activation, and DNA repair [10]. Three classes of histone interacting proteins have been described thus far, based on their function: the *writers* that place histone modifications, the *erasers* that can remove these modifications, and finally the *readers* that recognize the histone modifications and can deliver nucleosome, histone, or DNA-modifying enzymes.

3.1. Histone Acetylation. Histone acetylation occurs at either arginine-(R) or lysine-(K) residues and is a dynamic and reversible process that is regulated by two enzyme families, histone acetyltransferases (HAT) and histone deacetylases (HDAC). HATs catalyse the transfer of an acetyl group to the ε-amino group of the lysine residue on the histone protein and use acetyl-CoA as a cofactor. As a result chromatin adopts a more relaxed form (euchromatin) allowing the recruitment of transcription factors. HDACs reverse the acetylation of lysine residues and the local chromatin architecture becomes condensed (heterochromatin). Acetylation of lysine 16 of histone 4 (H4K16) appears to be crucial in chromatin folding and in the switch from the euchromatin state to heterochromatin [11]. Histone acetylation can also promote transcription by providing binding sites to proteins that are involved in gene activation, such as the bromodomain-containing family of proteins [12].

3.2. Histone Methylation. Histones can also be methylated at their lysine-(K) and arginine-(R) residues. Lysine residues can be monomethylated, dimethylated, or trimethylated whereas arginine residues can be mono- or dimethylated. Methyl marks are written by S-adenosylmethionine (SAM)-dependent methyltransferases and erased by either the Jumonji family of demethylases [13] or the lysine-specific histone demethylases 1 (LSD1) and 2 (LSD2) [14]. Histone methylation at lysine and arginine residues does not alter the chromatic structure, but rather acts as binding sites for other proteins that may condense chromatin [15] or have other effects. The different levels of lysine methylation are recognized by different methyl-lysine-binding domains and may be associated with either transcription activation or repression. H3K4me3, for example promotes transcription, whereas H3K27me3 is associated with gene silencing [10]. Arginine methylation of histone proteins has recently been shown to antagonize other histone marks, further increasing the histone code complexity [16].

4. Cancer and Epigenetic Modifications

In cancer, a global process of genomic hypomethylation occurs mostly at DNA-repetitive regions which results in activation of genes with growth and tumour promoting functions and loss of genome stability and imprinting [17]. In contrast, there are site-specific increases in CpG methylation in areas of the genome with a high density of CpG, termed CpG islands causing transcriptional silencing of tumour suppressor genes (TSG), such as *BRCA1* [18], *hMLH1* [19], *VHL* [20], *BIK* [21], and *MGMT* [22, 23].

Cancer contains not only DNA methylation aberrations, but also major disruption of the histone modification landscape [24]. Histone modifiers have been shown to be targets of aberrations and/or mutations in cancer such as mutated deacetylases [25], and amplified histone methyltransferases and demethylases [26].

4.1. When Genetics Meets Epigenetics in Cancer. Deregulation of the epigenetic machinery can also occur due to activation or inactivation of the epigenetic regulatory proteins. In other words, the enzymes that maintain and modify the epigenome are themselves frequent targets for mutation and/or epimutation in neoplasia [27]; for example, DNA methyltransferases themselves have been found to be genetically altered

in malignancies, such as *DNMT3A* [28] and *DNMT3B* in pancreatic and breast cancer cells [29]. Somatic *DNMT3A* mutations have been described in approximately 20% of acute myeloid leukemia (AML) patients, especially in those with an intermediate risk cytogenetic profile and although they did not affect the 5-methylcytosine content [30] they were associated with poor clinical outcome [30, 31]. How the lack of effect of *DNMT3A* mutations on 5-methylcytosine content is linked to an otherwise poor clinical outcome is not yet fully understood. It has been suggested that the R882 *DNMT3A* mutations alter functions of DNMT3A such as its ability to bind other proteins involved in transcriptional regulation and localization to chromatin regions containing methylated DNA [30]. Loss-of-function *TET2* mutations were also identified in myeloid neoplasms in 20–30% [32, 33] and have been associated with both good [34] and bad prognoses [35].

Genome sequencing has also revealed the presence of metabolic mutations in patients with myelodysplastic syndromes (MDS) and AML related to the isocitrate dehydrogenase (*IDH*) 1 and *IDH2* genes [36]. These mutations have been reported in approximately 30% of patients with normal karyotype AML [37, 38] and have been linked to the disruption of various processes such as bone marrow microenvironment changes and impaired differentiation suggesting a proleukemogenic effect. In an AML cohort, *IDH1* and *IDH2* mutations were mutually exclusive with *TET2* mutations while they shared the similar epigenetic defects with the *TET2* mutants. Epigenetic profiling revealed that AML patients with *IDH1/2* mutations displayed global hypermethylation and a specific hypermethylation signature [39]. MLL is another epigenetic modifier that is commonly mutated in acute leukemias and mainly due to translocations. In normal karyotype AML cases the incidence of MLL partial tandem duplications (MLL-PTD) is up to 8% whereas in cases of trisomy 11 the incidence reaches 25% [40]. Favorable AMLs such as those with t(8; 21) are MLL-PTD negative [41]. As MLL is a H3 K4 methyltransferase, translocations that replace the methyltransferase domain affect its function and have been linked with leukaemic transformation [42]. Mutations affecting the Polycomb repressive complex (PRC) components, such as EZH2, can also affect histone modifications and have recently been reported. EZH2 is the enzymatic component of the PRC2 complex and is a H3 K27 methyltransferase. Overexpression of EZH2 has been reported in various epithelial neoplasms and several types of leukemia [43–45] and has been shown to be due to, at least in part, the loss of transcriptional repression of specific microRNAs [44]. Activating mutations of *EZH2* have been reported in B-cell lymphomas [46] whereas missense, nonsense, and frameshift mutations have been reported in various myeloid malignancies [47, 48]. In AML, 3 cases so far have been described to carry *EZH2* mutations [27].

5. Clinical Use of Epigenetics

At present, there are two major areas of interest in the clinical use of epigenetics, namely, biomarkers and therapeutics. We now consider these areas.

5.1. Cancer Biomarkers. Methylated genomic DNA has a number of properties, which make it an attractive molecule for biomarker utility. First, it is stable in biofluids such as blood, urine, and saliva. Second, in the majority of cases methylation in CpG is acquired during malignant transformation and is therefore specific to neoplasia. Third, the techniques used for detection of methylated DNA are readily amenable to automation.

Several studies have explored the methylation status of gene promoters and its association with clinical parameters in primary patient samples from patients with haematological malignancies and solid tumours. Various methodologies have been used such as methylation-specific PCR (MSP), methylation-specific restriction enzyme digestion, HpaII tiny fragment enrichment by ligation-mediated PCR (HELP), bisulphite sequencing, and pyrosequencing. Either single genes or panels of genes in microarrays were studied. In MDS and AML methylation of several genes has been reported such as *MEG3*, *SNRPN* [49], *Plk2* [50], cyclin-dependent kinase inhibitors, e-cadherin [51], and various others reviewed in [52]. In multiple myeloma, methylation of the VHL promoter has been shown to correlate with bone disease [20] and methylation of the bcl-2 interacting killer (*BIK*) promoter has been shown to predict relapsed/refractory disease [21], while methylated *FHIT* has been shown to be an independent adverse prognostic factor [53].

In a study by Shen et al. [54] a panel of 10 hypermethylated genes was identified in patients with MDS. Quantitative pyrosequencing in a large cohort showed that patients with higher levels of methylation for these genes had shorter median overall and progressive-free survival (PFS) independent of age, sex, and the International Prognostic Scoring System (IPSS). Similarly, in solid tumours numerous methylated genes have been described. A substantial body of experimental evidence exists mechanistically associating acquired chemotherapy resistance with changes in the cancer cell epigenome and a number of genes have been identified, in which increased CpG island methylation and transcriptional downregulation are associated with resistance to specific agents such *hMLH1* [55] and *Plk2* [56] in ovarian cancer. Of note, methylation-dependent silencing of the methyl transferase *MGMT* in glioblastoma multiforme confers sensitivity to the alkylating agent temozolomide [23] but as with many such candidate biomarkers, clinical application to inform patient management is not yet routine.

The list of genes reported to be methylated in haematological neoplasms is extensive, and although several have been linked to clinical parameters and have been associated with survival or response to treatment, none of these markers has been used so far in the clinic to guide diagnosis or treatment, as opposed to gene mutations such as *NPM1* and *FLT3* that are now widely used to risk classify AML patients.

One of the major goals of investigators in oncology is that of individualized cancer therapy. Investigators continue to identify genes whose transcriptional silencing affects sensitivity to chemotherapeutic agents. The challenge now is to translate these findings into clinically usable tests to inform optimal deployment of anticancer drugs. It remains unlikely that a single gene methylation test will be sufficiently

informative to guide individual patient management and it is more likely that panels of genes will be required.

5.2. Cancer Therapeutics. Both epigenetic proteins and protein markers are good targets for the development of new anticancer treatments. The proof-of-concept for epigenetic therapies is the FDA and EMEA approval of demethylating agents and histone acetylase (HDAC) inhibitors for the treatment of MDS, AML and certain types of lymphomas, respectively. However, we should not forget that these agents are nonselective and their side effects are not clearly known.

5.2.1. DNA Methyltransferase Inhibitors (DNMTis) or Demethylating Agents. The two most well studied and in clinical use DNA methyltransferase inhibitors (DNMTi) are the azanucleosides azacytidine (5-azacytidine) and decitabine (5-aza′-2-deoxycytidine). Both are approved for use in the myelodysplastic syndromes and low-blast count AML and have improved the survival of patients with these diseases [57].

Unfortunately, clinical trials with DNMTi in solid tumours did not have the same results. A phase 1 study of decitabine with interleukin-2 in melanoma and renal cell carcinoma showed that decitabine caused grade 4 neutropenia in most patients [58]. Myelosuppression was also the predominant toxicity observed in a study combining decitabine with carboplatin [59]. However, in a phase II trial low-dose decitabine was found to restore sensitivity to carboplatin in patients with heavily pretreated ovarian cancer resulting in a high response rate (RR) and prolonged PFS [60]. In both studies, there was evidence that decitabine induced dose-dependent demethylation in marker genes such as *MLH1, RASSF1A, HOXA10*, and *HOXA11* [60]. It is possible that such an approach could efficiently be coupled with the use of epigenetic biomarkers predictive of chemosensitivity [56].

A major likely reason for the disappointing activity of demethylating agents in solid tumours is limited incorporation into cells, which are proliferating relatively slowly. These limitations may be less relevant for newer DNMTis which are independent of replication for incorporation into DNA. A second explanation for these results is that agents such as azacytidine, which cause global hypomethylation, likely reactivate expression of multiple silenced genes including oncogenes and tumour suppressors in different cell types and in different cancers. Demethylation could therefore cause both therapeutic and deleterious effects. For example, the oncogene *NT5E* is overexpressed in aggressive metastatic melanomas, yet transcriptionally silenced by methylation in breast cancer with more favorable prognosis [61].

A third and key possible explanation why DNMTi have advanced less rapidly in the clinic in solid tumours than in haematological malignancies is that of toxicity. Both decitabine and azacytidine are active in haematological malignancy at lower (less toxic) doses than are required for demethylation in epithelial malignancies. It is clearly of interest, therefore, that transient exposure of cells to low (relatively non-toxic) doses of these agents could induce a "memory" response with sustained reduction in CpG island methylation and reactivation of expression of previously silenced genes [62]. These observations imply that low-dose decitabine and azacytidine may have wider uses in management of neoplastic disease than previously believed. In a recently reported phase II trial Matei et al. [60] showed that pretreatment with low-dose azacytidine restored sensitivity to carboplatin in patients with drug resistant epithelial ovarian cancer and resulted in a high response rate and significantly improved clinical outcomes. This study clearly attests to the utility of low-dose azacytidine in solid tumours and sets the scene for further studies.

Newer azanucleosides are zebularine, S-110, and SGI-1027 that have shown antiproliferative activity in cell lines [63, 64], but have not entered the clinical trial setting yet.

5.2.2. Histone Deacetylase Inhibitors (HDACi). The HDACs catalyse removal of acetyl groups from lysine residues in the histones and functionally are transcriptional repressors. HDACs are divided into five classes: class I comprises HDAC1, HDAC2, HDAC3, and HDAC8; class IIa comprises HDAC4, HDAC5, HDAC7, and HDAC9; class IIb contains HDAC6 and HDAC10; class III comprises the sirtuins SIRT1-SIRT7 while class IV contains only HDAC11 [65]. The discovery of HDACi actually preceded the discovery of HDACs. Sodium butyrate was the first HDACi described to induce acetylation [66], and later on trichostatin (TSA), a fungal antibiotic, currently used in *in vitro* experiments, and valproic acid, a widely used antiepileptic, were identified. Valproic acid, in particular, has been used in combination with DNMTi and/or chemotherapy in patients with haematological malignancies [67, 68].

Currently HDACi that have been developed focus on class I and class II HDACs and can be further distinguished into chemically distinct subgroups based on their structure: aliphatic acids (phenylbutyrate, valproic acid), benzamides (entinostat), cyclic peptides (romidepsin), and hydroxamates (TSA, vorinostat/SAHA). Several HDACi are currently being tested in phase II-III trials, while two of them, vorinostat and romidepsin are the first FDA and EMEA approved agents for the treatment of progressive or recurrent cutaneous T cell lymphoma (CTCL) as second lines of treatment in 2006 and 2009, respectively [69], but convincing clinical evidence of activity of these agents in other cancer types is still lacking [70]. In non-small-cell lung cancer a number of HDACi such as entinostat, vorinostat, Pivanex, and CI-994 are in early phases of clinical development and first results have been reported [70, 71]. However, it appears that HDACi may need rational combinations to counterbalance the inherent potential of these compounds to reactivate tumor-progression genes [72]. Newer compounds such as givinostat (ITF2357) have also been developed. Givinostat has been shown to selectively target cells harboring the JAK2 V617F mutation [73] and has been tested in combination with hydroxyurea in patients with polycythemia vera in a phase II study (NCT00928707). Panobinostat (LBH589) has shown activity as monotherapy in patients with Hodgkin's lymphoma, who relapsed or were refractory to autologous transplantation [74] but limited activity in MDS [75]. However, in solid tumors the results of panobinostat monotherapy or in combination with other agents were rather disappointing [76, 77]. Second

generation HDACi, such as ACY-1215, are more selective and have recently entered the clinical trial setting [78]. It would be really interesting to see the efficacy and safety profile of such compounds.

HDACi, however, do not deacetylate histones only. It becomes increasingly recognized that HDACi deacetylase other nonhistone proteins that are transcription factors, signal transducers, or even the products of oncogenes or TSG that are involved in oncogenesis [79]. This could partly explain the unacceptable toxicity [80] as well as the lack of efficacy of some compounds [81].

5.2.3. Combination of DNMTi and HDACi. The recognition that a subset of TSGs are silenced by a combination of CpG hypermethylation and histone hypoacetylation has prompted testing of combinations of the two classes of agents and trials of these are in progress. There is initial evidence to suggest that such combinations may greatly increase clinical efficacy without unacceptable toxicity. For example, in multiply pretreated metastatic non-small-cell lung cancer patients, the combination of azacytidine and the histone deacetylase inhibitor entinostat produced objective clinical responses and, importantly, four of 19 treated patients had therapeutic responses to further agents given immediately after epigenetic therapy [82]. Evidence that demethylation is key to the responses was shown by analysis from peripheral blood samples of a set of four marker genes. The therapy was well tolerated. These encouraging results are currently being extended in further studies. The combination of decitabine and pegylated interferon alfa-2b was tested in patients with unresectable or metastatic solid tumours (NCT00701298). In ongoing trials, the combination of azacytidine and entinostat is undergoing testing in resected stage I non-small-cell lung cancer (NCT01207726) and oral azacytidine in combination with carboplatin or Abraxane (nanoparticle paclitaxel) is being evaluated in patients with refractory solid tumours (NCT01478685).

In elderly previously untreated AML patients and high-risk MDS patients the combination of azacytidine and lenalidomide, an immunomodulator drug, is currently under investigation (NCT01442714). Both drugs as monotherapies have already shown efficacy in this group of patients so their combination seems very promising. Sequential treatment of azacytidine and lenalidomide in elderly patients with AML also showed encouraging clinical and biologic activity [83].

In a recent Phase I study decitabine was combined with bortezomib for the treatment of elderly poor risk AML patients and the combination showed good preliminary activity since response rates were very encouraging [84].

6. Future Promise: Therapeutics

The use of epidrugs on the intent to restore sensitivity to cytotoxic or hormonal drugs is a major goal in the setting of solid tumors [85–87]. Restoring hormonal sensitivity in breast cancer is of uppermost clinical importance and has been intensively studied over the last decades. In total 25% of breast cancers have the estrogen receptor-alpha (ER alpha) repressed mainly due to hypermethylation of the ER promoter and do not respond to endocrine therapy, and almost all hormone-sensitive tumors turn to be refractory at some point. It appears now that epigenetic therapy seems to offer a promising tool to restore/reverse hormonal sensitivity. Recent studies found that decitabine and histone HDACi such as trichostatin A, entinostat, and scriptaid can restore expression of ER mRNA and functional protein and aromatase, along with the enzymatic activity of aromatase, indicating a potential to restore long term responsiveness of a subset of ER-negative tumors to endocrine therapy [87–89].

Given the complexity and heterogeneity of the cancer cell epigenome, it is highly likely that some form of epigenomic profiling of individual cancers will be required to inform optimal use of the available agents, which induce modification of the cancer cell epigenome. For example, it would clearly be important to determine the epigenome of chemotherapy resistant cancer cells, to identify potentially deleterious silenced genes, before deploying epigenetic therapeutic strategies in an attempt to pharmacologically reverse resistance. Malignant melanoma is an interesting example of such an approach. In this tumor type, loss of 5-hydroxymethylcytosine (5-hmC) has diagnostic and prognostic implications, which relates to downregulation of IDH2 and TET family enzymes. Reintroducing active TET2 or IDH2 was found to suppress melanoma growth and increase tumor-free survival in animal models [90].

Identifying the epigenetically modified genes, which are principally involved in tumor resistance, can be achieved by comparative analysis of diagnostic (pretreatment) biopsy with a second biopsy at disease relapse. Such rebiopsying is rapidly becoming the standard of care in oncology, for example, in breast cancer [91].

The ability of the physician to exploit therapeutic opportunities created by epigenetic changes in the cancer cell epigenome may also offer new approaches to cancer management. For example, *ASS1*, which encodes arginine succinate synthetase, the rate-limiting enzyme in arginine biosynthesis, is silenced by methylation in some cancer types including renal cell carcinoma, hepatocellular carcinoma, malignant melanoma, glioblastoma multiforme (GBM), and platinum-resistant epithelial ovarian cancer. *ASL* encoding arginine succinate lyase (a second key enzyme in arginine biosynthesis) is also silenced by CpG island methylation in GBM [92]. Loss of either gene confers arginine auxotrophy and sensitivity to arginine deiminase. These observations imply a further form of epigenetic therapy in which biochemical abnormalities resulting from epigenetic changes can be targeted for clinical benefit.

As we previously discussed, several epigenetic modifiers such as EZH2, IDH1/2, and DNMT3A are genetically altered in cancer. These epigenetic modifiers provide now new therapeutic targets for clinical development. What seems to be needed though is a better selection of patients who will benefit from such treatments as well as identification of new druggable targets and compounds such as histone kinases [93] or inhibitors of histone methyltransferases [94] and sirtuins [95].

7. Conclusions

The biggest clinical impact of epigenetic modifying agents in neoplastic disorders thus far has been in haematological malignancies and the efficacy of DNMTis and HDACi in blood cancers clearly attests to the principle that therapeutic modification of the cancer cell epigenome can produce clinical benefit. Although the efficacy of epigenetic therapy in solid tumours remains as yet unproven, there is every reason to believe that more rational use of existing agents, perhaps informed by individual patient epigenetic profiling, will improve the therapeutic index of this approach. Furthermore, an increasing number of viable new therapeutic targets are emerging from increased understanding of the epigenetic regulatory circuitry and its derangement in neoplasia.

Conflict of Interests

The authors have no conflict of interests to declare.

Acknowledgments

T. Crook is a Scottish senior clinical fellow in Medical Oncology. E. Hatzimichael is a scholar of the Hellenic Society of Hematology Foundation and a visiting scientist at the Computational Medicine Centre, Jefferson Medical College, Thomas Jefferson University. Work in the laboratory of T. Crook is supported by the Chief Scientific Officer of Scotland, The Leng Foundation, and The Anonymous Trust.

References

[1] R. Siegel, D. Naishadham, and A. Jemal, "Cancer statistics," *CA: A Cancer Journal for Clinicians*, vol. 62, pp. 10–29, 2012.

[2] E. S. Lander, L. M. Linton, B. Birren et al., "Initial sequencing and analysis of the human genome," *Nature*, vol. 409, pp. 860–921, 2001.

[3] D. Hanahan and R. A. Weinberg, "Hallmarks of cancer: the next generation," *Cell*, vol. 144, no. 5, pp. 646–674, 2011.

[4] P. A. Jones and P. W. Laird, "Cancer epigenetics comes of age," *Nature Genetics*, vol. 21, no. 2, pp. 163–167, 1999.

[5] E. J. Geutjes, P. K. Bajpe, and R. Bernards, "Targeting the epigenome for treatment of cancer," *Oncogene*, vol. 31, pp. 3827–3844, 2012.

[6] P. A. Jones and S. B. Baylin, "The fundamental role of epigenetic events in cancer," *Nature Reviews Genetics*, vol. 3, no. 6, pp. 415–428, 2002.

[7] M. Tahiliani, K. P. Koh, Y. Shen et al., "Conversion of 5-methylcytosine to 5-hydroxymethylcytosine in mammalian DNA by MLL partner TET1," *Science*, vol. 324, no. 5929, pp. 930–935, 2009.

[8] A. K. Maunakea, R. P. Nagarajan, M. Bilenky et al., "Conserved role of intragenic DNA methylation in regulating alternative promoters," *Nature*, vol. 466, no. 7303, pp. 253–257, 2010.

[9] K. D. Hansen, W. Timp, H. C. Bravo et al., "Increased methylation variation in epigenetic domains across cancer types," *Nature Genetics*, vol. 43, no. 8, pp. 768–775, 2011.

[10] T. Kouzarides, "Chromatin modifications and their function," *Cell*, vol. 128, no. 4, pp. 693–705, 2007.

[11] M. D. Shahbazian and M. Grunstein, "Functions of site-specific histone acetylation and deacetylation," *Annual Review of Biochemistry*, vol. 76, pp. 75–100, 2007.

[12] P. Filippakopoulos, S. Picaud, M. Mangos et al., "Histone recognition and large-scale structural analysis of the human bromodomain family," *Cell*, vol. 149, pp. 214–231, 2012.

[13] Y. I. Tsukada, J. Fang, H. Erdjument-Bromage et al., "Histone demethylation by a family of JmjC domain-containing proteins," *Nature*, vol. 439, no. 7078, pp. 811–816, 2006.

[14] Y. Shi, F. Lan, C. Matson et al., "Histone demethylation mediated by the nuclear amine oxidase homolog LSD1," *Cell*, vol. 119, no. 7, pp. 941–953, 2004.

[15] A. L. Nielsen, M. Oulad-Abdelghani, J. A. Ortiz, E. Remboutsika, P. Chambon, and R. Losson, "Heterochromatin formation in mammalian cells: interaction between histones and HP1 Proteins," *Molecular Cell*, vol. 7, no. 4, pp. 729–739, 2001.

[16] E. Guccione, C. Bassi, F. Casadio et al., "Methylation of histone H3R2 by PRMT6 and H3K4 by an MLL complex are mutually exclusive," *Nature*, vol. 449, no. 7164, pp. 933–937, 2007.

[17] M. Esteller, "Molecular origins of cancer: epigenetics in cancer," *New England Journal of Medicine*, vol. 358, no. 11, pp. 1148–1096, 2008.

[18] A. Dobrovic and D. Simpfendorfer, "Methylation of the BRCA1 gene in sporadic breast cancer," *Cancer Research*, vol. 57, no. 16, pp. 3347–3350, 1997.

[19] G. Deng, A. Chen, J. Hong, H. S. Chae, and Y. S. Kim, "Methylation of CpG in a small region of the hMLH1 promoter invariably correlates with the absence of gene expression," *Cancer Research*, vol. 59, no. 9, pp. 2029–2033, 1999.

[20] E. Hatzimichael, G. Dranitsaris, A. Dasoula et al., "Von Hippel-Lindau methylation status in patients with multiple myeloma: a potential predictive factor for the development of boneDisease," *Clinical Lymphoma and Myeloma*, vol. 9, no. 3, pp. 239–242, 2009.

[21] E. Hatzimichael, A. Dasoula, V. Kounnis et al., "Bcl2-interacting killer CpG methylation in multiple myeloma: a potential predictor of relapsed/refractory disease with therapeutic implications," *Leukemia & Lymphoma*, vol. 53, pp. 1709–1713, 2012.

[22] M. Esteller, "Epigenetics provides a new generation of oncogenes and tumour-suppressor genes," *British Journal of Cancer*, vol. 94, no. 2, pp. 179–183, 2006.

[23] M. Esteller, J. Garcia-Foncillas, E. Andion et al., "Inactivation of the DNA-repair gene MGMT and the clinical response of gliomas to alkylating agents," *New England Journal of Medicine*, vol. 343, no. 19, pp. 1350–1354, 2000.

[24] M. F. Fraga, E. Ballestar, A. Villar-Garea et al., "Loss of acetylation at Lys16 and trimethylation at Lys20 of histone H4 is a common hallmark of human cancer," *Nature Genetics*, vol. 37, no. 4, pp. 391–400, 2005.

[25] S. Ropero, M. F. Fraga, E. Ballestar et al., "A truncating mutation of HDAC2 in human cancers confers resistance to histone deacetylase inhibition," *Nature Genetics*, vol. 38, no. 5, pp. 566–569, 2006.

[26] P. A. C. Cloos, J. Christensen, K. Agger et al., "The putative oncogene GASC1 demethylates tri- and dimethylated lysine 9 on histone H3," *Nature*, vol. 442, no. 7100, pp. 307–311, 2006.

[27] E. Hatzimichael, G. Georgiou, L. Benetatos, and E. Briasoulis, "Gene mutations and molecularly targeted therapies in acute myeloid leukemia," *American Journal of Blood Research*, vol. 3, pp. 29–51, 2013.

[28] X. J. Yan, J. Xu, Z. H. Gu et al., "Exome sequencing identifies somatic mutations of DNA methyltransferase gene DNMT3A in acute monocytic leukemia," *Nature Genetics*, vol. 43, no. 4, pp. 309–317, 2011.

[29] L. Simo-Riudalbas, S. A. Melo, and M. Esteller, "DNMT3B gene amplification predicts resistance to DNA demethylating drugs," *Genes Chromosomes and Cancer*, vol. 50, no. 7, pp. 527–534, 2011.

[30] T. J. Ley, L. Ding, M. J. Walter et al., "DNMT3A mutations in acute myeloid leukemia.," *The New England Journal of Medicine*, vol. 363, pp. 2424–2433, 2010.

[31] F. Thol, F. Damm, A. Ludeking et al., "Incidence and prognostic influence of DNMT3A mutations in acute myeloid leukemia," *Journal of Clinical Oncology*, vol. 29, no. 21, pp. 2889–2896, 2011.

[32] F. Delhommeau, S. Dupont, V. Della Valle et al., "Mutation in TET2 in myeloid cancers," *New England Journal of Medicine*, vol. 360, no. 22, pp. 2289–2301, 2009.

[33] S. Weissmann, T. Alpermann, V. Grossmann et al., "Landscape of TET2 mutations in acute myeloid leukemia," *Leukemia*, vol. 26, pp. 934–942, 2012.

[34] O. Kosmider, V. Gelsi-Boyer, M. Cheok et al., "TET2 mutation is an independent favorable prognostic factor in myelodysplastic syndromes (MDSs)," *Blood*, vol. 114, no. 15, pp. 3285–3291, 2009.

[35] W. C. Chou, S. C. Chou, C. Y. Liu et al., "TET2 mutation is an unfavorable prognostic factor in acute myeloid leukemia patients with intermediate-risk cytogenetics," *Blood*, vol. 118, pp. 3803–3810, 2011.

[36] P. S. Ward, J. Patel, D. R. Wise et al., "The common feature of leukemia-associated IDH1 and IDH2 mutations is a neomorphic enzyme activity converting α-ketoglutarate to 2-hydroxyglutarate," *Cancer Cell*, vol. 17, no. 3, pp. 225–234, 2010.

[37] E. R. Mardis, L. Ding, D. J. Dooling et al., "Recurring mutations found by sequencing an acute myeloid leukemia genome," *New England Journal of Medicine*, vol. 361, no. 11, pp. 1058–1066, 2009.

[38] D. Rakheja, S. Konoplev, L. J. Medeiros, and W. Chen, "IDH mutations in acute myeloid leukemia," *Human Pathology*, vol. 43, pp. 1541–1551, 2012.

[39] M. E. Figueroa, O. Abdel-Wahab, C. Lu et al., "Leukemic IDH1 and IDH2 mutations result in a hypermethylation phenotype, disrupt TET2 function, and impair hematopoietic differentiation," *Cancer Cell*, vol. 18, pp. 553–567, 2010.

[40] G. Rege-Cambrin, E. Giugliano, L. Michaux et al., "Trisomy 11 in myeloid malignancies is associated with internal tandem duplication of both MLL and FLT3 genes," *Haematologica*, vol. 90, no. 2, pp. 262–264, 2005.

[41] C. Steudel, M. Wermke, M. Schaich et al., "Comparative analysis of MLL partial tandem duplication and FLT3 internal tandem duplication mutations in 956 adult patients with acute myeloid leukemia," *Genes Chromosomes and Cancer*, vol. 37, no. 3, pp. 237–251, 2003.

[42] A. V. Krivtsov and S. A. Armstrong, "MLL translocations, histone modifications and leukaemia stem-cell development," *Nature Reviews Cancer*, vol. 7, no. 11, pp. 823–833, 2007.

[43] S. Varambally, S. M. Dhanasekaran, M. Zhou et al., "The polycomb group protein EZH2 is involved in progression of prostate cancer," *Nature*, vol. 419, no. 6907, pp. 624–629, 2002.

[44] L. Benetatos, E. Voulgaris, G. Vartholomatos, and E. Hatzimichael, "Non-coding RNAs and EZH2 interactions in cancer: long and short tales from the transcriptome," *International Journal of Cancer*, 2012.

[45] J. A. Simon and C. A. Lange, "Roles of the EZH2 histone methyltransferase in cancer epigenetics," *Mutation Research*, vol. 647, no. 1-2, pp. 21–29, 2008.

[46] C. J. Sneeringer, M. P. Scott, K. W. Kuntz et al., "Coordinated activities of wild-type plus mutant EZH2 drive tumor-associated hypertrimethylation of lysine 27 on histone H3 (H3K27) in human B-cell lymphomas," *Proceedings of the National Academy of Sciences of the United States of America*, vol. 107, no. 49, pp. 20980–20985, 2010.

[47] T. Ernst, A. J. Chase, J. Score et al., "Inactivating mutations of the histone methyltransferase gene EZH2 in myeloid disorders," *Nature Genetics*, vol. 42, no. 8, pp. 722–726, 2010.

[48] G. Nikoloski, S. M. C. Langemeijer, R. P. Kuiper et al., "Somatic mutations of the histone methyltransferase gene EZH2 in myelodysplastic syndromes," *Nature Genetics*, vol. 42, no. 8, pp. 665–667, 2010.

[49] L. Benetatos, E. Hatzimichael, A. Dasoula et al., "CpG methylation analysis of the MEG3 and SNRPN imprinted genes in acute myeloid leukemia and myelodysplastic syndromes," *Leukemia Research*, vol. 34, no. 2, pp. 148–153, 2010.

[50] L. Benetatos, A. Dasoula, E. Hatzimichael et al., "Polo-like kinase 2 (SNK/PLK2) is a novel epigenetically regulated gene in acute myeloid leukemia and myelodysplastic syndromes: genetic and epigenetic interactions," *Annals of Hematology*, vol. 90, pp. 1037–1045, 2011.

[51] J. R. Melki, P. C. Vincent, and S. J. Clark, "Concurrent DNA hypermethylation of multiple genes in acute myeloid leukemia," *Cancer Research*, vol. 59, no. 15, pp. 3730–3740, 1999.

[52] M. A. McDevitt, "Clinical applications of epigenetic markers and epigenetic profiling in myeloid malignancies," *Seminars in Oncology*, vol. 39, pp. 109–122, 2012.

[53] S. Takada, K. Morita, K. Hayashi et al., "Methylation status of fragile histidine triad (FHIT) gene and its clinical impact on prognosis of patients with multiple myeloma," *European Journal of Haematology*, vol. 75, no. 6, pp. 505–510, 2005.

[54] L. Shen, H. Kantarjian, Y. Guo et al., "DNA methylation predicts survival and response to therapy in patients with myelodysplastic syndromes," *Journal of Clinical Oncology*, vol. 28, no. 4, pp. 605–613, 2010.

[55] Y. Watanabe, H. Ueda, T. Etoh et al., "A change in promoter methylation of hMLH1 is a cause of acquired resistance to platinum-based chemotherapy in epithelial ovarian cancer," *Anticancer Research*, vol. 27, no. 3 B, pp. 1449–1452, 2007.

[56] N. Syed, H. M. Coley, J. Sehouli et al., "Polo-like kinase Plk2 is an epigenetic determinant of chemosensitivity and clinical outcomes in ovarian cancer," *Cancer Research*, vol. 71, no. 9, pp. 3317–3327, 2011.

[57] P. Fenaux, G. J. Mufti, E. Hellstrom-Lindberg et al., "Efficacy of azacitidine compared with that of conventional care regimens in the treatment of higher-risk myelodysplastic syndromes: a randomised, open-label, phase III study," *The Lancet Oncology*, vol. 10, no. 3, pp. 223–232, 2009.

[58] J. A. Gollob and C. J. Sciambi, "Decitabine up-regulates S100A2 expression and synergizes with IFN-γ to kill uveal melanoma cells," *Clinical Cancer Research*, vol. 13, no. 17, pp. 5219–5225, 2007.

[59] K. Appleton, H. J. Mackay, I. Judson et al., "Phase I and pharmacodynamic trial of the DNA methyltransferase inhibitor decitabine and carboplatin in solid tumors," *Journal of Clinical Oncology*, vol. 25, no. 29, pp. 4603–4609, 2007.

[60] D. Matei, F. Fang, C. Shen et al., "Epigenetic resensitization to platinum in ovarian cancer," *Cancer Research*, vol. 72, pp. 2197–2205, 2012.

[61] H. Wang, S. Lee, C. L. Nigro et al., "NT5E (CD73) is epigenetically regulated in malignant melanoma and associated with metastatic site specificity," *British Journal of Cancer*, vol. 106, pp. 1446–1452, 2012.

[62] H. C. Tsai, H. Li, L. Van Neste et al., "Transient low doses of DNA-demethylating agents exert durable antitumor effects on hematological and epithelial tumor cells," *Cancer Cell*, vol. 21, pp. 430–446, 2012.

[63] J. C. Cheng, C. B. Matsen, F. A. Gonzales et al., "Inhibition of DNA methylation and reactivation of silenced genes by zebularine," *Journal of the National Cancer Institute*, vol. 95, no. 5, pp. 399–409, 2003.

[64] J. Datta, K. Ghoshal, W. A. Denny et al., "A new class of quinoline-based DNA hypomethylating agents reactivates tumor suppressor genes by blocking DNA methyltransferase 1 activity and inducing its degradation," *Cancer Research*, vol. 69, no. 10, pp. 4277–4285, 2009.

[65] A. J. M. de Ruijter, A. H. van Gennip, H. N. Caron, S. Kemp, and A. B. P. van Kuilenburg, "Histone deacetylases (HDACs): characterization of the classical HDAC family," *Biochemical Journal*, vol. 370, no. 3, pp. 737–749, 2003.

[66] M. G. Riggs, R. G. Whittaker, J. R. Neumann, and V. M. Ingram, "n-butyrate causes histone modification in HeLa and Friend erythroleukaemia cells," *Nature*, vol. 268, no. 5619, pp. 462–464, 1977.

[67] E. Raffoux, A. Cras, C. Recher et al., "Phase 2 clinical trial of 5-azacitidine, valproic acid, and all-trans retinoic acid in patients with high-risk acute myeloid leukemia or myelodysplastic syndrome," *Oncotarget*, vol. 1, pp. 34–42, 2010.

[68] A. O. Soriano, H. Yang, S. Faderl et al., "Safety and clinical activity of the combination of 5-azacytidine, valproic acid, and all-trans retinoic acid in acute myeloid leukemia and myelodysplastic syndrome," *Blood*, vol. 110, no. 7, pp. 2302–2308, 2007.

[69] H. M. Prince, M. J. Bishton, and S. J. Harrison, "Clinical studies of histone deacetylase inhibitors," *Clinical Cancer Research*, vol. 15, no. 12, pp. 3958–3969, 2009.

[70] S. E. Witta, R. M. Jotte, K. Konduri et al., "Randomized phase II trial of erlotinib with and without entinostat in patients with advanced non-small-cell lung cancer who progressed on prior chemotherapy," *Journal of Clinical Oncology*, vol. 30, pp. 2248–2255, 2012.

[71] C. Gridelli, A. Rossi, and P. Maione, "The potential role of histone deacetylase inhibitors in the treatment of non-small-cell lung cancer," *Critical Reviews in Oncology/Hematology*, vol. 68, no. 1, pp. 29–36, 2008.

[72] K. T. Lin, Y. W. Wang, C. T. Chen, C. M. Ho, W. H. Su, and Y. S. Jou, "HDAC inhibitors augmented cell migration and metastasis through induction of PKCs leading to identification of low toxicity modalities for combination cancer therapy," *Clinical Cancer Research*, vol. 18, pp. 4691–4701, 2012.

[73] V. Guerini, V. Barbui, O. Spinelli et al., "The histone deacetylase inhibitor ITF2357 selectively targets cells bearing mutated JAK2V617F," *Leukemia*, vol. 22, no. 4, pp. 740–747, 2008.

[74] A. Younes, A. Sureda, D. Ben-Yehuda et al., "Panobinostat in patients with relapsed/refractory Hodgkin's lymphoma after autologous stem-cell transplantation: results of a phase II study," *Journal of Clinical Oncology*, vol. 30, pp. 2197–2203, 2012.

[75] S. Dimicoli, E. Jabbour, G. Borthakur et al., "Phase II study of the histone deacetylase inhibitor panobinostat (LBH589) in patients with low or intermediate-1 risk myelodysplastic syndrome," *American Journal of Hematology*, vol. 87, no. 1, pp. 127–129, 2012.

[76] J. H. Strickler, A. N. Starodub, J. Jia et al., "Phase I study of bevacizumab, everolimus, and panobinostat (LBH-589) in advanced solid tumors," *Cancer Chemotherapy and Pharmacology*, vol. 70, no. 2, pp. 251–258, 2012.

[77] H. Wang, Q. Cao, and A. Z. Dudek, "Phase II study of panobinostat and bortezomib in patients with pancreatic cancer progressing on gemcitabine-based therapy," *Anticancer Research*, vol. 32, pp. 1027–1031, 2012.

[78] L. Santo, T. Hideshima, A. L. Kung et al., "Preclinical activity, pharmacodynamic, and pharmacokinetic properties of a selective HDAC6 inhibitor, ACY-1215, in combination with bortezomib in multiple myeloma," *Blood*, vol. 119, no. 11, pp. 2579–2589, 2012.

[79] B. N. Singh, G. Zhang, Y. L. Hwa, J. Li, S. C. Dowdy, and S. W. Jiang, "Nonhistone protein acetylation as cancer therapy targets," *Expert Review of Anticancer Therapy*, vol. 10, no. 6, pp. 935–954, 2010.

[80] A. Cashen, M. Juckett, A. Jumonville et al., "Phase II study of the histone deacetylase inhibitor belinostat (PXD101) for the treatment of myelodysplastic syndrome (MDS)," *Annals of Hematology*, vol. 91, pp. 33–38, 2012.

[81] J. D. Hainsworth, J. R. Infante, D. R. Spigel, E. R. Arrowsmith, R. V. Boccia, and H. A. Burris, "A phase II trial of panobinostat, a histone deacetylase inhibitor, in the treatment of patients with refractory metastatic renal cell carcinoma," *Cancer Investigation*, vol. 29, no. 7, pp. 451–455, 2011.

[82] R. A. Juergens, J. Wrangle, F. P. Vendetti et al., "Combination epigenetic therapy has efficacy in patients with refractory advanced non-small cell lung cancer," *Cancer Discovery*, vol. 1, pp. 598–607, 2011.

[83] D. A. Pollyea, H. E. Kohrt, L. Gallegos et al., "Safety, efficacy and biological predictors of response to sequential azacitidine and lenalidomide for elderly patients with acute myeloid leukemia," *Leukemia*, vol. 26, pp. 893–901, 2012.

[84] W. Blum, S. Schwind, S. S. Tarighat et al., "Clinical and pharmacodynamic activity of bortezomib and decitabine in acute myeloid leukemia," *Blood*, vol. 119, pp. 6025–6031, 2012.

[85] L. Shen, Y. Kondo, S. Ahmed et al., "Drug sensitivity prediction by CpG island methylation profile in the NCI-60 cancer cell line panel," *Cancer Research*, vol. 67, no. 23, pp. 11335–11343, 2007.

[86] M. E. Hegi, D. Sciuscio, A. Murat, M. Levivier, and R. Stupp, "Epigenetic deregulation of DNA repair and its potential for therapy," *Clinical Cancer Research*, vol. 15, no. 16, pp. 5026–5031, 2009.

[87] P. Raha, S. Thomas, and P. N. Munster, "Epigenetic modulation: a novel therapeutic target for overcoming hormonal therapy resistance," *Epigenomics*, vol. 3, pp. 451–470, 2011.

[88] G. J. Sabnis, O. Goloubeva, S. Chumsri, N. Nguyen, S. Sukumar, and A. M. H. Brodie, "Functional activation of the estrogen receptor-α and aromatase by the HDAC inhibitor entinostat sensitizes ER-negative tumors to letrozole," *Cancer Research*, vol. 71, no. 5, pp. 1893–1903, 2011.

[89] D. Sharma, N. K. Saxena, N. E. Davidson, and P. M. Vertino, "Restoration of tamoxifen sensitivity in estrogen receptor-negative breast cancer cells: tamoxifen-bound reactivated ER recruits distinctve corepressor complexes," *Cancer Research*, vol. 66, no. 12, pp. 6370–6378, 2006.

[90] C. G. Lian, Y. Xu, C. Ceol et al., "Loss of 5-hydroxymethylcytosine is an epigenetic hallmark of melanoma," *Cell*, vol. 150, pp. 1135–1146, 2012.

[91] A. Sharma, T. Crook, A. Thompson, and C. Palmieri, "Surgical oncology: why biopsying metastatic breast cancer should be routine," *Nature Reviews Clinical Oncology*, vol. 7, no. 2, pp. 72–74, 2010.

[92] N. Syed, J. Langer, K. Janczar et al., "Epigenetic status of argininosuccinate synthetase and argininosuccinate lyase modulates autophagy and cell death in glioblastoma," *Cell Death and Disease*, vol. 4, article e458, 2013.

[93] D. Huertas, M. Soler, J. Moreto et al., "Antitumor activity of a small-molecule inhibitor of the histone kinase Haspin," *Oncogene*, vol. 31, pp. 1408–1418, 2012.

[94] J. Tan, X. Yang, L. Zhuang et al., "Pharmacologic disruption of polycomb-repressive complex 2-mediated gene repression selectively induces apoptosis in cancer cells," *Genes and Development*, vol. 21, no. 9, pp. 1050–1063, 2007.

[95] E. Lara, A. Mai, V. Calvanese et al., "Salermide, a Sirtuin inhibitor with a strong cancer-specific proapoptotic effect," *Oncogene*, vol. 28, pp. 781–791, 2009.

Hindawi Publishing Corporation
Journal of Drug Delivery
Volume 2013, Article ID 107573, 7 pages
http://dx.doi.org/10.1155/2013/107573

Review Article

Convection-Enhanced Delivery for Targeted Delivery of Antiglioma Agents: The Translational Experience

Jonathan Yun,[1] Robert J. Rothrock,[1] Peter Canoll,[2] and Jeffrey N. Bruce[1,3]

[1] *Gabriele Bartoli Brain Tumor Laboratory, Departments of Neurosurgery, Columbia University Medical Center, 1130 St. Nicholas Avenue Room 1001, New York, NY 10032, USA*
[2] *Pathology and Cell Biology, Columbia University Medical Center, 1130 St. Nicholas Avenue Room 1001, New York, NY 10032, USA*
[3] *Department of Neurological Surgery, Neurological Institute of New York, 710 West 168th Street, New York, NY 10032, USA*

Correspondence should be addressed to Jeffrey N. Bruce; jnb2@columbia.edu

Received 23 November 2012; Accepted 10 December 2012

Academic Editor: Andreas G. Tzakos

Recent improvements in the understanding of glioblastoma (GBM) have allowed for increased ability to develop specific, targeted therapies. In parallel, however, there is a need for effective methods of delivery to circumvent the therapeutic obstacles presented by the blood-brain barrier and systemic side effects. The ideal delivery system should allow for adequate targeting of the tumor while minimizing systemic exposure, applicability across a wide range of potential therapies, and have existing safe and efficacious systems that allow for widespread application. Though many alternatives to systemic delivery have been developed, this paper will focus on our experience with convection-enhanced delivery (CED) and our focus on translating this technology from pre-clinical studies to the treatment of human GBM.

1. Introduction

Malignant gliomas are among the most pernicious of human tumors and are characterized as regionally invasive, usually recurring within two centimeters of their origin after resection [1]. Although many advances in treatment have been made, they have yielded only modest survival benefits [2]. Numerous chemotherapeutic drugs have demonstrated significant antitumor activity in preclinical studies, but often this effectiveness is not translated into clinical trials in humans. A major factor contributing to this is the limitation of systemic delivery, namely, the impermeability of the blood-brain barrier as well as dose-limiting toxicities of many compounds. This highlights the need for efficient, specific methods of delivery in the treatment of human GBM.

The ideal delivery method would be one that achieves adequate coverage of the tumor volume while minimizing any unwanted toxicities. Optimal delivery requires three important components: the ability to target the tumor while minimizing local and systemic effects, applicability over a wide range of therapies, and a safe, efficacious method of continuous delivery with noninvasive methods to monitor volumes of distribution (Vd) of agents. In this paper, we describe our experience with convection-enhanced delivery (CED) across these three domains and highlight the translational goals of this work. The ultimate goal is to safely bring such systems and therapies to human trials, and eventually, to optimize these methods in clinical practice and establish standards of care.

2. Convection-Enhanced Delivery

Convection-enhanced delivery, pioneered by Bobo et al., delivers agents directly into the tumor and the surrounding parenchyma with continuous, positive-pressure infusion [3]. While other methods of delivery exist, such as through intraarterial and intrathecal routes, these are often limited by the blood-brain and blood-CSF barrier as well as unwanted toxicities. Furthermore, compared to diffusion-based drug

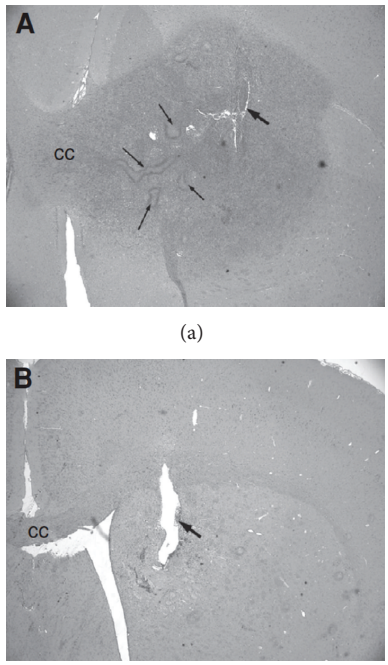

(a)

(b)

Figure 1: (a) The local delivery of PBS for 7 days into PDGF-expression retrovirus-induced tumor (large arrow—injection site) demonstrates a large proliferative lesion with notable pseudopalisading necrosis (small arrows) and invasion across the corpus callosum (CC). (b) The delivery of topotecan for 7 days results in significant decrease in tumor cells. (Figure reprinted with permission from Lopez et al. [5].)

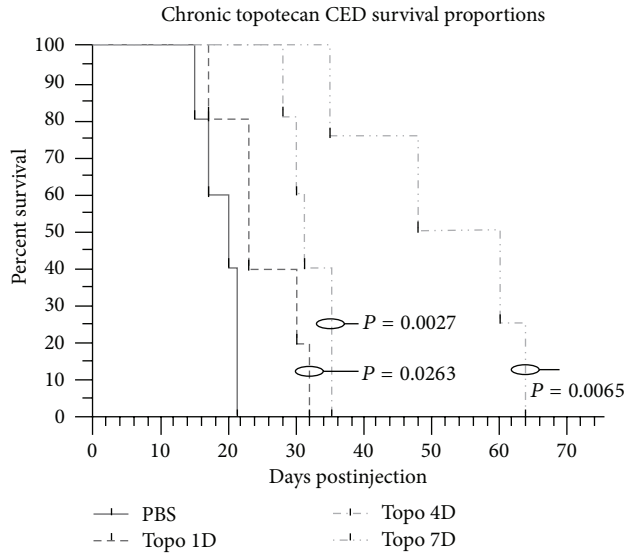

Figure 2: The local delivery of topotecan by convection-enhanced delivery resulted in significant survival advantage when compared to PBS treated controls. This effect was greater with longer periods of therapy. (Figure reprinted with permission from Lopez et al. [5].)

delivery (i.e., carmustine wafers), convective delivery allows for larger volumes of distribution, as it is not limited by diffusive spread by concentration gradients [4]. Importantly, CED allows direct access to the tumor bed, achieving high local concentrations of drug with minimal systemic absorption.

One of the first therapeutic agents given via CED for malignant gliomas in a clinical trial was diphtheria toxin conjugated to transferrin (TF-CRM107) [9]. This pioneering clinical trial highlighted the capability of CED to maximize therapeutic effect while limiting toxicity, as adverse events were limited. Several Phase I and II studies with other targeted cytotoxins followed in succeeding years, including IL-4, IL-13, transforming growth factor (TGF)-a conjugated to pseudomonas exotoxin, herpes simplex virus (HSV)-1-tk gene-containing liposomes, and 131I-labeled chimeric monoclonal antibody to histone H1 (Cotara) [10–14]. These trials demonstrated tumor specificity and adequate agent distribution with adverse effects similarly limited to target tissue damage and minimal to no systemic toxicity. These trials were limited, however, by the specificity of the delivered agents, which targeted only a subpopulation of tumor cells. Prior to our clinical trial, paclitaxel was the only conventional chemotherapeutic agent delivered via CED in a clinical trial [15]. This was mainly because paclitaxel does not cross the BBB, thus allowing the investigators to demonstrate that DW-MRI could be used to approximate the volume of distribution of CED. The trial resulted in a large incidence (40%) of chemical meningitis, a major drawback to the choice of paclitaxel [15, 16]. Though these studies highlighted initial challenges in the application of CED, they demonstrated the importance of careful and rational selection of agents for use in this method of delivery.

3. Early Experiences: CED of Topotecan

Our initial experience with CED of antitumor agents utilized the cytotoxic agent topotecan. Topotecan is a camptothecin-class drug and acts as a topoisomerase-I inhibitor. It causes single-strand DNA breaks during DNA replication [17, 18]. This drug was selected after we demonstrated in vitro cytotoxicity against various malignant glioma cell lines [19]. Due to its activity in cells in the S-phase of division, topotecan is ideal for the treatment of mitotically active glioma cells in the setting of relatively quiescent brain tissue. Previous experience with topotecan demonstrated poor penetration of the blood-brain barrier and significant dose-limiting toxicities, limiting systemic administration [20–23]. However, these same properties make it an ideal drug for administration via CED.

In addition, an important aspect of the choice of topotecan was its effect on a vital cellular process, namely, the role of topoisomerase I on DNA processes. This focus on conventional chemotherapeutic agents as opposed to targeted therapies allows for greater coverage of heterogeneous glioma subpopulations. While targeted therapies can be successful in eliminating a specific subpopulation of glioma cells that express a certain antigen, this provides a selective advantage for remaining neoplastic cells.

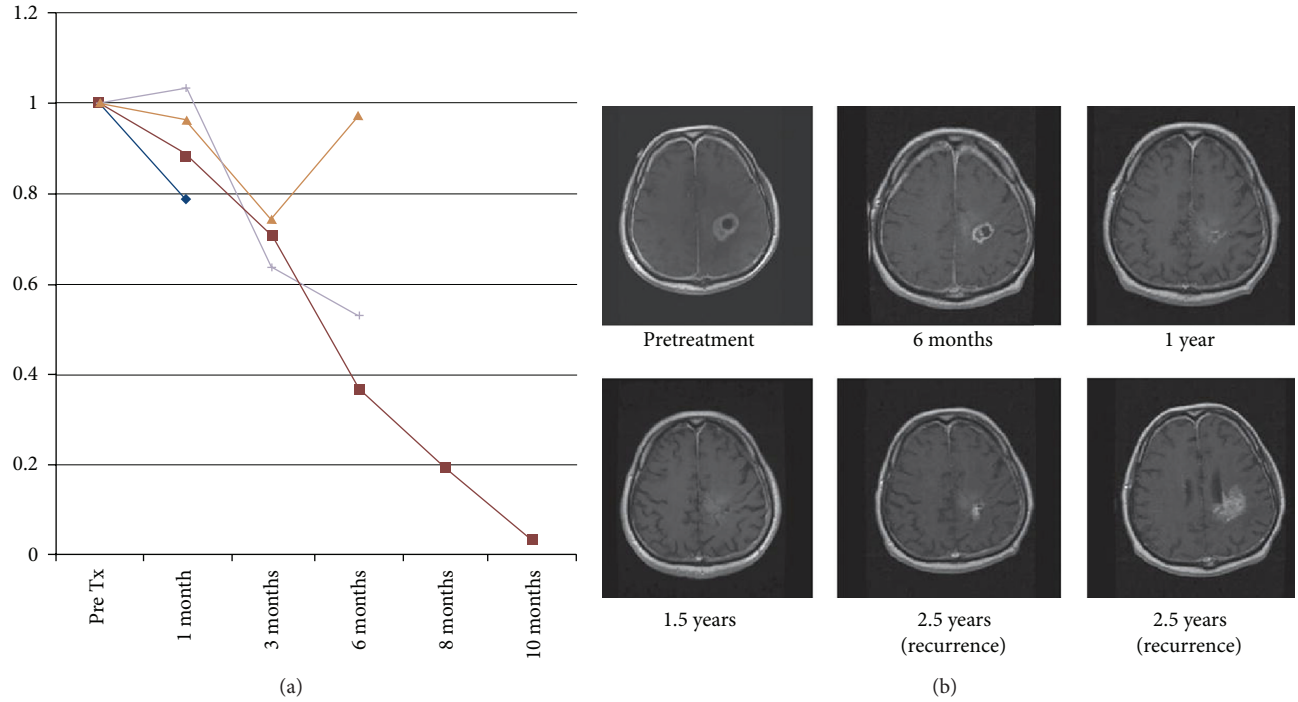

Figure 3: (a) 4 patients of the 16 treated demonstrated an immediate decrease in contrast enhancing volume following CED of topotecan, classified as early responders. (b) Serial T1 weighted, contrast MRI sequences from a selected patient demonstrating significant response with complete resolution at 1.5 years. Recurrence was noted at 2.5 years posttreatment. (Figure reprinted with permission from Bruce et al. [6].)

Preclinical testing of topotecan that was performed in a model of glioblastoma was developed using a PDGF-B expressing retrovirus injected stereotactically into the adult white matter of rats to infect glial progenitors [19]. This resulted in the consistent development of tumors that closely resembled glioblastoma, with pseudopalisading necrosis, invasion, glomeruloid vascular proliferation, and survival of 14–19 days [24]. Topotecan was delivered using an implantable osmotic pump connected to an intracerebral infusion cannula (Alzet; Cupertino, CA) that was implanted into the tumor. A significant survival advantage was demonstrated in glioma-bearing rats treated with topotecan at concentrations significantly less than those used in systemic studies. Further, we found that animals treated for a longer period of time demonstrated increased survival benefit (1 d versus 4 d versus 7 d) [5] (Figure 1). Importantly, no adverse effects of the medication were observed.

Given the promising results of our preclinical studies, a Phase I, dose escalation clinical trial was undertaken to treat patients with recurrent glioblastoma with CED of topotecan. Topotecan was delivered to 18 patients with radiographically and pathologically confirmed recurrent high-grade glioma. While not primarily designed to test treatment efficacy, this clinical trial demonstrated that the CED of topotecan resulted in radiographic tumor regression in 69% of patients, with 25% demonstrating an early response, at a drug concentration nontoxic to normal brain with minimal drug-associated systemic toxicity [6] (Figure 2). This demonstrated that CED is an effective method of bypassing the blood-brain barrier to achieve targeted antitumor effect with minimal dose-limiting toxicities. Furthermore, topotecan proved to be a potent antitumor drug when delivered appropriately and directly to the tumor.

4. CED as a Platform to Assess Novel Antitumor Agents

Various classes of drugs have been proposed as potential antitumor agents. CED is a valuable platform to assess the feasibility of administering these agents in vivo. For example, virus-mediated gene therapy has proven to be a promising modality to allow for tumor-specific delivery of gene constructs. However, the initial experience with these agents has been hindered by poor distribution [25]. We have found that CED is a viable method of distributing adenoviral particles widely across white matter tracts in a rodent model (Figure 3(a)). Furthermore, with the modification of these particles with supraparamagnetic iron oxide particles (Figure 5), we were able to characterize MRI signatures that would allow of the real-time monitoring of vector distribution (Figure 3(b)) [7].

CED allows for direct assessment of newly selected drugs by maximizing the specific delivery to the tumor, especially as the molecular understanding of human GBM continues to identify new potential targets. Based on the work of Verhaak et al., GBM has been subdivided based on 4 distinct molecular signatures: classical, neural, proneural, and

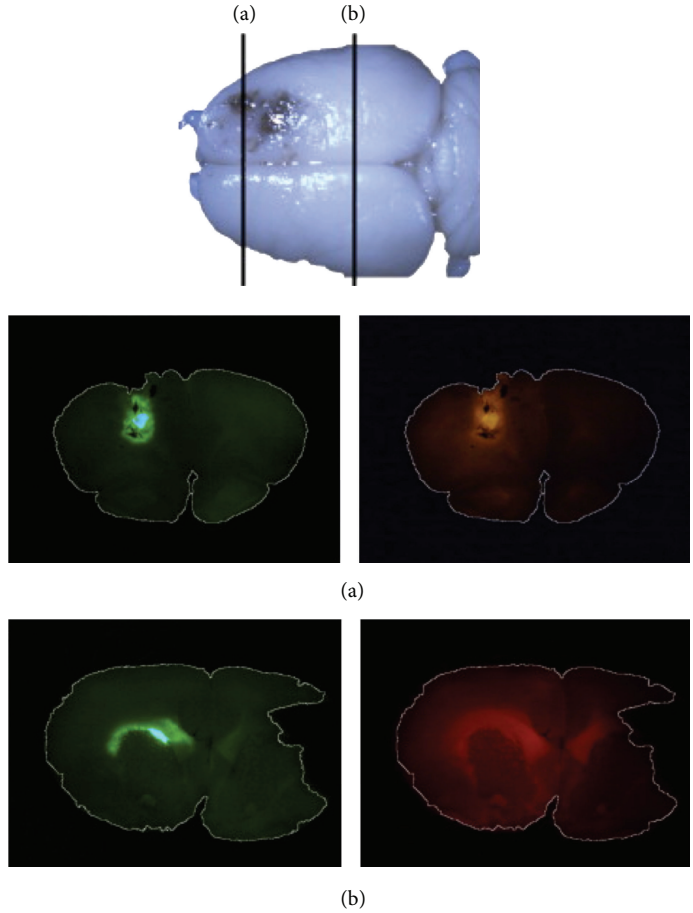

Figure 4: Infusion of an adenoviral vector (Ad5) expressing GFP and rhodamine-dextran demonstrates distribution of the vector throughout the ipsilateral white matter at (a) rostral and (b) caudal sections of the brain. (Figure reprinted with permission from Yun et al. [7].)

mesenchymal [26]. Our group has developed a mouse model of glioma which is induced by injecting a retrovirus that expresses PDGF-B and cre recombinase into the subcortical white matter of transgenic mice that harbor floxed alleles of the tumor suppressor genes, PTEN and p53. We found that the expression profile of these tumors closely resembles the proneural subtype of GBM [27]. This model provides a powerful tool to assess therapies in treating this specific subtype of GBM. Also, by understanding the molecular profile of this subtype, rational selection of antitumor agents can be pursued.

Within human TCGA data, we found that topoisomerases are differentially expressed across the 4 GBM subtypes, with proneural subtype showing the highest levels of both TOP2a and TOP2b expressions. The elevated expression of topoisomerase II seen in the proneural subgroup suggested that these tumors might be particularly sensitive to inhibitors of topoisomerase II. We also found elevated expression of topoisomerase II compared to topoisomerase I in our murine model of proneural GBM (Carminucci et al. [28]).

Based on these findings, we hypothesized that etoposide, a topoisomerase II inhibitor, would exhibit effective cytotoxicity against the proneural subtype of GBM. We are currently undergoing preclinical testing with local, continuous delivery of etoposide in our mouse model of proneural GBM, which demonstrates significant antitumor activity and prolonged survival (Carminucci et al. [28]). We hope to translate these findings into early Phase I and II trials and to assess clinical and radiographic response with an understanding of the specific molecular subtypes of tumors treated.

5. Prolonged CED with Implantable Subcutaneous Pumps

In our initial clinical trial, we demonstrated the ability of CED to deliver and effectively treat tumors with chemotherapy, all while bypassing the blood brain barrier and minimizing systemic toxicity. These clinical studies utilized externalized catheters, which, due to an increasing risk of infection with longer placement, shortened the treatment period to 4 days [6]. As mentioned above, in our rodent model, we demonstrated that prolonged delivery of topotecan is associated with increased survival. Therefore, we sought to develop a system for prolonged delivery that could be safely applied in the clinical setting.

To this end, we have employed an implantable subcutaneous pump (Synchromed II, Medtronic; Minneapolis, MN),

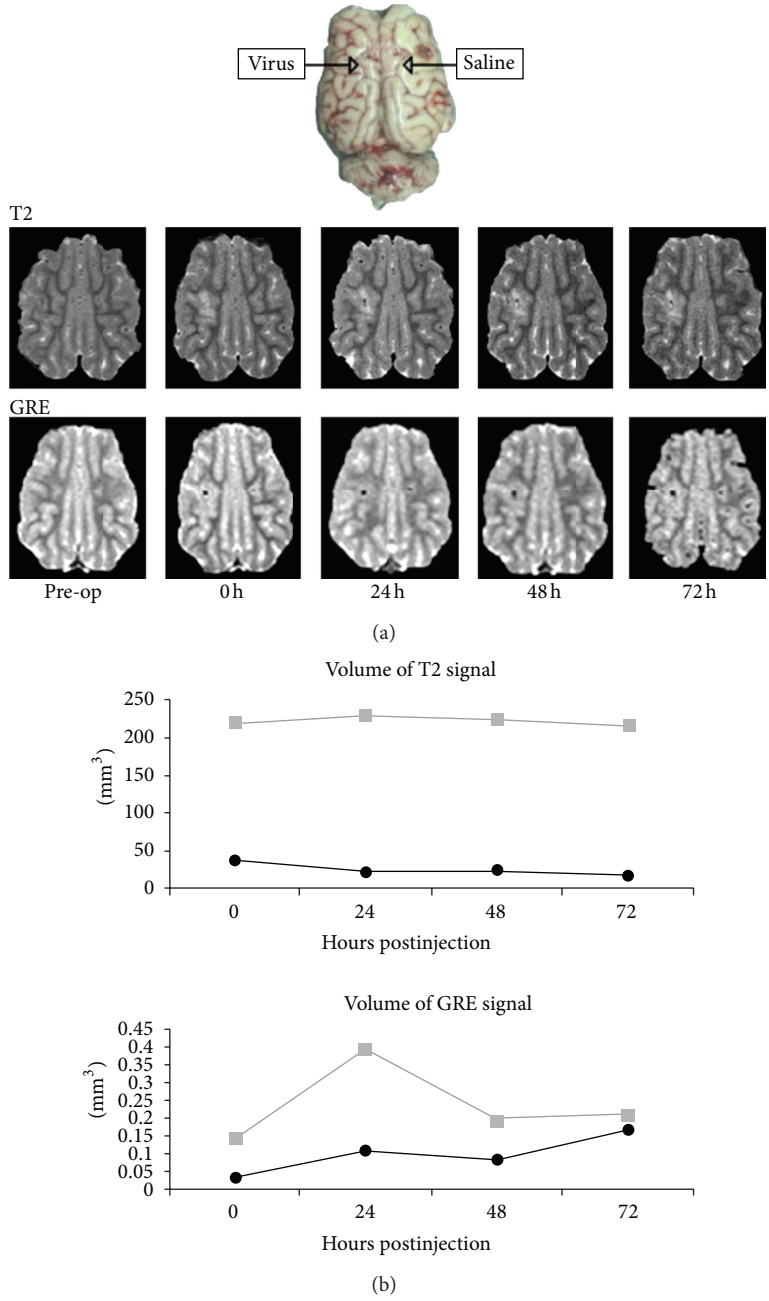

Figure 5: (a) Local injection of a superparamagnetic iron oxide nanoparticle labeled adenovirus demonstrates a T2-intense, GRE positive signal at the site of injection when compared to the contralateral, saline-injected side. (b) Volume analysis demonstrates a greater T2-intense volume with adenovirus injection when compared to saline. (Figure reprinted with permission from Yun et al. [7].)

already FDA approved for the treatment of spasticity and chronic pain. To assess this system in the pre-clinical setting, the pig model was used due to the larger size of the brain in comparison to the rodent model and its similarity to human gray/white matter composition. The pump was implanted into a subcutaneous pocket in the pig's back, and silastic catheter was tunneled subcutaneously and inserted into the frontal white matter. The reservoir was filled with a mixture of topotecan and/or gadolinium and was infused over a period of 10 days. The volumes of distribution were followed with serial MRI, and safety and toxicity were assessed on a daily basis [8].

In this study, we demonstrated safety of topotecan with prolonged intracerebral infusion in nontumor bearing animals. Furthermore, topotecan retained its antitumor bioactivity after prolonged exposure to physiologic conditions. We demonstrated stability of the volume of distribution of gadolinium with prolonged delivery, with rapid reabsorption of contrast following cessation of infusion [8] (Figure 4). Along with the tolerability of the implanted pump, these

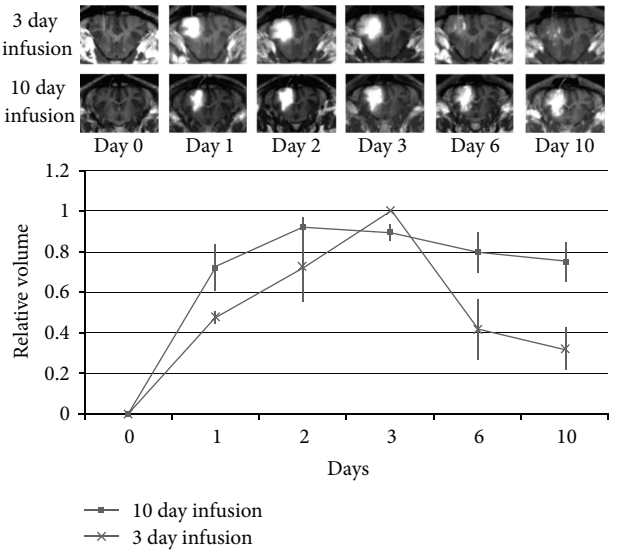

Figure 6: Prolonged infusion (10 d) with an implanted subcutaneous pump results in stable volumes of distribution. The maximum relative volume was reached 2-3 days after infusion was initiated. With infusion discontinued at day 3, enhancing volume is seen to dissipate. (Figure reprinted with permission from Sonabend et al. [8].)

findings provide justification for translation of this system to clinical trials, and we hope to employ this system for the treatment of human gliomas.

6. Challenges

The administration of therapeutics via CED is not without its challenges, most notably the leakage of refluxed infusate along the catheter [29]. Other risks include infection, as well as those related to the drug, including potential systemic events if the agent is able to cross the blood-brain barrier. In our experience, however, the biologically active doses of the therapeutic agent administered via CED are well below systemic dose limiting toxicities. As Saito et al. have demonstrated, the volume of distribution (Vd) (Figure 6) achieved by CED is dependent on multiple compound specific factors (i.e., lipophilicity), as well as anatomical variables (i.e., tumor architecture and white matter tracks) [30]. The potential volumes achievable with CED, however, are greater than the volumes achieved by implantable wafers and diffusion-based therapies [31].

7. Discussion

Convection-enhanced delivery provides a method of local delivery of antitumor agents directly to the tumor and the surrounding infiltrative edges. Benefits of this system include volumes of distribution not limited by the physical characteristics of the drug or diffusive spread along concentration gradients [4]. This allows for the administration of a wide range of antitumor drugs that have been previously limited by systemic toxicities and poor distribution.

Further, this method of delivery allows for greater flexibility with drug development and selection, as the effects of the blood brain barrier and systemic metabolism are minimized with direct, targeted delivery to the tumor. With the development of an implantable system that allows for prolonged delivery, it is conceivable that GBM can be treated chronically with single or multiple, sequential agents. Thus, our experience with CED demonstrates the ability to target tumors for the local delivery of a wide range of therapies, with systems that allow for a safe transition to the treatment of patients.

Conflict of Interests

The authors report no conflict of interests.

References

[1] F. G. Barker II, S. M. Chang, P. H. Gutin et al., "Survival and functional status after resection of recurrent glioblastoma multiforme," *Neurosurgery*, vol. 42, no. 4, pp. 709–723, 1998.

[2] R. Stupp, W. P. Mason, M. J. Van Den Bent et al., "Radiotherapy plus concomitant and adjuvant temozolomide for glioblastoma," *The New England Journal of Medicine*, vol. 352, no. 10, pp. 987–996, 2005.

[3] R. H. Bobo, D. W. Laske, A. Akbasak, P. F. Morrison, R. L. Dedrick, and E. H. Oldfield, "Convection-enhanced delivery of macromolecules in the brain," *Proceedings of the National Academy of Sciences of the United States of America*, vol. 91, no. 6, pp. 2076–2080, 1994.

[4] M. Y. Chen, R. R. Lonser, P. F. Morrison, L. S. Governale, and E. H. Oldfield, "Variables affecting convection-enhanced delivery to the striatum: a systematic examination of rate of infusion, cannula size, infusate concentration, and tissue-cannula sealing time," *Journal of Neurosurgery*, vol. 90, no. 2, pp. 315–320, 1999.

[5] K. A. Lopez, A. M. Tannenbaum, M. C. Assanah et al., "Convection-enhanced delivery of topotecan into a PDGF-driven model of glioblastoma prolongs survival and ablates both tumor-initiating cells and recruited glial progenitors," *Cancer Research*, vol. 71, no. 11, pp. 3963–3971, 2011.

[6] J. N. Bruce, R. L. Fine, P. Canoll et al., "Regression of recurrent malignant gliomas with convection-enhanced delivery of topotecan," *Neurosurgery*, vol. 69, pp. 1272–1279, 2011.

[7] J. Yun, A. M. Sonabend, I. V. Ulasov et al., "A novel adenoviral vector labeled with superparamagnetic iron oxide nanoparticles for real-time tracking of viral delivery," *Journal of Clinical Neuroscience*, vol. 19, pp. 875–880, 2012.

[8] A. M. Sonabend, R. M. Stuart, J. Yun et al., "Prolonged intracerebral convection-enhanced delivery of topotecan with a subcutaneously implantable infusion pump," *Neuro-Oncology*, vol. 13, pp. 886–893, 2011.

[9] D. W. Laske, R. J. Youle, and E. H. Oldfield, "Tumor regression with regional distribution of the targeted toxin TF- CRM107 in patients with malignant brain tumors," *Nature Medicine*, vol. 3, no. 12, pp. 1362–1368, 1997.

[10] R. W. Rand, R. J. Kreitman, N. Patronas, F. Varricchio, I. Pastan, and R. K. Puri, "Intratumoral administration of recombinant circularly permuted interleukin-4-Pseudomonas exotoxin in patients with high-grade glioma," *Clinical Cancer Research*, vol. 6, no. 6, pp. 2157–2165, 2000.

[11] F. W. Weber, F. Floeth, A. Asher et al., "Local convection enhanced, delivery of IL4-Pseudomonas exotoxin (NBI-3001) for treatment of patients with recurrent malignant glioma," *Acta Neurochirurgica*, no. 88, pp. 93–103, 2003.

[12] S. Kunwar, "Convection enhanced delivery of IL13-PE38QQR for treatment of recurrent malignant glioma: presentation of interim findings from ongoing phase 1 studies," *Acta neurochirurgica*, vol. 88, pp. 105–111, 2003.

[13] J. H. Sampson, G. Akabani, G. E. Archer et al., "Progress report of a Phase I study of the intracerebral microinfusion of a recombinant chimeric protein composed of transforming growth factor (TGF)-α and a mutated form of the Pseudomonas exotoxin termed PE-38 (TP-38) for the treatment of malignant brain tumors," *Journal of Neuro-Oncology*, vol. 65, no. 1, pp. 27–35, 2003.

[14] S. J. Patel, W. R. Shapiro, D. W. Laske et al., "Safety and feasibility of convection-enhanced delivery of Cotara for the treatment of malignant glioma: initial experience in 51 patients," *Neurosurgery*, vol. 56, no. 6, pp. 1243–1252, 2005.

[15] Z. Lidar, Y. Mardor, T. Jonas et al., "Convection-enhanced delivery of paclitaxel for the treatment of recurrent malignant glioma: a phase I/II clinical study," *Journal of Neurosurgery*, vol. 100, no. 3, pp. 472–479, 2004.

[16] G. Pöpperl, R. Goldbrunner, F. J. Gildehaus et al., "O-(2-[18F]fluoroethyl)-L-tyrosine PET for monitoring the effects of convection-enhanced delivery of paclitaxel in patients with recurrent glioblastoma," *European Journal of Nuclear Medicine and Molecular Imaging*, vol. 32, no. 9, pp. 1018–1025, 2005.

[17] R. P. Hertzberg, M. J. Caranfa, and S. M. Hecht, "On the mechanism of topoisomerase I inhibition by camptothecin: evidence for binding to an enzyme-DNA complex," *Biochemistry*, vol. 28, no. 11, pp. 4629–4638, 1989.

[18] Y. H. Hsiang, R. Hertzberg, S. Hecht, and L. F. Liu, "Camptothecin induces protein-linked DNA breaks via mammalian DNA topoisomerase I," *Journal of Biological Chemistry*, vol. 260, no. 27, pp. 14873–14878, 1985.

[19] M. G. Kaiser, A. T. Parsa, R. L. Fine, J. S. Hall, I. Chakrabarti, and J. N. Bruce, "Tissue distribution and antitumor activity of topotecan delivered by intracerebral clysis in a rat glioma model," *Neurosurgery*, vol. 47, no. 6, pp. 1391–1399, 2000.

[20] H. S. Friedman, T. Kerby, S. Fields et al., "Topotecan treatment of adults with primary malignant glioma. The Brain Tumor Center at Duke," *Cancer*, vol. 85, pp. 1160–1165, 1999.

[21] F. Goldwasser, X. Buthaud, M. Gross et al., "Decreased topotecan platelet toxicity with successive topotecan treatment cycles in advanced ovarian cancer patients," *Anti-Cancer Drugs*, vol. 10, no. 3, pp. 263–265, 1999.

[22] D. Macdonald, G. Cairncross, D. Stewart et al., "Phase II study of topotecan in patients with recurrent malignant glioma," *Annals of Oncology*, vol. 7, no. 2, pp. 205–207, 1996.

[23] M. L. Rothenberg, "Topoisomerase I inhibitors: review and update," *Annals of Oncology*, vol. 8, no. 9, pp. 837–855, 1997.

[24] M. Assanah, R. Lochhead, A. Ogden, J. Bruce, J. Goldman, and P. Canoll, "Glial progenitors in adult white matter are driven to form malignant gliomas by platelet-derived growth factor-expressing retroviruses," *Journal of Neuroscience*, vol. 26, no. 25, pp. 6781–6790, 2006.

[25] F. F. Lang, J. M. Bruner, G. N. Fuller et al., "Phase I trial of adenovirus-mediated p53 gene therapy for recurrent glioma: biological and clinical results," *Journal of Clinical Oncology*, vol. 21, no. 13, pp. 2508–2518, 2003.

[26] R. G. W. Verhaak, K. A. Hoadley, E. Purdom et al., "Integrated Genomic Analysis Identifies Clinically Relevant Subtypes of Glioblastoma Characterized by Abnormalities in PDGFRA, IDH1, EGFR, and NF1," *Cancer Cell*, vol. 17, no. 1, pp. 98–110, 2010.

[27] L. Lei, A. M. Sonabend, P. Guarnieri et al., "Glioblastoma models reveal the connection between adult glial progenitors and the proneural phenotype," *PLoS ONE*, vol. 6, no. 5, article e20041, Article ID e20041, 2011.

[28] A. S. Carminucci, B. Amendolara, R. Leung et al., "Convection-enhanced delivery of etoposide is effective against amurine model of proneural GBM," *Neuro-Oncology*. In press.

[29] R. Saito and T. Tominaga, "Convection-enhanced delivery: from mechanisms to clinical drug delivery for diseases of the central nervous system," *Neurologia Medico-Chirurgica*, vol. 52, pp. 531–538, 2012.

[30] R. Saito, M. T. Krauze, C. O. Noble et al., "Tissue affinity of the infusate affects the distribution volume during convection-enhanced delivery into rodent brains: implications for local drug delivery," *Journal of Neuroscience Methods*, vol. 154, no. 1-2, pp. 225–232, 2006.

[31] D. Allhenn, M. A. Boushehri, and A. Lamprecht, "Drug delivery strategies for the treatment of malignant gliomas," *International Journal of Pharmaceutics*, vol. 436, pp. 299–310, 2012.

Hindawi Publishing Corporation
Journal of Drug Delivery
Volume 2013, Article ID 957605, 13 pages
http://dx.doi.org/10.1155/2013/957605

Review Article

The Sulfatase Pathway for Estrogen Formation: Targets for the Treatment and Diagnosis of Hormone-Associated Tumors

Lena Secky,[1] Martin Svoboda,[1] Lukas Klameth,[1,2] Erika Bajna,[1] Gerhard Hamilton,[2] Robert Zeillinger,[2] Walter Jäger,[3] and Theresia Thalhammer[1]

[1] *Department of Pathophysiology and Allergy Research, Center for Pathophysiology, Infectiology and Immunology, Medical University of Vienna, Waehringer Guertel 18-20, 1090 Vienna, Austria*
[2] *Ludwig Boltzmann Cluster Translational Oncology, Waehringer Guertel 18-20, 1090 Vienna, Austria*
[3] *Department of Clinical Pharmacy and Diagnostics, University of Vienna, 1090 Vienna, Austria*

Correspondence should be addressed to Theresia Thalhammer; theresia.thalhammer@meduniwien.ac.at

Received 4 October 2012; Accepted 17 December 2012

Academic Editor: Andreas G. Tzakos

The extragonadal synthesis of biological active steroid hormones from their inactive precursors in target tissues is named "intracrinology." Of particular importance for the progression of estrogen-dependent cancers is the *in situ* formation of the biological most active estrogen, 17beta-estradiol (E2). In cancer cells, conversion of inactive steroid hormone precursors to E2 is accomplished from inactive, sulfated estrogens in the "sulfatase pathway" and from androgens in the "aromatase pathway." Here, we provide an overview about expression and function of enzymes of the "sulfatase pathway," particularly steroid sulfatase (STS) that activates estrogens and estrogen sulfotransferase (SULT1E1) that converts active estrone (E1) and other estrogens to their inactive sulfates. High expression of STS and low expression of SULT1E1 will increase levels of active estrogens in malignant tumor cells leading to the stimulation of cell proliferation and cancer progression. Therefore, blocking the "sulfatase pathway" by STS inhibitors may offer an attractive strategy to reduce levels of active estrogens. STS inhibitors either applied in combination with aromatase inhibitors or as novel, dual aromatase-steroid sulfatase inhibiting drugs are currently under investigation. Furthermore, STS inhibitors are also suitable as enzyme–based cancer imaging agents applied in the biomedical imaging technique positron emission tomography (PET) for cancer diagnosis.

1. Introduction

Estrogens play an important role in regulating cell proliferation and apoptosis in cancer cells of hormone-sensitive tumors in the breast, ovary, endometrium, and other various hormone-sensitive tissues, for example, colon. They are also important for the pathogenesis of nonmalignant disease, including the metabolic syndrome and Type 2 diabetes, diseases often associated with a higher risk for certain malignancies.

The biological most active estrogen, 17beta-estradiol (E2), is important for the homeostasis of cellular metabolism and growth. In premenopausal women, most of the E2 is produced by the gonads and functions as a circulating hormone. This is described by the term "endocrinology." After the menopause, the levels of circulating estrogens are low, and most of E2 is produced from adrenal steroid precursors at extragonadal sites in various organs including breast, brain, liver, bone, and fat. Extragonadal production of estrogens from adrenergic precursors in target tissues is also important in men having low levels of circulating estrogens. In target tissues, estrogen acts locally either in an intracrine or paracrine way. Production of E2 in the tissue where it regulates cellular processes is described by the term "intracrinology" [1].

Two pathways are important for the local E2 production in target tissues, namely, the "sulfatase pathway," in which biological inactive steroid sulfates are the source for E2, and the "aromatase pathway," in which E2 is derived from androgenic precursors [2].

Estrogens exert many biological effects through binding and activation of nuclear estrogen receptors (ER), ERalpha and ERbeta, as well as through membrane-associated

receptors. Activation of genomic and/or nongenomic signaling pathways contributes to the regulation of cell proliferation and differentiation [3]. Estrogens control the production and activity of components in the cell cycle progression, including cyclines, cyclin-dependent kinases, and their inhibitors [4]. Additionally, direct cancerogenic effects of estrogens can occurs via formation of electrophilic, redox-active estrogen ortho-quinones from catechol estrogens. The concurrent formation of reactive oxygen species and superoxide anions can damage DNA and cellular proteins [5].

In serum and tissues like the female breast, estrogens are mainly present in their inactive sulfated form [5, 6]. The important precursor for E2 in the "sulfate pathway" is inactive estrone-3-sulfate (E1S). This is the most abundant estrogen in women at all ages as well as in men. Levels of E1S in blood are 5–10-fold higher than that of unconjugated estrogens, estrone (E1), estradiol (E2), and estriol (E3). As it has also a longer half-life than E2, it is considered as storage form for estrogens in some organs, for example, breast, from where active E1 is liberated by removal of the sulfate through STS [7, 8].

To create E2, E1S is taken up into the cells. There, after the removal of sulfate, E1 is reduced by reductive members of the superfamily of 17beta-hydroxysteroid dehydrogenases (17beta-HSDs) to form E2. Oxidative 17β-HSDs catalyze the conversion of E2 to E1. Reductive 17beta-HSDs also inactivate androgens and catalyze also the formation of other estrogens, for example, 5alpha-androstenediol. Since 17beta-HSDs modulate the concentration of active estrogens and androgens, inhibitors of these enzymes may be applied in cancer therapy [9, 10] (Figure 1).

Polar estrogen sulfates, particularly, E1S, are taken up into cells by specific transport proteins from different families of SLC transporters including the family of organic anion transporters SLC21 or organic anion transporting polypeptides (OATPs). Within this concept, transporters from the OATP (SLC21) family such as OATP1A2, OATP1B3, OATP2B1, and OATP3A1 contribute to the cellular accumulation of E1S [11, 12], while ABC-efflux pumps from the MRP-family (ABCC1 and ABCC2), and the breast-cancer resistance protein (BCRP, ABCG2) mediates the efflux of E1S from the cells [13] (Figure 2). Uptake, biotransformation and excretion are transcriptionally regulated by nuclear receptors, for example, the pregnane X receptor. Furthermore, the variability in the expression levels and gene variants of transporters and enzymes can affect expression and function. These mechanisms may therefore influence the susceptibility of individuals to certain malignancies [14, 15].

As sulfated estrogens are unable to bind to the estrogen receptors, sulfonation of estrogens results in their inactivation. Therefore, conjugation with sulfate protects cells and tissues from an excess of active estrogens, and this may contribute to the prevention of hormone-dependent cancer cells. It further indicates that the balance between sulfate conjugation by the Phase 2 metabolizing enzyme estrogen sulfotransferases (SULT1E1) and the removal of the sulfate by the steroid sulfotransferase (STS) is important to store the hormone in an inactive form in the cells [16, 17].

Conjugation of lipophilic estrogens with sulfate is a main pathway for estrogen inactivation in estrogen target tissues. Sulfate conjugation of E2 is catalyzed by the Phase 2 drug metabolizing enzymes of the family of cytosolic sulfotransferases (SULTs) [18]. The isoform SULT1E1 is known as estrogen sulfotransferase, as it catalyzes the sulfonation of E1 and E2 with high efficiency at physiological concentrations. The sulfate conjugation of androgenic precursors, for example, dehydroepiandrosterone (DHEA), is mainly achieved by another SULT isoenzyme, namely, the SULT2A1 enzyme [18]. Both, 5alpha-androstenediol-sulfat (Diol-S) and dehydroepiandrosterone (DHEA) are mainly derived from the circulation. Diol-S is converted to 5alpha-androstenediol (5-Diol) by STS. It is converted into testosterone by 3beta-HSD. Dehydroepiandrosterone-sulfate (DHEA-S) is desulfonated to dehydroepiandrosterone (DHEA) and converted by 3beta-HSD to 4alpha-androstenedione (4-Dione), a precursor for testosterone formed by 17beta-HSD. Testosterone is converted to E2 by the aromatase (CYP19). 5-Diol binds and activates estrogen receptors, but with lower affinity than E2 [19].

As depicted in Figures 1 and 3, sulfonation of E2 forms inactive estradiol sulfate (E2S), which can be reactivated following removal of the sulfate by the cytosolic estrogen sulfatase STS. Sulfate (SO_4^{2-}) is obtained from the diet and the intracellular metabolism of sulfur-containing amino acids, including methionine and cysteine, and is an important nutrient for human growth and development.

The sulfuryl group donor (cosubstrate) for the SULT-catalyzed reaction to add the sulfate moiety to hydroxyl groups is 3′-phosphoadenosine 5′-phosphosulfate (PAPS). The reaction products are sulfated estrogens and adenosine 3′, 5′-diphosphate (PAP). PAPS is generated by PAPS-synthesizing enzymes (PAPSS). Two isoforms, namely, PAPSS1 and PAPSS2, are known to be expressed in various tissues [20]. PAPSS1 might be important for growth of estrogen-sensitive breast cancer cells as a recent study revealed that overexpression of SULT1E1 and PAPSS1 resulted in growth inhibition [21].

2. Steroid Sulfatase (STS)

The steroid sulfatase (STS) belongs to the family of arylsulfatases in the sulfatase superfamily, whose members catalyze the hydrolysis of sulfate ester bonds in various endogenous and exogenous substrates.

STS is also known as arylsulfatase C, and in contrast to the cytosolic expression of arylsulfatases A and B, this enzyme is located in the endoplasmic reticulum of various tissues [23]. STS has a central role in the formation of active sex steroid hormones, as it hydrolyzes several steroid sulfates, including E1S and DHEA-S to E1 and DHEA, respectively [17].

The human STS gene is localized on the X-chromosome and consists of 10 exons. Inactivating mutations in STS gene have been associated with X-linked ichthyosis. Six different promoters were detected to drive STS expression giving rise to transcripts with unique first exons, and exon 1 alpha was associated with the promoter that drives expression in the placenta [24]. Induction of STS transcription by estradiol through binding to ER and via activation of

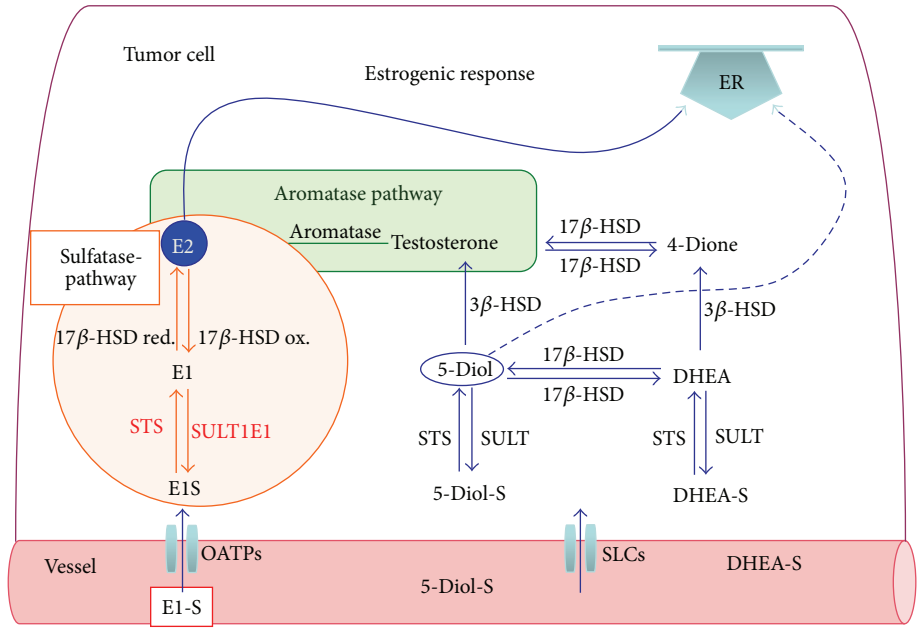

Figure 1: Estrone sulfate (E1S), androstenediol-sulfate (Adione-S), and dehydroepiandrosterone-sulfate (DHEA-S) are taken up into cells by organic anion transporting polypeptides (OATPs) and other transporters from the SLC-family. The "sulfatase pathway," estrone-3-sulfate (E1S), is taken up by the cells and is activated by the removal of sulfate by the steroid sulfatase (STS). E1 is converted to the biological most active estrogen, 17beta-estradiol (E2), by reductive 17beta-hydroxysteroid dehydrogenases (17beta-HSDs). E2 binds and activates estrogen receptors. Vice versa, the conversion of E2 to less active E1 is catalysed by oxidative 17beta-HSDs. For inactivation, E1 is sulfonated by estrogen sulfotransferase SULT1E1 to E1S. The "aromatase pathway," 5alpha-androstenediol-sulfat (Diol-S) and dehydroepiandrosterone (DHEA), are mainly derived from the circulation. Diol-S is converted 5alpha-androstenediol (5-Diol) by STS. It is converted into testosterone by 3beta-HSD. DHEA-S is hydrolyzed to form DHEA, which is further converted by 3beta-hydroxysteroid dehydrogenase to form androstenedione (4-Dione). Testosterone is formed by 17beta-HSD from 4-Dione. Testosterone is converted to E2 by the aromatase (CYP19). 5-Diol binds and activates estrogen receptors, but with lower affinity than E2 (see [20, 22]).

estrogen-response elements in the promoter region results in driving the 1a and 1b transcripts in breast carcinoma [25]. Furthermore, regulation of STS activity by tumor necrosis factor alpha and interleukin 6 was found in breast cancer, most likely through a posttranslational modification [26].

3. Estrogen Sulfotransferase (SULT1E1)

Cytosolic sulfotransferases transfer sulfate from active sulfate (5′phosphadenosine-3′-phosphosulfate) to nucleophilic groups of their substrates. Belonging to the group of Phase 2 detoxification enzymes, they catalyze the biotransformation of hydroxysteroid and thyroid hormones, phenols, arylamines, and primary alcohols.

Four SULT families have been identified, namely, the phenol-metabolizing SULT1, the hydroxysteroid sulfating SULT2, and the SULT family 4 and 6 [18]. The two latter families are poorly characterized for their substrate specificity and tissue distribution.

At least six SULT isoforms catalyze the sulfate conjugation of E2, but only two, namely, SULT1E1 and SULT2A1 mediate the sulfonation of estrone (E1).

SULT1E1 is considered as the "estrogen sulfotransferase," as it has the highest affinity for E2 and E1 from all SULTs. It is the only SULT that displays an affinity for E1, E2, and various synthetic estrogens in a physiological concentration range (in the nanomolar range) [26]. Deletion of SULT1E1 genes results in reproductive abnormalities involving both male and female animals [27]. In the liver, the pregnane X receptor was found to represses the SULT1E1 gene, which may block inactivation of estrogens [28]. The SULT1E1 gene is located on chromosome 4q3.12, and its mRNA is detectable in a great variety of tissues. This would suggest that SULT1E1 may protect peripheral tissues from an excess of estrogens. Various SNPs has been detected in the human SULT1E1 gene, and some are linked to the recurrence of hormone-dependent cancer [29].

4. Enzymes in the Sulfatase Pathway in Estrogen-Associated Cancer

Data on the expression of enzymes in the sulfatase pathway in some estrogen-associated cancers are given in the following sections. Generally, the data on the expression of enzymes

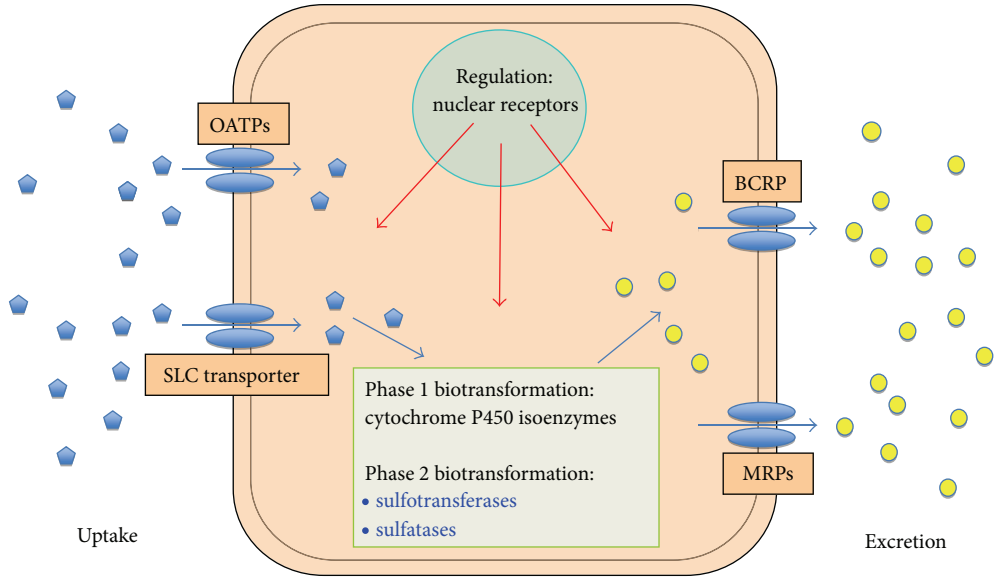

Figure 2: Uptake of E1S from the blood by organic anion transporting polypeptides (OATPs) and other SLC-Transporters. Biotransformation is mediated by phase 1 biotransformation (cytochrome P450 and isoenzymes) and phase 2 biotransformation (sulfotransferase and sulfatase). The excretion of sulfated estrogens is achieved by the breast cancer resistant protein (BCRP, ABCG2) and multidrug resistance related proteins (MRPs). Uptake, biotransformation and excretion is transcriptionally regulated by nuclear receptors, for example, the pregnane X receptor (PXR), which acts as a xenobiotic-activated transcription factor.

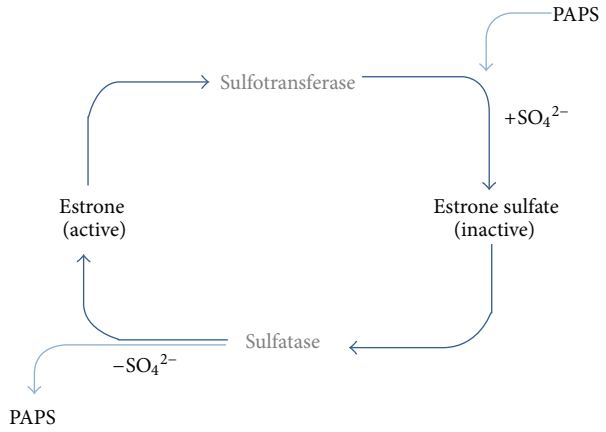

Figure 3: Conjugation of estrone (E1) with sulfate by the estrogen sulfotransferases (SULT) results in the formation of inactive estrone sulfate (E1S). Sulfated estrone is reactivated by the steroid sulfatase (STS) which catalyzes the removal of sulphate, forming estrone (E1). The sulfuryl group donor for the sulfotransferase-catalyzed sulfation is 3′-phosphoadenosine 5′-phosphosulfate (PAPS). The enzymatic reaction requires the acceptor (R-OH) and the donor PAPS to bind to a sulfotransferase. PAPS is synthesized by PAPS-synthesizing enzymes (PAPSS1 and PAPSS2). 3′-phosphoadenosine 5′-phosphosulfate synthase (PAPSS) catalyzes the biosynthesis of PAPS, which serves as the sulfate donor (see [22]).

for the formation of E2 are rather inconsistent. This might be due to the fact that expression of enzymes in the estrogen metabolism and the concentration of circulating steroids are highly variable even in healthy persons, and they are even more varying in patients with cancer. Therefore, selection of patients with defined clinical parameters is important for studying these pathways.

Cancer in a certain organ is not a uniform disease. A specific histological pattern and the molecular signature allow division of most hormone-dependent cancers into various subgroups. These are subgroups of cancer in a certain organ which have a different etiology and will produce a different response to a certain therapeutic regimen. However, even in a defined tumor type, there are great variations in the expression levels of different proteins in different tumor regions. This means that the expression in the tumor center can be completely different from that in one tumor front adjacent to the tumor center or in the front adjacent to the noncancerous tissue.

So far, most studies were done in rather heterogeneous collectives of patients with a certain tumor in an organ. Also, assessment of target proteins by immunohistochemistry was mostly done on undefined tumor regions. This may explain the often conflicting data on the expression of enzymes and targets in molecular pathways [30].

4.1. Breast Cancer. Breast cancer remains the leading cause of cancer in woman worldwide. It occurs in both men and women, although male breast cancer is rare (approx. 1% of the rate in women) [30]. In 2008, the estimated incidence of breast cancer in woman was 1,384.155 cases, and the mortality was 458.503 cases [31]. Estimated new cases and deaths from breast cancer in women are 226.800 and 39.510 women in the United States in 2012 [30].

More than 70% of breast cancers express ERs and progesterone receptors, PG-A and PG-B. Therefore, a major concern is whether or not the application of hormone replacement

therapy (HRT) would increase the risk of breast cancer in postmenopausal women. According to the 2012 analysis published in the Cochrane Database Syst. Rev., hormone-replacement therapy with estrogens only did not increase the risk of breast cancer in postmenopausal women at a mean age of 60 years, but the combined continuous therapy with estrogens and progesterone-derivates significantly increased the risk for this cancer [32]. The breast cancer risk associated with HRT is higher for estrogen receptor-positive cancers than for estrogen receptor-negative cancers and for low-grade cancers compared with high-grade cancers. The increased risk of breast cancer dissipates within 2 years after finishing HRT [33].

50–70% of all invasive breast cancers are invasive ductal tumors, which arise in the milk ducts of the breast. According to the expression pattern of specific genes, cancers are further subdivided into four major molecular subtypes: luminal A, luminal B, triple negative/basal-like, and HER2 type tumors. Both luminal A and luminal B tumors express ERs, while the triple negative/basal-like tumors and HER2-type tumors are negative for ERs and PGs. Lobular carcinomas (10–20%) start from cells in the lobuli and can also be divided in these subtypes [34].

The luminal A breast cancer is the most common subtype, representing 50–60% of the total. It is characterized by the expression of ER targeted genes that are typically present in the luminal epithelium lining the mammary ducts, absence of HER2, a low proliferation rate, and a low histological grade. Based on their molecular profile, all cases of lobular carcinoma *in situ* and most of the infiltrating lobular carcinomas belong to this subtype. Luminal B molecular profile tumors (10%–20% of all breast cancers) are more aggressive, have a higher histological grade, and a worse prognosis [35].

Several data show that estrogens are enriched in breast cancer tissue as compared to normal tissue. They surplus the plasma levels by 23-fold in women at reproductive age and 23-fold in postmenopausal patients. In older women, nearly all E2 is locally produced, but also in younger women up to 75% originate from the local production [35]. In breast cancer, the STS pathway with the reduction of E1 to E2 is catalyzed by reductive 17beta-HSDs. This is the most prominent pathway and prevail the aromatase pathway with estrogen production from testosterone and its precursors by 50–200-fold [6]. Indeed, many studies showed that STS activity is much higher than aromatase activity in breast tumors, the activity of the enzyme is also higher in the carcinoma than in the nonmalignant tissue, and expression of tissue-specific transcripts of STS is controlled by ERalpha signaling in normal and cancerous breast tissue [36]. Studies in patients with ERalpha-positive breast cancer showed that expression of more active STS isoforms under estrogen therapy may cause upregulation of E2, which would further promote cancer progression [36]. Moreover, high levels of STS mRNA expression in tumors are associated with a poor prognosis [37].

Breast tumors expressing ERs may benefit from adjuvant endocrine therapy with antiestrogens such as tamoxifen, which is applied in pre- and postmenopausal women. In postmenopausal women blocking the estrogen production by inhibitors of estrogen formation, for example, aromatase inhibitors is an effective therapy for cancer prevention [38, 39]. But some tumors are intrinsically resistant against endocrine therapy, or others acquire resistance against hormonal treatment later. STS and 17beta-HSDs in local estrogen production provide novel potential targets for endocrine therapy [10, 40]. Therefore, the development of combined of STS/aromatase inhibitors and STS/17 beta-HSD type 1 inhibitors will be required in the future.

4.2. Endometrial Carcinoma. Endometrial carcinoma is the most frequent gynecological malignancy in other in industrialized nation including the USA. 47.130 new cases and 8.010 deaths from endometrial cancer in the United States are estimated for 2012. In 90% of all cases, endometrial carcinomas occur sporadic. Most endometrial cancers are adenocarcinomas. They are subclassified into type 1 or type 2 tumors. Type 1 tumors (80% of all sporadic cases) are found in pre- and postmenopausal women and develop from precursor lesions (hyperplasia, intraepithelial neoplasia) through excessive stimulation by estrogens, if it is either not counteracted by progesterons or lasts over a prolonged time. Data from the 100 Million women study showed that estrogens increase the risk of endometrial cancer, while progestagens counteract the adverse effect of estrogens on the endometrium in women with a mean age of sixty. Because estrogens stimulate the proliferation and progesterons the differentiation of endometrial cells, continuous HRT with the estrogen-progestagen combination will reduce the risk of these carcinomas, which are sensitive to these hormones [41, 42].

Two major subtypes of endometrial carcinomas can be discriminated. In type 1 tumors, PTEN gene silencing together with defects in DNA mismatch repair genes and/or mutations in the K-ras and/or beta-catenin genes are frequently present and contribute to the malignant transformation via hyperplasia, intraepithelial neoplasia, and to the carcinoma. These type 1 endometrioid endometrial cancers are well differentiated and estrogen sensitive. Type 2 tumors develop either *de novo* or from metaplasia to serous-papillary or clear-cell carcinomas. They carry mutations in TP53 and Her-2/neu and seem to arise from a background of atrophic endometrium [43]. Overall, type 1 tumors have usually a better prognosis than high grade, estrogen-independent type 2 tumors [44].

In the endometrium, ERalpha and ERbeta are expressed, and as shown for other hormone-dependent tumors, ERalpha levels are higher than that of ERbeta. Since ERbeta is considered to have antiproliferative and proapoptotic effects, it may act as repressor for ERalpha. If ERbeta is reduced, E2 would rather act through ERalpha signaling.

Indeed, many studies showed that the receptors are differently expressed in normal and cancerous endometrium, but results are controversial. Higher, lower, and no changes in ratio between ERalpha and ERbeta were reported [45, 46]. Similar to the data from breast cancer, the levels of E2, E1, and E1S were found to be higher in cancer patients than in healthy postmenopausal women. Highest levels are seen for E1 [47]. Furthermore, the concentrations of estrogens are

several times higher in the cancerous endometrium than in the surrounding normal tissue [48].

Since the majority of the endometrial cancer patients are postmenopausal women, local formation of E2 from circulating precursors either from circulating androgens via the aromatase pathway or from E1S via the sulfatase pathway becomes important. Data on the expression of aromatase in endometrial cancer are rather inconsistent. Although aromatase inhibitors have become the gold standard for endocrine treatments in the postmenopausal patients with estrogen-dependent breast carcinoma, the therapeutic value of aromatase-inhibitors in estrogen-sensitive endometrioid carcinoma is also not clear [49].

Regarding aromatase expression in endometrial cancer, early studies [50, 51] showed that mRNA levels and the activity of the enzyme are higher in endometrial carcinomas than in the normal endometrium. It was demonstrated that aromatase is mainly located in stromal cells rather than in cancer cells. Interactions between stroma and tumor cells will provide E2 for the proliferation of cancer cells. This was shown in a coculture of Ishikawa cells (an endometrial carcinoma cell line) with stromal cells [52]. In a more recent study, aromatase mRNA expression was shown to be present in peritumoral tissue but not in the endometrial cancer [47]. In another study, aromatase was higher expressed in well-differentiated tumors than in normal tissue and in high grade tumors. However, overall aromatase mRNA levels in the endometrial carcinomas were shown to be low [53]. In line with these findings, only weak staining for aromatase was seen in cancerous endometrium [54]. In the latter study, no significant differences in aromatase mRNA expression levels between cancerous and adjacent normal tissues were seen. However, in some specimens from endometrial cancer, 17beta-HSD (AKR1C3) active to form testosterone from androstenedione was upregulated. This may increase testosterone for conversion to E2 by aromatase, and its may act as an estrogenic 17beta-HSD to produce E2 from E1. All enzymes necessary for intracrine production of E2 via the sulfatase pathway, namely, STS, reductive 17beta-HSD type 1,5,7,12, and oxidative 17beta-HSD type 2,4,8 are expressed in these tumors. These reductive 17beta-HSDs are thought to convert E1 to E2, and vice versa, oxidative 17beta-HSD isoenzymes to form E1 from E2 [54, 55]. The study of Lépine et al. [47] showed that 17beta-HSD enzymes, which convert E1 to E2, are highly expressed in normal tissue and are even higher in tumors. Additionally to the levels of 17beta-HSD isoenzymes, also levels of the sulfatase STS are increased. STS actives E1S, as it removes the sulfate group. In summary, this leads to an increase of levels of active estrogens in endometrial tumors [56].

Also SULT1E1, which inactivates E2 by producing E2S, is weakly expressed in these tumors. Utsunomiya et al. [57] demonstrated by immunohistochemistry that SULT1E1 is expressed in normal endometrium during the secretory phase in the menstruation cycle. In the majority of tumors, SULT1E1 levels were reduced, while STS levels were high.

4.3. Ovarian Carcinoma. Ovarian carcinoma that is the fifth most common cancer among women in Western countries is the most deadly gynecological malignancy. In 2012 in the USA, there are 22.380 estimated new cases and 15.500 deaths [30]. The estimate incidence of ovarian cancer worldwide was 224.747 cases in 2008 [31].

Ovarian carcinomas are now known as heterogeneous tumors. It is currently accepted that only gonadal, stromal tumors, and germ cell tumors (5% of all ovarian carcinomas) are tumors of cells present in the normal ovary. The great majority of the ovarian carcinomas develop in cells from outside the ovary, and involvement of the ovary is secondary [58–60]. Based on histopathological characteristics and the distinct molecular signature, five types of ovarian carcinomas that account for over 95% of all cases can be discriminated: high-grade serous carcinomas (HGSC), low-grade serous carcinomas (LGSC), endometrioid, clear-cell, and mucinous ovarian carcinomas [60]. Endometrioid (10%) and clear-cell (10%) carcinomas originate from endometriosis in the ovary, and HGSC and LGSC were previously thought to develop from the ovarian surface epithelium [61], but it is now agreed that they develop from the tubal epithelium in an independent way using different molecular pathways [60]. The most frequent HGSC (70–80% of all ovarian carcinomas) may arise from precursor lesions in the epithelial cells in the distal fimbriated end of the fallopian tube or the implantation of tubal-type epithelium into the ovary. SLGCs (5%) are associated with a serous borderline component. While HGSCs have a bad prognosis, LGSCs have a better outcome [62]. One reason is that because of absence of specific symptoms, HGSCS is usually detected at an advanced stage, in which the cancer has spread within the pelvis. In these cases, the five-year survival rate is less than 40%. Although HGSCs are initially sensitive to chemotherapy, they become resistant within a short period. TP 53 mutations are typically present in HGSCs, and mutations in BRAF, KRAS are characteristically found in LGSCs. Women with BRCA1/2 germline mutations are at high-risk factors for HGSCs (10% of all cases) [63]. Data on the expression of ERs and (PGs), whether they may serve as predictive biomarker for these tumors, are rather controversial, and only few studies discriminate between different tumor types. There is increasing evidence that ERalpha induces proliferation of ovarian cancer cell growth, whereas ERbeta has been described to mediate proapoptotic and antiproliferative effects. PR-A is a transcriptional inhibitor of ERalpha, and PR-B induces of cell differentiation. These four steroid hormone receptors were found to be commonly expressed in LGSCs, but their expression rate was significant reduced in HGSCs [64]. Recent epidemiological data showed that in patients with HGSCs, expression of ERs and PG-B receptor was associated with a favourable outcome as analysed by univariate analysis. In the multivariate analysis, only PR-B was an independent prognostic marker for the patient survival [65].

Steroid hormones may play a role in the development of sporadic ovarian cancer. While oral contraceptive have a protective effect, hormone replacement therapy with estrogen only or in combination with progesterones may increase the risk of ovarian cancer. In the 100 million women study, the risks associated with HRT varied significantly according to the tumor histological type. In women with epithelial tumors, the relative risk for current versus never use of HRT was

greater for serous than for mucinous, endometrioid, or clear-cell tumors [66]. Data from a recent study in a large cohort of women (909.946 cases) in Denmark revealed that hormone users had higher risk of serous and endometrioid type cancers, but not of ovarian cancer of the mucinous and clear-cell type [67]. Compared with never users, women taking unopposed estrogen therapy had increased risks of both serous tumors and endometrioid tumors but decreased risk of mucinous tumors. Similar increased risks of serous and endometrioid tumors were found with estrogen/progestin therapy. Consistent with results from other studies [66], the authors found that ovarian cancer risk varied according to tumor histology [67].

In most studies on the expression of steroid hormone receptors and on the expression of enzymes involved in the local estrogen synthesis in ovarian cancers cells, there is no discrimination between different types of ovarian cancer.

The aromatase pathway is active in ovarian cancer, but so far clinical studies using antiestrogens or aromatase inhibitors were rather disappointing [68]. However, recent data suggest that endocrine therapy might benefit women with certain cancer subtypes. For example, women with recurrent LGSC and expression of ER, application of hormonal therapy might be of benefit [69]. Furthermore, aromatase inhibitors were found to be promising in the treatment of rare granulose tumors in the ovary [70].

Intracrine production of E2 through the sulfatase pathway from E1S may be of particular interest for the diagnosis and treatment of ovarian cancer in postmenopausal women, although formation of E2 from circulating estrogen sulfates occurs in younger women as well. 17beta-DSH type 1 and 5 and STS were previously detected in samples from ovarian cancer patients at the mRNA and protein levels [71–73]. Steroid sulfatase enzymatic activity was determined [74]. STS was detected in ovarian surface epithelium and granulosa cells. In an immunohistochemical study, STS was detected in 30% of serous and 50% of mucinous adenocarcinoma specimens [75]. Also studies in our lab show high levels of STS and moderate to low expression of SULT1E1 in a collective of patients with advanced ovarian cancer (Figure 4).

Further studies in estrogen receptor alpha-expressing OVCAR-3 cells showed that STS is inhibited by the STS inhibitor STX64. As STS expression is highly variable and found at high levels in tumors of nearly all patients, blocking the sulfatase pathway may be of values for these patients [75]. Also the aromatase pathway to convert the androgens to estrogen is active in ovarian cancer cells and will lead via the conversion of dehydroepiandrostenedione to androstenedione to the production of E2. Therefore, a combined inhibitor for both, STS and aromatase, might be suitable for these patients [76].

4.4. Colorectal Cancer. Estimated new cases and deaths from colon and rectal cancer in the USA, in 2012, were 103.170 new cases of colon cancer and 40.290 cases of rectal cancer. 51.690 deaths were from colorectal cancer [30]. These cancers accounts for approx. 10% of new cancer diagnoses among women worldwide with an incidence of 571.204 cases and

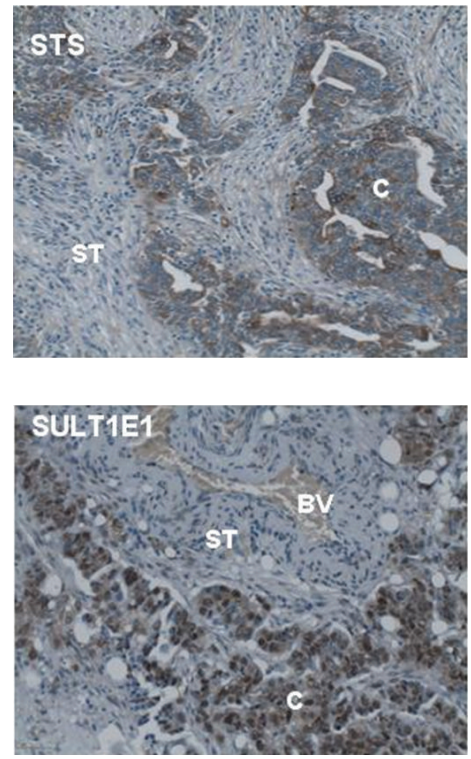

Figure 4: STS (steroid sulfatase) and SULT1E1 (estrogen sulfotransferase 1E1) in high-grade serous ovarian carcinoma. Immunoreactivity of STS and SULT1E1 is demonstrated in paraffin-embedded tissue sections from ovarian carcinoma. Sections were probed with an antibody against STS (GTX 105498, GeneTex, Irvine, CA) and SULT1E1 (NBP1-56977, Novus Biol., Littleton, CO), respectively. STS and SULT1E immunoreactivity is visible in the cancer cells (C). ST = tumor stroma, BV = blood vessel.

a mortality of 288.654 worldwide [31]. Colorectal cancer is the third leading cause of cancer for women after lung and breast cancer. Screening programmes for colorectal cancer in man and woman over the age of 50, now widely applied in many industrialized countries, are leading to a reduction in the incidence and mortality of colorectal cancer (similar to data shown for the USA) [77].

Estrogens were found to play a role in the pathogenesis of colorectal carcinomas and may have a protective role [78]. Many epidemiological studies have found a reduction in the risk of colon cancer associated with use of estrogen/progesterone-based regimens of HRT. Although overall diagnoses were decreased, a larger proportion of poor prognosis tumors was detected among these patients [79]. In the estrogen-alone group, there was no reduction in the risk of colorectal cancer. Therefore, a recent evaluation of the outcome of various studies on HRT led to the conclusion that application of any HRT regimen to prevent colorectal cancer is not recommended [80].

In many colon carcinoma specimens and colon cancer cell lines, ERbeta [81], aromatase, STS, SULT1E1 [82], and 17βHSDs [83] are expressed. It was also demonstrated that concentrations of estrogens in the cancer tissue were twice of those in normal colonic mucosa [82]. Moreover, higher

intratumoral concentrations of total estrogens were significantly associated with poorer survival. Thereby, the ratio between STS and SULT1E1 will determine the intratumoral concentration of total estrogens and determine the clinical outcome of the patients. However, these findings are not fully supported by epidemiological data on the application of estrogens to prevent colon cancer (see above).

Other findings would support the beneficial effects of estrogens. The gene coding for 17beta-HSD1 was found to be reduced by promoter methylation in colon cancer. This will reduce the formation of E2 from E1 via this 17beta-HSD [84]. Expression of type 2 and 4 isoenzymes of the 17beta-HSD family was also shown to be significantly decreased in tumors compared to normal mucosa [85]. Importantly, downregulation of ERbeta was found to be associated with a poor prognosis in the patients [86, 87].

4.5. Estrogen Sulfates in Metabolic Disease Related to Cancer. The incidences of breast cancer as well as of the metabolic syndrome with obesity, insulin resistance, hyper-insulinemia, high blood pressure, and type 2 diabetes have increased over the past decades in industrialized countries. The loss of the sensitivity of cells to insulin is associated with changes in the signaling of chemokines, cytokines, growth hormones, and steroid hormones [88–90]. This may explain why metabolic disease goes along with an increased risk of certain cancers, for example, breast and colon cancer. Studies in patients with the metabolic syndrome showed that levels of SULT1E1 for the inactivation of estrogens correlate with the expression of proinflammatory factors. The risk appears to be higher in postmenopausal than in premenopausal women, suggesting the importance of intracrine estrogen formation [89, 90]. Although there is sufficient evidence for a relation between metabolic syndrome and certain cancers, the exact molecular mechanism for the metabolic syndrome in the carcinogenesis is not thoroughly understood yet. Nevertheless, various potential direct and indirect links exist between obesity, metabolic syndrome, type 2 diabetes, and an increased risk of colon cancer. Modification of insulin and insulin-like growth factors pathway, leptin signaling, adipose-tissue induced changes in estrogens and androgens, and inflammatory molecules may contribute [90].

It is well known that E2 is an important regulator of the energy balance and metabolic homeostasis not only in women but also in men [91]. In postmenopausal women, low circulating estrogen levels lead to accumulation of visceral fat, insulin resistance/glucose intolerance, and osteoporosis [92]. As estrogen promotes the differentiation of bone marrow-derived mesenchymal stem cells to bone-building osteoblasts, low estrogen levels will favor adipocyte formation. Differentiation of adipocytes is reduced by SULT1E1 [93]. As a consequence, decreasing estrogen levels is associated with a decreased bone mass and accumulation of fat [94]. Similar changes are observed in men with estrogen deficiency or during ageing with declining levels of steroid hormones.

Local estrogen synthesis is also effectively carried out in adipocytes and human bone cells. E1S is a major source of local bioactive estrogen formation [95]. Also, SULT1E1 is also expressed at higher rate in malignant bone tumors than in benign ones [96]. In adipocytes, all enzymes important for the local formation of estrogen are expressed, and their levels increase after adipocyte differentiation [97]. In SULT1E1 knock-out mice, loss of SULT1E1 causing an excess of estrogens leads to the formation of smaller patches from white fat and insulin resistance [97].

In type 2 diabetes, induction of hepatic SULT1E1 is most frequently observed. Loss of SULT1E1 improves the metabolic function in a female mouse model of type 2 diabetes, restores insulin sensitivity, and blocks hepatic gluconeogenesis and lipogenesis [98]. Since in diabetes, upregulation of SULT1E1 decreases E2 levels, inactivation of the enzyme will prevent loss of estrogens and normalize estrogenic activity in the liver. This beneficial effects of SULT1E1 inactivation were absent in ovariectomized mice. These effects were also sex specific, as SULT1E1 loss in males worsened the diabetic phenotype and led to a decreased islet beta-cell mass, failure of glucose-stimulated insulin secretion, increased macrophage infiltration, and inflammation in white adipose tissue. The authors suggest that inhibition of SULT1E1 at least in females may represent a novel approach in the therapy of type 2 diabetes [98, 99]. However, it has to be considered that type 2 diabetes mostly occurs in women after the menopause when local formation of steroid hormones from adrenal precursors becomes important. Since extragonadal estrogen production is typical for primates [2], the benefit of increasing levels of active estrogens by reducing SULT1E1 may have to be studied in a proper model for type 2 diabetes in this group. In any case, higher estrogen levels are thought to have beneficial effects on type 2 diabetes, but the risk of the induction of hormone-sensitive cancers may be considered as well.

5. Steroid Sulfatase Inhibitors as Agents for a Therapy of Hormone-Sensitive Tumors

Hormone therapy is used to treat both early and advanced breast cancer and to prevent breast cancer in women who are at high-risk of developing the disease. Currently, the most widely used therapies for the treatment of hormone-dependent cancer is to block the action of steroid hormones. Adjuvant endocrine therapy with the selective estrogen receptor modulator (SERM) tamoxifen is recommended for premenopausal women with a history of atypical hyperplasia to reduce breast cancer risk. Raloxifene, another selective estrogen receptor modulator, was found to be equivalent to tamoxifen in reducing the risk of developing invasive breast cancer in postmenopausal women. However, it did not provide the same level of risk reduction for developing non-invasive breast cancer. Aromatase inhibitors, which block the conversion of androstenedione to estrone, are applied in postmenopausal women. Currently, third-generation aromatase inhibitors, which comprise the nonsteroidal compounds anastrozole and letrozole, and the steroidal exemestane are finding widespread application in the clinic (for reviews see [100, 101]). However, the development of resistance to the endocrine therapy is still a major therapeutic problem and limits the clinical benefit of their application.

Regarding the fact that local formation of E2 from E1S via the sulfatase pathway is more effective in some hormone-dependent tumors than formation of E2 via the aromatase pathway [102], STS inhibitors offer an attractive strategy to reduce estrogenic stimulation of hormone-sensitive tumors [103]. Furthermore, high levels of STS and low SULT1E1 expression are regarded as prognostic factors in hormone-sensitive cancer, for example, of the breast. Blocking STS may therefore offer an additional benefit in the therapy, and STS inhibitors are under development [104, 105].

The first approach was to block the desulfonation of E1S by offering nonhydrolysable E1S analogues, for example, sulfates of the flavonoid daidzein. However, these compounds possess high intrinsic estrogenic activity. Therefore, different STS inhibitors have been developed, a number of successful products in which the sulfate moiety was replaced by a sulfamate, for example, estrone 3-o-sulfamate were introduced, and estradiol 3-sulfamate was introduced into clinical trials but failed because of the estrogenic effects of the products. To prevent the estrogenic effects, sulfamate-based nonsteroidal inhibitors were introduced, and the most successful derivate was the cyclopentane carboxylate derivative STX64 (irosustat), which is present in clinical development (Phase 2 clinical trials) for the treatment of patients with advanced breast cancer and other hormone-dependent cancer. The structure is a tricyclic coumarin-based sulfamate. It undergoes desulfonylation as a result of its mechanism of STS inhibition [104].

Regarding the benefit of the therapeutic application of aromatase inhibitors and present knowledge on the importance of the inhibition of STS, compounds to inhibit both pathways (so-called DASIs) are now under investigation. They may provide a new therapeutic concept. One approach to create such DASIs is the insertion of a pharmacophore for STS inhibition into an established aromatase inhibitor, for example, letrozole. For example, the pharmacophore for STS inhibition, a phenol sulfamate ester, and the pharmacophore for aromatase inhibition, an N-containing heterocyclic ring, are incorporated into a single molecule. Another group of DASIs comprises derivatives of a known STS inhibitor incorporating a heme-ligating heterocyclic ring [105]. Many of these novel inhibitors of both enzymes were found to be effective in preclinical studies. This approach offers the opportunity for further continuing preclinical development of such dual inhibitors.

6. Steroid Sulfatase as a Target for Biomedical Positron Emission Tomography Imaging

Positron emission tomography (PET) is a biomedical imaging technique in which compounds labelled with positron emitting radioisotopes, for example, ^{1}1C, ^{18}F, are applied to monitor processes in cells. For PET, trace amounts of positron-emitting radionuclide-labelled compounds are retained in cells in different tissues either because of their binding to specific receptors or by being taken up into cells by specific transmembrane transporters where they undergo an enzyme-catalyzed conversion. As PET provides tomographic images of the distribution of the radioactive traces in tissues, the technique is widely used to diagnose cancer and cancer metastasis [106], and multitargeted anticancer agents are now developed as enzyme-based cancer imaging agents. For breast cancer diagnosis, STS catalyzing the hydrolysis of steroid sulfates to estrogens is an attractive target, and this is also true for aromatase. To target both enzymes, ^{11}C-labelled sulfamate derivatives were designed as potential PET dual aromatase-steroid sulfatase inhibitor (DASSI) radiotracers [107]. Another enzyme, which is highly expressed in a great variety of tumors, is carbonic anhydrase 2 (CA2), and recently a bis(sulfamoyl)estradiol derivative, which functions as a dual-function STS-CA2 inhibitor, was developed. This compound has a high antiproliferative potential in many tumor cells [108]. Additionally, antiangiogenic effects were shown *in vitro* and *in vivo,* and it may therefore be a good candidate for cancer treatment and molecular imaging of cancer.

7. Summary and Conclusion

Circulating inactive steroids in estrogen-dependent tumors are converted to the biological most active estrogen, 17beta-estradiol in the sulfatase, and aromatase pathway. In the sulfate pathway, estrone-3-sulfate (E1S) is desulfonated by steroid sulfatase (STS) to estrone (E1). Estrogens are inversely inactivated by sulfonation via the estrogene sulfotransferase (SULT)1E1 to the sulfated estrogens. E1 is converted to E2 by 17beta-hydroxsteroid dehydrogenases (17beta-HSDs) and vice versa. In the aromatase pathway, E1 and E2 are synthesized from the circulating precursors androstenedione and testosterone, respectively. The mechanism for the uptake and production of biological active steroids at extragonadal sites is described with the term "intracrinology." Importantly, the *in situ* formation of E2 at the sites of their actions will influence the growth and progression of hormone-dependent tumors. This paper gives an overview about expression and function of enzymes of the sulfatase pathway, particularly of STS, in breast, endometrial, ovarian, and colorectal cancer. High expression of STS together with the overexpression of 17beta-HSDs may lead to an increased production of active E2. Higher levels of E2 and other active estrogens can result in the stimulation of tumor growth and progression of hormone-sensitive tumors of the breast, endometrium, and ovary. Altered sulfonation of estrogens is also implicated in the pathogenesis of the metabolic syndrome and type 2 diabetes. Here, the increased secretion of proinflammatory cytokines and chemokines by metabolic disturbed cells seems to contribute to carcinogenesis. Indeed, these diseases share common risk factors with cancers of the breast and ovary. Because in hormone-sensitive tumors, for example, breast cancer, estrogen formation by the sulfatase pathway exceeds that of the aromatase pathway by several folds (50–100-fold), blocking the sulfatase pathway should reduce the growth of estrogen-sensitive cancer. Various inhibitors of sulfate-removing STS were synthesized and offer a promising therapeutic approach to combat estrogen-sensitive tumors, particularly, if these compounds also inhibit enzymes of other cancer progression pathways (aromatase, carboanhydrase 2). One compound STX-64, lacking estrogenic effects,

is currently undergoing clinical trials. Furthermore STS inhibitors might also be suitable as enzyme-based cancer imaging agents applied in the biomedical imaging technique positron emission tomography for the diagnosis and therapy of estrogen-sensitive cancer.

Acknowledgment

This study was supported by FP-6 STREP Project (OVCAD 2005-018698).

References

[1] F. Labrie, "Extragonadal synthesis of sex steroids: intracrinology," *Annales d'Endocrinologie*, vol. 64, no. 2, pp. 95–107, 2003.

[2] F. Labrie, "Intracrinology," *Molecular and Cellular Endocrinology*, vol. 78, no. 3, pp. C113–C118, 1991.

[3] D. C. Leitman, S. Paruthiyil, O. I. Vivar et al., "Regulation of specific target genes and biological responses by estrogen receptor subtype agonists," *Current Opinion in Pharmacology*, vol. 10, no. 6, pp. 629–636, 2010.

[4] R. D. Koos, "Minireview: putting physiology back into estrogens' mechanism of action," *Endocrinology*, vol. 152, no. 12, pp. 4481–4488, 2011.

[5] J. L. Bolton and G. R. J. Thatcher, "Potential mechanisms of estrogen quinone carcinogenesis," *Chemical Research in Toxicology*, vol. 21, no. 1, pp. 93–101, 2008.

[6] J. R. Pasqualini, G. Chetrite, C. Blacker et al., "Concentrations of estrone, estradiol, and estrone sulfate and evaluation of sulfatase and aromatase activities in pre- and postmenopausal breast cancer patients," *Journal of Clinical Endocrinology and Metabolism*, vol. 81, no. 4, pp. 1460–1464, 1996.

[7] G. S. Chetrite, J. Cortes-Prieto, J. C. Philippe et al., "Comparison of estrogen concentrations, estrone sulfatase and aromatase activities in normal, and in cancerous, human breast tissues," *Journal of Steroid Biochemistry and Molecular Biology*, vol. 72, no. 1-2, pp. 23–27, 2000.

[8] H. Sasano, Y. Miki, S. Nagasaki, and T. Suzuki, "*In situ* estrogen production and its regulation in human breast carcinoma: from endocrinology to intracrinology," *Pathology International*, vol. 59, no. 11, pp. 777–789, 2009.

[9] S. Marchais-Oberwinkler, C. Henn, G. Möller et al., "17β-hydroxysteroid dehydrogenases (17β-HSDs) as therapeutic targets: protein structures, functions, and recent progress in inhibitor development," *Journal of Steroid Biochemistry and Molecular Biology*, vol. 125, no. 1-2, pp. 66–82, 2011.

[10] D. Poirier, "Contribution to the development of inhibitors of 17β-hydroxysteroid dehydrogenase types 1 and 7: key tools for studying and treating estrogen-dependent diseases," *Journal of Steroid Biochemistry and Molecular Biology*, vol. 125, no. 1-2, pp. 83–94, 2011.

[11] M. Roth, A. Obaidat, and B. Hagenbuch, "OATPs, OATs and OCTs: the organic anion and cation transporters of the SLCO and SLC22A gene superfamilies," *British Journal of Pharmacology*, vol. 165, no. 5, pp. 1260–1287, 2012.

[12] N. Banerjee, C. Allen, and R. Bendayan, "Differential role of organic anion-transporting polypeptides in estrone-3-sulphate uptake by breast epithelial cells and breast cancer cells," *Journal of Pharmacology and Experimental Therapeutics*, vol. 342, no. 2, pp. 510–519, 2012.

[13] R. G. Deeley, C. Westlake, and S. P. C. Cole, "Transmembrane transport of endo- and xenobiotics by mammalian ATP-binding cassette multidrug resistance proteins," *Physiological Reviews*, vol. 86, no. 3, pp. 849–899, 2006.

[14] N. J. Lakhani, J. Venitz, and W. D. Figg, "Pharmacogenetics of estrogen metabolism and transport in relation to cancer," *Current Drug Metabolism*, vol. 4, no. 6, pp. 505–513, 2003.

[15] M. Svoboda, J. Riha, K. Wlcek et al., "Organic anion transporting polypeptides (OATPs): regulation of expression and function," *Current Drug Metabolism*, vol. 12, no. 2, pp. 139–153, 2011.

[16] T. Suzuki, Y. Miki, Y. Nakamura et al., "Steroid sulfatase and estrogen sulfotransferase in human carcinomas," *Molecular and Cellular Endocrinology*, vol. 340, no. 2, pp. 148–153, 2011.

[17] A. Purohit, L. W. L. Woo, and B. V. L. Potter, "Steroid sulfatase: a pivotal player in estrogen synthesis and metabolism," *Molecular and Cellular Endocrinology*, vol. 340, no. 2, pp. 154–160, 2011.

[18] J. Lindsay, L. L. Wang, Y. Li, and S. F. Zhou, "Structure, function and polymorphism of human cytosolic sulfotransferases," *Current Drug Metabolism*, vol. 9, no. 2, pp. 99–105, 2008.

[19] D. M. Otterness and R. Weinshilboum, "Human dehydroepiandrosterone sulfotransferase: molecular cloning of cDNA and genomic DNA," *Chemico-Biological Interactions*, vol. 92, no. 1–3, pp. 145–159, 1994.

[20] F. Labrie, V. Luu-The, A. Bélanger et al., "Is dehydroepiandrosterone a hormone?" *Journal of Endocrinology*, vol. 187, no. 2, pp. 169–196, 2005.

[21] Y. Xu, X. Liu, F. Guo et al., "Effect of estrogen sulfation by SULT1E1 and PAPSS on the development of estrogen-dependent cancers," *Cancer Science*, vol. 103, no. 6, pp. 1000–1009, 2012.

[22] N. Gamage, A. Barnett, N. Hempel et al., "Human sulfotransferases and their role in chemical metabolism," *Toxicological Sciences*, vol. 90, no. 1, pp. 5–22, 2006.

[23] D. Ghosh, "Human sulfatases: a structural perspective to catalysis," *Cellular and Molecular Life Sciences*, vol. 64, no. 15, pp. 2013–2022, 2007.

[24] M. J. Reed, A. Purohit, L. W. L. Woo et al., "Steroid sulfatase: molecular biology, regulation, and inhibition," *Endocrine Reviews*, vol. 26, no. 2, pp. 171–202, 2005.

[25] S. P. Newman, A. Purohit, M. W. Ghilchik et al., "Regulation of steroid sulphatase expression and activity in breast cancer," *Journal of Steroid Biochemistry and Molecular Biology*, vol. 75, no. 4-5, pp. 259–264, 2000.

[26] S. Honma, K. Shimodaira, Y. Shimizu et al., "The influence of inflammatory cytokines on estrogen production and cell proliferation in human breast cancer cells," *Endocrine Journal*, vol. 49, no. 3, pp. 371–377, 2002.

[27] Y. M. Qian, X. J. Sun, M. H. Tong et al., "Targeted disruption of the mouse estrogen sulfotransferase gene reveals a role of estrogen metabolism in intracrine and paracrine estrogen regulation," *Endocrinology*, vol. 142, no. 12, pp. 5342–5350, 2001.

[28] S. Kodama, F. Hosseinpour, J. A. Goldstein, and M. Negishi, "Liganded pregnane X receptor represses the human sulfotransferase SULT1E1 promoter through disrupting its chromatin structure," *Nucleic Acids Research*, vol. 39, no. 19, pp. 8392–8403, 2011.

[29] S. J. Hebbring, A. M. Moyer, and R. M. Weinshilboum, "Sulfotransferase gene copy number variation: pharmacogenetics and function," *Cytogenetic and Genome Research*, vol. 123, no. 1–4, pp. 205–210, 2009.

[30] S. Ogino, C. S. Fuchs, and E. Giovannucci, "How many molecular subtypes? Implications of the unique tumor principle in personalized medicine," *Expert Review of Molecular Diagnostics*, vol. 12, no. 6, pp. 621–628, 2012.

[31] International Agency for Research on Cancer. World Health Organizationl, "Estimated cancer Incidence, Mortality, Prevalence and Disability-adjusted life years (DALYs) Worldwide in 2008," 2008, http://globocan.iarc.fr/.

[32] C. Farquhar, J. Marjoribanks, A. Lethaby et al., "Long term hormone therapy for perimenopausal and postmenopausal women," *Cochrane Database of Systematic Reviews*, no. 2, Article ID CD004143, 2009.

[33] S. A. Narod, "Hormone replacement therapy and the risk of breast cancer," *Nature Reviews Clinical Oncology*, vol. 8, no. 11, pp. 669–676, 2011.

[34] S. Masuda, "Breast cancer pathology: the impact of molecular taxonomy on morphological taxonomy," *Pathology International*, vol. 62, no. 5, pp. 295–302, 2012.

[35] A. H. Sims, A. Howell, S. J. Howell, and R. B. Clarke, "Origins of breast cancer subtypes and therapeutic implications," *Nature Clinical Practice Oncology*, vol. 4, no. 9, pp. 516–525, 2007.

[36] T. Zaichuk, D. Ivancic, D. Scholtens et al., "Tissue-specific transcripts of human steroid sulfatase are under control of estrogen signaling pathways in breast carcinoma," *Journal of Steroid Biochemistry and Molecular Biology*, vol. 105, no. 1–5, pp. 76–84, 2007.

[37] S. J. Stanway, P. Delavault, A. Purohit et al., "Steroid sulfatase: a new target for the endocrine therapy of breast cancer," *Oncologist*, vol. 12, no. 4, pp. 370–374, 2007.

[38] R. D. Rao and M. A. Cobleigh, "Adjuvant endocrine therapy for breast cancer," *Oncology*, vol. 26, no. 6, pp. 541–547, 2012.

[39] M. Cazzaniga and B. Bonanni, "Breast cancer chemoprevention: old and new approaches," *Journal of Biomedicine and Biotechnology*, vol. 2012, Article ID 985620, 15 pages, 2012.

[40] J. Geisler, H. Sasano, S. Chen, and A. Purohit, "Steroid sulfatase inhibitors: promising new tools for breast cancer therapy?" *Journal of Steroid Biochemistry and Molecular Biology*, vol. 125, no. 1-2, pp. 39–45, 2011.

[41] V. Beral, D. Bull, and G. Reeves, "Million Women Study Collaborators. Endometrial cancer and hormone-replacement therapy in the Million Women Study," *The Lancet*, vol. 265, no. 9470, pp. 1543–1551, 2005.

[42] A. Doll, M. Abal, M. Rigau et al., "Novel molecular profiles of endometrial cancer-new light through old windows," *Journal of Steroid Biochemistry and Molecular Biology*, vol. 108, no. 3–5, pp. 221–229, 2008.

[43] L. C. Horn, M. Dietel, and J. Einenkel, "Hormone replacement therapy (HRT) and endometrial morphology under consideration of the different molecular pathways in endometrial carcinogenesis," *European Journal of Obstetrics Gynecology and Reproductive Biology*, vol. 122, no. 1, pp. 4–12, 2005.

[44] V. H. W. M. Jongen, J. M. Briët, R. A. De Jong et al., "Aromatase, cyclooxygenase 2, HER-2/neu, and P53 as prognostic factors in endometrioid endometrial cancer," *International Journal of Gynecological Cancer*, vol. 19, no. 4, pp. 670–676, 2009.

[45] M. Saegusa and I. Okayasu, "Changes in expression of estrogen receptors α and β in relation to progesterone receptor and pS2 status in normal and malignant endometrium," *Japanese Journal of Cancer Research*, vol. 91, no. 5, pp. 510–518, 2000.

[46] T. Šmuc, R. Rupreht, J. Šinkovec et al., "Expression analysis of estrogen-metabolizing enzymes in human endometrial cancer," *Molecular and Cellular Endocrinology*, vol. 248, no. 1-2, pp. 114–117, 2006.

[47] J. Lépine, E. Audet-Walsh, J. Grégoire et al., "Circulating estrogens in endometrial cancer cases and their relationship with tissular expression of key estrogen biosynthesis and metabolic pathways," *Journal of Clinical Endocrinology and Metabolism*, vol. 95, no. 6, pp. 2689–2698, 2010.

[48] N. V. Bochkareva, L. A. Kolomiets, I. V. Kondakova et al., "Sex hormone profile in uterine systemic and local blood flow in endometrial hyperplasia and carcinoma versus estrogen metabolism enzymes concentration," *Voprosy Onkologii*, vol. 54, no. 6, pp. 729–733, 2008.

[49] K. Ito, H. Utsunomiya, H. Niikura et al., "Inhibition of estrogen actions in human gynecological malignancies: new aspects of endocrine therapy for endometrial cancer and ovarian cancer," *Molecular and Cellular Endocrinology*, vol. 340, no. 2, pp. 161–167, 2011.

[50] S. E. Bulun, K. Economos, D. Miller, and E. R. Simpson, "CYP19 (aromatase cytochrome P450) gene expression in human malignant endometrial tumors," *Journal of Clinical Endocrinology and Metabolism*, vol. 79, no. 6, pp. 1831–1834, 1994.

[51] K. Watanabe, H. Sasano, N. Harada et al., "Aromatase in human endometrial carcinoma and hyperplasia: immunohistochemical, in situ hybridization, and biochemical studies," *American Journal of Pathology*, vol. 146, no. 2, pp. 491–500, 1995.

[52] N. Takahashi-Shiga, H. Utsunomiya, Y. Miki et al., "Local biosynthesis of estrogen in human endometrial carcinoma through tumor-stromal cell interactions," *Clinical Cancer Research*, vol. 15, no. 19, pp. 6028–6034, 2009.

[53] N. Pathirage, L. A. Di Nezza, L. A. Salmonsen et al., "Expression of aromatase, estrogen receptors, and their coactivators in patients with endometrial cancer," *Fertility and Sterility*, vol. 86, no. 2, pp. 469–472, 2006.

[54] T. Šmuc and T. L. Rižner, "Aberrant pre-receptor regulation of estrogen and progesterone action in endometrial cancer," *Molecular and Cellular Endocrinology*, vol. 301, no. 1-2, pp. 74–82, 2009.

[55] K. M. Cornel, R. F. Kruitwagen, B. Delvoux et al., "Overexpression of 17β-hydroxysteroid dehydrogenase type 1 increases the exposure of endometrial cancer to 17β-estradiol," *Journal of Clinical Endocrinology and Metabolism*, vol. 97, no. 4, pp. 591–601, 2012.

[56] O. Abulafia, Y. C. Lee, A. Wagreich et al., "Sulfatase activity in normal and neoplastic endometrium," *Gynecologic and Obstetric Investigation*, vol. 67, no. 1, pp. 57–60, 2009.

[57] H. Utsunomiya, K. Ito, T. Suzuki et al., "Steroid sulfatase and estrogen sulfotransferase in human endometrial carcinoma," *Clinical Cancer Research*, vol. 10, no. 17, pp. 5850–5856, 2004.

[58] J. Prat, "New insights into ovarian cancer pathology," *Annals of Oncology*, vol. 23, supplement 10, pp. 111–117, 2012.

[59] J. Li, O. Fadare, L. Xiang et al., "Ovarian serous carcinoma: recent concepts on its origin and carcinogenesis," *Journal of Hematology and Oncology*, vol. 5, no. 1, p. 8, 2012.

[60] R. J. Kurman and I. M. Shih, "Molecular pathogenesis and extraovarian origin of epithelial ovarian cancer—shifting the paradigm," *Human Pathology*, vol. 42, no. 7, pp. 918–931, 2011.

[61] N. Auersperg, "The origin of ovarian carcinomas: a unifying hypothesis," *International Journal of Gynecological Pathology*, vol. 30, no. 1, pp. 12–21, 2011.

[62] R. Vang, I. M. Shih, and R. J. Kurman, "Ovarian low-grade and high-grade serous carcinoma: pathogenesis, clinicopathologic

and molecular biologic features, and diagnostic problems," *Advances in Anatomic Pathology*, vol. 16, no. 5, pp. 267–282, 2009.

[63] H. D. Nelson, L. H. Huffman, R. Fu, and E. L. Harris, "Genetic risk assessment and BRCA mutation testing for breast and ovarian cancer susceptibility: systematic evidence review for the U.S. Preventive Services Task Force," *Annals of Internal Medicine*, vol. 143, no. 5, pp. 362–379, 2005.

[64] K. K. Wong, K. H. Lu, A. Malpica et al., "Significantly greater expression of ER, PR, and ECAD in advanced-stage low-grade ovarian serous carcinoma as revealed by immunohistochemical analysis," *International Journal of Gynecological Pathology*, vol. 26, no. 4, pp. 404–409, 2007.

[65] M. Lenhard, L. Tereza, S. Heublein et al., "Steroid hormone receptor expression in ovarian cancer: progesterone receptor B as prognostic marker for patient survival," *BMC Cancer*, vol. 12, no. 1, p. 553, 2012.

[66] V. Beral, "Ovarian cancer and hormone replacement therapy in the Million Women Study," *The Lancet*, vol. 369, no. 9574, pp. 1703–1710, 2007.

[67] L. S. Morch, E. Lokkegaard, A. H. Andreasen et al., "Hormone therapy and different ovarian cancers: a national cohort study," *American Journal of Epidemiology*, vol. 175, no. 12, pp. 1234–1242, 2012.

[68] K. M. Sjoquist, J. Martyn, R. J. Edmondson, and M. L. Friedlander, "The role of hormonal therapy in gynecological cancers-current status and future directions," *International Journal of Gynecological Cancer*, vol. 21, no. 7, pp. 1328–1333, 2011.

[69] K. M. Schmeler, C. C. Sun, D. C. Bodurka et al., "Neoadjuvant chemotherapy for low-grade serous carcinoma of the ovary or peritoneum," *Gynecologic Oncology*, vol. 108, pp. 510–514, 2008.

[70] M. M. Alhilli, H. J. Long, K. C. Podratz, and J. N. Bakkum-Gamez, "Aromatase inhibitors in the treatment of recurrent ovarian granulosa cell tumors: brief report and review of the literature," *Journal of Obstetrics and Gynaecology Research*, vol. 38, no. 1, pp. 340–344, 2012.

[71] J. Bonser, J. Walker, A. Purohit et al., "Human granulosa cells are a site of sulphatase activity and are able to utilize dehydroepiandrosterone sulphate as a precursor for oestradiol production," *Journal of Endocrinology*, vol. 167, no. 3, pp. 465–471, 2000.

[72] J. C. Chura, C. H. Blomquist, H. S. Ryu, and P. A. Argenta, "Estrone sulfatase activity in patients with advanced ovarian cancer," *Gynecologic Oncology*, vol. 112, no. 1, pp. 205–209, 2009.

[73] J. C. Chura, H. S. Ryu, M. Simard et al., "Steroid-converting enzymes in human ovarian carcinomas," *Molecular and Cellular Endocrinology*, vol. 301, no. 1-2, pp. 51–58, 2009.

[74] L. Milewich and J. C. Porter, "In situ steroid sulfatase activity in human epithelial carcinoma cells of vaginal, ovarian, and endometrial origin," *Journal of Clinical Endocrinology and Metabolism*, vol. 65, no. 1, pp. 164–169, 1987.

[75] T. Okuda, H. Saito, A. Sekizawa et al., "Steroid sulfatase expression in ovarian clear cell adenocarcinoma: immunohistochemical study," *Gynecologic Oncology*, vol. 82, no. 3, pp. 427–434, 2001.

[76] P. M. Wood, L. W. L. Woo, M. P. Thomas et al., "Aromatase and dual aromatase-steroid sulfatase inhibitors from the letrozole and vorozole templates," *ChemMedChem*, vol. 6, no. 8, pp. 1423–1438, 2011.

[77] A. Jemal, R. Siegel, E. Ward et al., "Cancer statistics, 2008," *CA: Cancer Journal for Clinicians*, vol. 58, no. 2, pp. 71–96, 2008.

[78] M. Barone, K. Lofano, N. De Tullio et al., "Dietary, endocrine, and metabolic factors in the development of colorectal cancer," *Journal of Gastrointestinal Cancer*, vol. 43, no. 1, pp. 13–19, 2012.

[79] H. S. Taylor and J. E. Manson, "Update in hormone therapy use in menopause," *Journal of Clinical Endocrinology and Metabolism*, vol. 96, no. 2, pp. 255–264, 2011.

[80] E. L. Barnes and M. D. Long, "Colorectal cancer in women: hormone replacement therapy and chemoprevention," *Climacteric*, vol. 15, no. 3, pp. 250–255, 2012.

[81] N. A. C. S. Wong, R. D. G. Malcomson, D. I. Jodrell et al., "ERβ isoform expression in colorectal carcinoma: an in vivo and in vitro study of clinicopathological and molecular correlates," *Journal of Pathology*, vol. 207, no. 1, pp. 53–60, 2005.

[82] R. Sato, T. Suzuki, Y. Katayose et al., "Steroid sulfatase and estrogen sulfotransferase in colon carcinoma: regulators of intratumoral estrogen concentrations and potent prognostic factors," *Cancer Research*, vol. 69, no. 3, pp. 914–922, 2009.

[83] M. A. English, P. M. Stewart, and M. Hewison, "Estrogen metabolism and malignancy: analysis of the expression and function of 17β-hydroxysteroid dehydrogenases in colonic cancer," *Molecular and Cellular Endocrinology*, vol. 171, no. 1-2, pp. 53–60, 2001.

[84] A. A. Rawluszko, K. Horbacka, P. Krokowicz, and P. P. Jagodziński, "Decreased expression of 17β-hydroxysteroid dehydrogenase type 1 is associated with DNA hypermethylation in colorectal cancer located in the proximal colon," *BMC Cancer*, vol. 19, no. 11, p. 522, 2011.

[85] O. O. Oduwole, V. V. Isomaa, P. A. Nokelainen et al., "Down-regulation of estrogen-metabolizing 17β-hydroxysteroid dehydrogenase type 2 expression correlates inversely with Ki67 proliferation marker in colon-cancer development," *International Journal of Cancer*, vol. 97, no. 1, pp. 1–6, 2002.

[86] L. Rath-Wolfson, O. Purim, E. Ram et al., "Expression of estrogen receptor β1 in colorectal cancer: correlation with clinicopathological variables," *Oncology Reports*, vol. 27, no. 6, pp. 2017–2022, 2012.

[87] A. Rudolph, C. Toth, M. Hoffmeister et al., "Expression of oestrogen receptor β and prognosis of colorectal cancer," *British Journal of Cancer*, vol. 107, no. 5, pp. 831–839, 2012.

[88] B. Arcidiacono, S. Iiritano, A. Nocera et al., "Insulin resistance and cancer risk: an overview of the pathogenetic mechanisms," *Experimental Diabetes Research*, vol. 2012, Article ID 789174, 12 pages, 2012.

[89] R. S. Ahima, "Digging deeper into obesity," *Journal of Clinical Investigation*, vol. 121, no. 6, pp. 2076–2079, 2011.

[90] K. Sikalidis and B. Varamini, "Roles of hormones and signaling molecules in describing the relationship between obesity and colon cancer," *Pathology and Oncology Research*, vol. 17, no. 4, pp. 785–790, 2011.

[91] E. R. Simpson, M. Misso, K. N. Hewitt et al., "Estrogen—the good, the bad, and the unexpected," *Endocrine Reviews*, vol. 26, no. 3, pp. 322–330, 2005.

[92] K. Blouin, M. Nadeau, J. Mailloux et al., "Pathways of adipose tissue androgen metabolism in women: depot differences and modulation by adipogenesis," *American Journal of Physiology*, vol. 296, no. 2, pp. E244–E255, 2009.

[93] T. Wada, C. A. Ihunnah, J. Gao et al., "Estrogen sulfotransferase inhibits adipocyte differentiation," *Molecular Endocrinology*, vol. 25, no. 9, pp. 1612–1623, 2011.

[94] J. W. Zhao, Z. L. Gao, H. Mei et al., "Differentiation of human mesenchymal stem cells: the potential mechanism for estrogen-induced preferential osteoblast versus adipocyte differentiation," *American Journal of the Medical Sciences*, vol. 341, no. 6, pp. 460–468, 2011.

[95] M. Muir, G. Romalo, L. Wolf et al., "Estrone sulfate is a major source of local estrogen formation in human bone," *Journal of Clinical Endocrinology and Metabolism*, vol. 89, no. 9, pp. 4685–4692, 2004.

[96] M. Svoboda, G. Hamilton, and T. Thalhammer, "Steroid hormone metabolizing enzymes in benign and malignant human bone tumors," *Expert Opinion on Drug Metabolism & Toxicology*, vol. 6, no. 4, pp. 427–437, 2010.

[97] V. K. Khor, R. Dhir, X. Yin et al., "Estrogen sulfotransferase regulates body fat and glucose homeostasis in female mice," *American Journal of Physiology*, vol. 299, no. 4, pp. E657–E664, 2010.

[98] J. Gao, J. He, X. Shi et al., "Sex-specific effect of estrogen sulfotransferase on mouse models of type 2 diabetes," *Diabetes*, vol. 61, no. 6, pp. 1543–1551, 2012.

[99] F. Mauvais-Jarvis, "Estrogen sulfotransferase: intracrinology meets metabolic diseases," *Diabetes*, vol. 61, no. 6, pp. 1353–1354, 2012.

[100] K. Visvanathan, R. T. Chlebowski, P. Hurley et al., "American Society of Clinical Oncology clinical practice guideline update on the use of pharmacologic interventions including tamoxifen, raloxifene, and aromatase inhibition for breast cancer risk reduction," *Journal of Clinical Oncology*, vol. 27, no. 19, pp. 3235–3258, 2009.

[101] J. Cuzick, A. DeCensi, B. Arun et al., "Preventive therapy for breast cancer: a consensus statement," *The Lancet Oncology*, vol. 12, no. 5, pp. 496–503, 2011.

[102] J. R. Pasqualini, "The selective estrogen enzyme modulators in breast cancer: a review," *Biochimica et Biophysica Acta*, vol. 1654, no. 2, pp. 123–143, 2004.

[103] L. W. L. Woo, A. Purohit, and B. V. L. Potter, "Development of steroid sulfatase inhibitors," *Molecular and Cellular Endocrinology*, vol. 340, no. 2, pp. 175–185, 2011.

[104] A. Purohit and P. A. Foster, "Steroid sulfatase inhibitors for estrogen- and androgen-dependent cancers," *The Journal of Endocrinology*, vol. 212, no. 2, pp. 99–110, 2012.

[105] L. L. Woo, A. Purohit, B. Malini et al., "Potent active site-directed inhibition of steroid sulphatase by tricyclic coumarin-based sulphamates," *Chemistry and Biology*, vol. 7, no. 10, pp. 773–791, 2000.

[106] I. Peñuelas, I. Dom´ınguez-Prado, M. J. Garc´ıa-Velloso et al., "PET tracers for clinical imaging of breast cancer," *Journal of Oncology*, vol. 2012, Article ID 710561, 9 pages, 2012.

[107] M. Wang, J. Mickens, M. Gao et al., "Design and synthesis of carbon-11-labeled dual aromatase-steroid sulfatase inhibitors as new potential PET agents for imaging of aromatase and steroid sulfatase expression in breast cancer," *Steroids*, vol. 74, no. 12, pp. 896–905, 2009.

[108] M. Wang, L. Xu, M. Gao et al., "Synthesis of 2-[^{11}C]methoxy-3,17β-*O*,*O*-bis(sulfamoyl)estradiol as a new potential PET agent for imaging of steroid sulfatase (STS) in cancers," *Steroids*, vol. 77, no. 8-9, pp. 864–970, 2012.

Hindawi Publishing Corporation
Journal of Drug Delivery
Volume 2013, Article ID 863539, 12 pages
http://dx.doi.org/10.1155/2013/863539

Review Article

Tumor-Specific Expression of Organic Anion-Transporting Polypeptides: Transporters as Novel Targets for Cancer Therapy

Veronika Buxhofer-Ausch,[1] Lena Secky,[2] Katrin Wlcek,[3] Martin Svoboda,[2] Valentinos Kounnis,[4] Evangelos Briasoulis,[4] Andreas G. Tzakos,[4,5] Walter Jaeger,[6] and Theresia Thalhammer[2]

[1] *Department of Medicine, Donauspital, Ludwig Boltzmann, Cluster for Translational Oncology, Vienna, Austria*
[2] *Institute of Pathophysiology and Allergy Research, Center for Pathophysiology, Immunology and Infectiology, Medical University of Vienna, Vienna, Austria*
[3] *Department of Clinical Pharmacology and Toxicology, University Hospital Zurich, Switzerland*
[4] *Cancer Biobank Center, University of Ioannina, Ioannina, Greece*
[5] *Department of Chemistry, University of Ioannina, Ioannina, Greece*
[6] *Department of Clinical Pharmacy and Diagnostics, University of Vienna, Vienna, Austria*

Correspondence should be addressed to Theresia Thalhammer; theresia.thalhammer@meduniwien.ac.at

Received 12 December 2012; Accepted 24 December 2012

Academic Editor: Vasso Apostolopoulos

Members of the organic anion transporter family (OATP) mediate the transmembrane uptake of clinical important drugs and hormones thereby affecting drug disposition and tissue penetration. Particularly OATP subfamily 1 is known to mediate the cellular uptake of anticancer drugs (e.g., methotrexate, derivatives of taxol and camptothecin, flavopiridol, and imatinib). Tissue-specific expression was shown for OATP1B1/OATP1B3 in liver, OATP4C1 in kidney, and OATP6A1 in testis, while other OATPs, for example, OATP4A1, are expressed in multiple cells and organs. Many different tumor entities show an altered expression of OATPs. OATP1B1/OATP1B3 are downregulated in liver tumors, but highly expressed in cancers in the gastrointestinal tract, breast, prostate, and lung. Similarly, testis-specific OATP6A1 is expressed in cancers in the lung, brain, and bladder. Due to their presence in various cancer tissues and their limited expression in normal tissues, OATP1B1, OATP1B3, and OATP6A1 could be a target for tumor immunotherapy. Otherwise, high levels of ubiquitous expressed OATP4A1 are found in colorectal cancers and their metastases. Therefore, this OATP might serve as biomarkers for these tumors. Expression of OATP is regulated by nuclear receptors, inflammatory cytokines, tissue factors, and also posttranslational modifications of the proteins. Through these processes, the distribution of the transporter in the tissue will be altered, and a shift from the plasma membrane to cytoplasmic compartments is possible. It will modify OATP uptake properties and, subsequently, change intracellular concentrations of drugs, hormones, and various other OATP substrates. Therefore, screening tumors for OATP expression before therapy should lead to an OATP-targeted therapy with higher efficacy and decreased side effects.

1. Introduction

Organic anion-transporting polypeptides (OATPs) encoded by the *SCLO* genes form the SLC family 21 (OATP family) mediating the transmembrane transport of a great variety of substrates [1]. OATPs are sodium-independent plasma membrane transporters for substrates from the endogenous metabolism, such as bile acids, steroid hormone conjugates, thyroid hormones, prostaglandins, cyclic nucleotides, drugs, and xenobiotics. In humans, eleven members of the OATP family, divided into six families which share >40% amino acid sequence identity, have been identified. OATPs share a largely common structure with 12 putative transmembrane regions and a large extracellular loop between the 9th and 10th transmembrane domains (Figure 1). While the families OATP3, 5, and 6 contain only a single member,

other families are further subdivided into subfamilies, which share a >60% amino acid sequence identity [2]. Members of the OATP family are expressed in a distinct pattern in excretory tissues (intestine, liver, and kidney) and on biological barriers of many organs including brain, breast, placenta, retina, ovary, and testis, where they may contribute to the absorption, distribution, and excretion of metabolic products, hormones, and drugs. OATPs work in concert with cellular metabolizing enzymes of phase 1 (cytochrome P450 isoenzymes) and phase 2 (glucuronosyltransferases, sulfotransferases, glutathione transferases, and others) enzymes as well as with efflux transporters (P-glycoprotein and breast cancer resistance protein ABCG2). The interplay between uptake, biotransformation, and efflux will strongly affect the distribution of drugs as OATP substrates [3].

There has been increasing evidence that OATPs may play an important role in the biology of various cancers. *De novo* expression of OATPs, like OATP1B1 and OATP1B3, normally only expressed in liver, has been identified in a variety of cancers (breast, colon, pancreas, stomach, prostate, bone, and ovary cancer) [4–6]. In patients with colon cancer, OATP1B3 confers resistance to anticancer drugs like paclitaxel (see Figure 3) [7]. In prostate cancer patients on androgen ablation therapy, variants of OATP1B3 with impaired function are associated with a longer progression-free and a longer overall survival, which is likely to be due to a reduced testosterone uptake into tumor cells [8, 9]. These findings recommend that therapeutic inhibition of OATP1B3 could be suitable for endocrine anticancer therapy. However, inhibiting this OATP therapeutically may interfere with normal physiological processes in the liver and impair the excretion of bilirubin, bile acids, drugs, and toxins. It may also cause drug interactions because of the inhibition of the hepatic uptake of OATP1B3 substrates and subsequently, with their biotransformation and excretion [10].

This paper focuses on the expression of OATP as a transporter for anticancer drugs and hormones in cancer. We provide an overview on the expression of specific OATPs and discuss their potential role as novel targets for anticancer therapy.

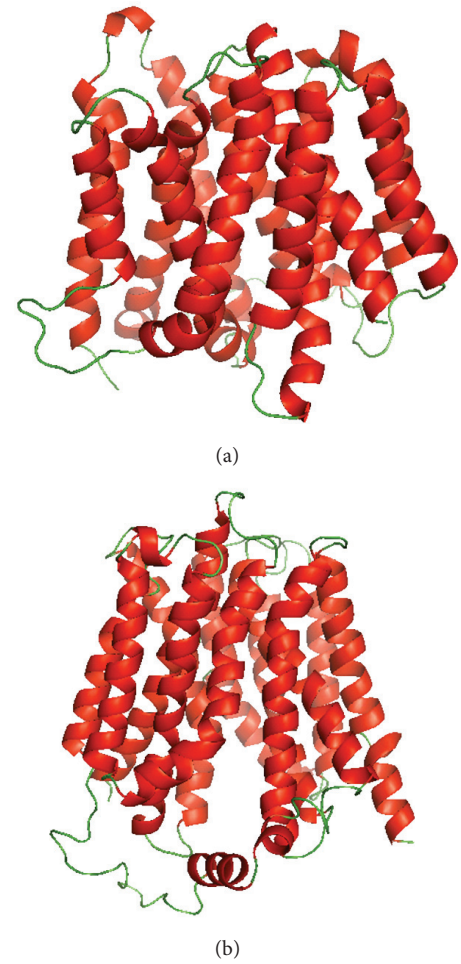

(a)

(b)

Figure 1: Ribbon representation of the three-dimensional model in (a) of OATP2B1 (built with modeller 9.11 using the structure template of the multidrug transporter EmrD from 2 *Escherichia coli*, pdbid: 2gfp) and in (b) of OATP1B3 (built with modeller 9.11 using the structure template of the *Escherichia coli* glycerol-3-phosphate transporter (PDB 1pw4)). The models were built by Modeller 9.11 program (San Francisco, CA, USA).

2. The OATP Family of Transporters

The best characterized family is the OATP1 family with three transporters OATP1A2, OATP1B1, and OATP1B3 that transport a number of typical OATP substrates including steroid hormone conjugates, thyroid hormones, prostaglandins, bile acids, and various drugs, for example, statins, antibiotics, and a number of anticancer drugs (for a review see [2]). The fourth member, OATP1C1, is regarded as thyroid hormone transporter, because of its high affinity for the thyroid hormones T_3 and T_4 [11]. However, it also transports steroid hormone conjugates [12].

The OATP2 family comprises two members, OATP2A1 and OATP2B1. OATP2A1 was originally identified as the prostaglandin transporter (PGT). It is thought to regulate prostaglandin (PG) levels in target tissues, for example, kidney, colon [13]. OATP2B1 has broader substrate specificity at an acidic pH (pH 6.8) for various endogenous products and drugs, while at pH 7.4, it transports mainly steroid hormone conjugates [2].

Typical OATP substrates (prostaglandins, thyroid hormones) are also transported by OATP3A1 and OATP4A1, but with varying affinity. For OATP3A1, transporting prostaglandins, thyroxin, vasopressin, deltorphin, and benzylpenicillin, two splice variants OATP3A1v1 and OATP3A1v2 were identified [2]. Additional substrates for the second member of the family 4, the "kidney-specific transporter" OATP4C1, which is important for the removal of uremic toxins, are cyclic nucleotides, the anticancer drug methotrexate, and other common OATP substrates, including thyroid hormones [14].

Transporters of the OATP family OATP5A1 and OATP6A1 are not characterized for their transport function yet. There is some evidence that OATP5A1 is involved in the chemoresistance to the oral anticancer drug satraplatin [15].

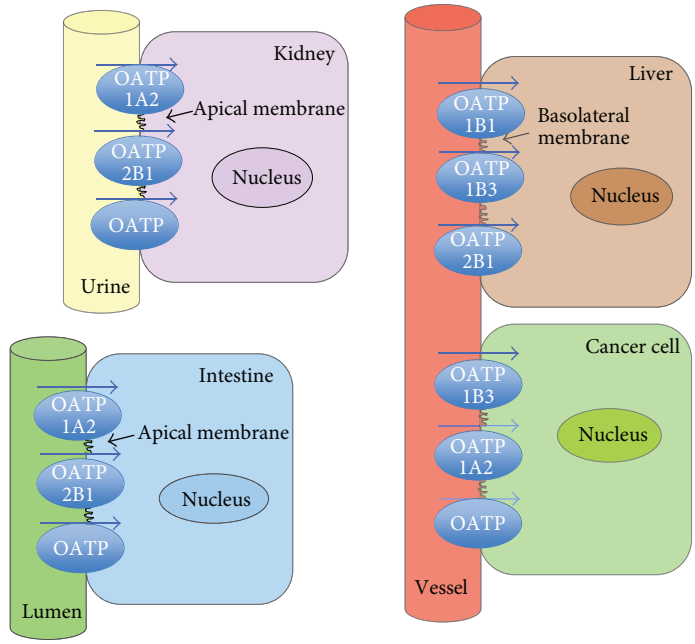

Figure 2: Expression of well-characterized OATPs of family 1 (OATP1A2, OATP1B1, and OATP1B3) and OATP2B1, in normal tissue and cancer cells (well-characterized OATPs are shown, and additional members of the OATP family are depicted as "OATP").

3. Relevance of OATP Expression in Cancer

3.1. The Specific Expression Pattern of OATPs in Cancer May Allow Therapeutic Targeting. Under physiological conditions, expression of OATP1B1, OATP1B3, and OATP6A1 is restricted to a certain tissue (Figure 2), but this pattern is no longer maintained under pathological conditions (inflammation, cancer). While in normal tissues, OATP1B1/OATP1B3 are expressed in liver and OATP6A1 in testis, the situation in cancer is different. These three OATPs are detectable in a number of different cancers. For example, "liver-specific" OATP1B3 becomes expressed in colon [16], pancreas [17], breast [18], prostate [19], lung [20], and ovarian cancer [3, 5]. "Testis-specific" OATP6A1 is highly expressed in lung [21] and brain cancer [22]. This altered expression pattern may be of a diagnostic value. It may also allow a targeted delivery of drugs. However, it has to be considered that it may also cause systemic adverse drug effects. But applying, for example, OATP1B3 substrates locally for tumors in the gastrointestinal tract or prostate, may allow an effective therapy with less side effects from the hepatic OATP1B3. Furthermore, OATP6A1-directed antibodies could be useful in the local therapy of cancers in lung, brain, and other organs expressing this OATP.

3.2. OATP Expression and Its Relevance for Cancer Progression

3.2.1. OATPs May Affect the Intracellular Concentration of Cancer Chemotherapeutics. Uptake of anticancer drugs by specific carriers plays an important role in tissue distribution, urinary and biliary excretion of drugs in healthy tissues [23]. They also provide intracellular drug concentrations necessary to reach a cytotoxic effect in cancer cells, because many cytotoxic drugs (methotrexate, taxol derivatives, imatinib, irinotecan, and flavopiridol) are substrates for OATPs (see Figure 3).

So far, mostly OATP1A2, OATP1B1, and OATP1B3 have been carefully studied for the transport properties of anticancer drugs using *Xenopus laevis* oocytes or cancer cell lines expressing these carriers (see [6]). From the data obtained, it is obvious that a cancer-specific expression pattern of individual OATPs will influence the intracellular accumulation of drugs that are substrates for specific OATPs. Therefore, the expression pattern will influence the sensitivity of cancer cells for a certain drug.

3.2.2. OATP Confers Resistance to Apoptosis after Anticancer Chemotherapy. After camptothecin and oxaliplatin treatment, OATP1B3 overexpression provides a survival advantage for wild-type p53 expressing colon cancer cell lines by altering p53-dependent survival pathways [7].

3.2.3. OATPs May Provide Steroid Hormones to Hormone-Sensitive Cancers. The steroid hormone precursors, estrone sulfate (E1S), dehydroepiandrosterone sulfate (DHEAS), and the androgen testosterone, are substrates for a number of different OATPs (see Figure 4). Overexpression of these OATPs in cancer may increase the cellular levels of hormones, for example, estrogens and androgens, which drive the proliferation of hormone-dependent cancer cells.

E1S is one of the most abundant estrogen precursors in postmenopausal women and important for the growth of estrogen-dependent breast cancer cells [25]. Seven out of eleven OATPs were found to transport E1S. For example, OATP1B3 expressed in the estrogen-dependent human

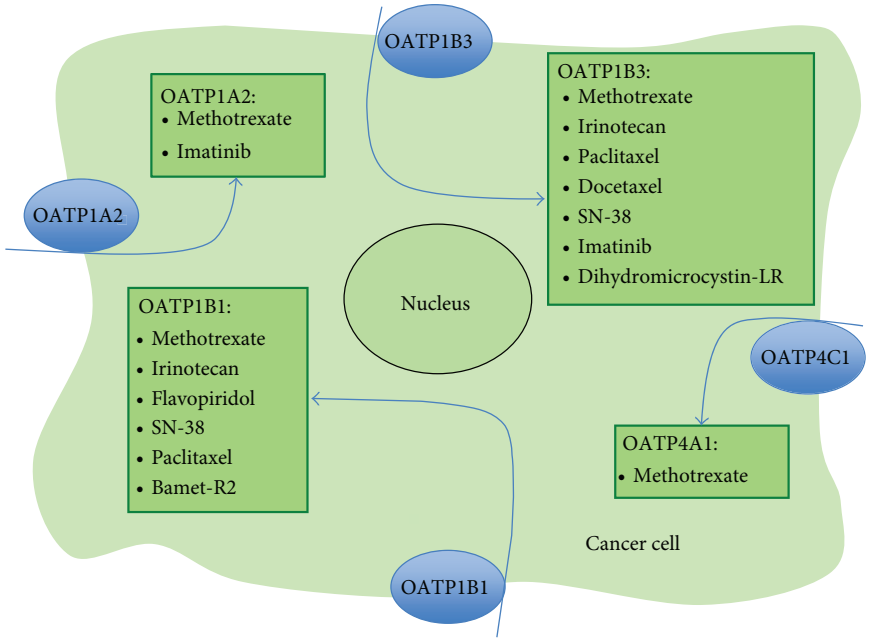

Figure 3: Selected anticancer drugs as substrates for organic anion-transporting polypeptides [2, 5, 6, 24].

breast cancer cell line MCF-7 contributes to E1S uptake [18]. The expression of steroid hormone-transporting OATP1A2, OATP1B1, OATP1B3, OATP2B1, and OATP3A1 was found to be higher in breast cancer cell lines than in the nonmalignant breast cell line MCF10A. Furthermore, specific OATP-mediated E1S uptake was observed only in malignant cells [26]. Enhanced expression of estrogen sulfates transporting OATPs may lead to the increased accumulation of steroid hormones in estrogen-sensitive tumor cells.

OATP1A2 is also important in prostate cancer. Growth of the androgen-sensitive prostate cancer cell line LnCAP is stimulated by the androgen precursor DHEAS. The steroid hormone precursor is taken up into the cells by OATP1A2, and there, it is converted by the steroid sulfatase (STS) to active, growth stimulating DHEA. Thus, OATP1A2 together with STS is postulated to be a pharmacological target for prostate cancer treatment [27]. Other OATPs important for the growth of prostate cancer are OATP1B3, mediating the uptake of testosterone (see Figure 4), and OATP2B1, for which DHEAS is a substrate [6].

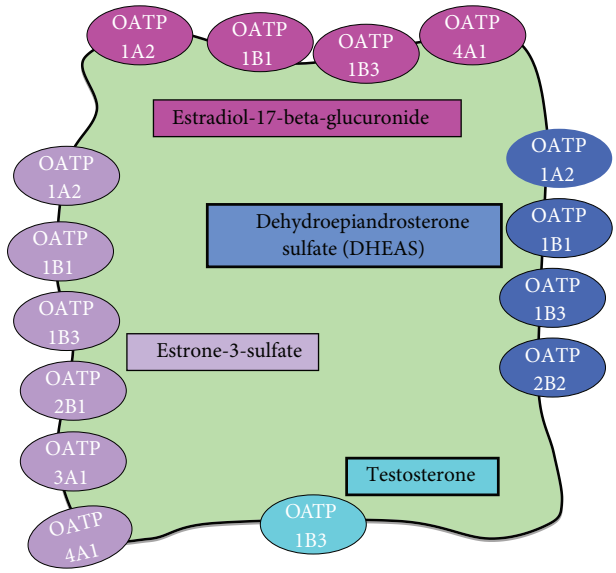

Figure 4: Transport of steroid hormones by OATP substrates [6].

3.3. OATP Expression Is a Predictive Factor for the Clinical Outcome of Tumors. In some tumors, OATPs show a specific expression pattern, and there is also evidence that specific OATPs might be predictive for tumor progression. For example, OATP1B3 immunoreactivity was found to be a potent prognostic factor in human breast, prostate, and colon cancer.

4. OATP Expression in Breast Cancer

In breast cancer, OATP1B3 immunoreactivity was detectable in 50% of breast cancer patients. Its expression was significantly associated with a hormone-dependent growth mechanism of the breast cancer, but patients expressing this OATP had a better prognosis [28]. Also in another study, a better prognosis was seen for estrogen receptor-positive patients who expressed OATP1B3. For another E1S transporting OATP, namely OATP2B1, no relation to the clinical progression of breast cancer was found [29]. Although expression of OATPs for the transport of estrogen precursors, including E1S, would rather lead to an increased proliferation of hormone-dependent tumors, but as this OATP also transports anticancer drugs, these patients may better respond to anticancer therapy.

Furthermore, a number of other OATPs known to transport estrogens, for example, OATP2B1, OATP3A1, and

OATP4A1 were found to be expressed in breast tissue and some are reduced in malignant tissues [30]. For example, OATP3A1 was recently found to be highly important for the transport of E1S in breast cancer cell lines [26], and this may also be the case in the cancer tissue.

It has also to be considered that apart from their role in estrogen homeostasis, expression of specific OATPs for which anticancer drugs are substrates (e.g., OATP1B1/OATP1B3 for paclitaxel) [31] may allow cancer patients to respond better to tumor therapy [28].

5. OATP Expression in Prostate Cancer

Testosterone (T) deprivation therapy is important to treat advanced, androgen-sensitive prostate cancer, but it is highly variable in its effectiveness. Also acquired resistance to androgen ablation is still a major therapeutic problem. Production of testosterone in testis is regulated by the hypothalamic-pituitary axis. Secretion of hypothalamic luteinizing hormone-releasing factor in the hypothalamus and gonadotropic luteinizing hormone in the pituitary regulate gametogenesis and synthesis of steroid hormones including T in testis. T is taken up by prostate cancer cells via OATP1B3. In prostate cancer cells, T is converted into dihydrotestosterone (DHT) by 5-alpha-reductase. Activation of the androgen receptor by DHT leads to a stimulation of cancer cell proliferation (see Figure 5). Mutations in T-transporting OATP1B3 were first found to limit the response to androgen-deprivation therapy in patients [9].

Later, it was shown that mutations in the gene coding for OATP2B1 were also associated with time to progression. Expression of the OATP2B1 genotype, which allows a more efficient uptake of androgens into cell, is associated with enhanced tumor progression. Patients carrying mutations in OATP2B1 and OATP1B3, which allows them to import androgens more efficiently into the cancer cells, were found to have a shorter period for progression-free survival [32]. Furthermore, increased intratumoral androgen levels and an increased expression of OATP1B1, OATP1B3, OATP2A1, OATP2B1, OATP3A1 und OATP4A1 in hormone-resistant metastases compared to untreated prostate cancers was also shown [9].

In line with these findings, the risk for androgen ablation-insensitive metastases is increased in patients with variant alleles for OATP2B1 or OATP1B3. The data so far suggest that OATPs could be potential biomarkers for assessing risk of androgen-insensitive metastases in patients who should be treated earlier with a non-hormonal based anticancer therapy [9].

6. OATP Expression in Colorectal Cancer

Using tissue microarrays, OATP1B3 immunoreactivity was detectable in the majority (56%) of colon tumor samples from 278 patients with all tumor stages. Similar to prostate cancer where expression OATP1B3 is significantly related to the Gleason score as a marker for tissue dedifferentiation [5], higher OATP1B3 levels in colon are associated with earlier tumor stage and they are found in better differentiated tumors. However, they are not predictive for the 5-year survival and for tumor recurrence. Within lower tumor grades, OATP1B3 expression is associated with an improved 5-year survival, while the tumor recurrence in patients with poorly differentiated tumors is independent on the expression of this OATP [16].

7. OATP Expression in Pancreatic Cancer

Extensive research has failed to produce any therapy efficient enough to substantially extend the median survival of treated patients beyond 6 months. Currently available therapies remain palliative on their intent [33–35]. Therefore, identification of new molecular targets and discovery of novel targeted therapies is of top priority for pancreatic cancer research. In a recent study, the expression of OATP1A2, OATP1B1, and OATP1B3 was studied by immunohistochemistry in a sample of 12 patients as well as on the mRNA level in two pancreatic cancer cell lines [17]. Quantitative analysis was done by the HistoQUEST Software using the TissueFaxs Microscopic Image Analysis System (TissueGnostics, Vienna, Austria). The three studied polypeptides were found ubiquitously expressed in all studied pancreatic cancer biopsy samples. Methods used confirmed extensive immunostaining of the entire cancer cell tissue with the antibodies against these OATPs. In detail, the OATP1A2 expression signal was weak in one sample and moderate to strong in all others. OATP1B1 was found to be weakly expressed in all 12 cases. Immunostaining with the mMDQ antibody against OATP 1B1/1B3 was proved to be the most intense. Nine cases demonstrated moderate expression and three cases stained strong. OATP 1B1 and 1B3 mRNA expression in two cell lines, MIA PaCa-2 and Bx-PC3, was comparable to that in normal liver, which was taken as a control, because both of these transporters are considered "liver-specific". Their mRNA expression, however, in normal pancreas was either undetectable (OATP 1B1) or 30–60 times lower than that in normal liver (OATP 1B3).

The OATPs investigated in this study were all found to be ubiquitously expressed at the protein and the mRNA level which flags them as appropriate candidates for *in vitro* studying of OATP-targeted anticancer compounds [17].

8. OATP Expression in Liver Cancer

In tumors of the liver, the expression of OATP1B1 and OATP1B3 is reduced along the degree of tissue dedifferentiation. This could reflect the reduction of metabolic function of liver cells in more advanced tumors [5]. In hepatocellular carcinoma patients, which undergo liver transplantation, expression levels of these OATPs are negatively related to tumor-related death after recurrence, but the expression of the OATPs is not correlated to the regression-free survival [36]. On the other hand, we showed that some OATPs (OATP2A1, OATP3A1, OATP4A1, and OATP5A1) become upregulated in primary and metastatic liver cancer as compared to nonmalignant liver. In these patients, OATP-derived

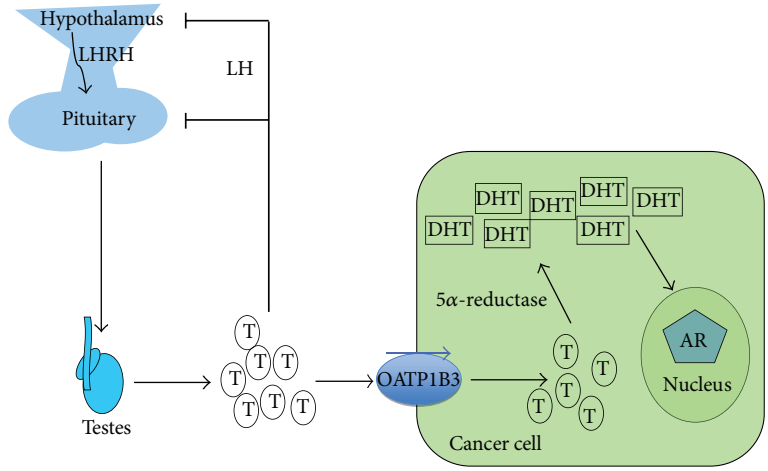

Figure 5: OATP1B3 provides androgens for prostate cancer cell proliferation. Production of Testosterone (T) in testis is regulated by the hypothalamic-pituitary axis via section of LHR (hypothalamic luteinizing hormone-releasing factor) and LH (gonadotropic luteinizing hormone). These hormones regulate gonadal function, including gametogenesis and synthesis of steroid hormones including testosterone (T), which is released into the circulation. It is taken up by prostate cancer cells via OATP1B3. In prostate cancer cells, T is converted into dihydrotestosterone (DHT) by 5-alpha-reductase. DHT activates the androgen receptor (AR) leading to a stimulation of cancer cell proliferation [9, 32].

immunoreactivity is located in the plasma membranes and, occasionally, in the cytoplasm of tumor cells. In some tumors, staining is also seen in bile duct cells and in stromal cells [37]. This pattern suggests that particular OATPs might be necessary to supply tumor cells with nutrients, hormones, or tissue factors in cells working in a close interaction between the tumor and its environment. These OATPs might be further exploited for the discovery of novel anticancer agents [38].

9. Members of the OATP Family: Role in the Transport of Anticancer Drugs and Hormones

9.1. OATP1A2. OATP1A2 (gene symbol, SLCO1A2) mediates the cellular uptake of a wide range of endogenous substrates including estrogen conjugates, DHEAS, thyroid hormones, prostaglandins, and bile acids. These groups are "typical OATP substrates" as they are transported by the vast majority of OATPs. But there is a diverging affinity for individual drugs. Figure 3 gives an overview on anticancer drugs as substrates for individual OATPs (see [2]).

OATP1A2 is also a transporter for many drugs, including statins, morphine derivates, and antibiotics. Importantly, the folate antimetabolite methotrexate and imatinib, a drug applied for many forms of leukemia, are OATP1A2 substrates [6].

This OATP is highly expressed at physiological barriers, for example, blood-brain barrier, the brush border membrane of the distal nephron, bile duct cells, and endothelial cells of the blood-brain barrier, and in the apical membranes of epithelial cells in the small intestine, suggesting a particular role of this OATP in drug disposition. OATP1A2 levels are low in all regions of the intestine [38, 39], but the transporter colocalizes with MDR1 to the brush border domain of enterocytes [40]. Therefore, OATP1A2 could be of pharmacological relevance if the levels of this OATP are induced by pharmacological administration of, for example, Vitamin D(3) or pregnane-X-receptor (PXR) ligands [41]. The bioavailability of oral applied anticancer drugs, for example, imatinib, and drugs given frequently to cancer patients, like deltorphin II and nadolol, could be influenced by the induction of intestinal OATP1A2 [42]. Interaction between OATP1A2 substrates may change intracellular concentrations of drugs which may influence the efficacy of the therapy and/or lead to serious side effects.

According to its localization in the basolateral membrane of the distal nephron, it may also regulate the renal excretion of anticancer drugs. This is suggested from the finding that SLCO1A2 mutations influence the imatinib clearance in patients with chronic myeloid leukemia [42]. On the other hand, another study reported that the imatinib absorption was not related to OATP1A2 variants [43]. Also methotrexate is mostly excreted via the kidney, and OATP1A2 may mediate the tubular reabsorption of methotrexate. Altered expression of OATP1A2 in the kidney may therefore contribute to drug-induced toxicity. Whether OATP1A2 mutations may influence drug clearance in patients is not known yet but could occur, as methotrexate transport is altered in *Xenopus laevis* oocytes expressing different OATP1A2 variants [44].

Finally, high expression levels of OATP1A2 in tumor cells in breast, prostate, and bone cancer will influence cellular levels of anticancer drugs imatinib and methotrexate and determine their local efficacy [26, 27].

The ligand-activated transcription factor PXR is known to play a role in the regulated expression of drug metabolizing enzymes and transporters. Data in breast cancer revealed that the PXR activator rifampicin can stimulate OATP1A2 expression. On the other hand, a statistical analysis of data from approximately 100 patients suggests that variations in genes coding for PXR, OATP1A2, and the OATPs 1B1, 1B3,

and 2B1 do not contribute to breast carcinogenesis [45]. At the protein level, protein kinase C was shown to regulate the correct insertion of OATP1A2 into the plasma membrane in part by clathrin-dependent pathways. Inhibition of PKC activity blocks the transport function of this OATP [46, 47].

9.2. OATP1B1/1B3. OATP1B1 and OATP1B3 are highly expressed in normal liver and are regarded as "liver-specific" OATPs. OATP1B3 is also expressed in various human cancer tissues, and some studies suggest that its expression levels are associated with the prognosis and clinical outcome of tumors [28, 48].

Both transporters from the 1B family are carriers for typical OATP substrates including hormones and conjugates, bile acids, statins, antibiotics, and a number of other drugs [2]. Also some anticancer drugs, for example, methotrexate, docetaxel, the irinotecan metabolite SN-38, and the immunosuppressive drug rapamycin, are transported by both OATPs (reviewed in [6]). The camptothecin derivatives gimatecan and BNP1350 [49], the cyclin-dependent kinase inhibitor flavopiridol [50], and the cisplatin bile acid derivatives Bamet-R2 [cis-diamminechlorocholylglycinate-platinum(II)], Bamet-UD2 [cis-diammine-bisursodeoxy-cholate-platinum(II)] [51] are substrates for OATP1B1. Substrates for OATP1B3 are the Her-2 tyrosine kinase inhibitor CP-724,714 [52], imatinib [53], and PKI166, a specific inhibitor of the tyrosine kinase activity of two epidermal growth factor receptors [54].

Both OATPs are polymorphic, and, so far, a number of variants with altered drug affinity and transport kinetics were identified and characterized *in vitro* (reviewed in [55, 56]). Expression of different variants in patients may alter the bioavailability of anticancer drugs as shown in animal studies, where absence of the analog of human OATP1B1/1B3 in mice led to a decrease in the docetaxel clearance. However, in patients, the reduced function of OATP1B1 or OATP1B3 variants did not alter docetaxel clearance. Therefore, only functional defects in both OATPs may influence the disposition of docetaxel [57]. Uptake of SN-38 was reduced in cell lines expressing three common variants of OATP1B1. An influence on the pharmacokinetics of SN-38 was also proposed for patients with the respective variants [58]. Indeed, patients with the SLCO1B1∗15 polymorphism had lower clearance of irinotecan [59].

Gadoxetic acid, which is used for liver magnetic resonance imaging in patients with liver cancer, is also an OATP1B1/OATP1B3 substrate. Although the pharmacokinetic characteristics for the drug were not influenced by SNP, in people carrying certain OATP1B1 variants, the magnetic resonance imaging signals were disturbed [60].

OATP1B1 and OATP1B3 expressions were shown to be reduced in primary and metastatic liver cancer. However, OATP1B3 is expressed in many cancers, for example, in colon, breast, pancreas, ovary, testis, bladder, prostate, and so forth [5], where it may influence tumor growth and survival in an organ-specific way [61]. Overexpression in colon cancer may contribute chemoresistance as it promotes the survival of colon cancer cells after treatment with anticancer drugs dependent on p53 expression [7]. In ovarian cancer cell lines, OATP1B1 and OATP1B3 were identified as high-affinity paclitaxel transporters. As both OATPs are expressed in 50% of cancer samples, they might have a role in the disposition of paclitaxel during first-line therapy of ovarian cancer [31].

Although OATP1B3 is frequently found in tumors, the molecular entity of cancer-associated OATP1B3 is still poorly addressed. Recently, a new OATP1B3 mRNA variant named cancer-type OATP1B3 was identified and found to be highly expressed in colon and lung cancer specimens. However, the translation product of this gene has not been characterized yet, and therefore, no statement on its impact on cancer growth and progression can be made [62].

By mediating the uptake of steroid hormones in hormone-sensitive tumor cells, these OATPs may promote the cell survival. OATP1B3 expression is regulated by transcription factors like the farnesoid-X-receptor (FXR), the hepatocyte nuclear factor (HNF) 1-alpha, and HNF3-beta. HNF1-alpha and HNF3-beta might contribute to its liver-specific expression, and FXR might play a role in its transcriptional activation by bile acids [63].

9.3. OATP1C1. OATP1C1 is a transporter with the highest affinity for thyroid hormones, and it could be important for the transport of these hormones in target tissues. Although it has some affinity for other OATP substrates, no cancer drugs were identified to be transported by this OATP. It is expressed in bone tumors too [64]. OATP1C1 might also contribute to the excretory system of the colon [65].

9.4. OATP2A1. The prostaglandin transporter OATP2A1 is widely expressed in different organs (e.g., brain, gastrointestinal tissues, kidney, heart, liver, ovary, lung, prostate, skeletal muscle, and spleen) [66]. At the protein level, OATP2A1 was detected in the luminal membrane of endothelial cells forming the blood-brain barrier and the blood-tumor barrier [67], in the pyloric glands of the antrum and in parietal cells in the gastrointestinal tract [68], as well as in the luminal and glandular epithelium of the endometrium [69]. The prostaglandin carrier mediates the transport of several prostanoids including prostaglandin E(2) and PGF(2-alpha).

High mRNA expression was detected in many other tumors including cancers of breast, liver, ovary, lung, and bone. It was shown to be downregulated at the mRNA and protein level in colorectal cancer, where it seems to contribute to the regulation of extracellular proinflammatory PGE(2) levels [70]. PGE(2) is taken up into cells from the extracellular milieu by OATP2A1, where it can be inactivated by oxidation to inactive 15-keto PGE(2) by the 15-hydroxyprostaglandin dehydrogenase [66].

9.5. OATP2B1. The ubiquitously expressed OATP2B1 has a high affinity for steroid hormone conjugates; OATP2B1 transports other OATP substrates including thyroid hormones, PGE(2), and many drugs. No anticancer agents were identified as a substrate for OATP so far. OATP2B1 expression was found to be regulated by steroid hormones. Progesterone was shown to stimulate OATP2B1-mediated

transport of precursors for steroid hormone synthesis, E1S, DHEA, and pregnenolone sulfate, but not of other OATP substrates [71].

OATP2B1 expression was also demonstrated in human gliomas, where it was localized to endothelial cells at the blood-brain barrier and blood-tumor barrier [72]. Increased expression was found in breast cancer specimens as compared to nonmalignant breast [30]. In breast cancer, its expression increases with increased tumor grade [29]. Furthermore, OATP2B1 mRNA expression was higher in bone cysts than in osteosarcoma tissues [64].

9.6. OATP3A1. OATP3A1 was shown to transport hormone and conjugates, prostaglandins, vasopressin, and benzylpenicillin and other antibiotics. Highest levels of this OATP were found in testis, brain, lung, spleen, human osteoblast-like cells, and bone-marrow stromal cell. High levels of this OATP were found in breast cancer, where it was detected in the membrane and cytoplasm of malignant cells in breast tumor specimens [73].

9.7. OATP4A1. The expression pattern of OATP4A1 is similar to that of OATP3A1. OATP4A1 is highly expressed in various carcinomas, for example, breast, lung, colon, and ovarian carcinoma, and metastatic tumors of colorectal cancer in liver. OATP4A1 and also OATP2B1 are significantly highly expressed in the colon of patients with inflammatory bowel disease than in normal colonic tissue [38]. In colorectal neoplasia, increased expression of prostaglandin E(2) transporting OATP4A1 and OATP2B1 may lead to a decreased sensitivity to cyclic nucleotides [65].

9.8. OATP4C1. OAT4C1 is expressed mainly in the kidney but is also found in some tumors, for example, colon. Human OATP4C1 were previously shown to transport cardiac glycosides, thyroid hormone, cAMP, and methotrexate [24]. In the rat kidney, Oatp4c1 reduced hypertension, cardiomegaly, and inflammation in the setting of renal failure. This was related to its excretory function in kidney. SLCO4C1 overexpression decreased plasma levels of the uremic toxins, for example, guanidino succinate, and dimethylarginine [74]. Statins, which act as inducers of nuclear aryl hydrocarbon receptors, upregulate SLCO4C1 transcription [75].

9.9. SLCO5A1. This poorly characterized OATP was detected at the mRNA levels in many tissues including heart, skeletal muscle, brain, breast, and blood cells. At the mRNA level it was described in cancers of the liver, bone, and breast. In normal breast tissue, OATP5A1 is located at the cell membrane of epithelial cells lining the milk ducts. In breast cancer, OATP5A1 loses the membrane localization as immunoreactivity was also visible in the cytoplasm of milk duct cells [73].

Haploinsufficiency of the gene coding for OATP5A1 together with that encoding the heparan sulfate 6-O-endosulfatase 1 acting as a regulator of numerous growth factors in skeletal embryonic development were found to cause a rare autosomal dominant disorder, the mesomelia-synostoses syndrome. It is characterized by mesomelic limb shortening, acral synostoses, and multiple congenital malformations [76].

9.10. OATP6A1. OATP6A1 was originally identified as a cancer/testis (CT) antigen strongly expressed at the mRNA level only in normal testis. Weak expression was seen in spleen, brain, and placenta [22]. Like other CT antigens, OATP6A1 is expressed in a number of cancers (brain, urinary bladder, and lung). Because of its high immunogenic potential, these CT antigens would be of potential utility as a target for antibody-based therapy for a variety of tumor types [77].

10. Regulation of OATP Expression

Altered expression of OATPs after malignant transformation of tissues raises the question about mechanisms involved in the regulation of the expression of these transporters. Although data on regulatory mechanisms for the expression of OATPs are still rare, regulation of OATP1B1, OATP1B3, OATP2A1, OATP2B1, and OATP4A1 were studied on the transcriptional and posttranscriptional levels. Activation of transcription factors, DNA-dependent gene silencing, and posttranscriptional modifications are involved in the regulation of their expression [31]. In cancer, these processes may change the expression levels of transporters and/or shift the transporter from the plasma membrane to cytosolic compartments leading to changes in OATP functional properties [6].

Transcriptional regulation by different nuclear receptors plays an important role in the regulation of OATP expression. For example, in breast carcinoma tissue and cancer cell lines, expression of OATP1A2 is closely correlated to the expression of the pregnane-X-receptor (PXR) [78]. This chemosensitizing nuclear receptor is activated by a wide range of drugs and xenobiotics, including rifampicin, capable to induce OATP1A2 in these cell lines [79]. In the breast cancer cell line T47-D, induction of OATP1A2 by rifampicin was accompanied by an increased cell proliferation, for which increased uptake of E1S could be responsible. Both increased uptake and cell proliferation after rifampicin can be inhibited by the application of PXR antagonists. Also expression of OATP1B3 and OATP1B1 are regulated by nuclear receptors, but in contrast to OATP1A2, PXR activation by rifampicin inhibits OATP1B3 expression.

Alterations in the cytokine pattern by viral infection and inflammation reduce the expression of OATP1B1, OATP1B3, and OATP2B1 as studies in patients suffering from hepatitis C showed [80]. Interferon gamma, tumor necrosis factor-alpha, interleukin-1-beta, and -6 were shown to decrease mRNA expression of the three OATPs in isolated hepatocytes [81].

DNA methylation-dependent gene silencing was demonstrated to regulate the expression of OATPs. Holla et al. showed [70] that the application of a demethylating agent or a histone deacetylase inhibitor could partially restore the reduced expression of OATP2A1 in colorectal cancer cell lines. Furthermore, the analysis of the DNA methylation

profile of OATPs in colon cancer cell lines revealed that GpG nucleotides around the transcriptional start site of OATP1B3 possess different methylation patterns leading to distinct expression pattern in these cell lines [82].

On the posttranscriptional level, phosphorylation and glycosylation may alter subcellular localization of the OATPs. For example, altered phosphorylation in breast cancer shifts the OATP2B1 from the plasma membrane to cytosolic compartments. Activation of protein kinase C by phorbol ester results in increased OATP2B1 phosphorylation, subsequent rapid clathrin-dependent internalization, and lysosomal degradation [46, 47].

11. Conclusions

The physiological expression pattern of OATPs is altered in malignancies. As many anticancer drugs are substrates for OATPs, expression of these transporters in tumors may affect the intracellular concentration of drugs, and, therefore, influence their effectiveness. Furthermore, expression levels of these influx transporters, known to work in concert with efflux transporters and drug-metabolizing enzymes, respectively, may play a crucial role in chemoresistance mechanisms. OATPs may also influence hormone-dependent tumor growth, because they mediate the uptake of steroid hormone precursors (E1S, DHEAS) into cancer cells. These precursors can be converted to the active estrogens and androgens by steroid sulfatase and 17-beta-dehydrogenases, respectively.

Furthermore, OATPs, highly and exclusively expressed in certain cancer types, may serve as novel biomarkers for the response to anticancer drugs and/or hormonal therapy. Whether OATPs may be targets for cancer-directed therapy has to be further evaluated.

Further research is also required to determine these transporters in individual tumors. *In vivo* models are necessary to investigate their potential to alter the response to clinically established and novel anticancer substrates as well as to therapeutically applied hormones. Expanding our understanding of the different expression patterns of OATPs in tumors will finally aid oncologists when prescribing anticancer drugs known to be transported by OATPs.

Abbreviations

Bamet-R2: cis-Diamminechloro-cholylglycinate-platinum(II)
Bamet-UD2: cis-Diammine-bisursodeoxy-cholate-platinum(II)
C/T: Cancer/testis antigen
DHT: Dihydrotestosterone
HNF: Hepatocyte nuclear factor
FXR: Farnesoid-X-receptor
LH: Gonadotropic luteinizing hormone
LHR: Hypothalamic luteinizing hormone-releasing factor
OATP: Organic-anion transporting polypeptide
SLCO: Solute carrier for organic anions, OATP protein
PG: Prostaglandin
PXR: Pregnane-X-receptor
SN-38: Active metabolite of irinotecan
T: Testosterone
A: Androgen receptor (AR).

Acknowledgment

This work is supported by the "Medical-Scientific Fund of the Mayor of the City of Vienna" (P10004 to VBA).

References

[1] M. A. Hediger, M. F. Romero, J. B. Peng, A. Rolfs, H. Takanaga, and E. A. Bruford, "The ABCs of solute carriers: physiological, pathological and therapeutic implications of human membrane transport proteins," *Pflugers Archiv European Journal of Physiology*, vol. 447, no. 5, pp. 465–468, 2004.

[2] B. Hagenbuch and C. Gui, "Xenobiotic transporters of the human organic anion transporting polypeptides (OATP) family," *Xenobiotica*, vol. 38, no. 7-8, pp. 778–801, 2008.

[3] M. Svoboda, J. Riha, K. Wlcek, W. Jaeger, and T. Thalhammer, "Organic anion transporting polypeptides (OATPs): regulation of expression and function," *Current Drug Metabolism*, vol. 12, no. 2, pp. 139–153, 2011.

[4] I. Sainis, D. Fokas, K. Vareli, A. G. Tzakos, V. Kounnis, and E. Briasoulis, "Cyanobacterial cyclopeptides as lead compounds to novel targeted cancer drugs," *Marine Drugs*, vol. 8, no. 3, pp. 629–657, 2010.

[5] H. Pressler, T. M. Sissung, D. Venzon, D. K. Price, and W. D. Figg, "Expression of OATP family members in hormone-related cancers: potential markers of progression," *PLoS One*, vol. 6, no. 5, Article ID e20372, 2011.

[6] A. Obaidat, M. Roth, and B. Hagenbuch, "The expression and function of organic anion transporting polypeptides in normal tissues and in cancer," *Annual Review of Pharmacology and Toxicology*, vol. 52, pp. 135–151, 2012.

[7] W. Lee, A. Belkhiri, A. C. Lockhart et al., "Overexpression of OATP1B3 confers apoptotic resistance in colon cancer," *Cancer Research*, vol. 68, no. 24, pp. 10315–10323, 2008.

[8] T. M. Sissung, H. Pressler, D. K. Price, and W. D. Figg, "SLCO transport genes in prostate cancer-letter," *Cancer Epidemiology, Biomarkers and Prevention*, vol. 20, no. 10, pp. 2326–2327, 2011.

[9] J. L. Wright, E. M. Kwon, E. A. Ostrander et al., "Expression of SLCO transport genes in castration-resistant prostate cancer and impact of genetic variation in SLCO1B3 and SLCO2B1 on prostate cancer outcomes," *Cancer Epidemiology Biomarkers and Prevention*, vol. 20, no. 4, pp. 619–627, 2011.

[10] Y. Shitara, "Clinical importance of OATP1B1 and OATP1B3 in drugdrug interactions," *Drug Metabolism and Pharmacokinetics*, vol. 26, no. 3, pp. 220–227, 2011.

[11] W. M. van der Deure, P. S. Hansen, R. P. Peeters et al., "Thyroid hormone transport and metabolism by organic anion transporter 1C1 and consequences of genetic variation," *Endocrinology*, vol. 149, no. 10, pp. 5307–5314, 2008.

[12] F. Pizzagalli, B. Hagenbuch, B. Stieger, U. Klenk, G. Folkers, and P. J. Meier, "Identification of a novel human organic anion transporting polypeptide as a high affinity thyroxine

transporter," *Molecular Endocrinology*, vol. 16, no. 10, pp. 2283–2296, 2002.

[13] T. Nomura, R. Lu, M. L. Pucci, and V. L. Schuster, "The two-step model of prostaglandin signal termination: in vitro reconstitution with the prostaglandin transporter and prostaglandin 15 dehydrogenase," *Molecular Pharmacology*, vol. 65, no. 4, pp. 973–978, 2004.

[14] H. Adachi, T. Suzuki, M. Abe et al., "Molecular characterization of human and rat organic anion transporter OATP-D," *American Journal of Physiology—Renal Physiology*, vol. 285, no. 6, pp. F1188–F1197, 2003.

[15] U. Olszewski-Hamilton, M. Svoboda, T. Thalhammer, V. Buxhofer-Ausch, K. Geissler, and G. Hamilton, "Organic anion transporting polypeptide 5A1 (OATP5A1) in small cell lung cancer (SCLC) cells: possible involvement in chemoresistance to satraplatin," *Biomarkers in Cancer*, vol. 3, pp. 31–40, 2011.

[16] A. C. Lockhart, E. Harris, B. J. Lafleur et al., "Organic anion transporting polypeptide 1B3 (OATP1B3) is overexpressed in colorectal tumors and is a predictor of clinical outcome," *Clinical and Experimental Gastroenterology*, vol. 1, no. 1, pp. 1–7, 2008.

[17] V. Kounnis, E. Ioachim, M. Svoboda et al., "Expression of organic anion-transporting polypeptides 1B3, 1B1, and1A2 in human pancreatic cancer reveals a new class of potential therapeuticTargets," *Journal of OncoTargets and Therapy*, vol. 4, pp. 27–32, 2011.

[18] T. Maeda, M. Irokawa, H. Arakawa et al., "Uptake transporter organic anion transporting polypeptide 1B3 contributes to the growth of estrogen-dependent breast cancer," *Journal of Steroid Biochemistry and Molecular Biology*, vol. 122, no. 4, pp. 180–185, 2010.

[19] A. Hamada, T. Sissung, D. K. Price et al., "Effect of SLCO1B3 haplotype on testosterone transport and clinical outcome in caucasian patientswith androgen-independent prostatic cancer," *Clinical Cancer Research*, vol. 14, no. 11, pp. 3312–3318, 2008.

[20] N. R. Monks, S. Liu, Y. Xu, H. Yu, A. S. Bendelow, and J. A. Moscow, "Potent cytotoxicity of the phosphatase inhibitor microcystin LR and microcystin analogues in OATP1B1- and OATP1B3-expressing HeLa cells," *Molecular Cancer Therapeutics*, vol. 6, no. 2, pp. 587–598, 2007.

[21] S. M. Oba-Shinjo, O. L. Caballero, A. A. Jungbluth et al., "Cancer-testis (CT) antigen expression in medulloblastoma," *Cancer Immunity*, vol. 8, article 7, 2008.

[22] S. Y. Lee, B. Williamson, O. L. Caballero et al., "Identification of the gonad-specific anion transporter SLCO6A1 as a cancer/testis (CT) antigen expressed in human lung cancer," *Cancer Immunity*, vol. 4, p. 13, 2004.

[23] M. J. Cutler and E. F. Choo, "Overview of SLC22A and SLCO families of drug uptake transporters in the context of cancer treatments," *Current Drug Metabolim*, vol. 12, no. 8, pp. 793–807, 2011.

[24] T. Mikkaichi, T. Suzuki, T. Onogawa et al., "Isolation and characterization of a digoxin transporter and its rat homologue expressed in the kidney," *Proceedings of the National Academy of Sciences of the United States of America*, vol. 101, no. 10, pp. 3569–3574, 2004.

[25] J. R. Pasqualini, G. Chetrite, C. Blacker et al., "Concentrations of estrone, estradiol, and estrone sulfate and evaluation of sulfatase and aromatase activities in pre- and postmenopausal breast cancer patients," *Journal of Clinical Endocrinology and Metabolism*, vol. 81, no. 4, pp. 1460–1464, 1996.

[26] N. Banerjee, C. Allen, and R. Bendayan, "Differential role of organicanion-transporting polypeptides in estrone-3-sulphate uptake by breast epithelialcells and breast cancer cells," *Journal of Pharmacology and Experimental Therapeutics*, vol. 342, no. 2, pp. 510–519, 2012.

[27] H. Arakawa, T. Nakanishi, C. Yanagihara et al., "Enhanced expression of organic anion transportingpolypeptides (OATPs) in androgen receptor-positive prostate cancer cells:Possible role of OATP1A2 in adaptive cell growth under androgen-depletedconditions," *Biochemical Pharmacology*, vol. 84, no. 8, pp. 1070–1077, 2012.

[28] M. Muto, T. Onogawa, T. Suzuki et al., "Human liver-specific organic anion transporter-2 is a potent prognostic factor for human breast carcinoma," *Cancer Science*, vol. 98, no. 10, pp. 1570–1576, 2007.

[29] W. Al Sarakbi, R. Mokbel, M. Salhab, W. G. Jiang, M. J. Reed, and K. Mokbel, "The role of STS and OATP-B mRNA expression in predicting the clinical outcome in human breast cancer," *Anticancer Research*, vol. 26, no. 6, pp. 4985–4990, 2006.

[30] K. Wlcek, M. Svoboda, T. Thalhammer, F. Sellner, G. Krupitza, and W. Jaeger, "Altered expression of organic anion transporter polypeptide (OATP) genes in human breast carcinoma," *Cancer Biology & Therapy*, vol. 7, no. 9, pp. 1450–1455, 2008.

[31] M. Svoboda, K. Wlcek, B. Taferner et al., "Expression of organic anion-transporting polypeptides 1B1 and 1B3 in ovarian cancer cells: relevance for paclitaxel transport," *Biomedicine and Pharmacotherapy*, vol. 65, no. 6, pp. 417–426, 2011.

[32] M. Yang, W. Xie, E. Mostaghel et al., "SLCO2B1 and SLCO1B3 may determine time to progression for patients receiving androgen deprivation therapy for prostate cancer," *Journal of Clinical Oncology*, vol. 29, no. 18, pp. 2565–2573, 2011.

[33] J. D. Berlin, P. Catalano, J. P. Thomas, J. W. Kugler, D. G. Haller, and A. B. Benson, "Phase III study of gemcitabine in combination with fluorouracil versus gemcitabine alone in patients with advanced pancreatic carcinoma: eastern Cooperative Oncology Group trial E2297," *Journal of Clinical Oncology*, vol. 20, no. 15, pp. 3270–3275, 2002.

[34] H. Burris, M. Moore, J. Andersen et al., "Improvements in survival and clinical benefit with gemcitabine as first-line therapy for patients with advanced pancreas cancer: a randomized trial," *Journal of Clinical Oncology*, vol. 15, no. 6, pp. 2403–2413, 1997.

[35] E. Briasoulis, N. Pavlidis, C. Terret et al., "Glufosfamide administered using a 1-hour infusion given as first-line treatment for advanced pancreatic cancer. A phase II trial of the EORTC-new drug development group," *European Journal of Cancer*, vol. 39, no. 16, pp. 2334–2340, 2003.

[36] F. Vasuri, R. Golfieri, M. Fiorentino et al., "OATP 1B1/1B3 expression in hepatocellular carcinomas treated with orthotopic liver transplantation," *Virchows Archiv*, vol. 459, no. 2, pp. 141–146, 2011.

[37] K. Wlcek, M. Svoboda, J. Riha et al., "The analysis of organic anion transporting polypeptide (OATP) mRNA and protein patterns in primary and metastatic liver cancer," *Cancer Biology and Therapy*, vol. 11, no. 9, pp. 801–811, 2011.

[38] K. A. Wojtal, J. J. Eloranta, P. Hruz et al., "Changes in mRNA expression levels of solute carrier transporters in inflammatory bowel disease patients," *Drug Metabolism and Disposition*, vol. 37, no. 9, pp. 1871–1877, 2009.

[39] I. Tamai, "Oral drug delivery utilizing intestinal OATP transporters," *Advanced Drug Delivery Reviews*, vol. 64, no. 6, pp. 508–514, 2012.

[40] H. Glaeser, D. G. Bailey, G. K. Dresser et al., "Intestinal drug transporter expression and the impact of grapefruit juice in humans," *Clinical Pharmacology & Therapeutics*, vol. 81, no. 3, pp. 362–370, 2007.

[41] J. J. Eloranta, C. Hiller, M. Jüttner, and G. A. Kullak-Ublick, "The SLCO1A2 gene, encoding human organic anion-transporting polypeptide 1A2, is transactivated by the vitamin D receptor," , *Molecular Pharmacology*, vol. 82, no. 1, pp. 37–46, 2012.

[42] Y. Yamakawa, A. Hamada, T. Shuto et al., "Pharmacokinetic impact of SLCO1A2 polymorphisms on imatinib disposition in patients with chronic myeloid Leukemia," *Clinical Pharmacology and Therapeutics*, vol. 90, no. 1, pp. 157–163, 2011.

[43] K. Eechoute, R. M. Franke, W. J. Loos et al., "Environmental and genetic factors affecting transport of imatinib by OATP1A2," *Clinical Pharmacology and Therapeutics*, vol. 89, no. 6, pp. 816–820, 2011.

[44] I. Badagnani, R. A. Castro, T. R. Taylor et al., "Interaction of methotrexate with organic-anion transporting polypeptide 1A2 and its genetic variants," *Journal of Pharmacology and Experimental Therapeutics*, vol. 318, no. 2, pp. 521–529, 2006.

[45] C. Justenhoven, E. Schaeffeler, S. Winter et al., "Polymorphisms of the nuclear receptor pregnane X receptor and organic anion transporter polypeptides 1A2, 1B1, 1B3, and 2B1 are not associated with breast cancer risk," *Breast Cancer Research and Treatment*, vol. 125, no. 2, pp. 563–569, 2011.

[46] K. Köck, A. Koenen, B. Giese et al., "Rapid modulation of the organic anion transporting polypeptide 2B1 (OATP2B1, SLCO2B1) function by protein kinase C-mediated internalization," *Journal of Biological Chemistry*, vol. 285, no. 15, pp. 11336–11347, 2010.

[47] F. Zhou, A. C. Lee, K. Krafczyk, L. Zhu, and M. Murray, "Protein kinase C regulates the internalization and function of the human organic anion transporting polypeptide 1A2," *British Journal of Pharmacology*, vol. 162, no. 6, pp. 1380–1388, 2011.

[48] N. Sharifi, A. Hamada, T. Sissung et al., "A polymorphism in a transporter of testosterone is a determinant of androgen independence in prostate cancer," *British Journal of Urology International*, vol. 102, no. 5, pp. 617–621, 2008.

[49] R. L. Oostendorp, E. van de Steeg, C. M. M. van der Kruijssen et al., "Organic anion-transporting polypeptide 1B1 mediates transport of gimatecan and BNP1350 and can be inhibited by several classic ATP-binding cassette (ABC) B1 and/or ABCG2 inhibitors," *Drug Metabolism and Disposition*, vol. 37, no. 4, pp. 917–923, 2009.

[50] W. Ni, J. Ji, Z. Dai et al., "Flavopiridol pharmacogenetics: clinical and functional evidence for the role of SLCO1B1/OATP1B1 in flavopiridol disposition," *PLoS One*, vol. 5, no. 11, Article ID e13792, 2010.

[51] O. Briz, M. A. Serrano, N. Rebollo et al., "Carriers involved in targeting the cytostatic bile acid-cisplatin derivatives cis-diammine-chloro-cholylglycinate-platinum(II) and cis-diammine-bisursodeoxycholate-platinum(II) toward liver cells," *Molecular Pharmacology*, vol. 61, no. 4, pp. 853–860, 2002.

[52] B. Feng, J. J. Xu, Y. A. Bi et al., "Role of hepatic transporters in the disposition and hepatotoxicity of a HER2 tyrosine kinase inhibitor CP-724,714," *Toxicological Sciences*, vol. 108, no. 2, pp. 492–500, 2009.

[53] S. Hu, R. M. Franke, K. K. Filipski et al., "Interaction of imatinib with human organic ion carriers," *Clinical Cancer Research*, vol. 14, no. 10, pp. 3141–3148, 2008.

[54] T. Takada, H. M. Weiss, O. Kretz, G. Gross, and Y. Sugiyama, "Hepatic transport of PKI166, an epidermal growth factor receptor kinase inhibitor of the pyrrolo-pyrimidine class, and its main metabolite, ACU154," *Drug Metabolism and Disposition*, vol. 32, no. 11, pp. 1272–1278, 2004.

[55] J. D. Clarke and N. J. Cherrington, "Genetics or environment in drug transport: the case of organic anion transporting polypeptides and adverse drug reactions," *Drug Metabolism and Pharmacokinetics*, vol. 8, no. 3, pp. 349–360, 2012.

[56] T. Nakanishi and I. Tamai, "Genetic polymorphisms of OATP transporters and their impact on intestinal absorption and hepatic disposition of drugs," *Drug Metabolism and Pharmacokinetics*, vol. 27, no. 1, pp. 106–121, 2012.

[57] A. J. de Graan, C. S. Lancaster, A. Obaidat et al., "Influence of polymorphic OATP1B-Type carriers on the disposition of docetaxel," *Clinical Cancer Research*, vol. 18, no. 16, pp. 4433–4440, 2012.

[58] T. Nozawa, H. Minami, S. Sugiura, A. Tsuji, and I. Tamai, "Role of organic anion transporter OATP1B1 (OATP-C) in hepatic uptake of irinotecan and its active metabolite, 7-ethyl-10-hydroxycamptothecin: in vitro evidence and effect of single nucleotide polymorphisms," *Drug Metabolism and Disposition*, vol. 33, no. 3, pp. 434–439, 2005.

[59] K. Sai, Y. Saito, K. Maekawa et al., "Additive effects of drug transporter genetic polymorphisms on irinotecan pharmacokinetics/pharmacodynamics in Japanese cancer patients," *Cancer Chemotherapy and Pharmacology*, vol. 66, no. 1, pp. 95–105, 2010.

[60] A. Nassif, J. Jia, M. Keiser et al., "Visualization of hepatic uptake transporter function in healthy subjects by using gadoxetic acid-enhanced MR imaging," *Radiology*, vol. 264, no. 3, pp. 741–750, 2012.

[61] T. Abe, M. Unno, T. Onogawa et al., "LST-2, a human liver-specific organic anion transporter, determines methotrexate sensitivity in gastrointestinal cancers," *Gastroenterology*, vol. 120, no. 7, pp. 1689–1699, 2001.

[62] M. Nagai, T. Furihata, S. Matsumoto et al., "Identification of a new organic anion transporting polypeptide 1B3 mRNA isoform primarily expressed in human cancerous tissues and cells," , *Biochemical and Biophysical Research Communications*, vol. 418, no. 4, pp. 818–823, 2012.

[63] H. Ohtsuka, T. Abe, T. Onogawa et al., "Farnesoid X receptor, hepatocyte nuclear factors 1α and 3β are essential for transcriptional activation of the liver-specific organic anion transporter-2 gene," *Journal of Gastroenterology*, vol. 41, no. 4, pp. 369–377, 2006.

[64] R. Liedauer, M. Svoboda, K. Wlcek et al., "Different expression patterns of organic anion transporting polypeptides in osteosarcomas, bone metastases and aneurysmal bone cysts," *Oncology Reports*, vol. 22, no. 6, pp. 1485–1492, 2009.

[65] K. Kleberg, G. M. Jensen, D. P. Christensen et al., "Transporter function and cyclic AMP turnover in normal colonic mucosa from patients with and without colorectal neoplasia," *BMC Gastroenterology*, vol. 12, no. 1, p. 78, 2012.

[66] V. L. Schuster, "Prostaglandin transport," *Prostaglandins and Other Lipid Mediators*, vol. 68-69, pp. 633–647, 2002.

[67] K. Choi, H. Zhuang, B. Crain, and S. Doré, "Expression and localization of prostaglandin transporter in Alzheimer disease brains and age-matched controls," *Journal of Neuroimmunology*, vol. 195, no. 1-2, pp. 81–87, 2008.

[68] K. Mandery, K. Bujok, I. Schmidt et al., "Influence of cyclooxygenase inhibitors on the function of the prostaglandin transporter organic anion-transporting polypeptide 2A1 expressed in human gastroduodenal mucosa," *Journal of Pharmacology and Experimental Therapeutics*, vol. 332, no. 2, pp. 345–351, 2010.

[69] J. Kang, P. Chapdelaine, P. Y. Laberge, and M. A. Fortier, "Functional characterization of prostaglandin transporter and terminal prostaglandin synthases during decidualization of human endometrial stromal cells," *Human Reproduction*, vol. 21, no. 3, pp. 592–599, 2006.

[70] V. R. Holla, M. G. Backlund, P. Yang, R. A. Newman, and R. N. DuBois, "Regulation of prostaglandin transporters in colorectal neoplasia," *Cancer Prevention Research*, vol. 1, no. 2, pp. 93–99, 2008.

[71] A. Koenen, K. Köck, M. Keiser, W. Siegmund, H. K. Kroemer, and M. Grube, "Steroid hormones specifically modify the activity of organic anion transporting polypeptides," *European Journal of Pharmaceutical Sciences*, vol. 47, no. 4, pp. 774–780, 2012.

[72] H. Bronger, J. König, K. Kopplow et al., "ABCC drug efflux pumps and organic anion uptake transporters in human gliomas and the blood-tumor barrier," *Cancer Research*, vol. 65, no. 24, pp. 11419–11428, 2005.

[73] J. Kindla, T. T. Rau, R. Jung et al., "Expression and localization of the uptake transporters OATP2B1, OATP3A1 and OATP5A1 in non-malignant and malignant breast tissue," *Cancer Biology and Therapy*, vol. 11, no. 6, pp. 584–591, 2011.

[74] T. Toyohara, T. Suzuki, R. Morimoto et al., "SLCO4C1 transporter eliminates uremic toxins and attenuates hypertension and renal inflammation," *Journal of the American Society of Nephrology*, vol. 20, no. 12, pp. 2546–2555, 2009.

[75] T. Suzuki, T. Toyohara, Y. Akiyama et al., "Transcriptional regulation of organic anion transporting polypeptide SLCO4C1 as a new therapeutic modality to prevent chronic kidney disease," *Journal of Pharmaceutical Sciences*, vol. 100, no. 9, pp. 3696–3707, 2011.

[76] B. Isidor, O. Pichon, R. Redon et al., "Mesomelia-synostoses syndrome results from deletion of sulf1 and slco5a1 genes at 8q13," *American Journal of Human Genetics*, vol. 87, no. 1, pp. 95–100, 2010.

[77] D. Atanackovic, I. Blum, Y. Cao et al., "Expression of cancer-testis antigens as possible targets for antigen-specific immunotherapy in head and neck squamous cell carcinoma," *Cancer Biology and Therapy*, vol. 5, no. 9, pp. 1218–1225, 2006.

[78] Y. Miki, T. Suzuki, C. Tazawa, B. Blumberg, and H. Sasano, "Steroid and xenobiotic receptor (SXR), cytochrome P450 3A4 and multidrug resistance gene 1 in human adult and fetal tissues," *Molecular and Cellular Endocrinology*, vol. 231, no. 1-2, pp. 75–85, 2005.

[79] H. E. Meyer Zu Schwabedissen, R. G. Tirona, C. S. Yip, R. H. Ho, and R. B. Kim, "Interplay between the nuclear receptor pregnane X receptor and the uptake transporter organic anion transporter polypeptide 1A2 selectively enhances estrogen effects in breast cancer," *Cancer Research*, vol. 68, no. 22, pp. 9338–9347, 2008.

[80] K. Ogasawara, T. Terada, T. Katsura et al., "Hepatitis c virus-related cirrhosis is a major determinant of the expression levels of hepatic drug transporters," *Drug Metabolism and Pharmacokinetics*, vol. 25, no. 2, pp. 190–199, 2010.

[81] M. le Vee, E. Jouan, A. Moreau, and O. Fardel, "Regulation of drug transporter mRNA expression by interferon-γ in primary human hepatocytes," *Fundamental and Clinical Pharmacology*, vol. 25, no. 1, pp. 99–103, 2011.

[82] S. Imai, R. Kikuchi, H. Kusuhara, and Y. Sugiyama, "DNA methylation and histone modification profiles of mouse organic anion transporting polypeptides," *Drug Metabolism Disposition*, vol. 41, no. 1, pp. 72–78, 2013.

Hindawi Publishing Corporation
Journal of Drug Delivery
Volume 2013, Article ID 172529, 13 pages
http://dx.doi.org/10.1155/2013/172529

Research Article

A Mathematical Model for Thermosensitive Liposomal Delivery of Doxorubicin to Solid Tumour

Wenbo Zhan and Xiao Yun Xu

Department of Chemical Engineering, Imperial College London, South Kensington Campus, London SW7 2AZ, UK

Correspondence should be addressed to Xiao Yun Xu; yun.xu@imperial.ac.uk

Received 9 October 2012; Accepted 13 December 2012

Academic Editor: Andreas G. Tzakos

The effectiveness of anticancer treatments is often hampered by the serious side effects owing to toxicity of anticancer drugs and their undesirable uptake by healthy cells *in vivo*. Thermosensitive liposome-mediated drug delivery has been developed as part of research efforts aimed at improving therapeutic efficacy while reducing the associated side effect. Since multiple steps are involved in the transport of drug-loaded liposomes, drug release, and its uptake, mathematical models become an indispensible tool to analyse the transport processes and predict the outcome of anticancer treatment. In this study, a computational model is developed which incorporates the key physical and biochemical processes involved in drug delivery and cellular uptake. The model has been applied to idealized tumour geometry, and comparisons are made between continuous infusion of doxorubicin and thermosensitive liposome-mediated delivery. Results show that thermosensitive liposome-mediated delivery performs better in reducing drug concentration in normal tissues, which may help lower the risk of associated side effects. Compared with direct infusion over a 2-hour period, thermosensitive liposome delivery leads to a much higher peak intracellular concentration of doxorubicin, which may increase cell killing in tumour thereby enhancing the therapeutic effect of the drug.

1. Introduction

As a common anticancer drug, doxorubicin is widely used in chemotherapy to treat various types of cancer, such as lymphoma, genitourinary, thyroid, and stomach cancer [1]. By interacting with DNA in cells, doxorubicin can inhibit the process of DNA replication. Because of this mechanism of action, high concentration of doxorubicin in normal tissues can cause serious damage to healthy cells, known as side effects. In clinical therapy, the most serious toxicity is life-threatening cardiomyopathy [2, 3], leading to heart failure. Side effects set a limit to the lifetime dose a patient can receive, which is approximately 550 mg per unit body surface area [1].

In order to improve the therapeutic benefit while reducing toxicity of doxorubicin in normal tissues, various treatment modalities have been developed. Recently, liposome-mediated doxorubicin delivery has been proposed as an alternative to direct intravenous administration. Some animal experiments have shown that liposomal doxorubicin delivery offers better effectiveness of anticancer treatments than bolus injection, but no obvious advantage over continuous infusion was reported [4]. The development of thermosensitive liposomes to enhance the effectiveness of anticancer treatment has been reported in many studies (e.g., [5–8]).

Following administration, the drug-loaded thermosensitive liposome-based nanoparticles are usually small enough to pass through the vasculature wall and then accumulate in the extracellular space in tumour. Localised heating can be performed several hours after drug administration. Upon heating to the phase transition temperature of the thermosensitive liposome, the encapsulated drug can be released from liposomes at a high rate. Some of the released drug may bind with proteins in blood and be cleared up by blood flow, whereas the rest will permeate through the vasculature wall entering the interstitial space. Drug in the interstitium may also bind with proteins present in the interstitial fluid, and be cleared up by the lymphatic system. Because of the

concentration gradient at the interface between tumour and normal tissues, drug exchange takes place between these tissues. The extracellular drug may pass through the cell membrane and be taken up by cells. Drug in tumour cells can also be transported back to the extracellular space. Given the many variables related to the properties of tumour, normal tissues, and anticancer drugs, mathematical models are needed to analyse the drug transport processes described above.

Previous numerical studies of liposome-mediated drug delivery have mainly focused on drug uptake by tumour cells with a simplified description of the transport processes involved. Harashima et al. [9, 10] and Tsuchihashi et al. [11] developed mathematical models for nonthermosensitive liposomal drug delivery, without considering the interaction between drug and proteins in blood plasma or interstitial fluid. El-Kareh and Secomb [12] used mathematical models to determine tumour cell uptake of thermosensitive liposome-mediated doxorubicin, but their model was formulated on a simplified tumour cord geometry, without accounting for the influence of blood and lymphatic vessels and the interstitial fluid flow, nor drug binding with proteins. However, each of these components may affect the outcome of anticancer therapy. Experimental results show that doxorubicin can easily bind with proteins [13].

In the present study, an improved mathematical model is developed and applied to an idealized geometry consisting of tumour and normal tissues. The model incorporates the key physical and biochemical processes involved, including time-dependent plasma clearance, liposome, and drug transport through the blood and lymphatic vessels, extracellular liposome, and drug transport (convection and diffusion), drug binding with proteins, lymphatic drainage, interactions with the surrounding normal tissues, and drug uptake by tumour cells. Therapeutic effect is evaluated based on the fraction of survival tumour cells by directly solving the pharmacodynamics equation using the predicted intracellular drug concentration. Comparisons are made of the predicted efficacies of direct intravenous administration and thermosensitive liposome-mediated delivery.

2. Mathematical Models

In solid tumours, the size and branching patterns of microvessels could vary considerably depending on the specific tumour type and its growth stage [14]. For a solid tumour at a specific stage, the distribution of blood vessels, lymphatic vessels, and tumour cells are spatially heterogeneous. However, owing to the lack of *in vivo* data on the heterogeneity of tumour vasculature, solid tumours are usually treated as a spatially homogeneous domain [15–18]. If the simulation window is much shorter than the growth rate of the tumour, it would be reasonable to assume that the key modelling parameters do not change with time in the simulation. The mathematical equations governing the physical and physiological processes of the liposome and drug transport as well as the pharmacokinetics of the drug are described below.

2.1. Interstitial Fluid Transport

2.1.1. Mass Conservation Equation. This is described by

$$\frac{\partial \rho}{\partial t} + \nabla \cdot (\rho \mathbf{v}) = \left(F_v - F_{\mathrm{ly}}\right) \rho, \tag{1}$$

where ρ and $\mathbf{v}$ are the density and velocity of the interstitial fluid, respectively. F_v is the interstitial fluid loss from the blood vessels per unit volume of tumour tissue, and F_{ly} is the fluid absorption rate by the lymphatics per unit volume of tumour tissue. F_v and F_{ly} are given by Starling's law

$$F_v = K_v \frac{S}{V} \left[p_v - p_i - \sigma_T \left(\pi_v - \pi_i\right)\right], \tag{2}$$

where K_v is the hydraulic conductivity of the microvascular wall, S/V is the surface area of blood vessels per unit volume of tumour tissue, p_v and p_i are the vascular and interstitial fluid pressures, respectively, σ_T represents the average osmotic reflection coefficient for plasma protein, π_v is the osmotic pressure of the plasma, and π_i is that of interstitial fluid.

The lymphatic drainage, F_{ly}, is related to the pressure difference between the interstitial fluid and lymphatics:

$$F_{\mathrm{ly}} = K_{\mathrm{ly}} \frac{S_{\mathrm{ly}}}{V} \left(p_i - p_{\mathrm{ly}}\right), \tag{3}$$

where K_{ly} is the hydraulic conductivity of the lymphatic wall, S_{ly}/V is the surface area of lymphatic vessels per unit volume of tumour tissue, and p_{ly} is the intralymphatic pressure.

2.1.2. Momentum Conservation Equation. Since the intercapillary distance (33–98 μm [19, 20]) is usually 2-3 orders of magnitude smaller than the length scale for drug transport (approximately 70 mm in this study), it is reasonable to treat the tumour and its surrounding tissues as porous media, for which the Navier-Stokes equations are applicable. By ignoring the gravitational effect, the momentum equation is expressed as

$$\frac{\partial (\rho \mathbf{v})}{\partial t} + \nabla \cdot (\rho \mathbf{v}\mathbf{v}) = -\nabla p_i + \nabla \cdot \boldsymbol{\tau} + \mathbf{F}, \tag{4}$$

where $\boldsymbol{\tau}$ is the stress tensor which is given by

$$\boldsymbol{\tau} = \mu \left[\nabla \mathbf{v} + (\nabla \mathbf{v})^T\right] - \frac{2}{3} \mu (\nabla \cdot \mathbf{v}) \mathbf{I}, \tag{5}$$

where $\mathbf{I}$ is the unit tensor. The last term in (4), $\mathbf{F}$, represents the Darcian resistance to fluid flow through porous media and is given by

$$\mathbf{F} = W \mu \mathbf{v} + \frac{1}{2} \mathbf{C} \rho |\mathbf{v}| \mathbf{v}, \tag{6}$$

and W is a diagonal matrix with all diagonal elements calculated as

$$\mathbf{W} = \kappa^{-1}, \tag{7}$$

where μ is the dynamic viscosity of interstitial fluid, $\mathbf{C}$ is the prescribed matrix of the inertial loss term, and κ is the permeability of the interstitial space. Since the velocity of interstitial fluid is very slow ($|\mathbf{v}| \ll 1$) [15], the inertial loss term can be neglected when compared to the Darcian resistance. In addition, the interstitial fluid is treated as incompressible with a constant viscosity. Hence, (6) can be reduced to

$$\mathbf{F} = W\mu\mathbf{v}. \tag{8}$$

2.2. Drug Transport. Drug transport is described by equations for the free and bound drug concentrations in the interstitial fluid and the intracellular concentration.

2.2.1. Free Doxorubicin Concentration in the Interstitial Fluid (C_{fe}). This is described by

$$\frac{\partial C_{fe}}{\partial t} + \nabla \cdot \left(C_{fe}\mathbf{v}\right) = D_{fe}\nabla^2 C_{fe} + S_i, \tag{9}$$

where D_{fe} is the diffusion coefficient of free doxorubicin. The source term, S_i, is the net rate of doxorubicin gained from the surrounding environment, which is given by

$$S_i = S_v + S_b + S_u, \tag{10}$$

S_v, S_b, and S_u represent the net doxorubicin gained from the blood/lymphatic vessels, association/dissociation with bound doxorubicin-protein, and influx/efflux from tumour cells, respectively,

$$S_v = F_{fp} - F_{fl}, \tag{11}$$

where F_{fp} is the doxorubicin gained from the blood capillaries in tumour and normal tissues, and F_{fl} is the doxorubicin loss to the lymphatic vessels per unit volume of tissue. Using the pore model [15–17, 21] for transcapillary exchange, F_{fp} and F_{fl} can be expressed as

$$\begin{aligned} F_{fp} &= F_v\left(1-\sigma_d\right)C_{fp} + P_{fe}\frac{S}{V}\left(C_{fp} - C_{fe}\right)\frac{\mathrm{Pe}_f}{e^{\mathrm{Pe}_f}-1}, \\ F_{fl} &= F_{\mathrm{ly}}C_{fe}, \end{aligned} \tag{12}$$

where C_{fp} is the concentration of doxorubicin in blood plasma, σ_d is the osmotic reflection coefficient for the drug molecules, and P_{fe} is the permeability of vasculature wall to free doxorubicin. Pe_f is the transcapillary Peclet number defined as

$$\mathrm{Pe}_f = \frac{F_v\left(1-\sigma_d\right)}{P_{fe}\left(S/V\right)}. \tag{13}$$

The net doxorubicin gained due to protein binding and cellular uptake is governed by (14), where D_c is the tumour cell density; k_a and k_d are the doxorubicin-protein binding and dissociation rates, respectively:

$$\begin{aligned} S_b &= k_d C_{be} - k_a C_{fe}, \\ S_u &= D_c\varepsilon - D_c\zeta. \end{aligned} \tag{14}$$

2.2.2. Bound-Doxorubicin Concentration in Interstitial Fluid (C_{be}). This is described by

$$\frac{\partial C_{be}}{\partial t} + \nabla \cdot \left(C_{be}\mathbf{v}\right) = D_{be}\nabla^2 C_{be} + F_{be} - S_b, \tag{15}$$

where D_{be} is the diffusion coefficient of the bound doxorubicin-protein. F_{be} represents the bound doxorubicin crossing the capillary wall into the interstitial fluid, which is given by

$$F_{be} = F_v\left(1-\sigma_d\right)C_{bp} + P_{be}\frac{S}{V}\left(C_{bp} - C_{be}\right)\frac{\mathrm{Pe}_b}{e^{\mathrm{Pe}_b}-1}, \tag{16}$$

where P_{be} is the permeability of vasculature wall to bound doxorubicin, and C_{bp} is the bound doxorubicin concentration in plasma. The transcapillary Peclet number is

$$\mathrm{Pe}_b = \frac{F_v\left(1-\sigma_d\right)}{P_{be}\left(S/V\right)}. \tag{17}$$

2.2.3. Intracellular Doxorubicin Concentration (C_i). Because mainly free doxorubicin can pass through the cell membrane and enter the intracellular space [12], the rate of cellular uptake is a function of free doxorubicin concentration in the interstitial fluid:

$$\begin{aligned} \frac{\partial C_i}{\partial t} &= \zeta - \varepsilon, \\ \zeta &= V_{\max}\frac{C_{fe}}{C_{fe} + k_e\varphi}, \\ \varepsilon &= V_{\max}\frac{C_i}{C_i + k_i}, \end{aligned} \tag{18}$$

where $V_{\max}$ is the rate of transmembrane transport, ζ and ε are cellular uptake and efflux functions, k_e and k_i are constants obtained from experimental data fitting, and φ is the volume fraction of extracellular space.

2.3. Thermosensitive Liposome-Mediated Drug Transport. Equations describing the transport of liposome-mediated drug include encapsulated drug concentration in the interstitial fluid, and released doxorubicin in plasma and interstitial fluid. Equations for drug transport include those for free drug concentration in plasma and interstitial fluid. Bound drug concentration in plasma and interstitial fluid as well as intracellular concentration are described using the same equations given in the preceding section.

2.3.1. Liposome Encapsulated Drug Concentration in the Interstitial Fluid (C_{le}). This is described by

$$\frac{\partial C_{le}}{\partial t} + \nabla \cdot \left(C_{le}\mathbf{v}\right) = D_l\nabla^2 C_{le} + S_l, \tag{19}$$

where D_l is the diffusion coefficient of liposome encapsulated drug. The source term S_l is the net rate of liposome encapsulated drug gained from the surrounding environment, which is given by

$$S_l = S_{lp} - S_r. \tag{20}$$

S_{lp} is the amount of liposome encapsulated drug from plasma. S_r represents released drug in the interstitial fluid:

$$S_{lp} = F_{lp} - F_{ll}, \tag{21}$$

where F_{lp} is the liposome encapsulated doxorubicin gained from the capillaries in tumour and normal tissues, and F_{ll} is the loss of liposome encapsulated doxorubicin through the lymphatic vessels per unit volume of tissue. Using the pore model for transcapillary exchange, F_{lp} and F_{ll} can be expressed as

$$\begin{aligned} F_{lp} &= F_v\left(1-\sigma_l\right)C_{lp} + P_l\frac{S}{V}\left(C_{lp}-C_{le}\right)\frac{\mathrm{Pe_l}}{e^{\mathrm{Pe_l}}-1}, \\ F_{ll} &= F_{\mathrm{ly}}C_{le}, \end{aligned} \tag{22}$$

where C_{lp} is the concentration of liposome in blood plasma, σ_l is the osmotic reflection coefficient for the liposome particles, and P_l is the permeability of vasculature wall to liposome. $\mathrm{Pe_l}$ is the transcapillary Peclet number defined as

$$\mathrm{Pe_l} = \frac{F_v\left(1-\sigma_l\right)}{P_l\left(S/V\right)}. \tag{23}$$

The amount of released liposome encapsulated drug in the interstitial fluid, S_r, is given by

$$S_r = k_{\mathrm{rel}}C_{le}, \tag{24}$$

where k_{rel} is the release rate of liposome.

2.3.2. Free Doxorubicin Concentration in Blood Plasma (C_{fp}). This is described by

$$\frac{\partial C_{fp}}{\partial t} = S_r - \frac{V_T}{V_B}F_{fp} - \frac{CL_{fp}C_{fp}}{V_D} - \left(k_aC_{fp} - k_dC_{bp}\right), \tag{25}$$

where F_{fp} represents the free doxorubicin crossing the capillary wall into the interstitial fluid. V_T is tumour volume, V_B is plasma volume, and V_D is the volume of distribution, which is a pharmacological theoretical volume that a drug would have to occupy to provide the same concentration as it is currently in blood plasma. CL_{fp} is the plasma clearance of drug. k_a and k_d are the association and disassociation rates with proteins.

2.3.3. Bound Doxorubicin Concentration in Blood Plasma (C_{bp}). This is described by

$$\frac{\partial C_{bp}}{\partial t} = \left(k_aC_{fp} - k_dC_{bp}\right) - \frac{V_T}{V_B}F_{be} - \frac{CL_{bp}C_{bp}}{V_D}, \tag{26}$$

where CL_{bp} is the plasma clearance of bound doxorubicin.

2.3.4. Free Doxorubicin Concentration in Interstitial Fluid (C_{fe}). This is described by

$$\frac{\partial C_{fe}}{\partial t} + \nabla\cdot\left(C_{fe}\mathbf{v}\right) = D_{fe}\nabla^2C_{fe} + S_f. \tag{27}$$

The source term S_f is the net rate of doxorubicin gained from the surrounding environment, which is given by

$$S_f = S_v + S_b + S_u + S_r. \tag{28}$$

Expressions for the terms on the right hand side have been given previously (see (11)–(14) and (24)).

2.4. Pharmacodynamics Model. During anticancer treatment, tumour cell density may change due to cell killing as a result of drug effect, tumour cell proliferation, and physiological degradation. This can be described by a pharmacodynamics model as given below:

$$\frac{dD_c}{dt} = -\frac{f_{\max}C_i}{EC_{50}+C_i}D_c + k_pD_c - k_gD_c^2. \tag{29}$$

The first term on the right hand side represents the effect of anticancer drug, where $f_{\max}$ is the cell-kill rate constant and EC_{50} is the drug concentration producing 50% of $f_{\max}$. k_p and k_g are cell proliferation rate constant and physiologic degradation rate, respectively. In this study, cell proliferation and physiologic degradation are assumed to reach equilibrium at the beginning of each treatment.

2.5. Model Geometry. A 2D idealized model with a realistic tumour size (Figure 1) is used in this study. The tumour is located at the centre, which is surrounded by a layer of normal tissue. The diameter of the tumour is 50 mm, and the thickness of the normal tissue is 10 mm. ANSYS ICEM CFD is used to create the geometry and generate the computational mesh. The final mesh consists of 3922 triangular elements. This is obtained based on mesh independence tests which show that the difference in predicted drug concentration between the adopted mesh and a 10-time finer mesh is less than 3%.

2.6. Model Parameters. Since the growth of tumour and normal tissues is ignored, all the geometric and transport parameters used in this study are assumed to be constant. These are summarized in Tables 1, 2, and 3 for parameters related to the tissue, liposome, and doxorubicin, respectively.

2.6.1. Vascular Permeability. Vascular permeability coefficient measures the capacity of a blood vessel (often capillary in tumour) wall to allow for the flow of substances, typically nutrients or pharmaceutical agents in and out of the vasculature. The permeability of polyethylene glycol coated liposomes of 100 nm through tumour capillaries was measured at 37°C by Yuan et al. [23] and Wu et al. [24] as 2.0×10^{-10} and $3.42\pm0.78\times10^{-9}$ m/s, respectively. In normal granulation tissues permeability of the same liposomes was $0.8-0.9\times10^{-9}$ m/s at the same temperature. Wu et al. [26] also measured the permeability of albumin (corresponding to albumin-bound doxorubicin) in tumour and granulation tissues at 37°C and obtained the values of $7.8\pm1.2\times10^{-9}$ m/s and $2.5\pm0.8\times10^{-9}$ m/s, respectively. The mean values of the above measurements are adopted in this study.

Table 1: Parameters for tumour and normal tissues (symbols are defined near the equations in which they first appear).

Parameter	Unit	Tumour Tissue	Normal Tissue	Reference
S/V	m^{-1}	20000	7000	[15–18]
K_v	m/Pa·s	2.10×10^{-11}	2.70×10^{-12}	[15–18]
K	m^2/Pa·s	3.10×10^{-14}	6.40×10^{-15}	[15–18]
ρ	kg/m^3	1000	1000	[18]
μ	kg/m·s	0.00078	0.00078	[18]
$1/\kappa$	m^{-2}	4.56×10^{16}	2.21×10^{17}	[15–18]
p_v	Pa	2080	2080	[15–18]
π_v	Pa	2666	2666	[15–18]
π_i	Pa	2000	1333	[15–18]
σ_T		0.82	0.91	[15–18]
$K_{ly}S_{ly}/V$	$(Pa\cdot s)^{-1}$	0	4.17×10^{-7}	[18]
p_{ly}	Pa	0	0	[18]
D_c	10^5 cell/m^3	1×10^{10}	1×10^{10}	[12, 22]
φ		0.4	—	[12, 22]

Table 2: Parameters for liposome (symbols are defined near the equations in which they first appear).

Parameter	Unit	In tumour	In normal Tissue	Reference
P_o	m/s	3.42×10^{-9}	8.50×10^{-10}	[23, 24]
h		71	—	—
D	m^2/s	9.0×10^{-12}	5.8×10^{-12}	[20, 23]
σ_l		0.95	1.0	—
A_1	kg/m^3	6.90×10^{-3}	6.90×10^{-3}	[25]
A_2	kg/m^3	8.37×10^{-5}	8.37×10^{-5}	[25]
k_1	s^{-1}	1.22×10^{-2}	1.22×10^{-2}	[25]
k_2	s^{-1}	4.17×10^{-6}	4.17×10^{-6}	[25]
t_h	hr	24	—	—
t_d	s	3600	—	—
$k_{rel\_37^\circ C}$	s^{-1}	0	—	—
$k_{rel\_42^\circ C}$	s^{-1}	0.0078	—	—

Gaber et al. [5] noticed a 76-fold increase in the liposome extracellular concentration on 45°C heating. The permeability to liposome at 42°C can be estimated by interpolation, which gives a 71-folder increase. Dalmark and Storm [40] measured the permeability of free doxorubicin at various temperatures, and their results showed that the permeability to doxorubicin at 42°C was 2.56-time higher at 37°C. Hence, temperature-dependent vascular permeability for both liposome and doxorubicin is adopted to allow for enhanced permeability at hyperthermia.

2.6.2. Reflection Coefficient. The reflection coefficient determines the efficiency of the oncotic pressure gradient in driving transport across the vascular wall. It is related to the sizes of drug and pores on the vasculature wall [41]. For the same drug, this parameter may vary in different types of tissues [42, 43]. Wolf et al. [32] measured the reflection coefficient for albumin and found this to be 0.82 ± 0.08. The sizes of albumin and liposome are 3.5 nm and 100 nm, respectively.

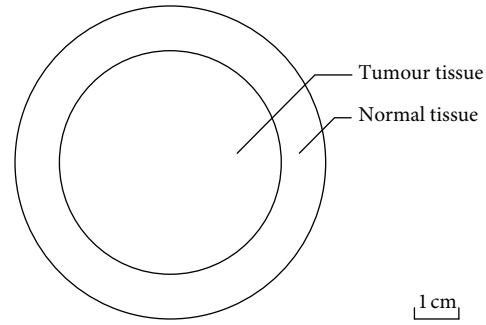

Figure 1: Model geometry.

The reflection coefficient for liposome is estimated to be greater than 0.90; hence it is assumed to be 0.95 in this study.

Because the size of liposome is much larger than the pore size on the vasculature wall in normal tissues (24–60 nm in diameter [44]), the reflection coefficient in normal tissue is assumed to be 1.0.

2.6.3. Liposome Release Rate (k_{rel}). Thermosensitive liposome is designed to release its contents rapidly on heating [6]. The release rate varies according to the composition of liposome, its preparation procedure, and heating temperature [45]. The relation between percentage release and exposure time is found to follow the first-order kinetics expressed as [46]

$$\%R(t) = R_c\left(1 - e^{-k_{rel}t}\right), \tag{30}$$

where $\%R(t)$ is the percentage of drug released at exposure time t; R_c is the total percentage of drug released at a given heating temperature. This equation is used to fit the experimental data obtained at 42°C [45]. From the best fitting curve (shown in Figure 2) obtained by using nonlinear least-squares method, the release rate is found to be 0.0078. At

Table 3: Parameters for doxorubicin (symbols are defined near the equations in which they first appear).

Parameter	Unit	Free doxorubicin	Bound doxorubicin	Reference
$P_{\text{Tumour\_}o}$	m/s	3.00×10^{-6}	7.80×10^{-9}	[18, 26]
h		2.56	—	—
P_{Normal}	m/s	3.75×10^{-7}	2.50×10^{-9}	[18, 26]
D_{Tumour}	m^2/s	3.40×10^{-10}	8.89×10^{-12}	[18, 22, 27–31]
D_{Normal}	m^2/s	1.58×10^{-10}	4.17×10^{-12}	[18, 22, 27–31]
MW	kg/mol	0.544	69.0	[12, 18]
σ_d		0.15	0.82	[18, 32]
k_a	s^{-1}	0.833	—	[22]
k_d	s^{-1}	—	0.278	[22]
$V_{\max}$	kg/10^5 cells s	4.67×10^{-15}	—	[22, 33]
k_e	kg/m^3	2.19×10^{-4}	—	[22, 33]
k_i	kg/m^3	1.37×10^{-12}	—	[22, 33]
$k_{\max}$	s^{-1}	1.67×10^{-5}	—	[34]
EC_{50}	kg/10^5 cells	5×10^{-13}	—	[34]
D	kg	8.56×10^{-5}	—	[1]
A	m^{-3}	74.6	74.6	[22, 35]
B	m^{-3}	2.49	2.49	[22, 35]
C	m^{-3}	0.552	0.552	[22, 35]
α	s^{-1}	2.43×10^{-3}	2.43×10^{-3}	[22, 35]
β	s^{-1}	2.83×10^{-4}	2.83×10^{-4}	[22, 35]
γ	s^{-1}	1.18×10^{-5}	1.18×10^{-5}	[22, 35]
k_p	s^{-1}	3.0×10^{-6}	—	[36]
k_g	s^{-1}	3.0×10^{-16}	—	[36]
$\text{CL}_{\text{tumour}}$	s^{-1}	1.48×10^{-5}	0	[35, 37–39]
$\text{CL}_{\text{tumour}}$	s^{-1}	2.43×10^{-3}	0	[35, 37–39]

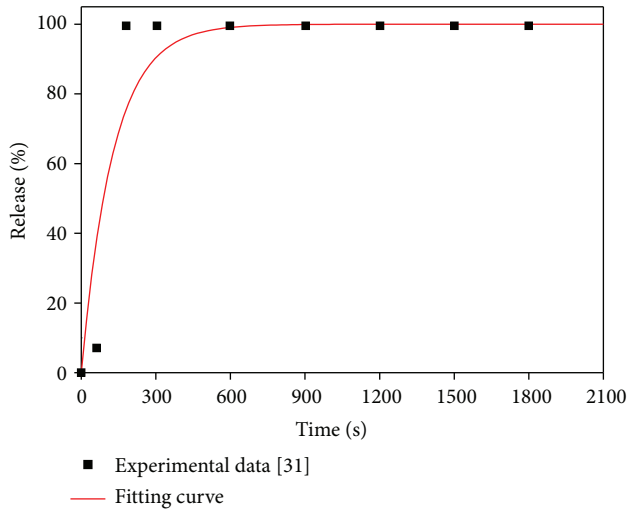

Figure 2: Liposome release rate at 42°C.

normal physiological temperature of 37°C, there should be no release; hence the release rate at 37°C is assumed to be zero.

2.6.4. Plasma Pharmacokinetics

(1) *Direct Continuous Infusion*. The doxorubicin concentration in blood plasma is modelled as an exponential decay function of time. The form of equation depends on the infusion mode. For continuous infusion, a triexponential decay function is assumed based on the plasma pharmacokinetics of doxorubicin:

$$C_v = \frac{D}{T}\left[\left(\frac{A}{\alpha}\left(1-e^{-\alpha t}\right)+\frac{B}{\beta}\left(1-e^{-\beta t}\right)+\frac{C}{\gamma}\left(1-e^{-\gamma t}\right)\right)\right] \quad (t < T),$$

$$C_v = \frac{D}{T}\left[\frac{A}{\alpha}\left(e^{\alpha T}-1\right)e^{-\alpha t}+\frac{B}{\beta}\left(e^{\beta T}-1\right)e^{-\beta t} + \frac{C}{\gamma}\left(e^{\gamma t}-1\right)e^{-\gamma t}\right] \quad (t \geq T), \tag{31}$$

where D is the dose of doxorubicin and T is the infusion duration. A, B, and C are compartment parameters and α, β, γ are compartment clearance rates.

Free doxorubicin in plasma can easily bind with proteins, such as albumin. Greene et al. [13] found that 74%–82% is present in the form of bound doxorubicin, and the percentage is independent of doxorubicin and albumin concentrations. Hence for direct infusion, the free (C_{fp}) and bound (C_{bp}) doxorubicin in plasma are given by

$$C_{fp} = (1-s)\,C_v; \qquad C_{bp} = sC_v, \tag{32}$$

where s is the percentage of bound doxorubicin, which is 0.75 in this study.

(2) *Thermosensitive Liposome-Mediated Drug Release.* The liposome encapsulated doxorubicin concentration in blood plasma is found to follow a 2-exponential decaying function of time [13], written as

$$C_{lp} = A_1 e^{-k_1 t} + A_2 e^{-k_2 t}, \quad (33)$$

where A_1 and A_2 are compartment parameters, and k_1 and k_2 are compartment clearance rates.

2.7. Boundary Conditions. Because the time scale for the simulation is assumed to be short enough to ignore the growth of tumour and normal tissues, the interface between the tumour and normal tissue as well as the outer surface of normal tissue are fixed. The interface between the tumour and normal tissues is treated as an internal boundary where all variables are continuous. The relative pressure at the outer surface of normal tissues is assumed to be constant at 0 Pa, where zero flux of drug is also specified.

2.8. Numerical Methods. The mathematical models described above are implemented into ANSYS FLUENT, which is a finite volume based computational fluid dynamics (CFD) code. Mass transfer equations describing the transport of drugs are coded by using the User Defined Scalar (known as UDS). These equations are solved in conjunction with the continuity and momentum equations using numerical algorithms available in FLUENT. Spatial discretisation is performed by employing the second order UPWIND scheme, while pressure-velocity coupling is achieved by the SIMPLEC algorithm. The absolute criteria for residual tolerances for solutions of the Navier-Stokes equations and the drug transport equations are 1×10^{-5} and 1×10^{-8}, respectively. The equations for the interstitial fluid flow are solved first to obtain a steady-state solution in the entire tumour and its surrounding normal tissues. The obtained pressure and velocity fields are then applied to the equations for drug transport. The second-order implicit backward Euler scheme is used for temporal discretisation, and a fixed time step size of 10 seconds is chosen, which is obtained after time-step sensitivity tests.

3. Results and Discussion

The microenvironment in tumour and normal tissues plays an important role in determining the efficiency of liposome and drug transport. The interstitial fluid pressure (IFP) determines the drug exchange between interstitial fluid and blood plasma, as well as tumour and normal tissues. The mean IFP predicted in the tumour region is 1533 Pa, which is almost identical to the value reported by Baxter and Jain [15]. The mean IFP in the normal tissue is 41 Pa.

The spatial distribution of IFP in tumour and normal tissues is shown in Figure 3. It is clear that pressures in the tumour and normal tissues are at different levels, and a thin layer of steep pressure gradient exists at the interface between the two regions.

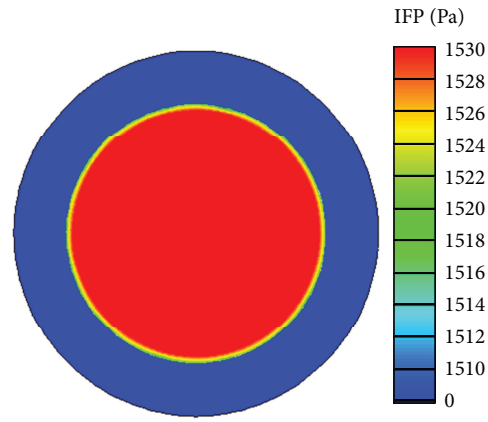

Figure 3: Interstitial fluid pressure distribution in tumour and normal tissues.

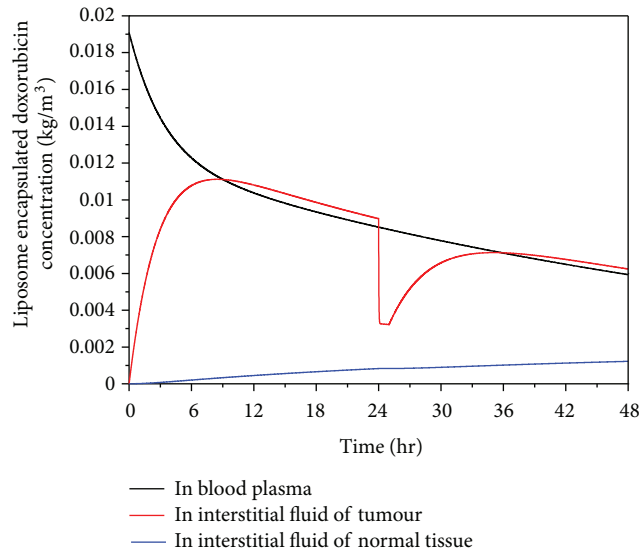

Figure 4: Liposome concentration in plasma and interstitial fluid as a function of time after start of treatment (dose = 50 mg/m^2).

Liposome encapsulated doxorubicin concentration is a key parameter that determines the doxorubicin concentration in tumour cells. Shown in Figure 4 are the predicted time courses of liposome encapsulated doxorubicin concentrations in blood plasma and interstitial space in tumour and normal tissues, for a total doxorubicin dose of 50 mg/m^2 encapsulated in thermosensitive liposomes.

Liposome encapsulated doxorubicin is administrated into blood in a very short duration, and its concentration in plasma decreases following an exponential decay function of time during the entire treatment period [13]. Its concentration in tumour increases rapidly in the initial stage after administration. This is because at this stage, the concentration in plasma is much higher than that in tumour, providing the driving force for liposome to pass through the vasculature wall and accumulate in tumour. The concentration in tumour

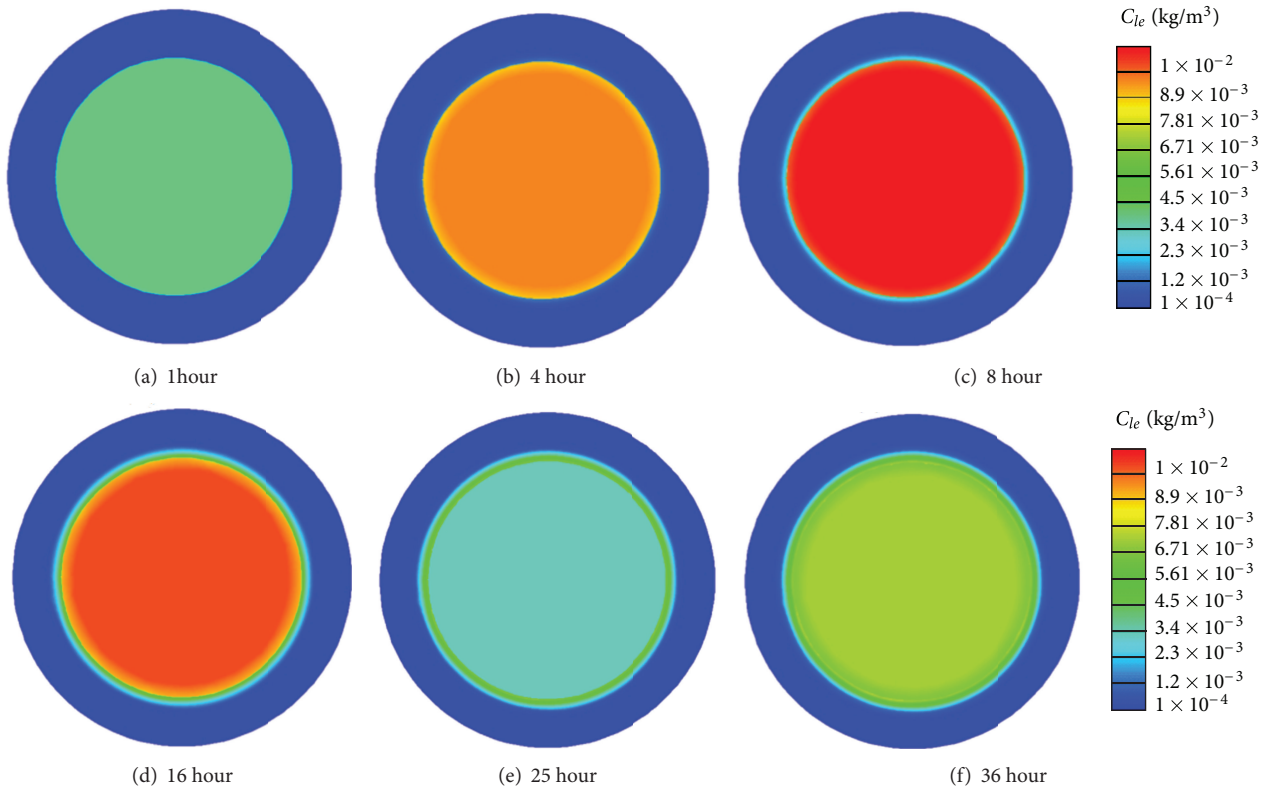

Figure 5: Spatial distribution of liposome encapsulated doxorubicin extracellular concentration in tumour and normal tissues.

reaches its peak when the concentration in tumour interstitial fluid and plasma reaches an equilibrium state. Upon heating at 24 hours after administration (heating lasts for 1 hour), doxorubicin is rapidly released from liposome, resulting in a sharp fall in the concentration of liposome encapsulated doxorubicin in the interstitial fluid of tumour, followed by a steady increase after heating ceases at 25 hour.

Since the size of liposome is too large to pass through the vasculature wall in normal tissues [44, 45], liposome encapsulated doxorubicin enters normal tissues by diffusion and convection from tumour, which can be seen clearly in Figure 5. This is the reason why the liposome encapsulated doxorubicin concentration in normal tissues increases slowly over time and stays at a very low level during the simulation time.

There is evidence for rapid and significant binding between free doxorubicin and proteins in plasma [12, 22]. Predicted free and bound doxorubicin concentrations in plasma for thermosensitive liposome delivery and 2-hour infusion of nonencapsulated doxorubicin are compared in Figure 6. Results show that 75% doxorubicin binds with proteins, which is consistent with the experimental data of Greene et al. [13].

For direct infusion of nonencapsulated doxorubicin, the infusion duration is 2 hours as recommended in the literature [12], and the total dose is 50 mg/m^2. The free and bound doxorubicin concentrations increase rapidly during the initial period following drug administration. For thermosensitive liposome delivery, the doxorubicin concentration remains at zero in the first 24 hours, since no doxorubicin is released from liposome before heating is applied. Upon heating to mild hyperthermia at 24 hours which lasts for one hour, doxorubicin is rapidly released from liposome causing much higher concentration in plasma. Because the temperature of tumour falls back to 37°C immediately after heating is stopped and assuming that encapsulated doxorubicin remains trapped within the core of liposome, the concentration declines rapidly to a low level. Although the concentration with both modes of administration drops to a low level after the infusions ends, 2-hour continuous infusion of nonencapsulated doxorubicin gives a slightly higher concentration over time.

Free and bound extracellular concentrations of doxorubicin in tumour and normal tissues are shown in Figures 7 and 8, respectively. Comparing the extracellular concentrations in these two figures with the plasma concentration in Figure 6, they all seem to follow the same trend. This means that plasma concentration has a direct influence on the extracellular concentration of both free and bound doxorubicin.

Despite thermosensitive liposome delivery gives higher peak values for both free and bound extracellular concentrations of doxorubicin in normal tissues, the concentration level is still lower than the half maximal (50%) inhibitory concentration (IC) of doxorubicin in normal tissue, which is 4.13×10^{-5} kg/m^3 [47]. However, the rate of cell killing is found to be related to the area under the extracellular concentration curve (AUC$_e$) [48, 49]. A simplified model

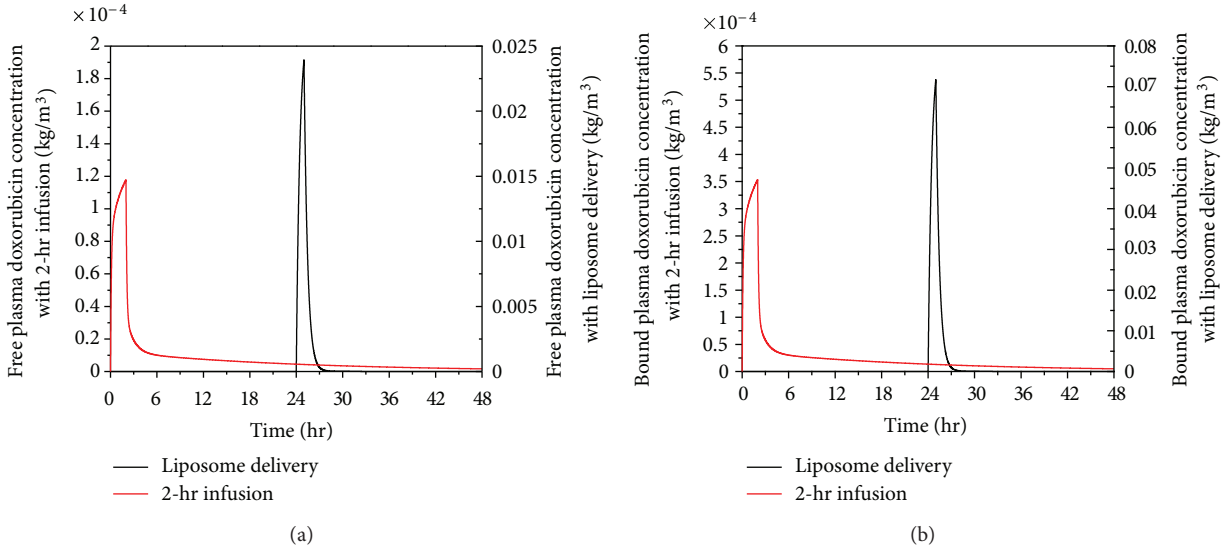

Figure 6: Spatial mean free (a) and bound (b) doxorubicin plasma concentration in tumour as a function of time under liposome delivery and 2-hr infusion of nonencapsulated doxorubicin (dose = 50 mg/m^2).

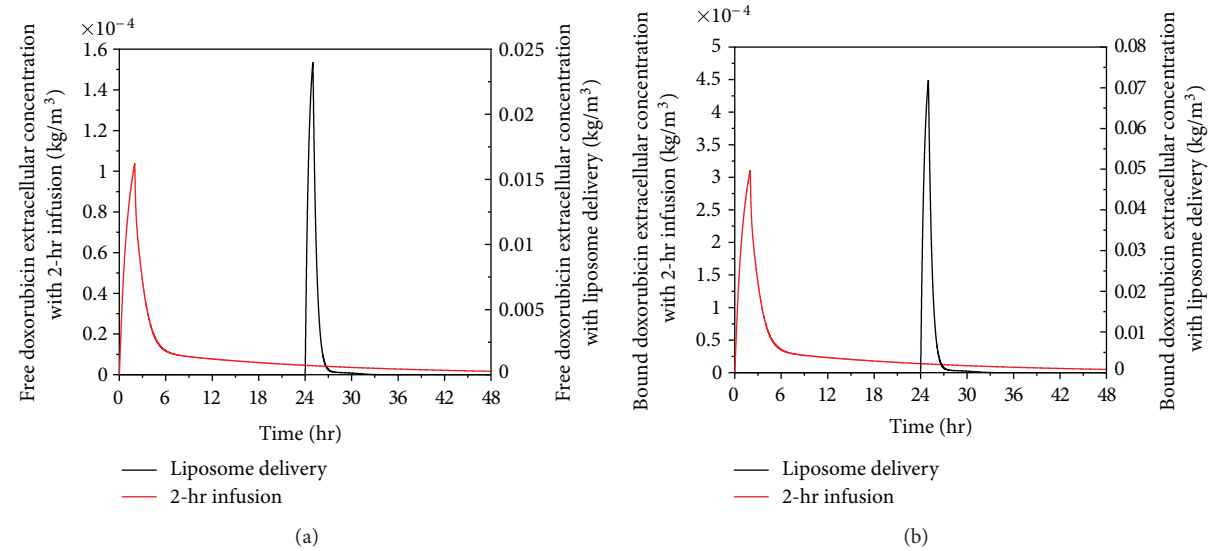

Figure 7: Spatial mean free and bound doxorubicin extracellular concentration in tumour as a function of time under thermosensitive liposome delivery and 2-hour infusion (dose = 50 mg/m^2).

in literature [49] shows that the logarithmic value of cell survival fraction is proportional to the AUC$_e$. Values for AUC$_e$ under 2-hour infusion and thermosensitive liposome delivery are compared in Table 4 which shows that the 2-hour infusion leads to high AUC$_e$ in the first 48 hours of the treatment, suggesting that 2-hour direct infusion of doxorubicin is likely to cause more cell death in normal tissues than thermosensitive liposome delivery.

Because heating can be controlled and localised in tumour, the temperature in normal tissues would be lower than the hyperthermia temperature required for the release of doxorubicin from liposomes. During the heating period, doxorubicin enters normal tissue only by diffusion and convection from tumour. This leads to doxorubicin being mainly concentrated in the region surrounding the tumour, as shown in Figure 9(b). However, under 2-hour direct infusion, doxorubicin is carried by blood into normal tissues. This leads to doxorubicin concentration reaching a higher level in the entire region of normal tissues, shown in Figure 9(a). Hence, thermosensitive liposome-mediated drug

Table 4: AUC$_e$ with various drug delivery modes in the first 48 hours.

	Free AUC$_e$ (kgs/m^3)	Bound AUC$_e$ (kgs/m^3)
Liposome delivery	1.59×10^{-6}	5.19×10^{-6}
2-hour infusion	2.30×10^{-6}	6.91×10^{-6}

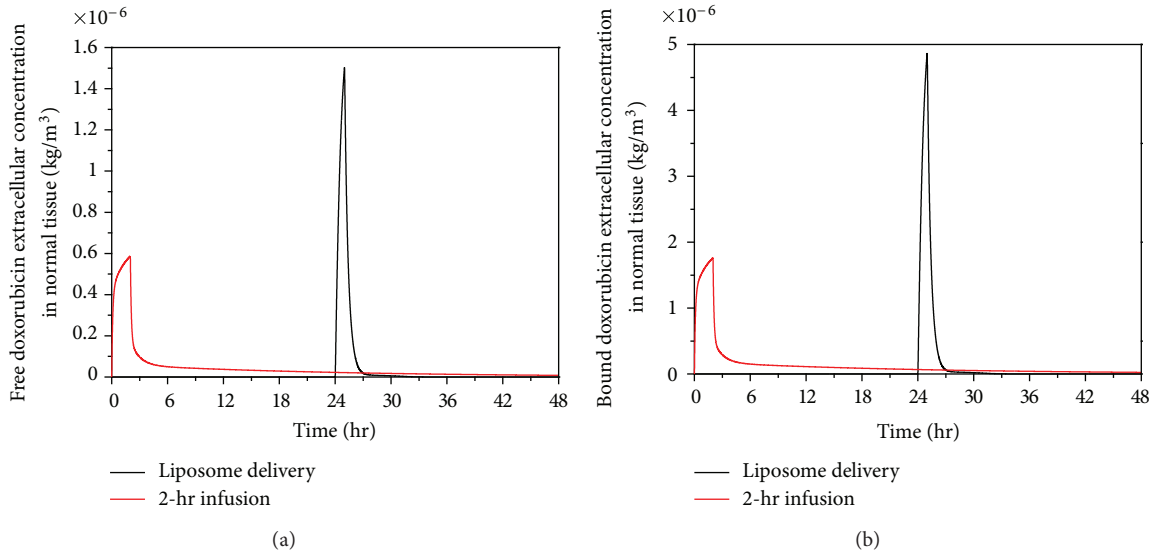

FIGURE 8: Spatial mean free and bound doxorubicin extracellular concentration in normal tissue as a function of time under thermosensitive liposome delivery and 2-hour infusion of nonencapsulated doxorubicin (dose = 50 mg/m^2).

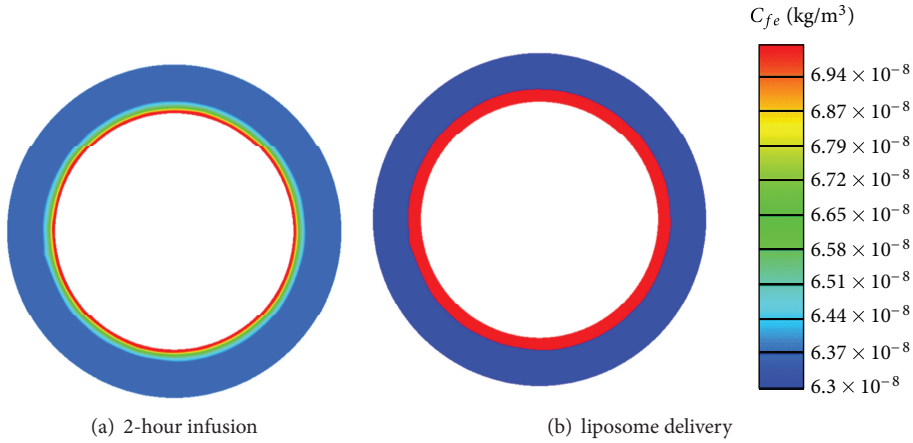

FIGURE 9: Spatial distribution of free doxorubicin extracellular concentration in normal tissues at 25-hour with 2-hour infusion and liposome delivery (dose = 50 mg/m^2).

delivery performs better in reducing drug concentration in the main region of normal tissues, which may help lower the risks of associated side effects.

Figure 10 presents the intracellular doxorubicin concentration in tumour for thermosensitive liposome delivery and 2-hour direct infusion. The intracellular concentration under 2-hour direct infusion displays a quick rise after drug administration until it reaches a peak and then decreases. The intracellular concentration under thermosensitive liposome delivery remains at zero until 24 hours, but there is a sharp rise to a high peak immediately after heating. However, as heating ceases and tumour tissue cools down to the physiological temperature range, no new doxorubicin is released and the intracellular concentration drops rapidly to a low level. Compared with 2-hour direct infusion, the thermosensitive liposome delivery leads to a much higher peak intracellular concentration.

Compared with the study reported by El-Kareh and Secomb [12], lower free doxorubicin extracellular and intracellular concentrations are found here. This is because the present model accounts for the effect of binding between doxorubicin and proteins in plasma. Since 75% doxorubicin is bound with proteins, less free doxorubicin is available in plasma for crossing the vasculature wall and entering the interstitial space, which leads to less drug uptake by tumour cells. Together with the experimental evidence [13], our predictions demonstrate that protein binding of anticancer drugs in plasma is an important factor that should be included in future mathematical models.

Figure 11 shows the fraction of survival cells by applying the pharmacodynamics model described by (29). As can be observed, the therapeutic effectiveness of 2-hour direct infusion can last for a longer period after administration. Fewer tumour cells are killed after 36 hours because the

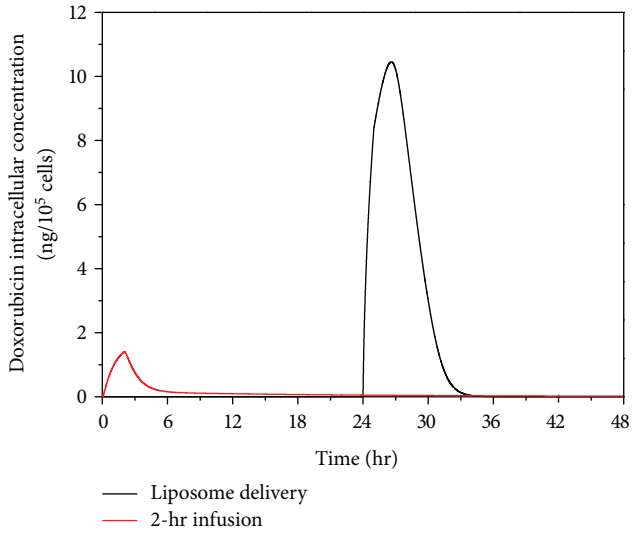

Figure 10: Doxorubicin intracellular concentration as a function of time, for thermosensitive liposome delivery and 2-hour direct infusion (dose = 50 mg/m^2).

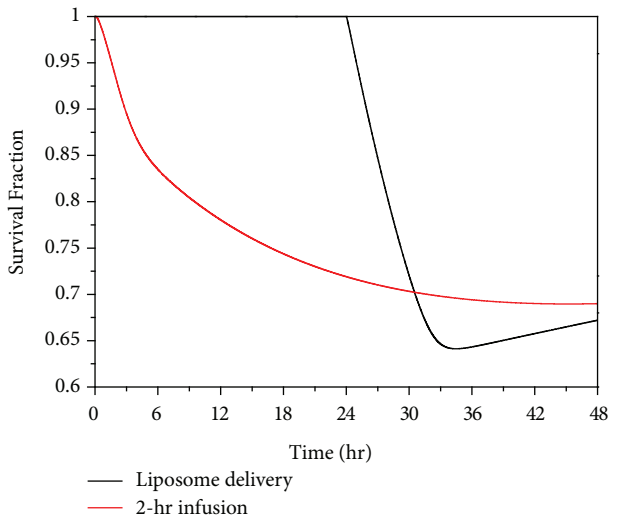

Figure 11: Temporal profiles of predicated tumour cell survival under 2-hour direct infusion and thermosensitive liposome delivery (dose = 50 mg/m^2).

intracellular concentration is below the threshold for cell killing (Figure 10). On the other hand, the effect of thermosensitive liposome delivery takes place after the start of heating. Highly effective tumour cell killing is observed since the intracellular concentration rises to a very high level in a short period of time (Figure 10). However, because temperature drops to the normal physiological range after heating, and no doxorubicin is released at this temperature, both the extra- and intracellular concentrations fall rapidly to a low level (Figures 7 and 10). Since the rate of cell killing caused by doxorubicin is slower than the rate of cell proliferation, the survival faction starts to rise after 34 hours. Nevertheless, thermosensitive liposome delivery leads to higher tumour cell death in a shorter time period than 2-hour direct infusion. On the other hand, the 2-hour direct infusion yields a higher extracellular concentration in normal tissues, which is undesirable as high drug concentration in normal tissue may increase the risk of side effects in patients.

Although the present numerical study offers some new insight into how anticancer treatment efficacy could be affected by different drug delivery modes, the mathematical models involve a number of assumptions. For example, realistic changes in tumour temperature during heating and after heating are ignored, and step changes are specified instead. In clinical practice, tumour temperature profiles (temperature versus time curve) may vary depending on the heating method applied. Moreover, temperature distribution in tumour tissue is likely to be nonuniform. These factors can influence the outcome of anticancer treatments. Other assumptions include an idealised geometry for the tumour and normal tissues, uniform transport properties, and a uniform distribution of microvasculature for administration of anticancer drug.

4. Conclusion

Doxorubicin delivery into solid tumour by direct continuous infusion and thermosensitive liposome are studied by mathematical modelling, and the anticancer effectiveness is evaluated in terms of the survival fraction of tumour cells. Our computational results show that thermosensitive liposome-mediated delivery offers a lower drug concentration in normal tissues than direct infusion of nonencapsulated doxorubicin, which may help reduce the risk of associated side effects. In addition, thermosensitive liposome delivery achieves a significantly higher peak intracellular concentration, and hence more rapid and effective tumour cell killing in a short time period of treatment.

References

[1] S. Goodman, A. Gilman, L. Brunton, J. Lazo, and K. Parker, *Goodman & Gilman's the Pharmacological Basis of Therapeutics*, McGraw-Hill, New York, 2005.

[2] E. Saltiel and W. McGuire, "Doxorubicin (Adriamycin) cardiomyopathy. A critical review," *Western Journal of Medicine*, vol. 139, no. 3, pp. 332–341, 1983.

[3] P. K. Singal and N. Iliskovic, "Doxorubicin-induced cardiomyopathy," *The New England Journal of Medicine*, vol. 339, no. 13, pp. 900–905, 1998.

[4] G. Storm, Q. G. C. M. van Hoesel, G. de Groot, W. Kop, P. A. Steerenberg, and F. C. Hillen, "A comparative study of the antitumor effect, cardiotoxicity and nephrotoxicity of doxorubicin given as a bolus, continuous infusion or entrapped in liposomes in the Lou/M Wsl rat," *Cancer Chemotherapy and Pharmacology*, vol. 24, no. 6, pp. 341–348, 1989.

[5] M. H. Gaber, N. Z. Wu, K. Hong, S. K. Huang, M. W. Dewhirst, and D. Papahadjopoulos, "Thermosensitive liposomes: extravasation and release of contents in tumor microvascular networks," *International Journal of Radiation Oncology Biology Physics*, vol. 36, no. 5, pp. 1177–1187, 1996.

[6] Y. Zou, M. Yamagishi, I. Horikoshi, M. Ueno, X. Gu, and R. Perez-Soler, "Enhanced therapeutic effect against liver W256

carcinosarcoma with temperature-sensitive liposomal Adriamycin administered into the hepatic artery," *Cancer Research*, vol. 53, no. 13, pp. 3046–3051, 1993.

[7] N. Z. Wu, R. D. Braun, M. H. Gaber et al., "Simultaneous measurement of liposome extravasation and content release in tumors," *Microcirculation*, vol. 4, no. 1, pp. 83–101, 1997.

[8] T. P. Chelvi, S. K. Jain, and R. Ralhan, "Hyperthermia-mediated targeted delivery of thermosensitive liposome-encapsulated melphalan in murine tumors," *Oncology Research*, vol. 7, no. 7-8, pp. 393–398, 1995.

[9] H. Harashima, M. Tsuchihashi, S. Iida, H. Doi, and H. Kiwada, "Pharmacokinetic/pharmacodynamic modeling of antitumor agents encapsulated into liposomes," *Advanced Drug Delivery Reviews*, vol. 40, no. 1-2, pp. 39–61, 1999.

[10] H. Harashima, S. Iida, Y. Urakami, M. Tsuchihashi, and H. Kiwada, "Optimization of antitumor effect of liposomally encapsulated doxorubicin based on simulations by pharmacokinetic/pharmacodynamic modeling," *Journal of Controlled Release*, vol. 61, no. 1-2, pp. 93–106, 1999.

[11] M. Tsuchihashi, H. Harashima, and H. Kiwada, "Development of a pharmacokinetic/pharmacodynamic (PK/PD)-simulation system for doxorubicin in long circulating liposomes in mice using peritoneal P388," *Journal of Controlled Release*, vol. 61, no. 1-2, pp. 9–19, 1999.

[12] A. W. El-Kareh and T. W. Secomb, "A mathematical model for comparison of bolus injection, continuous infusion, and liposomal delivery of doxorubicin to tumor cells," *Neoplasia*, vol. 2, no. 4, pp. 325–338, 2000.

[13] R. F. Greene, J. M. Collins, and J. F. Jenkins, "Plasma pharmacokinetics of adriamycin and adriamycinol: implications for the design of in vitro experiments and treatment protocols," *Cancer Research*, vol. 43, no. 7, pp. 3417–3421, 1983.

[14] P. Rubin and G. Casarett, "Microcirculation of tumors part I: anatomy, function, and necrosis," *Clinical Radiology*, vol. 17, no. 3, pp. 220–229, 1966.

[15] L. T. Baxter and R. K. Jain, "Transport of fluid and macromolecules in tumors. I. Role of interstitial pressure and convection," *Microvascular Research*, vol. 37, no. 1, pp. 77–104, 1989.

[16] L. T. Baxter and R. K. Jain, "Transport of fluid and macromolecules in tumors II. Role of heterogeneous perfusion and lymphatics," *Microvascular Research*, vol. 40, no. 2, pp. 246–263, 1990.

[17] L. T. Baxter and R. K. Jain, "Transport of fluid and macromolecules in tumors. III. Role of binding and metabolism," *Microvascular Research*, vol. 41, no. 1, pp. 5–23, 1991.

[18] Y. M. F. Goh, H. L. Kong, and C. H. Wang, "Simulation of the delivery of doxorubicin to hepatoma," *Pharmaceutical Research*, vol. 18, no. 6, pp. 761–770, 2001.

[19] J. R. Less, T. C. Skalak, E. M. Sevick, and R. K. Jain, "Microvascular architecture in a mammary carcinoma: branching patterns and vessel dimensions," *Cancer Research*, vol. 51, no. 1, pp. 265–273, 1991.

[20] F. Yuan, M. Dellian, D. Fukumura et al., "Vascular permeability in a human tumor xenograft: molecular size dependence and cutoff size," *Cancer Research*, vol. 55, no. 17, pp. 3752–3756, 1995.

[21] W. M. Deen, "Hindered transport of large molecules in liquid-filled pores," *AIChE Journal*, vol. 33, no. 9, pp. 1409–1425, 1987.

[22] S. Eikenberry, "A tumor cord model for Doxorubicin delivery and dose optimization in solid tumors," *Theoretical Biology and Medical Modelling*, vol. 6, no. 1, article 16, 2009.

[23] F. Yuan, M. Leunig, Shi Kun Huang, D. A. Berk, D. Papahadjopoulos, and R. K. Jain, "Microvascular permeability and interstitial penetration of sterically stabilized (stealth) liposomes in a human tumor xenograft," *Cancer Research*, vol. 54, no. 13, pp. 3352–3356, 1994.

[24] N. Z. Wu, D. Da, T. L. Rudoll, D. Needham, A. R. Whorton, and M. W. Dewhirst, "Increased microvascular permeability contributes to preferential accumulation of stealth liposomes in tumor tissue," *Cancer Research*, vol. 53, no. 16, pp. 3765–3770, 1993.

[25] A. Gabizon, R. Catane, B. Uziely et al., "Prolonged circulation time and enhanced accumulation in malignant exudates of doxorubicin encapsulated in polyethylene-glycol coated liposomes," *Cancer Research*, vol. 54, no. 4, pp. 987–992, 1994.

[26] N. Z. Wu, B. Klitzman, G. Rosner, D. Needham, and M. W. Dewhirst, "Measurement of material extravasation in microvascular networks using fluorescence video-microscopy," *Microvascular Research*, vol. 46, no. 2, pp. 231–253, 1993.

[27] R. K. Jain, "Transport of molecules in the tumor interstitium: a review," *Cancer Research*, vol. 47, no. 12, pp. 3039–3051, 1987.

[28] K. A. Granath and B. E. Kvist, "Molecular weight distribution analysis by gel chromatography on sephadex," *Journal of Chromatography A*, vol. 28, no. C, pp. 69–81, 1967.

[29] W. M. Saltzman and M. L. Radomsky, "Drugs released from polymers: diffusion and elimination in brain tissue," *Chemical Engineering Science*, vol. 46, no. 10, pp. 2429–2444, 1991.

[30] L. J. Nugent and R. K. Jain, "Extravascular diffusion in normal and neoplastic tissues," *Cancer Research*, vol. 44, no. 1, pp. 238–244, 1984.

[31] E. A. Swabb, J. Wei, and P. M. Gullino, "Diffusion and convection in normal and neoplastic tissues," *Cancer Research*, vol. 34, no. 10, pp. 2814–2822, 1974.

[32] M. B. Wolf, P. D. Watson, and D. R. C. Scott, "Integral-mass balance method for determination of solvent drag reflection coefficient," *American Journal of Physiology*, vol. 253, no. 1, p. 22/1, 1987.

[33] D. J. Kerr, A. M. Kerr, R. I. Freshney, and S. B. Kaye, "Comparative intracellular uptake of adriamycin and 4'-deoxydoxorubicin by non-small cell lung tumor cells in culture and its relationship to cell survival," *Biochemical Pharmacology*, vol. 35, no. 16, pp. 2817–2823, 1986.

[34] R. E. Eliaz, S. Nir, C. Marty, and F. C. Szoka, "Determination and modeling of kinetics of cancer cell killing by doxorubicin and doxorubicin encapsulated in targeted liposomes," *Cancer Research*, vol. 64, no. 2, pp. 711–718, 2004.

[35] J. Robert, A. Illiadis, and B. Hoerni, "Pharmacokinetics of adriamycin in patients with breast cancer: correlation between clinical short-term response," *European Journal of Cancer and Clinical Oncology*, vol. 18, no. 8, pp. 739–745, 1982.

[36] C. Liu, J. Krishnan, and X. Y. Xu, "A systems-based mathematical modelling framework for investigating the effect of drugs on solid tumours," *Theoretical Biology & Medical Modelling*, vol. 8, pp. 45–65, 2011.

[37] M. Winter, *Basic Clinical Pharmacokinetics, Plasma Protein Binding*, Lippincott Williams & Wilkins, Philadelphia, Pa, USA, 4th edition, 2003.

[38] L. Z. Benet and P. Zia-Amirhosseini, "Basic principles of pharmacokinetics," *Toxicologic Pathology*, vol. 23, no. 2, pp. 115–123, 1995.

[39] K. A. Rodvold, D. A. Rushing, and D. A. Tewksbury, "Doxorubicin clearance in the obese," *Journal of Clinical Oncology*, vol. 6, no. 8, pp. 1321–1327, 1988.

[40] M. Dalmark and H. H. Storm, "A Fickian diffusion transport process with features of transport catalysis. Doxorubicin transport in human red blood cells," *Journal of General Physiology*, vol. 78, no. 4, pp. 349–364, 1981.

[41] R. T. Tong, Y. Boucher, S. V. Kozin, F. Winkler, D. J. Hicklin, and R. K. Jain, "Vascular normalization by vascular endothelial growth factor receptor 2 blockade induces a pressure gradient across the vasculature and improves drug penetration in tumors," *Cancer Research*, vol. 64, no. 11, pp. 3731–3736, 2004.

[42] J. C. Parker, M. A. Perry, and A. E. Taylor, "Permeability of the microvascular barrier," in *Edema*, N. C. Staub and A. E. Taylor, Eds., pp. 143–187, Raven Press, New York, NY, USA, 1984.

[43] K. Aukland and R. K. Reed, "Interstitial-lymphatic mechanisms in the control of extracellular fluid volume," *Physiological Reviews*, vol. 73, no. 1, pp. 1–78, 1993.

[44] H. Sarin, "Physiologic upper limits of pore size of different blood capillary types and another perspective on the dual pore theory of microvascular permeability," *Journal of Angiogenesis Research*, vol. 2, no. 1, article 14, 2010.

[45] T. Tagami, M. Ernsting, and S. D. Li, "Optimization of a novel and improved thermosensitive liposome formulated with DPPC and a Brij surfactant using a robust in vitro system," *Journal of Controlled Release*, vol. 154, no. 3, pp. 290–297, 2011.

[46] M. Afadzi, C. Davies, and Y. H. Hansen, "Ultrasound stimulated release of liposomal calcein," in *Ultrasonics Symposium (IUS)*, vol. 2010, pp. 11–14, IEEE Conference, October 2010.

[47] J. Kirk, S. Houlbrook, N. S. A. Stuart, I. J. Stratford, A. L. Harris, and J. Carmichael, "Differential modulation of doxorubicin toxicity to multidrug and intrinsically drug resistant cell lines by anti-oestrogens and their major metabolites," *British Journal of Cancer*, vol. 67, no. 6, pp. 1189–1195, 1993.

[48] L. M. Levasseur, H. K. Slocum, Y. M. Rustum, and W. R. Greco, "Modeling of the time-dependency of in vitro drug cytotoxicity and resistance," *Cancer Research*, vol. 58, no. 24, pp. 5749–5761, 1998.

[49] S. Ozawa, Y. Sugiyama, Y. Mitsuhashi, T. Kobayashi, and M. Inaba, "Cell killing action of cell cycle phase-non-specific antitumor agents is dependent on concentration-time product," *Cancer Chemotherapy and Pharmacology*, vol. 21, no. 3, pp. 185–190, 1988.

Hindawi Publishing Corporation
Journal of Drug Delivery
Volume 2012, Article ID 842785, 11 pages
doi:10.1155/2012/842785

Research Article

Active Targeting to Osteosarcoma Cells and Apoptotic Cell Death Induction by the Novel Lectin *Eucheuma serra* Agglutinin Isolated from a Marine Red Alga

Keita Hayashi,[1] Peter Walde,[2] Tatsuhiko Miyazaki,[3] Kenshi Sakayama,[4] Atsushi Nakamura,[4] Kenji Kameda,[5] Seizo Masuda,[5] Hiroshi Umakoshi,[1] and Keiichi Kato[6]

[1] *Division of Chemical Engineering, Graduate School of Engineering Science, Osaka University, 1-3 Machikaneyama-cho, Toyonaka 560-8531, Osaka, Japan*
[2] *Department of Materials, ETH, Wolfgang-Pauli-Straße 10, 8093 Zürich, Switzerland*
[3] *Department of Pathogenomics, Graduate School of Medicine, Ehime University, Shitsukawa, Toon 791-0295, Ehime, Japan*
[4] *Department of Bone and Joint Surgery, Graduate School of Medicine, Ehime University, Shitsukawa, Toon 791-0295, Ehime, Japan*
[5] *Integrated Center for Science Shigenobu Station, Ehime University, Shitsukawa, Toon 791-0295, Ehime, Japan*
[6] *Department of Materials Science and Biotechnology, Graduate School of Science and Engineering, Ehime University, 3 Bunkyo-cho, Matsuyama 790-8577, Ehime, Japan*

Correspondence should be addressed to Peter Walde, peter.walde@mat.ethz.ch and Keiichi Kato, keiichi1017@mc.pikara.ne.jp

Received 30 September 2012; Accepted 21 November 2012

Academic Editor: Andreas G. Tzakos

Previously, we demonstrated that the novel lectin *Eucheuma serra* agglutinin from a marine red alga (ESA) induces apoptotic cell death in carcinoma. We now find that ESA induces apoptosis also in the case of sarcoma cells. First, propidium iodide assays with OST cells and LM8 cells showed a decrease in cell viability after addition of ESA. With 50 μg/ml ESA, the viabilities after 24 hours decreased to 54.7 ± 11.4% in the case of OST cells and to 41.7 ± 12.3% for LM8 cells. Second, using fluorescently labeled ESA and flow cytometric and fluorescence microscopic measurements, it could be shown that ESA does not bind to cells that were treated with glycosidases, indicating importance of the carbohydrate chains on the surface of the cells for efficient ESA-cell interactions. Third, Span 80 vesicles with surface-bound ESA as active targeting ligand were shown to display sarcoma cell binding activity, leading to apoptosis and complete OST cell death after 48 hours at 2 μg/ml ESA. The findings indicate that Span 80 vesicles with surface-bound ESA are a potentially useful drug delivery system not only for the treatment of carcinoma but also for the treatment of osteosarcoma.

1. Introduction

Osteosarcoma has one of the worst prognosis among all malignant tumors. Before 1970, the 5-year survival rate of the treated patients was only about 20% [1, 2]. The treatment of osteosarcoma currently involves surgical resection in combination with neoadjuvant chemotherapy. Despite advances in the neoadjuvant chemotherapy and in limb-salvage surgery, the disease-free survival rate still remains poor for patients with metastatic, recurrent, or unresectable osteosarcoma. Thus, novel selective therapeutic approaches against osteosarcoma are highly required.

Previously, we found that the novel lectin *Eucheuma serra* agglutinin (ESA), which was successfully isolated by Kawakubo et al. [3] from the marine red alga *Eucheuma serra*, specifically binds to carcinoma cell lines of human adenocarcinoma, human cervical squamous cell carcinoma, and marine adenocarcinoma but not to normal human fibroblasts or lymphocytes [4]. We also revealed, that the specific binding of ESA to carcinoma cells is based on specific

interactions between ESA and the unique sugar chains of high mannose type on the surface of the carcinoma cells [4]. In a more recent study, Hori et al. [5] investigated the specific interactions between ESA and various unique sugar chains of high mannose type in detail. Furthermore, we successfully elaborated the basis for a novel type of drug delivery system (DDS) for cancer therapy using ESA (i) as targeting ligand to carcinoma tumors and (ii) as inducer of apoptosis due to specific ESA binding to carcinoma cells [6]. Recently, the general potential of certain types of sugar binding proteins (lectins) as promising, alternative antitumor drugs has been emphasized [7]. The antitumor activity of these lectins might be related directly to specific intermolecular interactions between the lectins and the sugar chains on the tumor cell surface [8]. However, whether lectins also have antitumor activities against osteosarcomas has not been clarified yet.

Generally, carcinomas which originate in epithelial cells and sarcomas which originate in mesenchymal cells (e.g., osteosarcoma) are thought to be quite different in their tumorigenesis as well as in the phenotypes including cytoskeleton, binding molecules, proliferation procedure, and surface glycoproteins [9, 10]. Therefore, different therapeutic approaches have been employed for the treatment of sarcomas, if compared with the therapies applied for the treatment of carcinomas, except for the surgical treatment. On the other hand, the existence of cell surface-bound sugar chain structures, which are common among carcinomas and sarcomas, but not present in normal cells, has been suggested [11]. Moreover, the concept of epithelial-mesenchymal transition in tumors implies common structures and/or mechanism among carcinomas and sarcomas [12, 13]. Therefore, on the basis of our previous *in vitro* and *in vivo* studies with ESA bound to Span 80 vesicles for targeting carcinoma cells [6], we found it worthwhile to investigate whether the lectin ESA can also be applied in a therapeutic approach against osteosarcomas. Span 80 is generally known in the food and cosmetic industries as sorbitan monooleate, although commercial Span 80 is a heterogeneous mixture of sorbitan mono-, di-, tri-, and tetra-esters [14]. We have already demonstrated that nonionic vesicles prepared from Span 80 have promising physicochemical properties (high membrane fluidity with temperature dependent fusiogenicity) which make this type of vesicle an attractive possible alternative to the commonly used liposomes *in vitro* and *in vivo* [6, 14–22].

Aim of the work was to clarify the specificity of the binding of ESA to either OST cells or LM8 cells, both being osteosarcoma cell lines. Furthermore, the potential effectivity of ESA as ligand on the surface of Span 80 vesicles [6, 14, 18, 19, 21, 22] with targeting function and as possible apoptosis-inducer for the treatment of osteosarcoma was also examined. In the work presented, the interactions between ESA and OST cells and between ESA and LM8 cells were examined by means of fluorescence microscopy and flow cytometry. As a result of our study, the evidence is presented that ESA specifically binds to these two types of osteosarcoma cells, followed by induction of apoptosis due to this specific ESA binding to the cells. Furthermore, we could demonstrate that ESA has a considerable potential as novel type of ligand immobilized onto PEGylated Span 80 vesicles, an important step towards the potential development of a therapy for the treatment of refractory osteosarcoma, as novel lipidic microcapsule drug-delivery system (DDS) for transporting and delivering anticancer drugs for the treatment of cancer [6].

2. Material and Methods

2.1. Materials. *Eucheuma serra* agglutinin (ESA) was extracted from the red alga *Eucheuma serra*, by means of ethanol precipitation, followed by purification with fast protein liquid chromatography (FPLC), using a 10 mmol/L sodium phosphate buffer (pH = 7.4) [3]. Propidium iodide (PI), α-mannnosidase, β-mannnosidase, endoglycosidase H, and rhodamine 6G were obtained from Sigma-Aldrich (St. Louis, MO, USA). The "Annexin V-PE Apoptosis Detection Kit I" which contains Annexin V-PE and 7-amino-actinomycin D (7-ADD) was obtained from Becton Dickinson Biosciences (Franklin Lakes, NJ, USA). The caspase assay system was purchased from Promega (Madison, WI, USA). Fluorescein isothiocyanate, isomer I (FITC), Span 80, cholesterol, and lecithin from soybeans were obtained from Wako Pure Chemical Industries (Osaka, Japan). The lecithin was purified by acetone precipitation [23]. The phospholipid 1,2-dioleoyl-*sn*-glycero3-phosphoethanolamine-N-(succinyl) (SuPE) was obtained from Avanti Polar Lipids (Alabaster, AL, USA). DSPE-PEG_{2000} was from NOF Corporation (Tokyo, Japan). PBS (phosphate buffered saline) was composed of 137 mM NaCl, 2.7 mM KCl, 10 mM Na_2HPO_4 and 2 mM KH_2PO_4, (pH = 7.4).

2.2. Cells and Cell Cultures. Human osteosarcoma Takase (OST) cells were offered by Dr. Katsuro Tomita (Department of Orthopaedic Surgery, Kanazawa University School of Medicine, Japan), cultured in either ERDF medium (Kyokuto Pharmaceutical Industrial, Tokyo, Japan) or Dulbecco's Modified Eagle Medium (D-MEM) (Wako Pure Chemical Industries, Osaka, Japan) supplemented with 10% of fetal bovine serum (FBS) at 37°C in a humidified atmosphere consisting of 5% CO_2. Murine osteosarcoma cell line (LM8 cells) was obtained from RIKEN (RIKEN BRC Cell Bank). These LM8 cells were grown in D-MEM supplemented with 10% of FBS at 37°C in a humidified atmosphere consisting of 5% CO_2.

2.3. Cell Viability Assay. OST cells and LM8 cells were inoculated in 6-well culture plates at a cell density of 2.0×10^5 cells/mL suspended in D-MEM with 10% FBS. After 16 hours, the medium in each plate was exchanged with 10% FBS D-MEM containing various concentration of ESA. After incubation during one day, the cell number and the viabilities of both types of cells were evaluated by means of the "Propidium Iodide Nucleic Acid Stain" using flow cytometry [24]. The viability assay of OST cells for EPV was also performed by the same way as above. In a similar way, time-courses of the viability of both OST cells and LM8 cells were experimentally measured in medium with ESA at a concentration of 50 μg/mL.

2.4. Apoptosis Assay. Apoptosis was analyzed by using the "Annexin V-PE Apoptosis Detection Kit I" according to a previously published protocol [25–27]. OST cells or LM8 cells, at a concentration of 2×10^5 cells/mL, were suspended in D-MEM containing 10% FBS, and then inoculated in 6-well culture plates. After 16 hours inoculation, the medium in each plate was exchanged with 10% FBS, D-MEM containing 50 μg/mL ESA. The cell lines in each plate were incubated for different time periods, followed by twice washing with cold PBS. Using a cell counter, the washed cells were diluted to a concentration of 1×10^6 cells/mL by resuspending the cells in 0.1 M Hepes/NaOH (pH 7.4) containing 1.4 M NaCl and 25 mM $CaCl_2$ ("binding buffer"). Volumes of 100 μL of the cell suspensions were transferred to 1.5 mL Eppendorf tubes. Solutions of 5 μL of AnnexinV-PE and 5 μL of 7-ADD were added to the suspensions, followed by vortexing and incubation for 15 min at room temperature in the dark. Then, 400 μL "binding buffer" were added to each tube containing the incubated suspension, followed by analysis with a flow cytometer.

2.5. Caspase-3 Assay. Caspase-3 activity was evaluated spectrophotometrically at $\lambda = 405$ nm with the caspase-3 substrate Ac-DEVD-pNA. OST cells were suspended at 2.0×10^5 cells/mL in D-MEM with 10% FBS and then pipetted into 6-well culture plates. After 16 hours of incubation at 37°C and 5% CO_2, the medium in each plate was exchanged by 10% FBS, D-MEM containing either 50 μg/mL ESA, or 50 μg/mL ESA + ZVAD-FMK (=N-Benzyloxycarbonyl-Val-Ala-Asp(O-Me) fluoromethyl ketone) which is a known caspase-3 inhibitor, or PBS as control. Following culturing for 16 hours, the caspase-3 activity in these kinds of cells was measured with the caspase assay system (Promega, Madison, WI, USA), using a spectrophotometer U-2000 (HITACHI, Tokyo, Japan) according to the manufacturer's instructions.

2.6. Test of ESA Binding to the Cells. An amount of 1.22 mg/mL ESA was fluorescently labeled by addition of 1 mg/mL Rhodamine 6G (Rh6G) in 0.15 M sodium carbonate buffer (pH = 9.0), followed by removal of free FITC by using a PD-10 column (GE Healthcare, CT, USA). OST cells and LM8 cells, suspended at a concentration of 2.0×10^5 cells/mL, were cultured in 10% FBS ERDF medium. After 16 hours, the culture medium was exchanged with a culture medium containing 10% FITC-ESA solution, both types of cells were separately incubated for 3, 6, 9, 12, and 24 hours in a CO_2 incubator at 37°C, respectively.

After the incubation, both cells were washed with cold PBS twice. Both cell suspensions were then analyzed by flow cytometry using a FACS Calibur instrument (Becton Dickinson, Mansfield, MA, USA). In a similar way, the binding activities of ESA (labeled with either rhodamine 6G (Rh6G) or FITC) to the sugar chains on the surface of OST cells were examined by incubation with α-mannnosidase, or β-mannnosidase, or endoglycosidase H for 2 hours before adding fluorescenctly labeled ESA. After incubation for 1 hour, the ESA binding to the OST cells was evaluated by using a fluorescence microscope (BH2-RFC, Olympus Corp, Tokyo, Japan) and the flow cytometer.

2.7. Preparation of a Lipidic ESA-Conjugate. ESA-SuPE, a phospholipid-ESA conjugate, was prepared as follows: 100 μL of a SuPE solution (1.25 mg/mL in chloroform) were added to a test tube. A thin film of SuPE formed after evaporation of chloroform under a stream of nitrogen gas. Afterwards, 2.5 mL of an ESA solution (0.675 mg/mL) were added to the film to react with SuPE in 0.15 M sodium carbonate buffer (pH 9.0) at room temperature. The reaction mixture was incubated for 2 hours with vortexing for a few seconds every 30 min, followed by letting the suspension stand at 4°C overnight. Residual SuPE in the buffer solution was removed by gel filtration with a PD-10 column packed with Sephadex G-25 (GE Healthcare; Buckinghamshire, England).

2.8. Preparation of Different Types of Span 80 Vesicles. In the present work, four types of Span 80 vesicles were prepared. Type 1: Span 80 vesicles with immobilized ESA and immobilized PEG (EPV), containing as inner aqueous solution PBS. Type 2: Span 80 vesicles (called "control vesicles": CV) containing encapsulated FITC. Type 3: Span 80 vesicles with immobilized ESA (EV) containing encapsulated FITC. Type 4: Span 80 vesicles with immobilized ESA and immobilized PEG (EPV) containing encapsulated FITC. The vesicles of types 2, 3, and 4 contained a 0.15 M sodium carbonate buffer solution (pH = 9.0) containing 1 mg/mL FITC as inner aqueous solution.

The vesicles were prepared with the two-step emulsification method in pretty much the same way of as described in the previous papers [6, 19]. In this work, some minor modifications were applied for the preparation of EPV containing FITC. A volume of 0.6 mL of the inner aqueous solutions (the sodium carbonate buffer solution containing FITC as mentioned above) was added to 6 mL of a n-hexane solution containing Span 80 (264 mg), purified lecithin (24 mg) and cholesterol (12 mg), followed by the first emulsification for 6 min at 17,500 rpm using a micro-homogenizer NS-310E 2 (Microtec Co., Ltd., Funabashi, Japan). Afterwards, the solvent was removed in a rotary evaporator at 28°C under reduced pressure, yielding a water-lipid emulsion to which 6 mL of the ESA-SUPE solution (obtained as described above) containing Tween 80 (96 mg) and DSPE-PEG_{2000} (14.2 mg/mL) were added, followed by the second emulsification with the homogenizer for 2 min at 3500 rpm to obtain a heterogeneous Span 80 vesicle suspension. After stirring with a magnetic stirrer for 3 hours at room temperature, the vesicle suspension was stored overnight at 4°C. The vesicles were then purified by ultracentrifugation (50,000 rpm at 4°C for 120 min) in a Himac centrifuge CR15B (Hitachi Koki Co., Ltd., Tokyo, Japan). The lower phase was filtrated through 100-nm nucleopore track-etch polycarbonate membranes (Avanti Polar Lipids; Alabaster, AL, USA) and purified by gel filtration on a 7 cm (diameter) $\times$ 50 cm (length) column containing Biogel-A5m (Bio-Rad Laboratories, Richmond, CA, USA). CV containing FITC and EV containing FITC

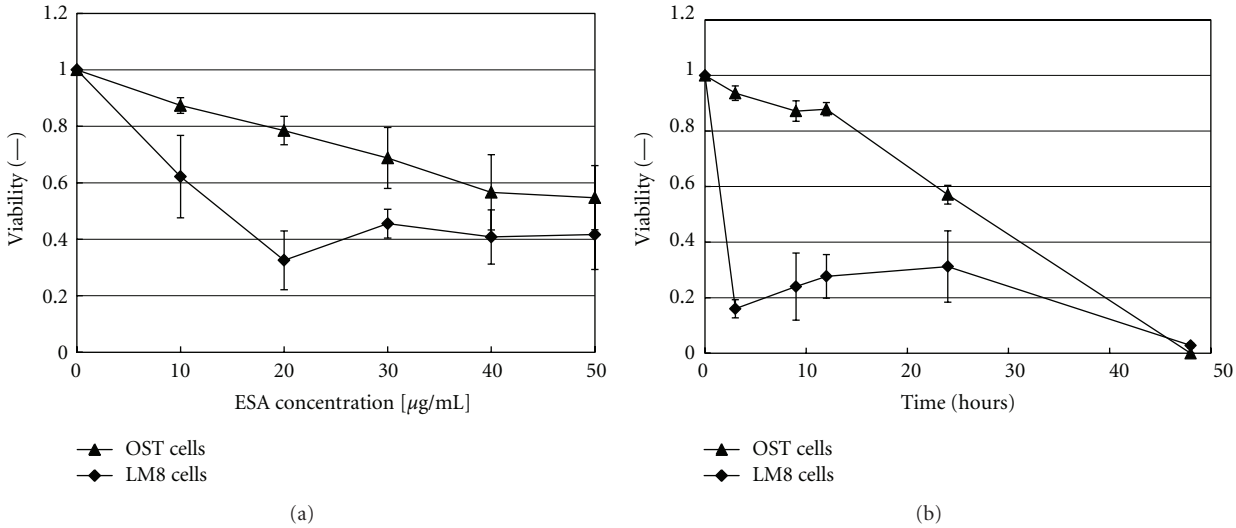

Figure 1: Cytotoxic effect of ESA on either OST cells or LM8 cells, as evaluated by means of propidium iodide staining. (a) Variation of the cell viability with increasing ESA concentration during incubation for 24 hours. (b) Time courses of the cell viabilities for [ESA] = 50 μg/mL. For both set of data, mean values and standard deviations for three separate measurements are shown.

were also prepared in the same manner as above, but without both ESA and PEG (for CV), and without DSPE-PEG$_{2000}$ (for EV), respectively. The diameters of CV, EV, and EPV, which contained FITC were 104 ± 7 nm, 100 ± 2 nm, and 103 ± 5 nm, respectively.

2.9. Analysis of the Binding of EPV to OST Cells. OST cells were inoculated in 6-well culture plates at a cell density of 2.0×10^5 cells/mL suspended in D-MEM with 10% FBS. The cells were incubated for 16 hours. Afterwards, the culture medium was exchanged with 1.8 mL D-MEM containing 10% FBS and 0.2 mL PBS, CV containing encapsulated FITC, EV containing encapsulated FITC, or EPV containing encapsulated FITC. The cells were then kept for 15 min in a CO_2 incubator at 37°C. After incubation, the OST cells were washed with cold PBS twice, followed by flow cytometric analysis.

3. Results

3.1. Effect of ESA on the Viabilities of OST Cells and LM8 Cells. The viabilities of OST cells and LM8 cells were measured in the concentration range from 10 μg/mL to 50 μg/mL to evaluate the possible anticancer activity of ESA. As shown in Figure 1(a), the proliferations of both osteosarcoma cell types were inhibited by ESA. The inhibitory effect against the cell viability increased with increasing amounts of added ESA. Addition of 50 μg/mL ESA, for example, decreased the cell viabilities of OST cells and LM8 cells to 54.7 ± 11.4% and 41.7 ± 12.3%, respectively. Furthermore, Figure 1(b) shows that the cell viabilities decreased with increasing elapsing time. The cell proliferation was inhibited completely by the addition of 50 μg/mL ESA after incubation for 48 hours. These experiments clearly demonstrate the anticancer activity of ESA in the case of these osteosarcoma cells.

3.2. Apoptosis Induction by ESA in Both OST Cells and LM8 Cells as Determined by Means of a Double Staining Test. Previously, we have already demonstrated that ESA induces apoptosis in carcinoma cells [4]. The findings presented above about the inhibition of sarcoma cell proliferation (see Section 3.1.) suggested that ESA may also induce apoptosis in sarcoma cells. Therefore, apoptosis induction in either OST cells or LM8 cells by ESA was examined by means of the double staining test for Annexin V-PE and 7-ADD.

The numerical values obtained from this analysis are displayed in Figure 2 and summarized in Table 1. As shown in Figure 2(a) and Table 1, the relative amount of cells in the lower right part of the diagram (indicating early stages of apoptosis) was 74.8% at an elapsing time of 3 hours after adding ESA, while in the case of the control cells (PBS-treated only, no ESA), the amount of the cells was 14.2% in the same part. Moreover, the amount of cells in the upper right part of the diagram (indicating dead cells) increased from 22.5% (at 3 hours after ESA addition) to 71.0% (at 24 hours). These results clearly show that ESA induced apoptosis in OST cells.

The same double staining test was also performed with LM8 cells. The results are also shown in Figure 2(b) and Table 1. The amount of cells in the lower right part of the diagram increased from 19.8% (control) to 68.2% at an elapsing time of 3 hours after adding ESA, being similar to the case of OST cells. The amount of cells in the upper right of the diagram also increased from 17.9% (at 3 hours) to 23.1% (at 24 hours). Thus, ESA also induced apoptosis in LM8 cells.

From the results in Sections 3.1 and 3.2, it was found that ESA specifically binds to OST cells and to LM8 cells, both being osteosarcoma cell lines, followed by induction of

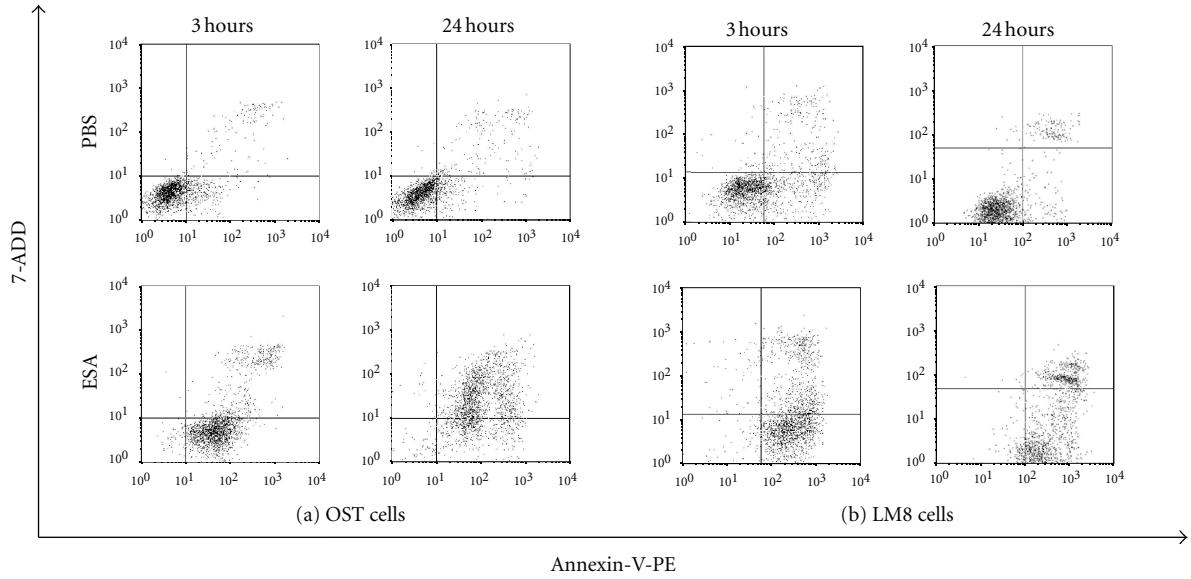

Figure 2: Apoptotic induction in either (a) OST cells or in (b) LM8 cells after adding ESA. The cells were cultured in 10% FBS D-MEM with 50 μg/mL ESA (bottom panel). As control, only PBS (no ESA) was added (top panel). The cells were incubated with ESA for either 3 hours or 24 hours. Induction of apoptosis in these cells was detected by means of the double staining assay for annexin V-PE and 7-ADD.

Table 1: Cell state dependence on elapsing time after the addition of ESA to OST cells or LM8 cells. The cell states are classified as "living", "apoptotic" or "dead", as obtained from the data shown in Figure 2.

Elapsing time (h)	OST cells			LM8 cells		
	living (%)	apoptotic (%)	dead (%)	living (%)	apoptotic (%)	dead (%)
3	2.5	74.8	22.5	10.3	68.2	17.9
24	3.5	24.1	71.0	7.9	68.8	23.1

Please note that cells appearing in the upper left part of the diagram in Figure 2 (Annexin V-PE negative and 7-ADD positive) are not included in the table.

apoptosis. In the following investigations we mainly focused on OST cells, although some experiments were also carried out with LM8 cells.

3.3. Caspase-3 Assay in OST Cells after Adding ESA. The activity of caspase-3 in OST cells was measured by using the caspase-3 assay in combination with the caspase-3 inhibitor ZVAD-FMK, as outlined in Section 2.5. The values reported on the y-axis of Figure 3 are proportional to the amount (i.e., the activity) of expressed caspase-3, arising from the induced apoptosis in the OST cells. Upon addition of ESA, a 2.3-fold increase in caspase-3 activity was observed in comparison with the control (without ESA: only PBS). On the other hand, the addition of ZVAD-FMK inhibited the expressed capase-3 to almost the same level as in the case of the control. These data indicate that ESA induces apoptotic cell death in OST cells, which confirms the independent results presented in Figure 2.

3.4. Examination of the Binding of ESA to OST Cells and to LM8 Cells by Flow Cytometric Measurements. To investigate the binding of ESA (labeled with FITC) to both OST cells and LM8 cells, flow cytometric measurements were performed. As shown previously [4], ESA hardly binds to normal cells. If ESA-FITC binding to cells occurs, a rightward shift of the flow cytometric curve is expected. This, indeed, was observed in the experiments with OST cells and LM8 cells, as shown in Figure 4. The fluorescence intensity of the cells treated with ESA-FITC increased significantly, as compared to the control cells (treated with PBS only). The curve shifts became larger with longer cell-incubation times: with both cell types, the shifts after 12 hours of incubation were larger than the shifts observed after 3 hours. This demonstrates binding of ESA-FITC to both cell types.

3.5. Fluorescence Microscopic Observation of the Binding of ESA to OST Cells That Were Pretreated with Glycosidases. In a previous study it was shown that ESA is a lectin that specifically binds to high-mannose type (HM) N-glycans [5]. The binding of ESA to OST cells that were pretreated with glycosidases was investigated by labeling cell-bound ESA with rhodamine 6G (Rh6G), see Section 2.6.

First, the OST cells were pretreated with glycosidases to cleave sugar chains on the cell surface. Incubation was for 2 hours using one of the following three glycosidases, α-mannnosidase, β-mannnosidase, or endoglycosidase H. The method of Rh6G labeling with ESA was performed by incubating ESA with Rh6G as mentioned in Section 2.6. Then, the ESA labeled with Rh6G was bound to the cells by

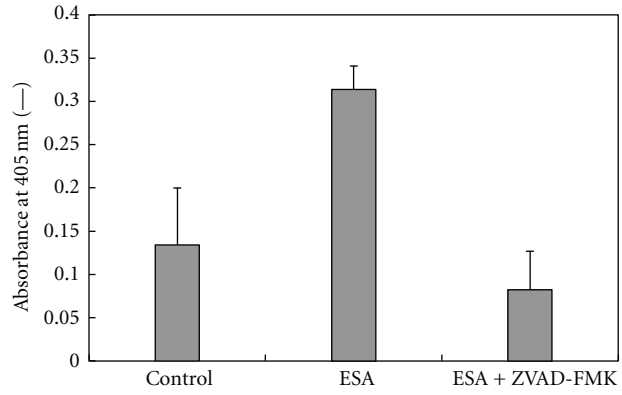

Figure 3: Determination of the caspase-3 activity of OST cells treated with ESA. The OST cells were cultured during 16 hours in D-MEM containing either a solution of 10% FBS and 50 μg/mL ESA in PBS or a solution of 50 μg/mL ESA and ZVAD-FMK (as caspase inhibitor) in PBS. Caspase-3 activity was determined from the absorbance values measured at 405 nm as "activity index" by use of a spectrophotometer. The values are means and standard deviations for three separate measurements.

incubating the cells for 1 hour, followed by a fluorescence microscopic observation of the labeled cells. As shown in Figure 5, non-treated OST cells (as control) displayed Rh6G fluorescence, but other OST cells that were pretreated with a glycosidases showed almost no fluorescence. This means that ESA could not recognize the molecular structure of the sugar-chains on the surface of OST cell that were cleaved by glycosidases; ESA only recognized the native structure of the sugar-chains of the OST cells. Thus, with these experiments it could be demonstrated that ESA specifically binds to OST cells, through recognition of the sugar chains on the surface of the cells.

3.6. Flow Cytometric Analysis of the Specific Binding of ESA to OST Cells Treated with Glycosidases. To confirm the specific binding of ESA to OST cells, a flow cytometric examination was also performed in a similar way as described in Sections 3.4 and 3.5. The results are shown in Figure 6(a) for cells treated with α-mannosidase and β-mannosidase, and in Figure 6(b) for cells treated with endoglycosidase H. In both cases, the decreases in fluorescence intensity in those cells that were treated with a glycosidase, if compared to untreated cells, were obvious. The intensity decrease in the case of treatment with α-mannosidase seemed to be smaller than in the case of β-mannosidase or endoglycosidase H. This is in good agreement with the images shown in Figure 5 obtained with an independent analysis. Weak Rh6G fluorescence was detectable in glycosidase-treated OST cells—although with rather low intensity—only if the treatment was with α-mannosidase. In the other two cases, there was no detectable fluorescence (Figure 5).

3.7. Possible Application of ESA as Sarcoma-Targeting Ligand Immobilized on Span 80 Vesicles. To test whether ESA could be used as osteosarcoma-targeting ligand on a vesicular DDS, Span 80 vesicles with surface bound ESA were prepared, and the interaction of these vesicles with OST cells was compared with the interaction of vesicles that did not have surface bound ESA. Three types of Span 80 vesicles were prepared and tested (see Section 2.9): CV (control vesicles, no ESA), EV (vesicles with immobilized ESA), and EPV (PEGylated vesicles with immobilized ESA). All these vesicles contained encapsulated FITC as fluorescent probe. The vesicles were then mixed with OST cells and incubated, as mentioned in Section 2.9. Then, flow cytometric measurements were performed. As shown in Figure 7, the fluorescence intensity in both cases was higher than for cells treated with CV containing FITC. This means that both types of vesicles with surface bound ESA, EPV, and EV bind to OST cells stronger than CV does. Furthermore, the fluorescence intensity of the cells treated with EPV containing FITC was found to be almost equal to the fluorescence intensity of the cells that were treated with EV containing FITC. Therefore, PEGylation did not hinder the binding of ESA to the sugar chains on the surface of the cells. Thus, Span 80 vesicles with immobilized ESA may be well suited for the development of a DDS for targeting osteosarcoma cells.

3.8. Cytotoxic Effects of EPV against OST Cells. In a final investigation, the anticancer activity of EPV against osteosarcoma cells was examined *in vitro*. The variation of the OST cells viability as a function of the concentration of added ESA (incubation time was 48 hours) is shown in Figure 8. EPV also clearly showed a strong anticancer activity against OST cells, inhibiting proliferation of OST cells completely in a culture medium that contained 2 μg/mL ESA. This result is promising as it shows that PEGylated Span 80 vesicles with immobilized ESA are potentially useful as drug carrier system with endogenous antitumor activity against osteosarcoma. In the ESA concentration range above about 2 μg/mL complete death of the OST cells was observed, as shown in Figure 8. This demonstrates that EPV not only can function as targeting unit (see Section 3.7), but also efficiently inhibit OST cell growth.

4. Discussion

It is known that the carbohydrate structures vary among the different cancer cell lines [27, 28]. In this work, we report about our findings that ESA has anticancer activity not only against carcinoma [4] but also against sarcoma. This conclusion is based on the observation that both types of osteosarcoma cells, OST cells and LM8 cells, were significantly destroyed if incubated with ESA at a concentration of 50 μg/mL during a period of 24 hours, as shown in Figure 1(a), and also destroyed completely if during 48 hours, as shown in Figure 1(b).

The effect of ESA on the viabilities of osteosarcroma cells was compared with the effect of ESA carcinoma cells studied previously [4], see S-2, Supplementary Material, available online at doi:10.1155/2012/842785. The Supplementary Material contains (i) data on the cytotoxicity and binding affinity of free ESA and EV for normal cells and for

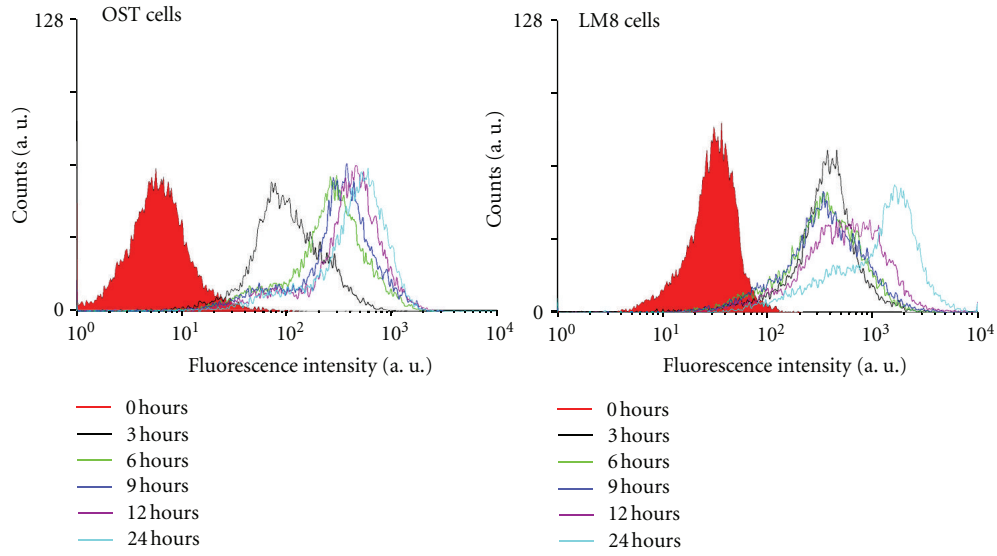

Figure 4: Specific binding of ESA to either OST cells or LM8 cells, as measured by using a flow cytometer. The cells were cultured with 10% FBS D-MEM containing FITC-labeled ESA at 37°C in a humidified atmosphere of 5% CO_2. After incubation for 0, 3, 6, 9, 12, and 24 hours, the cells were washed with PBS, followed by evaluation of the amount of ESA which was bound to the cells.

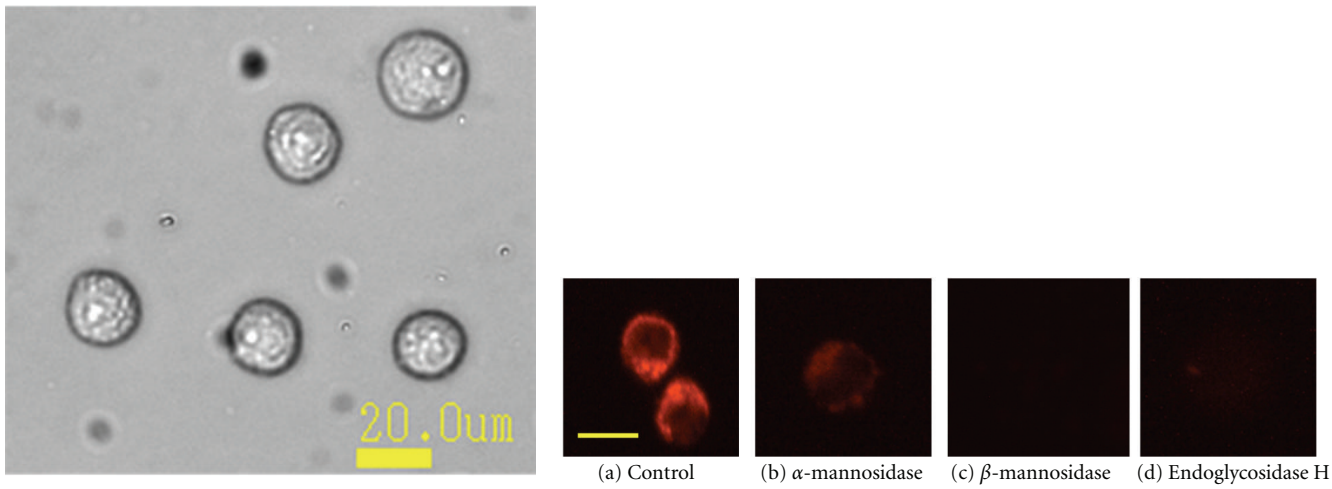

Figure 5: (A) Bright field image of OST cells. The diameter of the OST cells was 19.9 μm ± 1.5 μm. (B) Fluorescence microscopic observations of the binding of ESA to OST cells. The cells were pretreated for 2 hours with different glycosidases and then incubated with rhodamine 6G-labeled ESA. (a) Untreated cells (as control); (b) pretreated with α-mannosidase; (c) pretreated with β-mannosidase; and (d) pretreated with endoglycosidase H. After the pretreatment with the glycosidases, which led to a cleavage of some of the sugar chains on the surface of the OST cells, incubation of the pretreated cells with rhodamine 6G-labeled ESA occurred during 1 hour at 37°C in a humidified atmosphere of 5% CO_2. Scale bar shows approximately 20 μm. This scale was calculated from the bright field image.

cancer cells; and (ii) a comparison of the effect of free ESA on the cell viabilities of osteosarcoma and carcinoma cells. This comparison indicates that the antiproliferative activity of free ESA in sarcoma cells is higher than in carcinoma cells, which may be related to differences in the carbohydrate structure of the surface of the two cell types. This point needs to be investigated further.

We already reported [4] that ESA specifically binds to high mannose type sugar chains in the case of carcinoma cells, inducing apoptotic cell death. As shown in Figure 4 of the flow cytometric measurements, it was confirmed that ESA bound not only to carcinoma cells but also to sarcoma cells like OST cells and LM8 cells. Moreover, pretreatment of OST cells with different types of glycosidases, which cleaved the sugar chains on the surface of the OST cells, significantly decreased the binding of ESA to the cells (Figures 5 and 6). These results provide evidence that binding of ESA to the sarcoma cells occurs through specific interactions

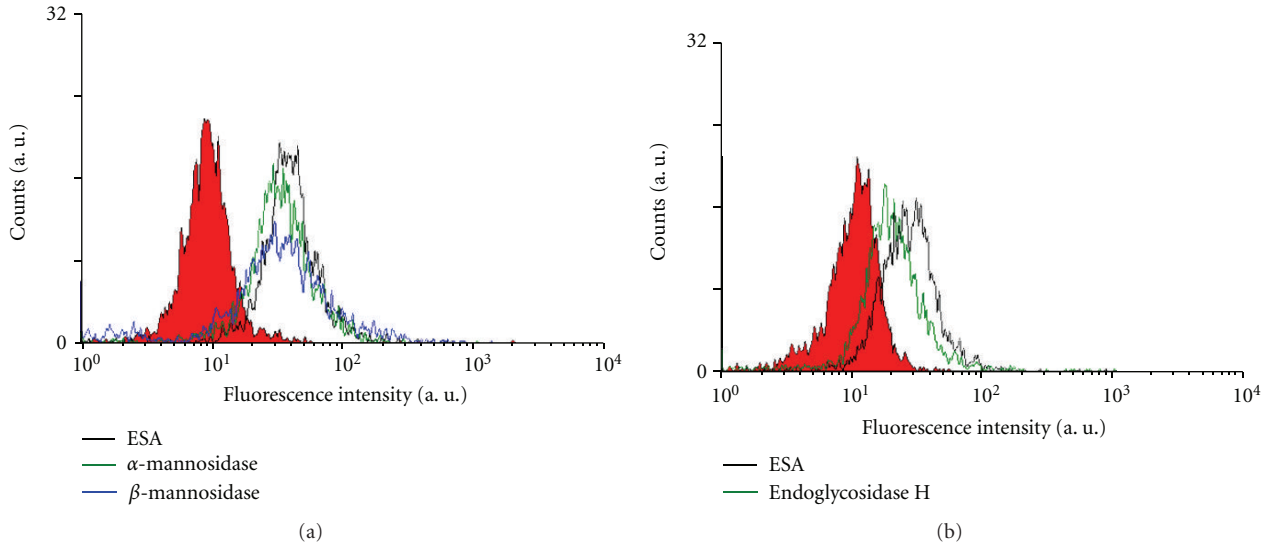

Figure 6: Flow cytometric analysis of OST cells that were pretreated with a glycosidase as described in the legend of Figure 5 and then incubated with FITC-labeled ESA (balck line). Pretreatment was with either α-mannosidase (green line) or with β-mannosidase (blue line) (a), or with endoglycosidase H (green line) (b). The filled curves represent control measurements with untreated cells. PBS was added to OST cells as control (red fill).

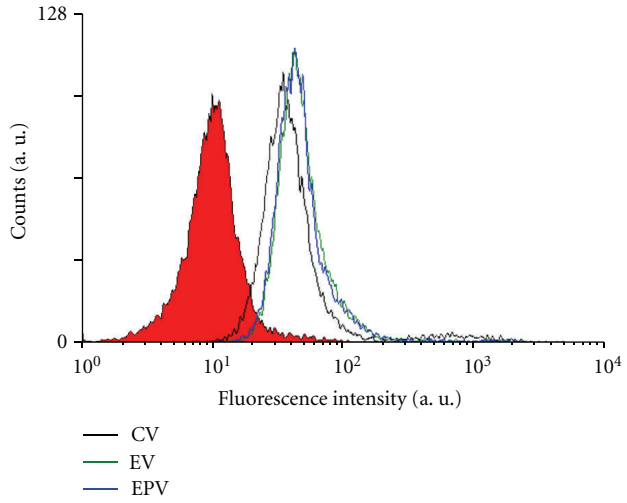

Figure 7: Flow cytometric analysis of the interaction between OST cells and different types of Span 80 vesicles containing entrapped FITC: control vesicles (CV, black line), vesicles with immobilized ESA (EV, green line), and PEGylated vesicles with immobilized ESA (EPV, blue line). Before analysis, the OST cells were incubated with the vesicles during 15 min at 37°C in a humidified atmosphere of 5% CO_2. PBS was added to OST cells as control (red fill).

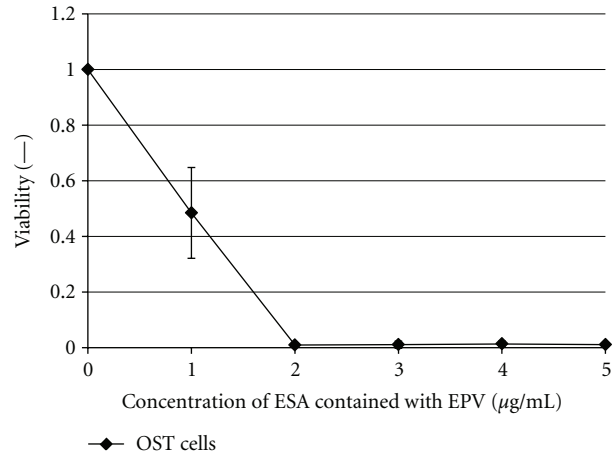

Figure 8: Cytotoxic effect of ESA in EPV on OST cells. The cell viability was evaluated with the propidium iodide staining. The OST cells were incubated during 48 hours at 37°C with EPV at the given concentration in D-MEM containing 10% FBS in a humidified atmosphere of 5% CO_2. Mean values and standard deviations for three separate measurements are plotted.

between ESA and carbohydrate chains on the cell surface. ESA exhibited higher affinity towards OST cells as compared to LM8 cells (Figure 4). The reason for this may be due to differences in the carbohydrate structure in the two cell types. This point needs to be also investigated, however, before any clear conclusion about the cell specificity can be drawn.

ESA induces apoptosis in osteosarcoma cells as shown by using the double staining test for Annexin-V and 7-ADD [25–27]. At an elapsing time of 3 hours after adding ESA, apoptosis in both OST cells and LM8 cells was obvious. Moreover, almost all of the OST cells were dead after 24 hours incubation with ESA (50 μg/mL), as shown in Figure 2(a). The number of LM8 cells appearing in the upper right region of the plot did not seem to increase (see Figure 2(b)). This apparent failure in staining is related to the apoptotic progress of the cell, and the apoptosis couldn't be correctly measured with the double staining method. In fact, in the analysis of the flow cytometry, in the LM8 cells often

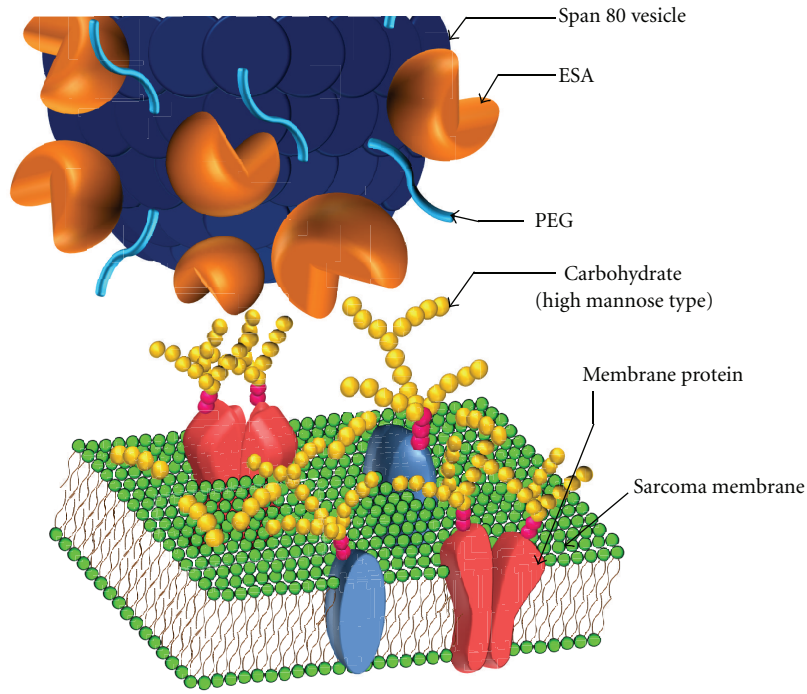

Figure 9: Graphical imaginary view indicating the binding between carbohydrate chains of high mannose type on sarcoma membrane and the ESA on the PEGylated Span 80 vesicle.

fragmented and therefore counted correctly, when incubated during 24 hours with ESA (data not shown).

Induction of apoptosis in OST cells by ESA was demonstrated by measuring the expression of caspase-3 (see Figure 3). It was shown that the addition of ESA to OST cells led to apoptosis in cells of sarcoma, because the caspase-3 expression is known to be directly related to the apoptosis mechanism [29]. Thus, ESA may be used as efficient tumor-targeting ligand and apoptosis inducer in a DDS in a sarcoma therapy. As shown in our previous work, PEGylated Span 80 vesicles with immobilized ESA (abbreviated as EPV) are rather promising drug carriers for the treatment of carcinoma cancers [6]. Therefore, the use of EPV may be expanded to the treatment of sarcoma.

The ability of ESA, and EPV, as targeting unit and apoptosis inducer in the case of cells of sarcoma was examined further by flow cytometry as well as cell viability measurements, choosing OST cells as typical sarcoma cell type. As shown with the flow cytometric measurements in Figure 6, targeting of ESA to OST cells *in vitro* was observed from the shift of the flow cytometric curve to the right hand side (see Figure 6). Furthermore, comparing EPV with CV in Figure 7 (as mentioned in Section 3.7.), it was found that the macromolecular structure of PEG on the vesicle surface did not hinder OST cell binding of ESA which was localized on the vesicle surface together with PEG. This is a very important phenomenon. It may be due to the high mobility of both ESA and PEG, because of the high membrane fluidity of Span 80 vesicles, as mentioned previously [19, 30]. Therefore, the use of Span 80 vesicles as DDS is very effective. In addition, EPV showed anticancer activity against OST cells since after an elapsing time of about 48 hours after the addition of EPV at an ESA concentration of 2 μg/mL, the OST cell viability was reduced to almost zero, as shown in Figure 8. It seems that the anticancer activities of ESA against OST cells in the vesicle system (Figure 8) is stronger than those in free ESA system (Figure 1). However, the activities of the two systems cannot be compared directly, because either the incubation time or the ESA concentration was different in the two systems. For example, for a direct comparison of the activities of the two systems against OST cells, the time-course of the viability upon addition of free ESA system (Figure 1(b)) should be measured at [ESA] = 2 μg/mL; at this concentration and after an incubation time of 48 hours, the cells were no more viable if the vesicles system was used (Figure 8). Unfortunately, the data obtained from measurements with free ESA at this low concentration showed great variations.

On the other hand, we have already examined [4, 6] the cytotoxicity of either ESA or EV for various carcinoma cancer cells and normal cells, followed by examining the binding affinities of ESA and EV to the cells. In these experiments, Colo201 (human colon adenocarcinoma), MCF-7 (human breast adenocarcinoma), HeLa (human cervix adenocarcinoma), and HB4C5 cells (human hybridoma cell line) were used as carcinoma cells, and MCF10-2A (non-tumorigenic epitherial cell line) and normal fibroblasts (from the umbilical cord) were also used as normal cells. ESA and EV showed cytotoxicity against carcinoma cells but not against normal cells, see S-1, Supplementary Material.

Figure 9 is a graphical imaginary view indicating the binding between carbohydrate chains of high mannose type

on sarcoma membranes and ESA on the PEGylated Span 80 vesicle.

5. Conclusions

In the study presented, the following main results were obtained: (i) ESA specifically binds to sarcoma cells and induces apoptotic death of the cells; (ii) the antiproliferative activity of ESA in sarcoma is higher than the activity in carcinoma; (iii) ESA immobilized onto PEGylated Span 80 vesicles (EPV) shows antitumor activity against OST cells without any entrapped antitumor agents. Furthermore, in a previous study, it was already revealed that ESA and EV (ESA-immobilized on Span 80 vesicles) hardly bind to normal cells (either MCF10-2A (non-tumorigenic epithelial cells) or normal fibroblasts from the umbilical cord); and cytotoxicity caused by ESA and EV was not observed for these normal cells. Therefore, ESA has considerable potential as novel type of targeting ligand against sarcoma.

Based on all these findings, we propose using EPV as possible DDS not only for the targeted treatment of carcinoma, but also for the targeted treatment of sarcoma. Furthermore, the administration of PEGylated Span 80 vesicles with immobilized ESA, in which anticancer drugs are encapsulated, is expected to express more effective antitumor activity against sarcoma as compared to empty EPV.

We already performed first *in vivo* experiments by using either EV or EPV with entrapped anticancer drugs toward the development of a sarcoma therapy. The results will be presented in a separate paper.

Conflict of Interests

No author has a financial conflict of interests to report.

Acknowledgments

This study was partly supported by the Grant-in-Aids for Research for Promoting Technological Seeds (no. 14-024 (type A) and no. 14-B03 (type B)) from Japan Science and Technology Agency (JST). We thank Dr. Yousuke Omokawa (Center for Marine Environmental Studies, Ehime University, Japan) for all the inspiring discussions on this study. The authors also thank the graduate students (Department of Materials Science and Biotechnology, Ehime University) of Mr. Hiroyuki Ohsawa, Mr. Fuminobu Moriki, and Miss Mayumi Ni-imura for their help in the microscopic and flow cytometric measurements and in the determination of the caspase-3 activity and the cell culture studies. The authors are also very grateful to Professor Takuya Sugahara and Professor Koichi Akiyama (Faculty of Agriculture, Ehime University) for the extraction of ESA from *Eucheuma serra*.

References

[1] M. A. Friedman and S. K. Carter, "The therapy of osteogenic sarcoma: current status and thoughts for the future," *Journal of Surgical Oncology*, vol. 4, no. 5, pp. 482–510, 1972.

[2] M. P. Link, A. M. Goorin, M. Horowitz et al., "Adjuvant chemotherapy of high-grade osteosarcoma of the extremity: updated results of the Multi-Institutional Osteosarcoma Study," *Clinical Orthopaedics and Related Research*, no. 270, pp. 8–14, 1991.

[3] A. Kawakubo, H. Makino, J. I. Ohnishi, H. Hirohara, and K. Hori, "The marine red alga *Eucheuma serra* J. Agardh, a high yielding source of two isolectins," *Journal of Applied Phycology*, vol. 9, no. 4, pp. 331–338, 1997.

[4] T. Sugahara, Y. Ohama, A. Fukuda, M. Hayashi, A. Kawakubo, and K. Kato, "The cytotoxic effect of *Eucheuma serra* agglutinin (ESA) on cancer cells and its application to molecular probe for drug delivery system using lipid vesicles," *Cytotechnology*, vol. 36, no. 1–3, pp. 93–99, 2001.

[5] K. Hori, Y. Sato, K. Ito et al., "Strict specificity for high-mannose type N-glycans and primary structure of a red alga *Eucheuma serra* lectin," *Glycobiology*, vol. 17, no. 5, pp. 479–491, 2007.

[6] Y. Omokawa, T. Miyazaki, P. Walde et al., "In vitro and in vivo anti-tumor effects of novel Span 80 vesicles containing immobilized *Eucheuma serra* agglutinin," *International Journal of Pharmaceutics*, vol. 389, no. 1-2, pp. 157–167, 2010.

[7] Q. Yan, Y. Li, Z. Jiang, Y. Sun, L. Zhu, and Z. Ding, "Antiproliferation and apoptosis of human tumor cell lines by a lectin (AMML) of *Astragalus mongholicus*," *Phytomedicine*, vol. 16, no. 6-7, pp. 586–593, 2009.

[8] B. Liu, H. J. Bian, and J. K. Bao, "Plant lectins: potential antineoplastic drugs from bench to clinic," *Cancer Letters*, vol. 287, no. 1, pp. 1–12, 2010.

[9] V. Kumar, A. K. Abbas, N. Fausto, and R. N. Mitchell, *Robbins and Cotran Pathologic Basis of Disease*, ELSEVIER, The Nederlands, 8th edition, 2009.

[10] R. A. Weinberg, "The retinoblastoma protein and cell cycle control," *Cell*, vol. 81, no. 3, pp. 323–330, 1995.

[11] J. J. Stastny and T. K. Das Gupta, "Isolation and analysis of lectin-reactive sarcoma-associated membrane glycoproteins," *Anticancer Research*, vol. 14, no. 2, pp. 587–591, 1994.

[12] J. P. Thiery and J. P. Sleeman, "Complex networks orchestrate epithelial-mesenchymal transitions," *Nature Reviews Molecular Cell Biology*, vol. 7, no. 2, pp. 131–142, 2006.

[13] J. P. Their, "Epithelial-mesenchymal transitions in tumor progression," *Nature Reviews Cancer*, vol. 2, no. 6, pp. 442–454, 2002.

[14] K. Kato, P. Walde, N. Koine, Y. Imai, K. Akiyama, and T. Sugahara, "Molecular composition of nonionic vesicles prepared from span 80 or span 85 by a two-step emulsification method," *Journal of Dispersion Science and Technology*, vol. 27, no. 8, pp. 1217–1222, 2006.

[15] K. Kato, T. Ikeda, and M. Shinozaki, "Lipid-membrane characteristics of large lipid-vesicles prepared by two-step emulsification technique and enzymatic NAD^+-recycling in the vesicles," *Journal of Chemical Engineering of Japan*, vol. 26, no. 2, pp. 212–216, 1993.

[16] K. Kato and K. Hirata, "Water permeability through the lipid membrane of a giant vesicle prepared by a two-step emulsification technique," *Solvent Extraction Research and Development*, vol. 1996, no. 3, pp. 62–73, 1996.

[17] K. Kato and J. Hirashita, "Preparation and function of a hybrid-type vesicle modified by Concanavalin A for a DDS directed toward a cancer therapy," in *Biochemical Engineering Marching Toward the Century of Biotechnology*, Z. Y. Shen, F. Ouyang, J. T. Yu, and Z. A. Cao, Eds., pp. 592–596, Tsinghua University Press, Beijing, China, 1997.

[18] K. Kato, P. Walde, H. Mitsui, and N. Higashi, "Enzymatic activity and stability of D-fructose dehydrogenase and sarcosine dehydrogenase immobilized onto giant vesicles," *Biotechnology and Bioengineering*, vol. 84, no. 4, pp. 415–423, 2003.

[19] K. Kato, P. Walde, N. Koine et al., "Temperature-sensitive nonionic vesicles prepared from Span 80 (sorbitan monooleate)," *Langmuir*, vol. 24, no. 19, pp. 10762–10770, 2008.

[20] T. Sugahara, S. Kawashima, A. Oda, Y. Hisaeda, and K. Kato, "Preparation of cationic immunovesicles containing cationic peptide lipid for specific drug delivery to target cells," *Cytotechnology*, vol. 47, no. 1–3, pp. 51–57, 2005.

[21] Y. Ohama, Y. Heiki, T. Sugahara et al., "Gene transfection into HeLa cells by vesicles containing cationic peptide lipid," *Bioscience, Biotechnology and Biochemistry*, vol. 69, no. 8, pp. 1453–1458, 2005.

[22] Y. Fukuda, T. Sugahara, M. Ueno et al., "The anti-tumor effect of Euchema serra agglutinin on colon cancer cells in vitro and in vivo," *Anti-Cancer Drugs*, vol. 17, no. 8, pp. 943–947, 2006.

[23] K. Inoue, T. Yamakawa, and S. Nojima, *Seikagaku Jikken Kouza*, vol. 3, Shishitsu no Kagaku, Tokyo Kagaku Dojin, Japan, 1974.

[24] C. Souchier, M. Ffrench, M. Benchaib, R. Catallo, and P. A. Bryon, "Methods for cell proliferation analysis by fluorescent image cytometry," *Cytometry*, vol. 20, no. 3, pp. 203–209, 1995.

[25] M. O'Brien and W. E. Bolton, "Comparison of cell viability probes compatible with fixation and permeabilization for combined surface and intracellular staining in flow cytometry," *Cytometry*, vol. 19, no. 3, pp. 243–255, 1995.

[26] M. van Engeland, L. J. Nieland, F. C. Ramaekers, B. Schutte, and C. P. Reutelingsperger, "Annexin V-affinity assay: a review on an apoptosis detection system based on phosphatidylserine exposure," *Cytometry*, vol. 31, no. 1, pp. 1–9, 1998.

[27] Y. J. Kim and A. Varki, "Perspectives on the significance of altered glycosylation of glycoproteins in cancer," *Glycoconjugate Journal*, vol. 14, no. 5, pp. 569–576, 1997.

[28] E. Gorelik, U. Galili, and A. Raz, "On the role of cell surface carbohydrates and their binding proteins (lectins) in tumor metastasis," *Cancer and Metastasis Reviews*, vol. 20, no. 3-4, pp. 245–277, 2001.

[29] M. O. Hengartner, "The biochemistry of apoptosis," *Nature*, vol. 407, no. 6805, pp. 770–776, 2000.

[30] K. Hayashi, T. Shimanouchi, K. Kato, T. Miyazaki, A. Nakamura, and H. Umakoshi, "Span 80 vesicles have a more fluid, flexible and "wet" surface than phospholipid liposomes," *Colloids and Surfaces B*, vol. 87, no. 1, pp. 28–35, 2011.

Hindawi Publishing Corporation
Journal of Drug Delivery
Volume 2012, Article ID 975763, 10 pages
doi:10.1155/2012/975763

Research Article

Chlorotoxin Fused to IgG-Fc Inhibits Glioblastoma Cell Motility via Receptor-Mediated Endocytosis

Tomonari Kasai,[1] Keisuke Nakamura,[1] Arun Vaidyanath,[2] Ling Chen,[3] Sreeja Sekhar,[1] Samah El-Ghlban,[1] Masashi Okada,[1] Akifumi Mizutani,[1] Takayuki Kudoh,[1] Hiroshi Murakami,[1] and Masaharu Seno[1]

[1] *Department of Medical and Bioengineering Science, Graduate School of Natural Science and Technology, Okayama University, Okayama 7008530, Japan*
[2] *Cell and Cancer Biology Branch, National Cancer Institute, National Institutes of Health, Bethesda, MD 20892, USA*
[3] *Department of Pathology, Tianjin Central Hospital of Gynecology Obstetrics, Tianjin 300100, China*

Correspondence should be addressed to Masaharu Seno, mseno@okayama-u.ac.jp

Received 30 August 2012; Revised 5 November 2012; Accepted 7 November 2012

Academic Editor: Andreas G. Tzakos

Chlorotoxin is a 36-amino acid peptide derived from *Leiurus quinquestriatus* (scorpion) venom, which has been shown to inhibit low-conductance chloride channels in colonic epithelial cells. Chlorotoxin also binds to matrix metalloproteinase-2 and other proteins on glioma cell surfaces. Glioma cells are considered to require the activation of matrix metalloproteinase-2 during invasion and migration. In this study, for targeting glioma, we designed two types of recombinant chlorotoxin fused to human IgG-Fcs with/without a hinge region. Chlorotoxin fused to IgG-Fcs was designed as a dimer of 60 kDa with a hinge region and a monomer of 30 kDa without a hinge region. The monomeric and dimeric forms of chlorotoxin inhibited cell proliferation at 300 nM and induced internalization in human glioma A172 cells. The monomer had a greater inhibitory effect than the dimer; therefore, monomeric chlorotoxin fused to IgG-Fc was multivalently displayed on the surface of bionanocapsules to develop a drug delivery system that targeted matrix metalloproteinase-2. The target-dependent internalization of bionanocapsules in A172 cells was observed when chlorotoxin was displayed on the bionanocapsules. This study indicates that chlorotoxin fused to IgG-Fcs could be useful for the active targeting of glioblastoma cells.

1. Introduction

Glioblastoma is one of the most malignant and consistently fatal brain cancers in adults. Treatment of glioma remains a challenge largely because of its rapid growth rate and the highly invasive nature of this disease, despite incremental advances in surgical and radiation therapies [1]. Glioma cells are considered to require the activation of matrix metalloproteinase (MMP)-2, which degrades the extracellular matrix (ECM) during invasion and migration [2, 3]. In the central nervous system, membrane type MMP-1 (MT1-MMP) has a more important role than MMP-2 during ECM remodeling, migration, infiltration, and invasion of gliomas [4]. MT1-MMP on cell surfaces is replenished by autodegradation or clathrin-dependent internalization, and its concentration is stabilized by the tissue inhibitor of MMP (TIMP)-2 [5, 6]. Malignant human gliomas express membrane-anchored MMPs and their endogenous TIMPs [7–10]. Many MMP inhibitors have been developed for human clinical trials, but effective candidates have not been obtained [10, 11].

Chlorotoxin (CTX) is a 36-amino acid peptide with four disulfide bridges and is derived from *Leiurus quinquestriatus* (scorpion) venom. CTX has been shown to inhibit low-conductance chloride channels in colonic epithelial cells [12]. Several experiments have used CTX to target brain tumors, exploiting its binding affinity to the glioma-specific chloride ion channel complex, MMP-2, and other

proteins [13, 14]. Recently, a conjugate of CTX and fluorescent dye was demonstrated to target brain tumors by visualizing cancer foci *in vivo* [15, 16].

Bionanocapsules (BNCs) are artificial hollow nanoparticles composed of the recombinant envelope L protein of hepatitis B virus, which has a specific affinity for human hepatocytes [17, 18]. To confer BNCs a high affinity for the IgG-Fc domain, the pre-S1 region of L protein was replaced with the ZZ motif in protein A derived from *Staphylococcus aureus* [19, 20]. BNCs displaying anti-human EGFR monoclonal antibodies were delivered successfully to glioma cells in a mouse model of brain tumors [19]. EGFR is expressed not only in tumors but also in normal epithelia; therefore, it may not always be feasible to target brain tumors with EGFR. Thus, we designed a CTX peptide fused to the human IgG-Fc domain (CTX-Fc) in this study to establish a more efficient and specific targeting vehicle for glioblastoma cells.

2. Materials and Methods

2.1. Cell Culture. A human cell line derived from glioblastoma, A172 (RCB2530), was provided by RIKEN BRC through the National BioResource Project of MEXT, Japan. Glioma cells were grown and subcultured in RPMI medium (Sigma-Aldrich, St Louis, MO, USA) supplemented with 10% fetal bovine serum (FBS, PAA Laboratories, Pasching, Austria) in the presence of 100 IU/mL penicillin and 100 μg/mL streptomycin (Nacalai Tesque, Kyoto, Japan). The cells were maintained at 37°C in a humidified incubator with 95% air and 5% CO_2.

2.2. Construction of Expression Plasmids. The expression plasmids for CTX fused to human IgG-Fcs (CTX-Fcs) were constructed as follows. An oligonucleotide coding for the CTX peptide was synthesized by Operon Biotechnologies (Tokyo, Japan) and cloned into pET28b (Novagen, Darmstadt, Germany). The DNA fragment coding human IgG-Fcs was excised from the plasmid pBO593 (coding with a hinge domain) and pBO807 (coding without a hinge domain, [20, 21]) using the restriction endonucleases, AgeI and NotI, and then ligated to the 3′-end of the CTX coding sequence downstream of a T7 promoter to code a dimeric form of CTX-Fc (D-CTX-Fc) and a monomeric form of CTX-Fc (M-CTX-Fc), respectively.

2.3. Expression and Purification of M/D-CTX-Fcs. *Escherichia coli* BL21 (DE3) pLysS (Novagen) was transformed with expression vectors for M/D-CTX-Fcs. Transformants were grown in 1 L of LB medium containing 50 μg/mL kanamycin and 10 μg/mL chloramphenicol at 37°C. Protein expression was induced by 0.4 mM isopropyl 1-thio-β-D-galactopyranoside. After expression induction, the transformants were cultured at 25°C for 16 h, and the bacteria were harvested. Cell pellets were thawed and homogenized in 20 mL of lysis buffer containing 10 mM Tris-HCl (pH 8.0), 10 mM EDTA, 0.2 M NaCl, and 10% sucrose. The inclusion bodies were collected by centrifugation at 12,000 ×g for 20 min. The inclusion bodies were washed three times with 0.5% Triton X-100. The insoluble fraction was resolved in 4 mL of 6 M guanidinium HCl containing 0.1 M Tris-HCl (pH 8.5). The solution was degassed by aspiration while purging the air with nitrogen gas and supplemented with 50 μL of 2-mercaptoethanol. After 1 h incubation at 37°C in a shaking water bath, the mixture was dispersed into a 20-fold volume of refolding buffer containing 10 mM Tris-HCl (pH 8.5), 0.1 M NaCl, and 0.5 mM oxidized glutathione. Refolding was conducted by incubation at 4°C for 18 h. The pH was then adjusted to 7.0 using acetic acid. Insoluble materials were removed by centrifugation at 12,000 ×g for 20 min. The solution containing refolded protein was applied to a cobalt resin column (TALON superflow metal affinity resin, Clontech, Mountain View, CA, USA), after equilibrating with equilibration buffer containing 50 mM phosphate buffer (pH 7.0) and 300 mM NaCl. The column was then washed with equilibration buffer containing 20 mM imidazole and 0.1% Triton X-100. M/D-CTX-Fcs were eluted with elution buffer containing 50 mM phosphate buffer (pH 7.0), 300 mM imidazole, and 300 mM NaCl. The eluted solution was dialyzed three times against phosphate-buffered saline (Dulbecco's formula, hereafter PBS) for 2 h each time. The purity of M/D-CTX-Fcs in the final preparations was assessed by SDS-PAGE, Coomassie Brilliant Blue (CBB) staining, and western blotting.

2.4. Preparation of CTX-Fc-BNCs. We mixed 2 nM (10 μg/mL) ZZ-tagged bionanocapsules (ZZ-BNCs) [19] with M-CTX-Fc or human IgG (Sigma-Aldrich) at a ratio of 1 : 20 and incubated them at 4°C for 1 h in PBS. The precipitates were removed by centrifugation at 12,000 ×g for 5 min.

2.5. Enzyme Immunoassay on Cell Surfaces. The enzyme immunoassay (EIA) was designed to evaluate the binding ability of CTX-Fcs to A172 cell surfaces. Each well of a 96-well plate (Greiner Bio-One, Frickenhausen, Germany) was coated with 10% skim milk (Wako Pure Chemical Industries, Osaka, Japan) in PBS at 25°C for 1 h and washed with PBS. Five thousand A172 cells/well were seeded in RPMI medium supplemented with 10% FBS, 100 IU/mL penicillin, and 100 μg/mL streptomycin. After 20 h of culture, the cells were washed three times with PBS and fixed with 4% paraformaldehyde in PBS. The cells were washed three times with PBS, covered with 10% skim milk in PBS at 25°C for 1 h, and then washed three times with PBS. The cells were incubated with M/D-CTX-Fcs in a range of 0–400 nM in PBS at 25°C for 1 h. The cells were then washed with PBS containing 0.1% Tween-20 (PBST), before adding 100 μL of protein A conjugated to horse radish peroxidase (HRP; Sigma-Aldrich), diluted to 1 : 500, and incubated at 25°C for 1 h. The wells were washed three times with PBST, and 100 μL 3,3′,5,5′-tetramethylbenzidine (TMB) Liquid Substrate System (Sigma-Aldrich) was added to test the peroxidase reaction. After 5 min, the reaction was quenched with 50 μL of 0.5 M sulfuric acid, and the absorbance at 450 nm was measured in each well using a microplate reader

(SH-9000; Corona Electric, Ibaraki, Japan). Each experiment was performed in triplicate, and the mean values and standard deviations were calculated.

2.6. Wound Healing Assay. Thirty thousand A172 cells were seeded into a 24-well plate in RPMI medium supplemented with 10% FBS, 100 IU/mL penicillin, and 100 μg/mL streptomycin. After 20 h incubation, each confluent monolayer was scratched using a 200 μL plastic pipette tip to create a wounded cell-free area and washed with RPMI medium supplemented with 10% FBS. The cells were incubated at 37°C with M/D-CTX-Fcs in a range of 0–300 nM in RPMI medium supplemented with 10% FBS, 100 IU/mL penicillin, and 100 μg/mL streptomycin and photographed at 0 and 12 h using an inverted microscope CKX41 (Olympus, Tokyo, Japan). The digital images were acquired with a digital camera U-CMDA3 (Olympus) using the imaging program DP2-BSW (Olympus). The distances between the edges of cell-free areas were measured using NIH Image J. The migration length was defined as the change in the distance between 0 and 12 h, which was normalized by the change in the absence of the stimulant.

2.7. Cell Migration Assay. The migration of A172 cells was assayed in 24-well plates with 8 μm pore cell culture inserts (BD, Franklin Lakes, NJ, USA). Five hundred microliters of RPMI medium supplemented with 10% FBS were added to each well, and 3×10^4 cells were seeded into each insert. The cells were incubated with M/D-CTX-Fcs in a range of 0–300 nM in RPMI medium supplemented with 1% BSA at 37°C. After 48 h of culture, the insert chambers were removed, and adherent cells on the bottom of each well were counted. The number of migrated cells was normalized by the number of adherent cells in the absence of CTX-Fcs.

2.8. Cell Proliferation Assay. The inhibition of cell growth by M/D-CTX-Fcs was evaluated using a 3-(4, 5-dimethylthiazol-2-yl)-2, 5-diphenyltetrazolium bromide (MTT) cleavage assay with A172 cells. The cells were seeded at 5×10^3 cells/well in 96-well plates in RPMI medium supplemented with 10% FBS. After 20 h of culture, M/D-CTX-Fcs in a range of 0–300 nM were added in triplicate, and the cells were further cultured for 48 h. The cells were then exposed to 5 mg/mL MTT in PBS at a final concentration of 1 mg/mL in culture for 5 h. Formazan crystals formed during the incubation period were dissolved overnight at 37°C by adding 10% SDS containing 20 mM HCl. The absorbance was measured at 570 nm. To assess the viability of cells treated with CTX after 48 h incubation with different concentrations of CTX, the wells were washed twice with RPMI medium supplemented with 10% FBS. The cells were further incubated for 24 h in RPMI medium supplemented with 10% FBS. The viable cells were evaluated using the MTT cleavage assay, as described above.

2.9. Confocal Microscopic Observation. For confocal microscopic observation, A172 cells were grown on 18 mm cover slips (Iwaki, Tokyo, Japan) in 12-well plates. The cells were incubated with 30 nM M/D-CTX-Fcs or 30 nM human IgG-Fc domain [20] in PBS containing 1% BSA for 15 min or 1 h at 4°C or 37°C. The cells were washed twice with PBS to evaluate specific binding to cell surfaces. The cells were fixed with 4% paraformaldehyde in PBS, permeabilized with 0.2% Triton X-100, and blocked with blocking solution containing 10% FBS or 1% BSA in PBS. The cells were washed with PBS and incubated with anti-early endosome antigen-1 (EEA-1) antibody (Cell Signaling Technology, Beverly, MA, USA) for 1 h at 25°C followed by Alexa 555-labelled anti-rabbit IgG (Molecular Probes Inc., Eugene, OR, USA) for 30 min at 25°C. The cells were washed with PBS and incubated with FITC-labeled anti-human IgG-Fc antibody (Sigma-Aldrich) for 30 min at 25°C. After further washes, the nuclei were stained with DAPI (Vector Laboratories Inc., Burlingame, CA, USA), and the cells were visualized using a confocal microscope IX81 (Olympus) with Fluoview FV-1000 (Olympus). To observe the binding of BNCs on cells, the cells were incubated with CTX-Fc-BNCs at 37°C for 1 h. The specific binding of CTX-Fcs was further assessed by competition with a CTX (Sigma-Aldrich). In the competitive assay, the cells were incubated primarily with 300 nM CTX in 1% BSA-PBS at 4°C for 20 min, followed by incubation with CTX-Fc-BNCs in the presence of 300 nM CTX at 37°C for 1 h. The cells were washed with PBS and fixed with 4% paraformaldehyde in PBS, permeabilized with 0.2% Triton X-100, and blocked with blocking buffer. The cells were washed with PBS and incubated with anti-human IgG-Fc antibody labeled with fluorescein isothiocyanate (FITC) (Sigma-Aldrich) for 1 h at 25°C. After further washes, the cells were visualized using a confocal microscope LSM 510 Meta (Carl Zeiss, Jena, Germany) equipped with an argon laser having an excitation laser line of 488 nm coupled with a bandpass filter of 505 nm.

2.10. Assessment of Internalization of CTX-Fc-BNCs. Cellular uptake of CTX-Fc-BNCs was evaluated. A172 cells in 60-mm dishes were washed three times with ice-cold PBS and incubated with 2 nM (10 μg/mL) of CTX-Fc-BNCs, human IgG-BNCs, or M-CTX-Fc for 1 h at 4°C or 37°C. After incubation, the cells were washed three times with ice-cold PBS to remove unbounded BNCs and were collected by treatment with 0.025% trypsin. After centrifugation at 5000 ×g for 5 min, the supernatant was discarded, and the cell pellet was washed three times with ice-cold PBS. The cells were then lysed in lysis buffer, incubated for 20 min on ice, and sonicated twice. The extracts were clarified by centrifugation at 12,000 ×g for 5 min at 4°C. Twenty microliters of anti-HBsAg microbead suspension were added to the extracts, and this mixture was incubated overnight at 4°C. After centrifugation at 12,000 ×g for 30 s at 4°C, the beads were washed three times in PBS, suspended in Laemmli buffer supplemented with β-mercaptoethanol, heated for 5 min at 95°C, and subjected to SDS-PAGE followed by western blotting.

2.11. Western Blotting and Image Analysis. Proteins resolved on SDS-PAGE were transferred to a polyvinylidene difluoride (PVDF) membrane (Millipore, Billerica, MA, USA). The membrane was blocked with 10% skim milk in 10 mM

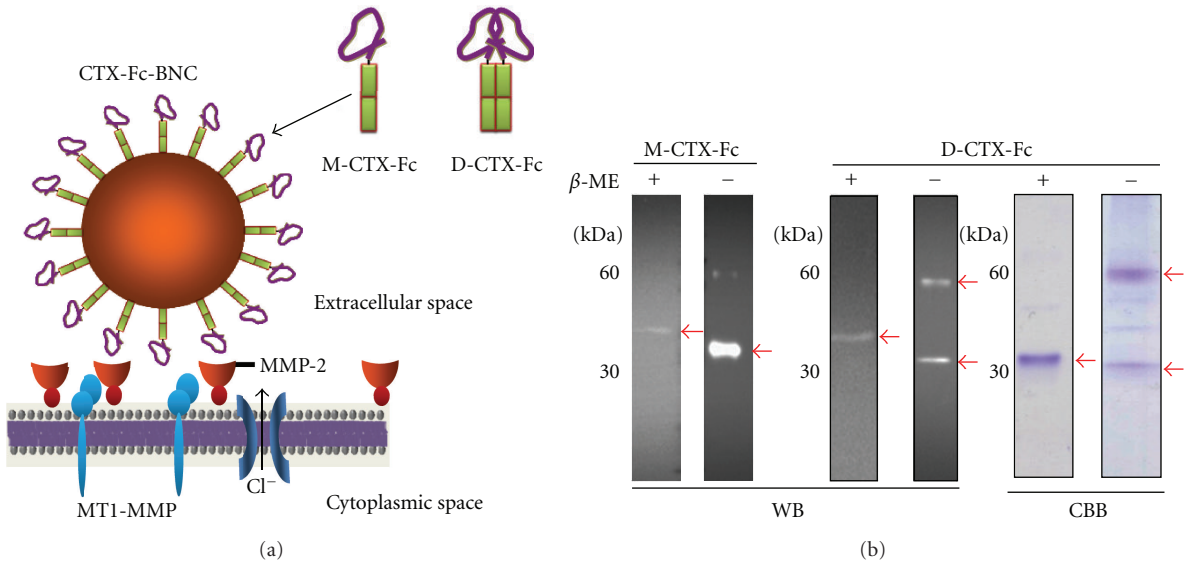

Figure 1: Design and preparation of M/D-CTX-Fcs. (a) Schematic diagrams of monomeric and dimeric CTX-Fcs and the multivalent display of M-CTX-Fc on the surface of ZZ-BNCs. (b) Reduced and nonreduced forms of M/D-CTX-Fcs. M/D-CTX-Fcs were subjected to SDS-PAGE and western blotting. Anti-human-IgG-Fc antibody reacted with the purified M/D-CTX-Fcs without significant degradation. Arrows indicate the purified protein. β-ME: beta-mercaptoethanol; WB: western blotting; CBB: Coomassie Brilliant Blue staining.

Tris-HCl (pH 7.4), 150 mM NaCl containing 0.1% Tween-20 (TBST). The blots were probed with anti-human IgG mouse monoclonal antibody conjugated with HRP (Life technologies, Carlsbad, CA, USA) diluted to 1 : 500 in TBST containing 10% skim milk. The HRP signal was developed using a Western Lightning Plus-ECL chemiluminescence reagent (PerkinElmer, Waltham, MA, USA), and the intensities of the bands were visualized using a Light-Capture II cooled CCD camera system (ATTO, Tokyo, Japan). The relative intensities of the blots were quantitatively analyzed using NIH Image J.

2.12. Statistical Analysis. The results were expressed as means ± standard deviations from at least three independent experiments. The data were analyzed using Student's t-test. $P < 0.05$ was considered statistically significant.

3. Results

3.1. Preparation of M/D-CTX-Fcs. Schematic representations of M/D-CTX-Fcs and ZZ-BNCs displaying M-CTX-Fcs are shown in Figure 1(a). The His-tagged CTX-Fc fusion protein was designed as a CTX peptide fused to the amino terminus of the human IgG-Fc domain with/without a hinge domain. The CTX-Fcs expressed in *E. coli* were observed as monomers of approximately 30 kDa under the reducing condition, whereas CTX-Fcs with a hinge domain were observed as dimers of approximately 60 kDa under the nonreducing condition, which was confirmed using CBB staining or western blotting (Figure 1(b)).

3.2. Intracellular Localization of M/D-CTX-Fcs in A172 Cells. Because of the high expression levels of MMP-2 [22], we evaluated the binding capabilities of M/D-CTX-Fcs on the surface of A172 glioblastoma cells. When the cells were incubated with M/D-CTX-Fcs at 4°C, the fluorescence from anti-human IgG labeled with FITC indicated the localization of the fused proteins on the plasma membrane. However, when the cells were incubated at 37°C, the fluorescence indicated that M/D-CTX-Fcs were localized intracellularly in A172 cells (Figure 2(a)). In contrast, the human IgG-Fc domain without a CTX domain produced no fluorescence at 4°C or 37°C indicating the specific binding of the CTX moiety to A172 cell surfaces (see Figure S1 in Supplementary Materials available online at doi:10.1155/2012/975763). We quantitatively evaluated the cell surface binding affinity by assaying sequentially diluted M/D-CTX-Fcs using the A172 cells fixed in EIA plates. The results showed that M-CTX-Fc had a higher affinity than D-CTX-Fc and that 100 nM of M-CTX-Fc saturated the binding (Figure 2(b)).

3.3. Effect of M/D-CTX-Fcs on the Migration of A172 Cells. The effect of M/D-CTX-Fcs on the migration of A172 cells was assessed (Figure 3(a)). Although M-, D-CTX-Fcs, and CTX at a concentration of 300 nM significantly inhibited the migration of the cells, M-CTX-Fc exhibited the inhibition clearly depending on the concentration. In the wound healing assay, the effect of inhibition by both M- and D-CTX-Fcs appeared to be dose dependent in the range of 3–300 nM (Figure 3(b)). The results showed that M-CTX-Fc had a more efficient inhibitory effect than D-CTX-Fc.

We then evaluated the effects of M/D-CTX-Fcs on the proliferation and viability of A172 cells. M-CTX-Fc strongly suppressed the cell viability compared with D-CTX-Fc and CTX (Figure 4(a)). IC_{50} was estimated at around 100 nM. After treatment with 300 nM M/D-CTX-Fcs for 48 h, the growth of cells resumed in the next 24 h when the medium

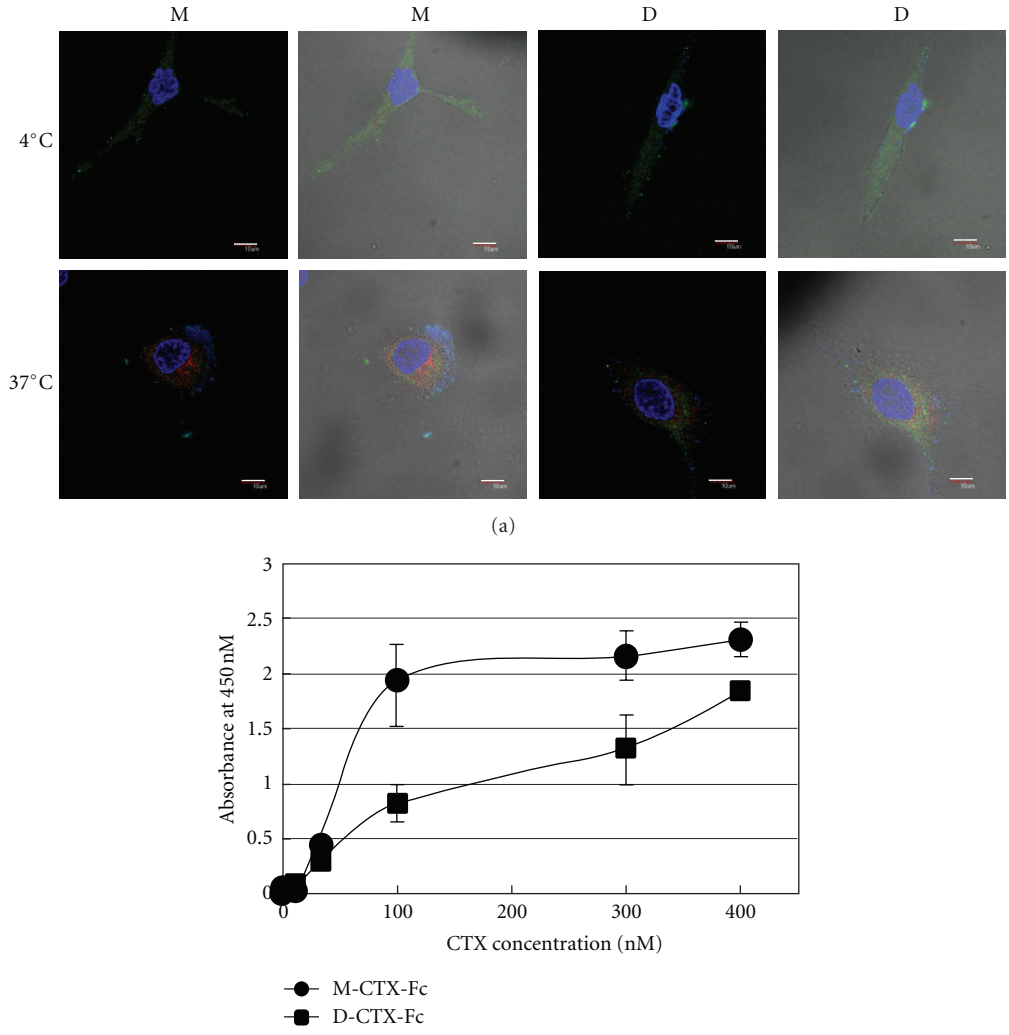

Figure 2: Immunofluorescence image and binding assay for M/D-CTX-Fcs using A172 cells. (a) The M/D-CTX-Fcs attached to cell surfaces at 4°C (upper). Fifteen minutes incubation at 37°C promoted the internalization of M/D-CTX-Fcs into cells (lower). The cells were stained with anti-human IgG antibody labeled with FITC, anti-EEA1 antibody and anti-rabbit IgG antibody labeled with alexa-555, and DAPI. Left: fluorescence image; right; composite image. M: M-CTX-Fc; D: D-CTX-Fc. Bars = 10 μm. (b) The binding ability of M/D-CTX-Fcs was evaluated by EIA. A172 cells were fixed on EIA plates and exposed to M/D-CTX-Fcs. The affinity of M-CTX-Fc for cell surfaces was higher than that of D-CTX-Fc.

was replaced with a medium without M/D-CTX-Fcs or CTX (Figure 4(b)).

3.4. Internalization of CTX-Fc-BNCs. The M-CTX-Fc was multivalently displayed on the surface of ZZ-BNCs, thereby exploiting the affinity of the ZZ peptide for the IgG-Fc region [20]. CTX-Fc-BNCs (2 nM, 10 μg/mL) were incubated with A172 cells at 37°C for 1 h, and the specific binding of CTX-Fc-BNCs was observed competing with free CTX (Figure 5(a)). To evaluate the internalization of CTX-Fc-BNCs, the cells were incubated with M-CTX-Fc, human IgG-BNCs, or CTX-Fc-BNCs at 37°C or 4°C. The incubation of cells at 37°C facilitated the intracellular localization of BNCs, indicating that the temperature-dependent internalization was attributable to a membrane-dependent mechanism (Figures 5(b) and 5(c)).

The mechanism of uptake of CTX-Fc-BNCs was assessed in A172 cells using endocytotic pathway inhibitors (Figure 6). To determine the effective concentration of CPZ, the cells were incubated with 2 nM of CTX-Fc-BNCs and CPZ in the range of 0–100 nM (Vaidyanath et al. 2011 [20], Figure S2). One hundred nanomolar of CPZ effectively inhibited the internalization of CTX-Fc-BNCs in A172 cells. The cells were treated with CPZ, an amphiphilic drug that inhibits the clathrin-mediated pathway, and the internalization of CTX-Fc-BNCs was reduced to the same level as that of human IgG-BNCs.

4. Discussion

Migration of glioma cells is considered to be correlated with MMP-2 expression and activity [2, 3]. Membrane-associated

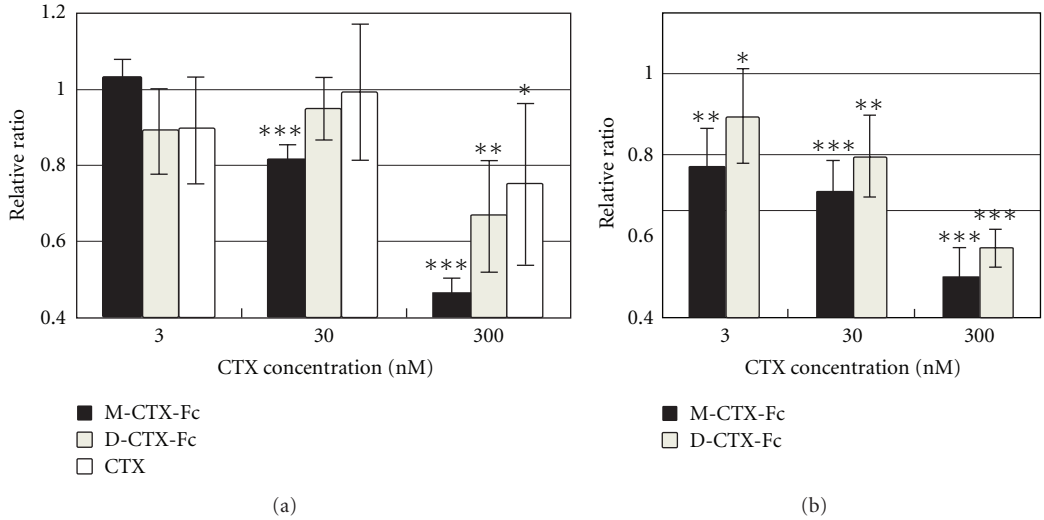

Figure 3: Cell migration and wound healing assays. (a) The effect of M/D-CTX-Fcs on the migration of A172 cells was assessed using a PET track-etched membrane culture insert (pore size, 8.0 μm). The cells were incubated with M/D-CTX-Fcs in the range of 0–300 nM. Translocated cell numbers were normalized against those in the absence of CTX. The results are shown as means ± SD. (b) The inhibition of cell migration by M/D-CTX-Fcs was assayed by wound healing. The effect on migration was evaluated based on the change in the distance. The data (mean ± S.D) presented are from three independent experiments. ($^*P < 0.1$, $^{**}P < 0.05$, $^{***}P < 0.01$).

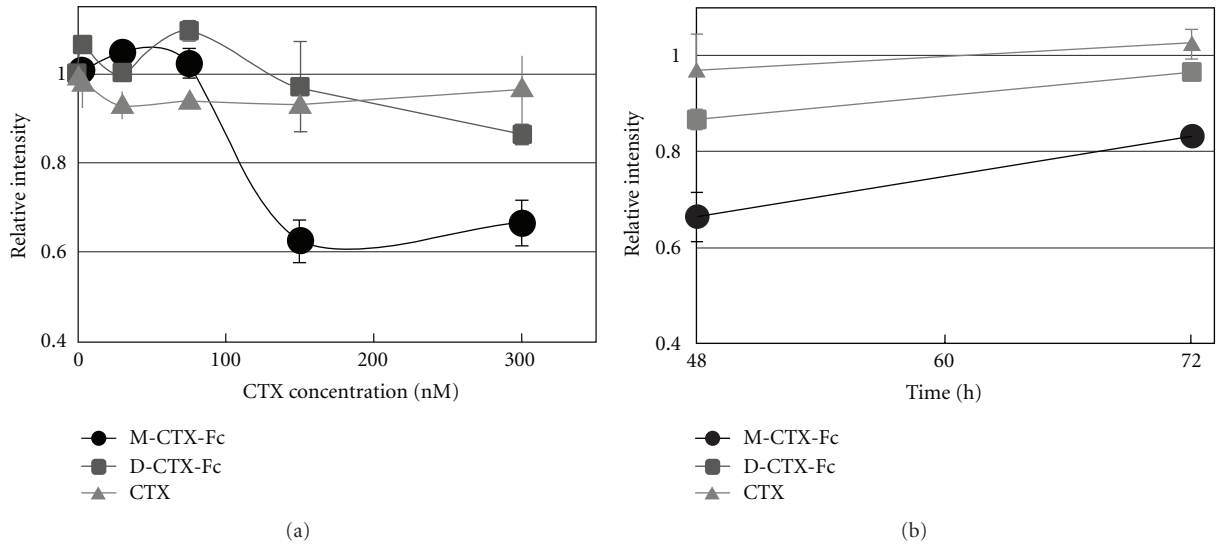

Figure 4: Proliferation inhibition activity. (a) The inhibition of cell growth in the presence of M/D-CTX-Fcs for 48 h. (b) The viable cells at 48 h were kept cultured without M/D-CTX-Fcs up to 72 h. Cell numbers in each well were assessed by MTT assay. The absorbance at 570 nm corresponding to the initial number of the cells was defined as 1.

MT1-MMP mediates proteolysis and activates the precursor of MMP-2 (pro-MMP-2), which localizes on the cell surface, and these events occur at the invasive edge of tumor cell nests [6, 23, 24]. Most MMPs have a hemopexin C-terminal domain (C domain), which is linked to the C terminus of the catalytic domain via a flexible proline-rich linker peptide [25–27]. It is considered that MMP-2 contributes to migration, invasion, translocation, and malignancy. In glioma cells, it was reported that CTX inhibits cell invasion by reducing MMP2 activity [13]. In addition, MMP-2 is associated with cell signaling by binding to integrins directly. The proteolytically activated form of the C terminus of MMP-2 can bind integrins on melanoma cells and blood vessels [28]. An angiogenic regulator, angiopoietin 2, induces invasion by stimulating MMP-2 expression and secretion in glioma cells [29]. In cancer, MMPs, such as MMP-2 and MT1-MMP, associate with tumor growth, tissue remodeling, tissue invasion, and metastasis. We designed and purified M/D-CTX-Fcs (Figure 1). M/D-CTX-Fcs were attached to A172 cell surfaces, and they localized intracellularly at 37°C (Figure 2). Furthermore, M/D-CTX-Fcs inhibited cell migration and proliferation in a dose-dependent manner (Figures 3 and 4). Collectively, CTX was shown to inhibit and arrest the cell proliferation machinery but without being

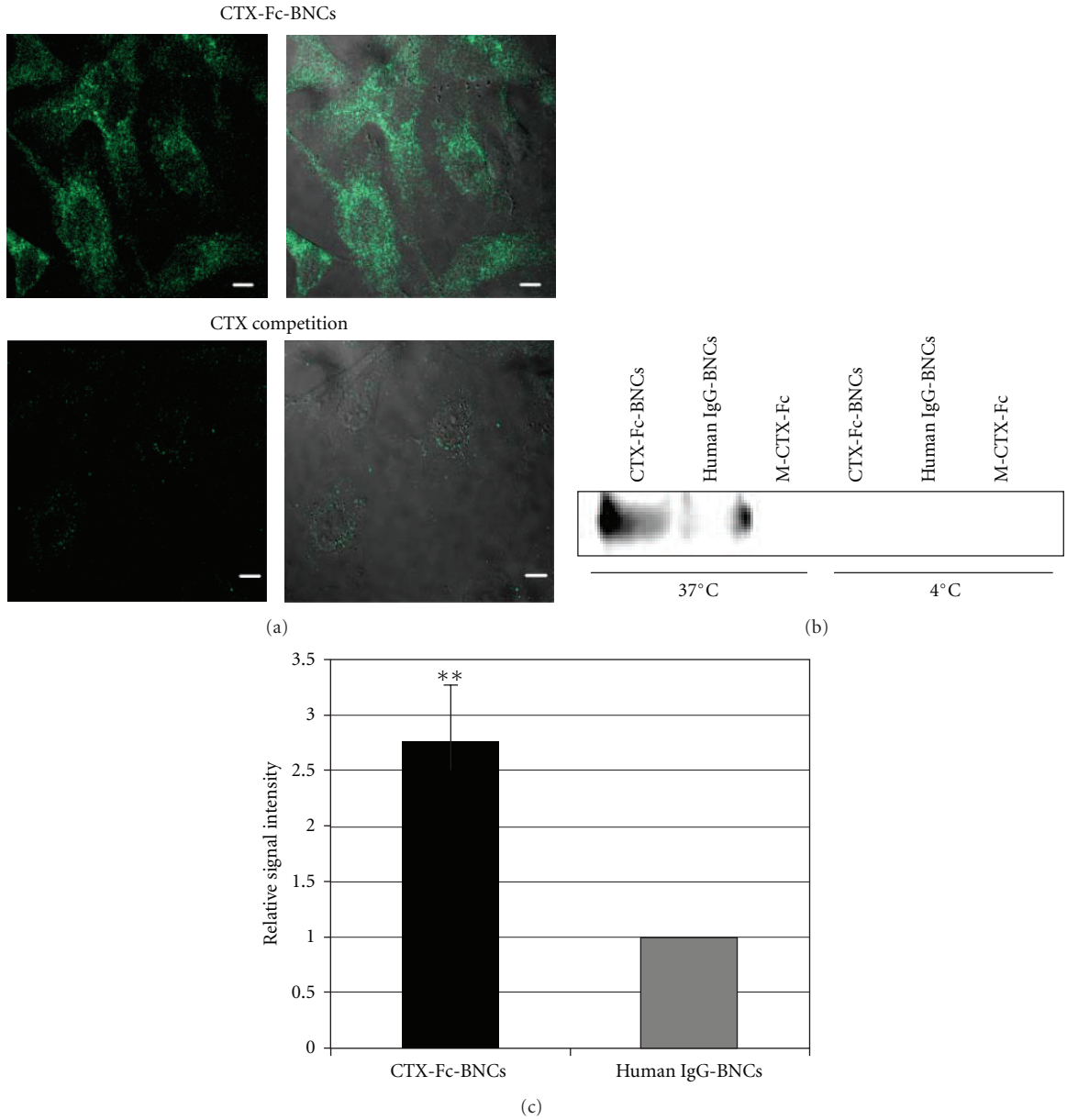

Figure 5: Evaluation of CTX-Fc-BNCs internalized by A172 cells. (a) A172 cells were incubated with CTX-Fc-BNCs at 37°C. In "CTX competition", the cells were treated primarily with CTX at 4°C for 20 min before incubating with CTX-Fc-BNCs. The cells were stained with anti-human IgG antibody labeled with FITC. Left: fluorescence image; right; composite image. Bars = 10 μm. (b) and (c) A172 cells were treated with CTX-Fc-BNCs, human IgG-BNCs, or M-CTX-Fc for 1 h at 4°C or 37°C. After incubation, the cells were trypsinized. The cytoplasmic fraction was immunoprecipitated with anti-HBsAg antibody conjugated to microbeads. (b) The precipitates were immunoblotted and detected with anti-human-IgG-Fc antibody. (c) The BNC bands in the CTX-Fc-BNCs or human IgG-BNCs treatment at 37°C were analyzed densitometrically using a CS Analyzer 3.0 and plotted in each graph to estimate the amount endocytosed. The data (mean ± S.D) presented are from three independent experiments ($^{**}P < 0.05$).

toxic to the cells (Figure 4(b)). These findings suggest that M/D-CTX-Fcs may be a potential ligand for the active targeting of glioblastoma cells.

Several MMPs are considered to regulate signaling pathways in cells [30]. MT1-MMP influences the cellular microenvironment and promotes cell invasion via degradation of ECM, shedding of CD44 and syndecan1, and activation of ERK, Akt, and FAK signaling [31, 32]. MT1-MMP is internalized, and like other membrane-binding molecules, it is regulated by endocytosis because of the functional role of internalization in the cytoplasmic tail [33]. The regulation of the activity and internalization of MT1-MMP are associated with integrin on endothelial cells [34]. Endocytosis and accumulation of MT1-MMP are mediated by the clathrin-dependent endocytic pathway [33]. CTX-Fc-BNCs were localized intracellularly at 37°C (Figure 5), which was inhibited by 100 nM CPZ, a blocker of clathrin-coated pit formation [21], and by 5 mM mβCD (Figure 6),

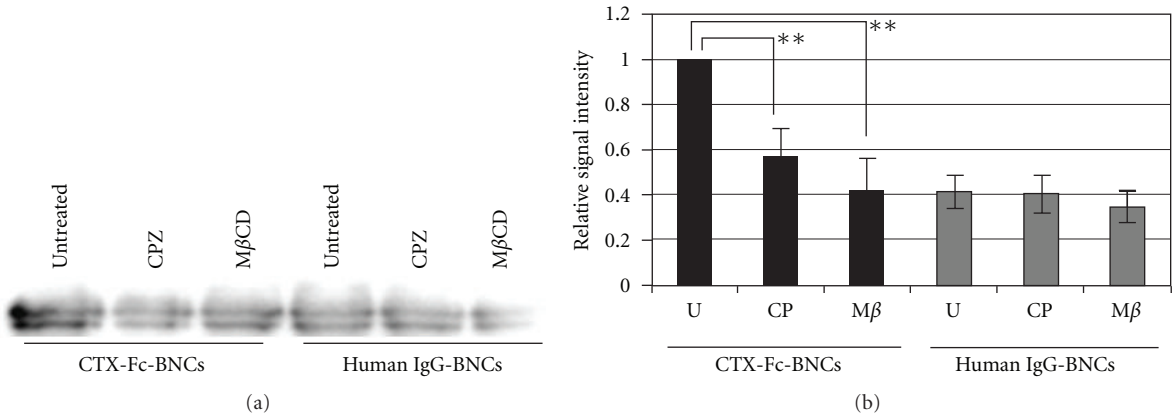

Figure 6: Assessment of the mechanism of CTX-Fc-BNCs internalization. A172 cells were treated with CTX-Fc-BNCs or human IgG-BNCs in the presence of 100 nM CPZ or 5 mM MβCD at 37°C for 1 h, followed by trypsinization. The cytoplasmic fraction was immunoprecipitated with anti-HBsAg antibody conjugated to microbeads. "Untreated" indicates that the cells were treated with CTX-Fc-BNCs in the absence of any inhibitors. (a) The precipitates were immunoblotted and detected using anti-human-IgG-Fc antibody. (b) The BNC bands were analyzed densitometrically using a CS Analyzer 3.0 and plotted in each graph to evaluate the amount endocytosed. U: untreated; CP: CPZ; Mβ: MβCD. The data (mean ± S.D) presented are from three independent experiments (**$P < 0.05$).

a cholesterol-dislodging oligosaccharide that inhibits caveolar formation and perturbs clathrin-coated endocytic vesicles [35, 36]. Because 300 nM CTX significantly reduced the green fluorescence of BNCs by competing with CTX-Fc-BNCs (Figure 5(a)), CTX-Fc-BNCs binding on A172 cell surfaces should be specific to the CTX-binding site such as MMP-2 and MT1-MMP. The internalization of CTX-Fc-BNCs was shown to be temperature dependent (Figure 5(b)). This suggests that cellular uptake of CTX-Fc-BNCs was receptor mediated.

Zhang et al. reported that CTX was displayed on polyethylene glycol (PEG-) coated iron oxide nanoparticles that were detectable in the tumor lesions of mouse and rat glioma models. They demonstrated the active targeting of glioma cells using a combination of CTX and supermagnetic or fluorescent compounds *in vivo* and *in vitro* [37–40]. CTX-displaying nanoparticles were able to pass the blood-brain barrier (BBB) or the blood-tumor barrier (BTB) after intravenous injection and accumulated in brain tumors [38, 41]. Many methods, such as intratumoral injection, intracavity injection, microdialysis, biodegradable polymers, and enhanced convection, have been used for local drug delivery to brain tumors [42]. Given the characteristic features of CTX-Fc-BNCs, the targeted intravenous injection of brain tumors with nanodrugs displaying CTX-Fcs should alleviate painful side effects in patients.

5. Conclusions

We designed a fusion protein between CTX and human IgG-Fcs. Depending on the presence of hinge region of Fc domain, the fusion protein exists as a monomer or a dimmer. The monomeric form, M-CTX-Fc, performed as an active targeting ligand to suppress the motility of A172 glioblastoma cells. We then constructed a protein nanocapsule displaying M-CTX-Fc as CTX-Fc-BNCs, which showed specific affinity to the surface of A172 cells and internalized into the cytoplasmic space. This internalization depended on the clathrin-mediated endocytosis pathway. Thus the internalization was enhanced by the multivalent display of the ligand on nanocapsules, which should be a promising drug delivery system for targeting glioblastoma when an appropriate anticancer agent is loaded.

Conflict of Interests

The authors report no conflict of interests. The authors alone are responsible for the content and writing of the paper.

Acknowledgments

This work was supported by a Grant-in-Aid for Scientific Research (B) from the Ministry of Education, Culture, Sports, Science and Technology of Japan (MEXT KAKENHI Grant no. 21300179) and by a Grant-in-Aid for Scientific Research (C) from the Japan Society for the Promotion of Science (JSPS KAKENHI Grant no. 24510151).

References

[1] A. Giese, R. Bjerkvig, M. E. Berens, and M. Westphal, "Cost of migration: invasion of malignant gliomas and implications for treatment," *Journal of Clinical Oncology*, vol. 21, no. 8, pp. 1624–1636, 2003.

[2] M. W. Roomi, V. Ivanov, T. Kalinovsky, A. Niedzwiecki, and M. Rath, "Inhibition of glioma cell line A-172 MMP activity and cell invasion in vitro by a nutrient mixture," *Medical Oncology*, vol. 24, no. 2, pp. 231–238, 2007.

[3] C. Wild-Bode, M. Weller, and W. Wick, "Molecular determinants of glioma cell migration and invasion," *Journal of Neurosurgery*, vol. 94, no. 6, pp. 978–984, 2001.

[4] A. T. J. Beliën, P. A. Paganetti, and M. E. Schwab, "Membrane-type 1 matrix metalloprotease (MT1-MMP) enables invasive migration of glioma cells in central nervous system white

matter," *Journal of Cell Biology*, vol. 144, no. 2, pp. 373–384, 1999.

[5] H. Sato and T. Takino, "Coordinate action of membrane-type matrix metalloproteinase-1 (MT1-MMP) and MMP-2 enhances pericellular proteolysis and invasion," *Cancer Science*, vol. 101, no. 4, pp. 843–847, 2010.

[6] S. Hernandez-Barrantes, M. Toth, M. M. Bernardo et al., "Binding of active (57 kDa) membrane type 1-matrix metalloproteinase (MT1-MMP) to tissue inhibitor of metalloproteinase (TIMP)-2 regulates MT1-MMP processing and pro-MMP-2 activation," *Journal of Biological Chemistry*, vol. 275, no. 16, pp. 12080–12089, 2000.

[7] L. Emdad, P. Dent, D. Sarkar, and P. B. Fisher, "Future approaches for the therapy of malignant glioma: targeting genes mediating invasion," *Future Oncology*, vol. 8, pp. 343–346, 2012.

[8] T. R. Alves, F. R. S. Lima, S. A. Kahn et al., "Glioblastoma cells: a heterogeneous and fatal tumor interacting with the parenchyma," *Life Sciences*, vol. 89, pp. 532–539, 2011.

[9] M. D. Groves, V. K. Puduvalli, K. R. Hess et al., "Phase II trial of temozolomide plus the matrix metalloproteinase inhibitor, marimastat, in recurrent and progressive glioblastoma multiforme," *Journal of Clinical Oncology*, vol. 20, no. 5, pp. 1383–1388, 2002.

[10] J. Yue, K. Zhang, and J. F. Chen, "Role of integrins in regulating proteases to mediate extracellular matrix remodeling," *Cancer Microenvironment*, vol. 5, no. 3, pp. 275–283, 2012.

[11] L. M. Coussens, B. Fingleton, and L. M. Matrisian, "Matrix metalloproteinase inhibitors and cancer: trials and tribulations," *Science*, vol. 295, no. 5564, pp. 2387–2392, 2002.

[12] J. A. DeBin, J. E. Maggio, and G. R. Strichartz, "Purification and characterization of chlorotoxin, a chloride channel ligand from the venom of the scorpion," *American Journal of Physiology*, vol. 264, no. 2, pp. C361–C369, 1993.

[13] J. Deshane, C. C. Garner, and H. Sontheimer, "Chlorotoxin inhibits glioma cell invasion via matrix metalloproteinase-2," *Journal of Biological Chemistry*, vol. 278, no. 6, pp. 4135–4144, 2003.

[14] L. Soroceanu, Y. Gillespie, M. B. Khazaeli, and H. Sontheimer, "Use of chlorotoxin for targeting of primary brain tumors," *Cancer Research*, vol. 58, no. 21, pp. 4871–4879, 1998.

[15] M. Veiseh, P. Gabikian, S. B. Bahrami et al., "Tumor paint: a chlorotoxin:Cy5.5 bioconjugate for intraoperative visualization of cancer foci," *Cancer Research*, vol. 67, no. 14, pp. 6882–6888, 2007.

[16] M. Akcan, M. R. Stroud, S. J. Hansen et al., "Chemical re-engineering of chlorotoxin improves bioconjugation properties for tumor imaging and targeted therapy," *Journal of Medicinal Chemistry*, vol. 54, no. 3, pp. 782–787, 2011.

[17] D. Yu, T. Fukuda, Tuoya et al., "Engineered bio-nanocapsules, the selective vector for drug delivery system," *IUBMB Life*, vol. 58, no. 1, pp. 1–6, 2006.

[18] T. Yamada, Y. Iwasaki, H. Tada et al., "Nanoparticles for the delivery of genes and drugs to human hepatocytes," *Nature Biotechnology*, vol. 21, no. 8, pp. 885–890, 2003.

[19] Y. Tsutsui, K. Tomizawa, M. Nagita et al., "Development of bionanocapsules targeting brain tumors," *Journal of Controlled Release*, vol. 122, no. 2, pp. 159–164, 2007.

[20] A. Vaidyanath, T. Hashizume, T. Nagaoka et al., "Enhanced internalization of ErbB2 in SK-BR-3 cells with multivalent forms of an artificial ligand," *Journal of Cellular and Molecular Medicine*, vol. 15, pp. 2525–2538, 2011.

[21] T. Hashizume, T. Fukuda, T. Nagaoka et al., "Cell type dependent endocytic internalization of ErbB2 with an artificial peptide ligand that binds to ErbB2," *Cell Biology International*, vol. 32, no. 7, pp. 814–826, 2008.

[22] M. Thier, E. Roeb, B. Breuer, T. A. Bayer, H. Halfter, and J. Weis, "Expression of matrix metalloproteinase-2 in glial and neuronal tumor cell lines: inverse correlation with proliferation rate," *Cancer Letters*, vol. 149, no. 1-2, pp. 163–170, 2000.

[23] H. Sato, T. Takino, Y. Okada et al., "A matrix metalloproteinase expressed on the surface of invasive tumour cells," *Nature*, vol. 370, no. 6484, pp. 61–65, 1994.

[24] S. Papparella, B. Restucci, O. Paciello, and P. Maiolino, "Expression of matrix metalloprotease-2 (MMP-2) and the activator membrane type 1 (MT1-MMP) in canine mammary carcinomas," *Journal of Comparative Pathology*, vol. 126, no. 4, pp. 271–276, 2002.

[25] R. Visse and H. Nagase, "Matrix metalloproteinases and tissue inhibitors of metalloproteinases: structure, function, and biochemistry," *Circulation Research*, vol. 92, no. 8, pp. 827–839, 2003.

[26] C. M. Overall, "Molecular determinants of metalloproteinase substrate specificity: matrix metalloproteinase substrate binding domains, modules, and exosites," *Applied Biochemistry and Biotechnology*, vol. 22, no. 1, pp. 51–86, 2002.

[27] E. M. Tam, T. B. Moore, G. S. Butler, and C. M. Overall, "Characterization of the distinct collagen binding, helicase and cleavage mechanisms of matrix metalloproteinase 2 and 14 (gelatinase A and MT1-MMP): the differential roles of the MMP hemopexin C domains and the MMP-2 fibronectin type II modules in collagen triple helicase activities," *Journal of Biological Chemistry*, vol. 279, no. 41, pp. 43336–43344, 2004.

[28] P. C. Brooks, S. Strömblad, L. C. Sanders et al., "Localization of matrix metalloproteinase MMP-2 to the surface of invasive cells by interaction with integrin $\alpha v\beta 3$," *Cell*, vol. 85, no. 5, pp. 683–693, 1996.

[29] B. Hu, M. J. Jarzynka, P. Guo, Y. Imanishi, D. D. Schlaepfer, and S. Y. Cheng, "Angiopoietin 2 induces glioma cell invasion by stimulating matrix metalloprotease 2 expression through the $\alpha v\beta 1$ integrin and focal adhesion kinase signaling pathway," *Cancer Research*, vol. 66, no. 2, pp. 775–783, 2006.

[30] K. Kessenbrock, V. Plaks, and Z. Werb, "Matrix metalloproteinases: regulators of the tumor microenvironment," *Cell*, vol. 141, no. 1, pp. 52–67, 2010.

[31] Y. Itoh and M. Seiki, "MT1-MMP: a potent modifier of pericellular microenvironment," *Journal of Cellular Physiology*, vol. 206, no. 1, pp. 1–8, 2006.

[32] A. Kwiatkowska, M. Kijewska, M. Lipko, U. Hibner, and B. Kaminska, "Downregulation of Akt and FAK phosphorylation reduces invasion of glioblastoma cells by impairment of MT1-MMP shuttling to lamellipodia and downregulates MMPs expression," *Biochimica et Biophysica Acta*, vol. 1813, no. 5, pp. 655–667, 2011.

[33] P. Osenkowski, M. Toth, and R. Fridman, "Processing, shedding, and endocytosis of membrane type 1-Matrix metalloproteinase (MT1-MMP)," *Journal of Cellular Physiology*, vol. 200, no. 1, pp. 2–10, 2004.

[34] B. G. Gálvez, S. Matías-Román, M. Yáñez-Mó, F. Sánchez-Madrid, and A. G. Arroyo, "ECM regulates MT1-MMP localization with $\beta 1$ or $\alpha v\beta 3$ integrins at distinct cell compartments modulating its internalization and activity on human endothelial cells," *Journal of Cell Biology*, vol. 159, no. 3, pp. 509–521, 2002.

[35] R. Chadda, M. T. Howes, S. J. Plowman, J. F. Hancock, R. G. Parton, and S. Mayor, "Cholesterol-sensitive Cdc42 activation

regulates actin polymerization for endocytosis via the GEEC pathway," *Traffic*, vol. 8, no. 6, pp. 702–717, 2007.

[36] S. K. Rodal, G. Skretting, Ø. Garred, F. Vilhardt, B. Van Deurs, and K. Sandvig, "Extraction of cholesterol with methyl-β-cyclodextrin perturbs formation of clathrin-coated endocytic vesicles," *Molecular Biology of the Cell*, vol. 10, no. 4, pp. 961–974, 1999.

[37] C. Sun, O. Veiseh, J. Gunn et al., "In vivo MRI detection of gliomas by chlorotoxin-conjugated superparamagnetic nanoprobes," *Small*, vol. 4, no. 3, pp. 372–379, 2008.

[38] O. Veiseh, C. Sun, C. Fang et al., "Specific targeting of brain tumors with an optical/magnetic resonance imaging nanoprobe across the blood-brain barrier," *Cancer Research*, vol. 69, no. 15, pp. 6200–6207, 2009.

[39] O. Veiseh, F. M. Kievit, J. W. Gunn, B. D. Ratner, and M. Zhang, "A ligand-mediated nanovector for targeted gene delivery and transfection in cancer cells," *Biomaterials*, vol. 30, no. 4, pp. 649–657, 2009.

[40] O. Veiseh, J. W. Gunn, F. M. Kievit et al., "Inhibition of tumor-cell invasion with chlorotoxin-bound superparamagnetic nanoparticles," *Small*, vol. 5, no. 2, pp. 256–264, 2009.

[41] R. Huang, W. Ke, L. Han, J. Li, S. Liu, and C. Jiang, "Targeted delivery of chlorotoxin-modified DNA-loaded nanoparticles to glioma via intravenous administration," *Biomaterials*, vol. 32, no. 9, pp. 2399–2406, 2011.

[42] D. R. Groothuis, "The blood-brain and blood-tumor barriers: a review of strategies for increasing drug delivery," *Neuro-Oncology*, vol. 2, no. 1, pp. 45–49, 2000.

Hindawi Publishing Corporation
Journal of Drug Delivery
Volume 2012, Article ID 592602, 13 pages
doi:10.1155/2012/592602

Research Article

Application of Collagen-Model Triple-Helical Peptide-Amphiphiles for CD44-Targeted Drug Delivery Systems

Margaret W. Ndinguri,[1,2] Alexander Zheleznyak,[3] Janelle L. Lauer,[1,4] Carolyn J. Anderson,[3,5] and Gregg B. Fields[1,2]

[1] *Department of Biochemistry, University of Texas Health Science Center, 7703 Floyd Curl Drive, San Antonio, TX 78229, USA*
[2] *Departments of Chemistry and Biology, Torrey Pines Institute for Molecular Studies, 11350 SW Village Parkway, Port St. Lucie, FL 34987, USA*
[3] *Mallinckrodt Institute of Radiology, Washington University School of Medicine, 510 S Kingshighway Boulevard, St. Louis, MO 63110, USA*
[4] *Department of Molecular Therapeutics, Scripps Florida, 130 Scripps Way, Jupiter, FL 33458, USA*
[5] *Department of Radiology, University of Pittsburgh, 200 Lothrop Street, Pittsburgh, PA 15219, USA*

Correspondence should be addressed to Gregg B. Fields, gfields@tpims.org

Received 17 July 2012; Revised 3 October 2012; Accepted 5 October 2012

Academic Editor: Walter Jäger

Cancer treatment by chemotherapy is typically accompanied by deleterious side effects, attributed to the toxic action of chemotherapeutics on proliferating cells from nontumor tissues. The cell surface proteoglycan CD44 has been recognized as a cancer stem cell marker. The present study has examined CD44 targeting as a way to selectively deliver therapeutic agents encapsulated inside colloidal delivery systems. CD44/chondroitin sulfate proteoglycan binds to a triple-helical sequence derived from type IV collagen, α1(IV)1263–1277. We have assembled a peptide-amphiphile (PA) in which α1(IV)1263–1277 was sandwiched between 4 repeats of Gly-Pro-4-hydroxyproline and conjugated to palmitic acid. The PA was incorporated into liposomes composed of DSPG, DSPC, cholesterol, and DSPE-PEG-2000 (1 : 4 : 5 : 0.5). Doxorubicin-(DOX-)loaded liposomes with and without 10% α1(IV)1263–1277 PA were found to exhibit similar stability profiles. Incubation of DOX-loaded targeted liposomes with metastatic melanoma M14#5 and M15#11 cells and BJ fibroblasts resulted in IC_{50} values of 9.8, 9.3, and >100 μM, respectively. Nontargeted liposomes were considerably less efficacious for M14#5 cells. In the $CD44^+$ B16F10 mouse melanoma model, CD44-targeted liposomes reduced the tumor size to 60% of that of the untreated control, whereas nontargeted liposomes were ineffective. These results suggest that PA targeted liposomes may represent a new class of nanotechnology-based drug delivery systems.

1. Introduction

The ultimate goal of targeted nanotechnology-based drug delivery systems (nanoDDSs) in cancer therapy is to improve the therapeutic index of cytotoxic agents by selectively increasing their concentration at the tumor site. Liposomes in particular have attracted much attention as site-specific drug delivery vehicles because of their biocompatibility [1, 2], and the ease with which they can be manipulated to accommodate targeting ligands to further increase the specificity and therefore the potency of encapsulated chemotherapeutics [3]. Numerous targeted liposomes have been developed and are in clinical trials [2].

The cell surface proteoglycan CD44 is overexpressed on a variety of tumor cells [4, 5], and cells with higher expression of CD44 have a greater migratory and invasive potential on hyaluronate-coated substrates [6]. In addition, 4- to 6-fold elevated CD44 expression is associated with tumor growth and metastasis [7]. CD44 interaction with hyaluronan induces ankyrin binding to MDR1 (P-glycoprotein), resulting in the efflux of chemotherapeutic agents and chemoresistance in tumor cells [8–10]. Interestingly, CD44 has been revealed as a cancer stem cell marker for numerous tumor types [5, 11–17]. A theory is emerging that CD44 positive cells within a tumor display true stem cell properties

such that one cell can give rise to an entire tumor [12]. This makes the development of CD44-targeted drugs important as few therapeutics are capable of killing 100% of the cells within a tumor.

Ligands that bind CD44 undergo endocytosis [18, 19], making this receptor a good candidate for targeted drug delivery [20–24]. CD44 in the chondroitin sulfate proteoglycan (CSPG) modified form is among the receptors uniquely overexpressed in metastatic melanoma [4]. Targeting strategies for drug delivery vehicles against the CD44 receptor in melanoma have included hyaluronan/hyaluronic acid (HA) and its fragments. HA liposomes containing DOX were previously shown to be significantly more effective than free DOX *in vitro* against B16F10 melanoma cells [21] and *in vivo* against a variety of mouse tumor models [22, 24]. HA liposomes have been used to effectively deliver mitomycin C *in vivo* in three mice tumor models [25] and antitelomerase siRNA *in vitro* to CD44-expressing lung cancer cells [26].

A possible disadvantage of using HA as a targeting ligand is that, as a high molecular weight species, it may be quickly removed from circulation by hepatic cells [27]. In an attempt to circumvent this possible problem, enzymatically degraded HA fragments of lower molecular weight (hexameric fragments) have been used by Eliaz and Szoka Jr. [20] as targeting moieties in DOX-loaded liposomes against the CD44-overexpressing B16F10 melanoma cells. The hexameric HA induced rapid dose-dependent CD44 receptor binding of the targeted liposomes to melanoma cells. However, the low molecular weight HA fragments were also found to have lower affinity to the CD44 receptor than the intact HA, thus diminishing the targeting capabilities.

Unfortunately, an approach that employs HA and/or its fragments as the targeting moiety to CD44 suffers from reduced selectivity because other cell surface receptors such as RHAMM have been shown to bind HA just as avidly as CD44 [28, 29]. In addition, HA binding to CD44 is not sensitive to distinct glycosylation patterns of this receptor, as, for example, the site of chondroitin sulfate (CS) modification is distant from the HA binding site (Figure 1). HA modified delivery systems will bind to any cell that possesses CD44, as recently shown for macrophages [30]. Finally, CS modification of CD44 (which occurs in melanoma) negatively regulates HA binding [31, 32].

In addition to binding to HA, CS modified CD44 binds collagen [42–44]. The sequence to which CD44 binds within the type IV collagen triple helix has been identified as α1 (IV)1263–1277 (gene-derived sequence Gly-Val-Lys-Gly-Asp-Lys-Gly-Asn-Pro-Gly-Trp-Pro-Gly-Ala-Pro) [41, 45]. Efficient binding is dependent upon CS modification of CD44 [41]. This sequence is not bound by collagen-binding integrins [41, 46]. We have previously constructed α1(IV)1263–1277 based triple-helical "peptide-amphiphiles" (PAs) [general structure C_n-(Gly-Pro-Hyp)$_4$-Gly-Val-Lys-Gly-Asp-Lys-Gly-Asn-Pro-Gly-Trp-Pro-Gly-Ala-Pro-(Gly-Pro-Hyp)$_4$-NH_2] specific for CD44/CSPG [41, 47–49]. M14#5 human melanoma cells bound to C_{14}, C_{16}, or C_{18} α1(IV)1263–1277 PA with EC_{50} approximately 0.08–0.5 μM [41, 46, 50]. The amphiphilic design of the PA construct facilitates the anchoring of the functional

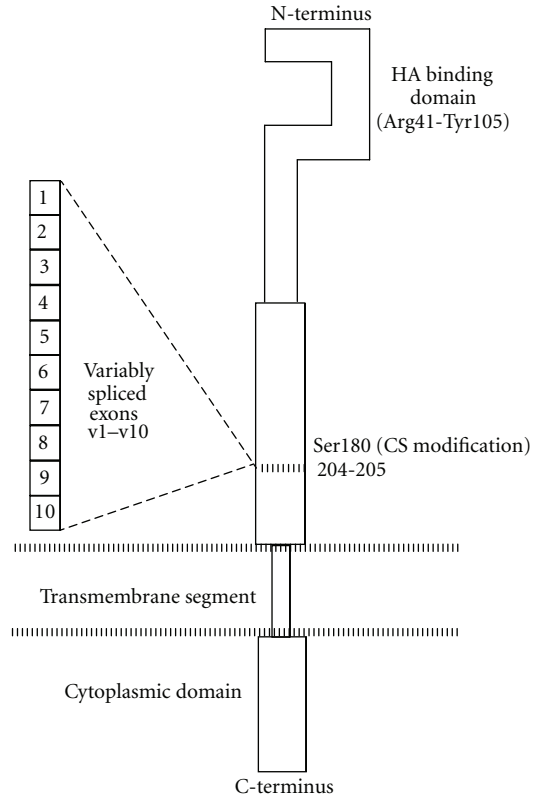

Figure 1: Schematic structure of CD44. The hyaluronate/hyaluronic acid (HA) binding site is in the *N*-terminal portion (Link module) of CD44 (residues Arg41-Tyr105) [33–35], while the CS modification primarily occurs at Ser180 [31]. The alternatively spliced variants of CD44 contain inserts at residues 204-205 of the parent protein [4]. Heparan sulfate modification occurs in exon v3 [36]; dermatin sulfate modification is observed for the nonspliced protein [37, 38], and CD176/Thomsen-Friedenreich antigen is found in spliced CD44 variants [39, 40]. The binding of α1(IV)1263–1277 to CD44 is dependent upon CS [41], and thus α1(IV)1263–1277 binding occurs in a region distinct from HA binding.

"head group" of the construct to the liposome surface by the insertion of the hydrophobic acyl "tail" into the lipid bilayer. This in turn allows the hydrophilic head group or targeting the portion of the PA to protrude outward from the liposomal surface making it available to interact with the CD44/CSPG receptor. The incorporation of the α1(IV)1263–1277 PAs into rhodamine-loaded liposomes did not destabilize these systems and conferred targeting selectivity to liposomes against cell lines varying in the CD44 expression based on the receptor/PA ligand recognition [23].

In the current study we evaluated the stability of distearoyl phosphatidylglycerol-(DSPG-)distearoyl phosphatidylcholine (DSPC) DOX-loaded liposomes both with and without the α1(IV)1263–1277 PA. We incorporated PEG-2000 into the liposomal systems to allow for increased circulation times *in vivo* [51–54]. The efficacies of the various liposomal nanoDDSs were evaluated by quantifying their cytotoxic effects against cell lines with varying levels of

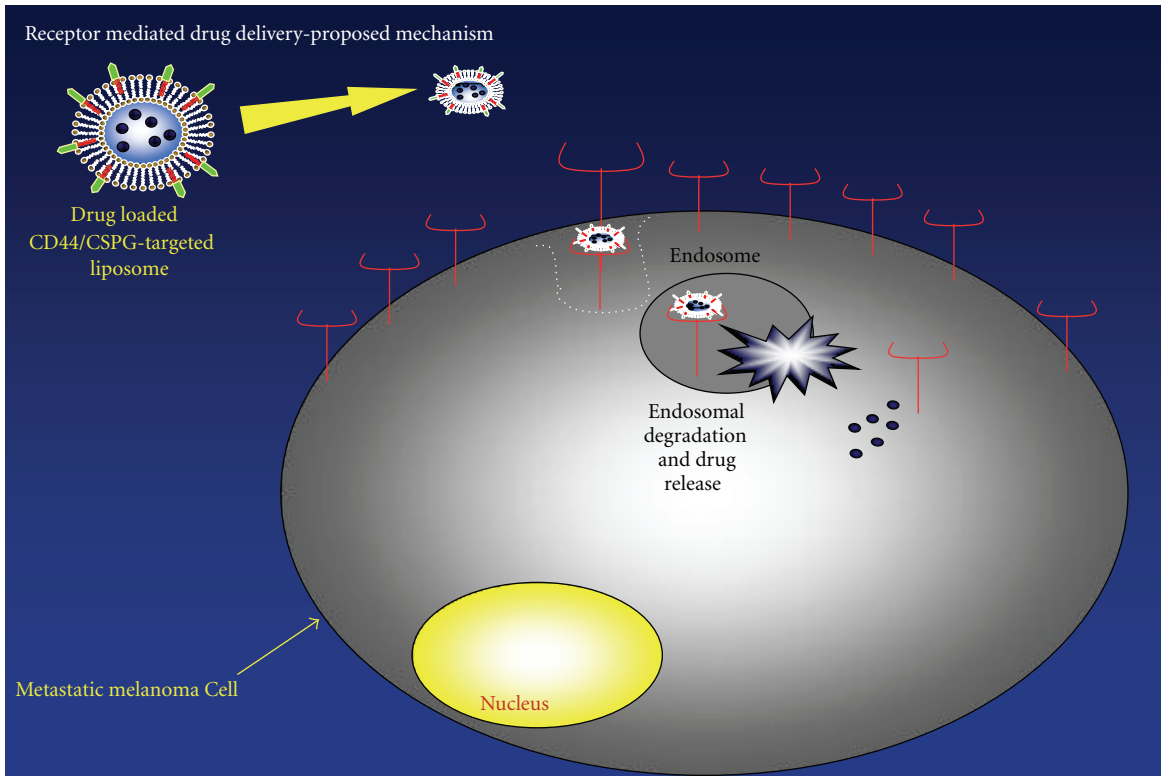

Scheme 1: Schematic depiction of targeted liposomal delivery to CD44/CSPG metastatic melanoma cells. The α1(IV)1263–1277 PA (red alkyl tail and green peptide head group) is incorporated into liposomes along with DOX (blue circles). The liposome targets CD44/CSPG (red) on the melanoma cell surface. The liposome-receptor complex is internalized via endocytosis and DOX released. The mechanism of delivery was described previously [23]. This scheme does not explicitly propose how liposomes are trafficked through different intracellular compartments.

CD44/CSPG expression (Scheme 1) and in a B16F10 mouse melanoma model system.

2. Materials and Methods

2.1. Chemicals. All phospholipids (Cat# 850365, 840465, and 880120) and cholesterol (Cat# 700000) were purchased from Avanti Polar Lipids. All chemicals and solvents used in the syntheses of the triple-helical peptide (THP) PA and vesicles, such as methanol (Cat# 42395), chloroform (Cat# 650498), *tert*-butyl ether (Cat# E127), *N*,*N*-dimethylformamide (Cat# D119), *N*,*N*-diisopropylethylamine (Cat# AC11522), DOX (Cat# BP2516), and palmitic acid (Cat# 129700025) [CH_3-$(CH_2)_{14}$-CO_2H, designated C_{16}], were from Fisher Scientific or Sigma-Aldrich. CellTiter-Glo Luminescen Cell Viability Assay kit (Gly-Phe-AFC) (Cat# AFC033) was purchased from Promega Corporation or MP Biomedicals. The appropriately protected amino acids, O-(1H-6-chlorobenzotriazole-1-yl)-1,1,3,3-tetramethyluronium hexafluorophosphate (HCTU) (Cat# 851012) and NovaPEG rink amide resin (Cat# 855047) were all obtained from EMD Biosciences. The preparation, purification, and characterization of the α1(IV)1263–1277 THP [(Gly-Pro-Hyp)$_4$-Gly-Val-Lys-Gly-Asp-Lys-Gly-Asn-Pro-Gly-Trp-Pro-Gly-Ala-Pro-(Gly-Pro-Hyp)$_4$-NH_2] PA possessing a C_{16} tail have been described previously [48].

2.2. Cell Culture Conditions. The M14#5 and M14#11 human metastatic melanoma cell lines were generously provided by Dr. Barbara Mueller. The BJ foreskin fibroblasts from a melanoma patient were obtained from the American Type Culture Collection (ATCC) (Cat# CRL-2522). Cell media (Cat# MT10-013-CV) and trypan blue (Cat# ICN1691049) were obtained from Fisher Scientific or CellGro, and all reagents required for cell culture were purchased from Invitrogen. Cells were maintained in DMEM supplemented with 10% fetal bovine serum (Cat# 10437028), 50 units/mL penicillin, and 0.05 mg/mL streptomycin (Cat# 15140163). Cells were cultured with complete medium at 37°C in a humidified atmosphere of 5% CO_2 in air. For all experiments cells were harvested from subconfluent (<80%) cultures using a trypsin-EDTA (Cat# 15400054) solution and then resuspended in fresh medium. Preparations of cells with a >90% viability, as determined by trypan blue exclusion, were used.

2.3. Preparation of DOX-Loaded Liposomes. The phospholipids and cholesterol were combined in fixed ratios (Table 1) and dissolved in an organic phase mixture of methanol, methyl *tert*-butyl ether, and chloroform (1 : 2 : 2.4) by vortexing for 0.5 h at room temperature. At this stage, if PA-targeted liposomes were the desired product (Table 1), the α1(IV)1263–1277 PA was added to the lipid organic

Table 1: Liposomal systems utilized for stability and cytotoxicity evaluations.

Liposome formulation	Molar ratio	Liposome diameter (nm)
Distearoyl phosphatidylglycerol (DSPG)	1	
Distearoyl phosphatidylcholine (DSPC)	4	
Cholesterol	5	84 ± 10
Distearoyl phosphatidylethanolamine poly(ethyleneglycol) 2000 (DSPE-PEG-2000)	0.5	
Distearoyl phosphatidylglycerol (DSPG)	1	
Distearoyl phosphatidylcholine (DSPC)	4	
Cholesterol	5	93 ± 10
α1(IV)1263-1277 peptide-amphiphile (PA)	0.5–1	
Distearoyl phosphatidylethanolamine poly(ethyleneglycol) 2000 (DSPE-PEG-2000)	0.5	

phase mixture. The organic phase was then removed under reduced pressure by rotary evaporation, leaving a thin lipid film at the bottom of the flask which was dried overnight *in vacuo*. The phospholipid film was then rehydrated in ammonium sulfate (125 mM), and the resulting dispersion was vortexed extensively. The dispersion was then stirred for 30 min at 60°C. The maintenance of this temperature for a sustained time was necessary as the lipid tails were mobilized and thus allowed the aqueous medium to traverse the lipid bilayers. The resulting multilamellar vesicle (MLV) suspension was then subjected to 10 freeze-thaw cycles, briefly sonicated, followed by 10 cycles of extrusion at 60°C through 100 nm double-stacked polycarbonate filters using a Lipex Extruder (Northern Lipids, Inc., Vancouver, British Columbia) at pressures typically at the lower end of the 250–700 psi range. The polycarbonate filters employed in the extrusion process were obtained from SPI Supplies (West Chester, PA). The extruded liposomes were dialyzed against a 200-fold volume of 5% glucose solution with four changes overnight. DOX was actively loaded into the liposomes by the creation of an ammonium sulfate gradient [55, 56]. The DOX was prepared by dissolving 10 mg/mL in 5% glucose. An aliquot of 250 μL of this solution was then added to each 0.1 mmol scale liposome batch and then incubated at 60°C for 2 h. The unencapsulated doxorubicin was separated from the DOX-loaded liposomes by dialysis against a 500-fold volume of PBS with 4 solution changes over 24–48 h. The size of liposomes was evaluated by dynamic light scattering as described [23]. Dynamic light scattering analysis, using a Zetasizer Nano Series, Nano ZG with Gateway 842GM (Malvren Instruments), was carried out at Louisiana State University (Department of Chemistry) to determine the mean diameter of the liposomes from each batch prepared (Table 1). Liposomes were used within 24 h of preparation or stored at 4°C and used within 1 week. The liposome phospholipid content was determined by the Stewart (ammonium ferrothiocyanate) assay as described previously [57–59]. The DOX concentration was determined by the measurement of absorbance at $\lambda = 480$ nm following liposome solubilization in 100% ethanol. To account for quenching effects, absorbance values were then compared to a standard curve generated using known concentrations of free DOX in the presence of empty liposomes with a drug : phospholipid ratio of 100 μg/μmol phospholipid. The DOX encapsulation efficiency was usually greater than 90%. The presence of the α1(IV)1263–1277 PA and DSPE-PEG-2000 in the liposomal bilayer was examined by MALDI-TOF mass spectrometry (MS) using an α-cyano-4-hydroxycinnamic acid matrix. The incorporation of the α1(IV)1263–1277 PA into liposomes was quantified by UV-visible spectroscopy using $\varepsilon_{280} = 5579\ M^{-1}\ cm^{-1}$ for Trp. The UV absorbance value for Trp was recorded in ethanol/PBS using a NanoDrop spectrophotometer (Thermo Scientific) and the concentration of the peptide determined using the Beer-Lambert law where $A = \varepsilon lc$.

2.4. Liposome Stability. The stability of the encapsulated doxorubicin in the various liposome systems was initially determined by monitoring DOX release from the vesicles (200 μL of 0.5 mg/mL vesicle solution) at 4, 25, and 37°C, over time. Briefly, a fresh batch of liposomes was prepared and loaded with DOX. The unencapsulated doxorubicin was separated from the DOX-loaded liposomes by dialysis against a 500-fold volume of PBS as described in *Preparation of DOX-Loaded Liposomes*. The fluorescence intensity for each vesicle sample in PBS at each temperature was measured at selected time points within a 30 d period using a Spectra Max Gemini EM Fluorescent Plate Reader (Molecular Devices) at $\lambda_{excitation} = 480$ nm and $\lambda_{emission} = 590$ nm. Complete release of DOX from the vesicles at each time point yields 100% dequenching and was obtained from control ethanol-treated liposome samples. The percentage release of DOX from the vesicles was determined from the fluorescence intensity of each sample relative to 100% dequenching, which can then be expressed in terms of percentage of DOX release.

2.5. Cytotoxicity Assay. The cytotoxicity of all liposomal systems used in this study, as well as free DOX, on the cells was determined using the CellTiter-Glo Luminescent Cell Viability Assay. The M14#5, M14#11, and BJ cells were plated on 96-well tissue cultured treated plates corning at a density of 5×10^3 cells per well and incubated for 24 h at 37°C and 5% CO_2. The culture medium was then replaced with 100 μL of medium containing various concentrations

of each liposomal system or free DOX. The cells were then exposed to the drug for 3 h; the cells were washed twice with sterile PBS following drug exposure. Fresh culture medium was then added, and the incubation was continued for 24 h. After the incubation period, 100 μL CellTiter Glo reagent was added to each well. The cells were allowed to incubate for an additional 3 h at 37°C and 5% CO_2. The cytotoxicity assays were done in triplicate and were repeated at least twice in separate experiments.

2.6. Tumor Growth In Vivo. B16F10 murine melanoma cells were prepared at the Washington University [60]. C57BL/6 mice were obtained from the Harlan Laboratories (Indianapolis, IN). Mice were housed under pathogen-free conditions according to the guidelines of the Division of Comparative Medicine, Washington University School of Medicine. The Washington University Animal Studies Committee approved all experiments.

Tumor cells (10^5 cells/100 μL in PBS) were injected subcutaneously in the neck of C57BL/6 anesthetized mice and allowed to grow 7–14 d until tumors were $\sim 5 \times 5$ mm. Eight mice per treatment group were inoculated with 10^5 tumor cells. The number of animals tested (n) was calculated by power analysis (probability of type I error $\alpha = 0.05$; probability of type II error $\beta = 0.20$) based on previous data. This was the minimum number of animals required to achieve statistical significance. Mice inoculated with tumor cells were divided into a control (saline treated) as well as groups treated with the various DOX-loaded liposomes at doses (5 mg/kg with an average mouse weighing ~20 g) corresponding to those used previously for DOX-loaded liposomes in melanoma mouse models [22]. Liposomes or saline was injected on days 0, 3, 5, 6, and 8, with day 0 being the first day of the regimen and all animals dosed on the same days. The experiment was terminated at 11 d after initiation of treatment regimen.

Mice were anesthetized by isoflurane (2% vaporized in O_2). Tumor size was determined by measuring the greatest length (L) and the greatest width (W) using calipers. The tumor size was calculated using the ellipsoid volume formula: $1/2 \times L \times W^2$ [61].

2.7. Statistics. The P values for cytotoxicity and tumor growth were calculated with the Student's t-test, two tailed by using Graph Pad Software.

3. Results

3.1. Construction and Characterization of Nontargeted and Targeted Liposomes. We have previously determined that liposomes composed of DSPG, DSPC, and cholesterol (molar ratio 1 : 4 : 5) form a stable liposomal delivery system [23, 62, 63]. In addition, the presence of the α1 (IV)1263–1277 PA did not affect the overall liposome stability. However, the earlier studies utilized ~1% of the α1(IV)1263–1277 PA [23], whereas efficient liposome-mediated targeting usually requires 5–23% of the peptide ligand [64–67]. Thus, the present study has examined the stability and efficacy of liposomes possessing either 5 or 10% α1(IV)1263–1277 PA.

The liposomes prepared herein also incorporated DSPE-PEG-2000. The presence of PEG on liposomes allows for increased circulation times *in vivo* compared to conventional liposomes, which has been attributed to the reduced interactions between the liposomal surface and cells of the reticuloendothelial system (RES) [51–53].

The phospholipid concentration of all the liposome systems was 0.5 mg/mL, as verified by the Stewart Assay [57]. The sizes of the targeted and nontargeted liposomes assembled here were characterized using dynamic light scattering. Liposomes were 84–93 nm (small unilamellar vesicles; SUVs) (Table 1), allowing for valid stability comparisons between each system. This size range was previously found to be optimal for efficacious liposomal drug delivery to tumors [68–70].

To confirm the incorporation of the α1(IV)1263–1277 PA and DSPE-PEG-2000, liposomes were treated with ethanol to liberate the α1(IV)1263–1277 PA and PEG from the lipid bilayer. MALDI-TOF mass spectral analysis of the resulting solution produced a peak corresponding to the mass of the α1(IV)1263–1277 PA ($[M+H]^+$ = 3813.3 Da, theoretical $[M+H]^+$ = 3813.3 Da) and a comb-like distribution of peaks corresponding to DSPE-PEG-2000, with the predominant peaks covering $[M+H]^+$ = 1727.9–2122.9 Da ($[M+H]^+$ = 1728.8–2123.7 Da for DSPE-PEG-2000 directly from the supplier, dissolved in ethanol). UV-visible spectroscopic analysis following dialysis indicated 96% incorporation of the PA into liposomes.

3.2. Stability of α1(IV)1263–1277 PA to Proteolysis. To determine the stability of the α1(IV)1263–1277 PA in serum-containing conditions, 17.5 μM PA was incubated at 37°C in either (a) water, (b) OptiMEM I media containing 4% FBS, (c) OptiMEM I media containing 10% FBS, 5 μg/mL insulin, 5 ng/mL epidermal growth factor, and 40 μg/mL bovine pituitary extract, or (d) 10% FBS in water. The samples were monitored by RP-HPLC at 0, 24, and 72 h. No hydrolysis of the α1(IV)1263–1277 PA was observed under these conditions (data not shown). Thus, the triple-helical nature of this ligand renders it reasonably stable to proteolysis (as has been observed for other THPs [71]).

3.3. Stability Comparison of DOX-Loaded Liposomes with and without α1(IV)1263–1277 PA. To determine the effect that the α1(IV)1263–1277 PA has on liposomal stability, DOX-loaded liposomes were prepared with and without 10% α1(IV)1263–1277 PA. The DOX : phospholipid ratios were 1.65 : 1 (1300 μg DOX : μmol phospholipid) and 1.93 : 1 (1520 μg DOX : μmol phospholipid) for targeted [+10% α1(IV)1263–1277 PA] and nontargeted [no α1(IV)1263–1277 PA] liposomes, respectively. Fluorescence intensity measurements for each vesicle sample at 4, 25, or 37°C were taken at selected time points over a 30 d period.

The targeted and nontargeted liposomes exhibited similar stability profiles over 918 h (38 d), with approximately 30–35% DOX release at 4°C (Figure 2) and 40–49% DOX

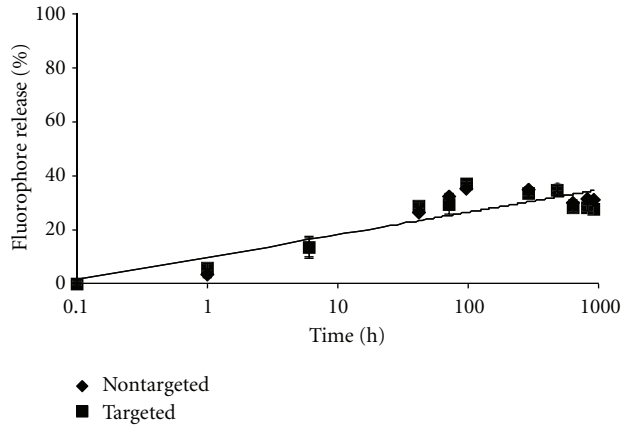

Figure 2: Temperature dependent stability comparisons between targeted [10% α1(IV)1263–1277 PA] and nontargeted DSPG-DSPC liposomes loaded with DOX and stored at 4°C for 30 d. DOX release was determined as described in Section 2.

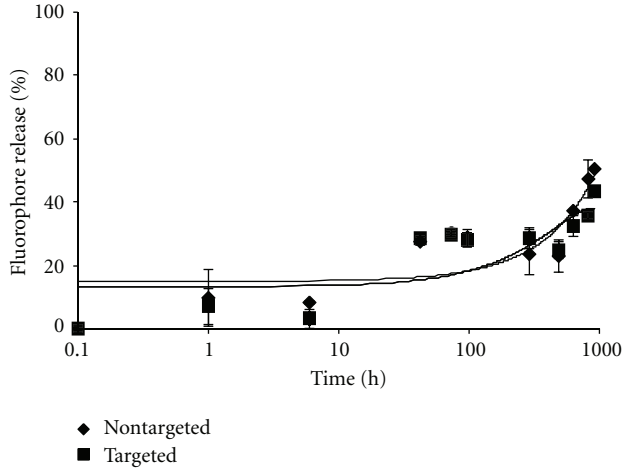

Figure 3: Temperature dependent stability comparisons between targeted [10% α1(IV)1263–1277 PA] and nontargeted DSPG-DSPC liposomes loaded with DOX and stored at 25°C for 30 d. DOX release was determined as described in Section 2.

release at 25 and 37°C (Figures 3 and 4). Within the first 6 h following preparation, the liposomes again demonstrated similar and minimal DOX release. Only ≤15% release was observed for both targeted and nontargeted liposomes when incubated at 4 or 25°C (Figures 2–3), and targeted liposomes were more stable than nontargeted liposomes after 6 h at 37°C (Figure 4). Data presented here are for the targeted liposomes possessing 10% PA, but similar results were observed for liposomes incorporating 5% PA (data not shown). Thus, the presence of the α1(IV)1263–1277 PA did not serve to destabilize the liposomes used in this study.

3.4. Cytotoxicity of DOX-Loaded Liposomes for Cells Varying in CD44/CSPG Content. Cytotoxicity experiments were performed on metastatic melanoma M14#5 and M14#11 and fibroblast BJ cell lines. BJ fibroblasts have ~60% of the CD44 content of M14#5 melanoma cells, while M14#11 melanoma

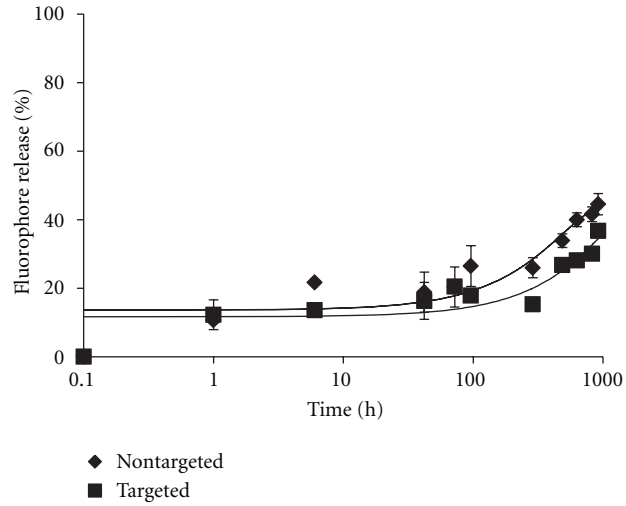

Figure 4: Temperature dependent stability comparisons between targeted [10% α1(IV)1263–1277 PA] and nontargeted DSPG-DSPC liposomes loaded with DOX and stored at 37°C for 30 d. DOX release was determined as described in Section 2.

cells have ~75% of the CD44 content [23]. The variation in CD44/CSPG content allowed for the examination of selectivity of liposome encapsulated DOX, free DOX, and empty liposomes (Scheme 1). Empty liposomes were included due to possible unpredictable cellular responses to specific lipids within a liposome [72]. Cytotoxicity results for targeted liposomes containing 5% PA were found to be inconsistent (data not shown), so only results with 10% PA are described below.

A dose-dependent response was observed for M14#5 cytotoxicity by DOX encapsulated targeted liposomes (Figure 5), with an IC_{50} value of 9.8 μM. Nontargeted liposomes were considerably less toxic for M14#5 cells (Figure 5) to where an IC_{50} value of 117.6 μM was observed. In contrast, there was little difference in cytotoxic effects between targeted and nontargeted liposomes for M14#11 (Figure 6). More precisely, the M14#11 cell IC_{50} values for targeted and nontargeted liposomes were 9.3 and 9.9 μM, respectively. Thus, the greatest difference between targeting and non-targeting was observed with the cells possessing the highest CD44 content. However, the potency of targeted liposomes with the M14#5 and M14#11 cells were relatively similar (IC_{50} values of 9.8 and 9.3 μM, resp.), despite their difference in CD44 content. This may be due to cell toxicity requiring a relatively low level of DOX delivery, so, even with M14#11 cells having ~75% of the CD44 content of M14#5 cells, the amount of DOX delivered was sufficiently toxic for both cell types. The greater efficacy of nontargeted liposomes for M14#11 cells (compared with M14#5 cells) could be due to liposomal interactions with other surface molecules that are more abundant in M14#11 cells. For example, M14#5 cells express CD44 but not melanoma-associated proteoglycan/melanoma chondroitin sulfate proteoglycan (MPG/MCSP/NG2), while M14#11 cells express both [41]. Nontargeted liposomes may associate with

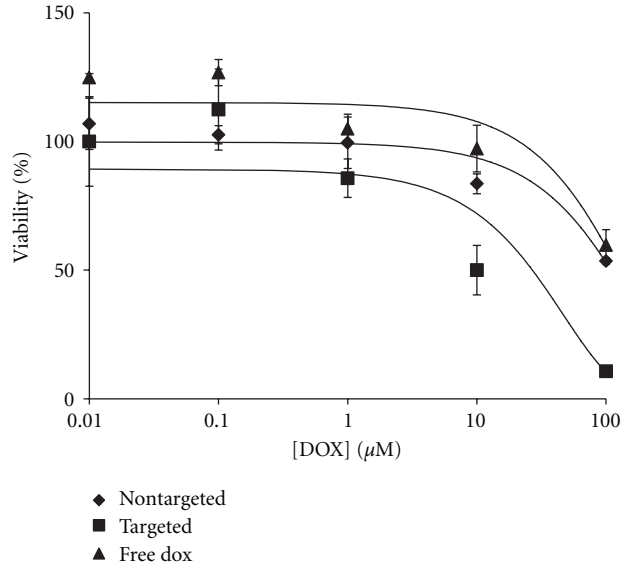

Figure 5: Cytotoxicity data of M14#5 cells incubated for 3 h with targeted [10% α1(IV)1263–1277 PA] and nontargeted DSPG-DSPC liposomes loaded with DOX and free DOX. The difference between targeted and nontargeted liposomes loaded with DOX is statistically significant as $^{**}P = 0.00305$ at 10 μM and $^{***}P = 0.00034$ at 100 μM.

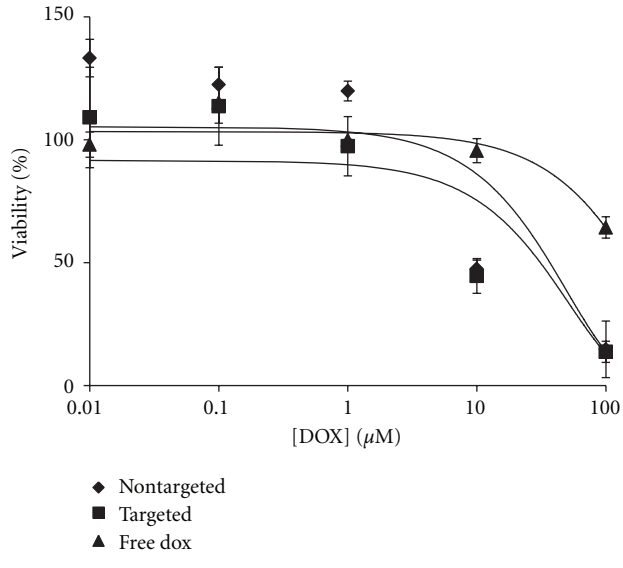

Figure 6: Cytotoxicity data of M14#11 cells incubated for 3 h with targeted [10% α1(IV)1263–1277 PA] and nontargeted DSPG-DSPC liposomes loaded with DOX and free DOX.

MPG/MCSP/NG2 and thus prove more cytotoxic to M14#11 cells compared with M14#5 cells.

To further evaluate the role of CD44 content in targeted delivery, the BJ fibroblast cell line was treated with free DOX and targeted and nontargeted liposomes (Figure 7). BJ fibroblasts showed a similar susceptibility to the effects of free DOX compared with the M14#5 cells (i.e., approximately

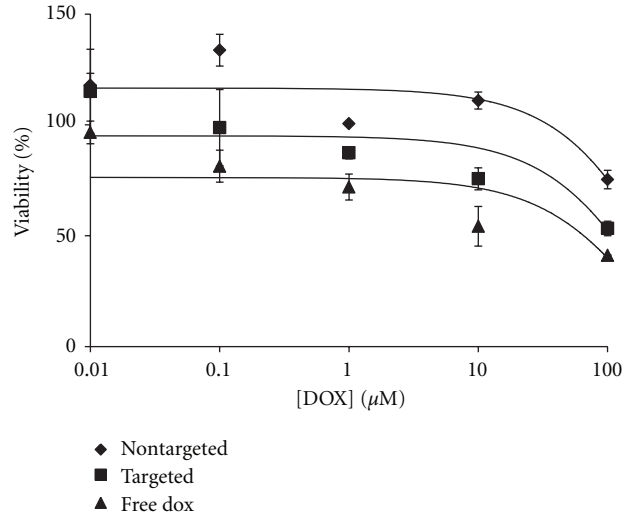

Figure 7: Cytotoxicity data of BJ cells incubated for 3 h with targeted [10% α1(IV)1263–1277 PA] and nontargeted DSPG-DSPC liposomes loaded with DOX and free DOX.

50–60% viable at [DOX] = 100 μM) (Figures 5 and 7). Comparing cytotoxicities based on targeted liposomal delivery of DOX, M14#5 cells were almost completely killed at a DOX concentration of 100 μM (Figure 5), while BJ cells were 60% viable (Figure 7). Thus, a positive correlation was observed between the CD44/CSPG content of M14#5 and BJ cells and the cytotoxic effects of targeted liposomes.

M14#11 melanoma cells were more susceptible to DOX than BJ fibroblasts (Figures 6 and 7). While the levels of CD44 are not the same for M14#11 cells and fibroblasts (see above), enhanced cytotoxicity made also have been influenced by different metabolic profiles of the cell types. While one presumes that the *mechanism* of DOX delivery and toxicity is same for all cell types, the metabolic rates and pathways in melanoma are different from normal cells [73], which could affect the efficiency of DOX action.

At low DOX concentrations, slight increases in cell adhesion were sometimes observed. The luminescence assay used to measure cell adhesion relies upon luciferase conversion of luciferin to oxyluciferin [74]. The luciferase activity is ATP and Mg^{2+} dependent, and thus ATP released from lysed cells directly regulates luciferase. It is possible that low concentrations of DOX could enhance luciferase activity, and thus the increase in cell adhesion is an assay artifact. If this were the case, however, one would expect the same increase in cell adhesion for all three cell types at low free DOX concentrations. This does not occur (Figures 5–7). Free DOX is only activating for M14#5 cells, while M14#11 cells and fibroblasts are activated by nontargeted liposomes. Due to the lack of a consistent trend, we believe that this slight activation is not an assay artifact. The slight activation by low levels of DOX is intriguing, but beyond the scope of the present study to further explore.

There was no significant cytotoxicity observed among the three cell lines upon incubation with empty liposomes (data not shown). Since empty liposomes were not cytotoxic,

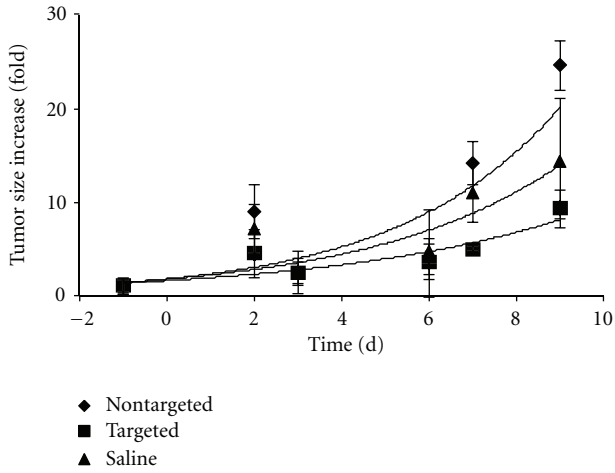

Figure 8: Effects of targeted [10% α1(IV)1263–1277 PA] and nontargeted DSPG-DSPC liposomes loaded with DOX and saline on tumor size in the B16F10 mouse melanoma model. Liposomes or saline was injected on days 0, 3, 5, 6, and 8. On day 7 $^{**}P = 0.003$ (between targeted and non-targeted) and $^{*}P = 0.0184$ (between targeted and saline control); on day 9 $^{**}P = 0.0022$ (between targeted and non-targeted) and $^{*}P = 0.0456$ (one tail, between targeted and saline control).

any cytotoxic effects observed here must be due solely to the cellular delivery of DOX by the respective liposomal systems.

3.5. Cytotoxicity of DOX-Loaded Liposomes to B16F10 Mouse Melanoma Model. The CD44-targeted DOX-loaded PEG liposomes and nontargeted DOX loaded PEG liposomes were tested in a B16F10 mouse melanoma model. Although the B16F10 cell line is of murine origin, it highly expresses CD44 [75] and serves as a good *in vivo* model of aggressive human melanoma. Tumor size measurement was utilized to quantify the efficacy of targeted drug delivery. Mice were treated on days 0, 3, 5, 6, and 8 with 5 mg/kg DOX-loaded liposomes. Treatment with nontargeted liposomes showed no significant decrease in tumor size compared with saline control (Figure 8). However, mice treated with the targeted DOX-loaded liposomes showed substantially decreased tumor size compared with nontargeted liposomes and the saline control (Figure 8).

4. Discussion

We have previously constructed triple-helical α1(IV)1263–1277 PAs, which have been shown to be specific for CD44/CSPG [41, 47–49]. In order to develop a targeted nanoDDS specific for metastatic melanoma, α1(IV)1263–1277 PA has been incorporated the into liposomes [23, 62]. The results of our prior study indicated that liposomes composed of DSPG, DSPC, and cholesterol (molar ratio 1 : 4 : 5) were the most suitable for *in vitro* and *in vivo* applications [23, 63]. These liposomes proved to be the most stable of the systems tested, and the presence of the α1(IV)1263–1277 PA did not affect the liposomal stability. Results obtained through a series of competitive displacement experiments verified CD44/α1(IV)1263–1277 PA liposome recognition [23, 62]. More specifically, α1(IV)1263–1277 PA liposomal rhodamine delivery correlated with cellular CD44 content and was inhibited in a dose-dependent fashion by exogenous α1(IV)1263–1277 PA [23]. Fluorescence microscopy revealed localization of α1(IV)1263–1277 PA liposomes to CD44-positive cells [62].

In the present study, we further modified DSPG/DSPC liposomes with the addition of PEG. Such modifications have previously been shown to increase liposome circulation times *in vivo* [53, 76–82]. We used 5 mol % of PEG-2000 in our liposomes (Table 1), the same amount of PEG used in the clinically approved drug Doxil (DOX encapsulated PEG-stabilized liposomes) [83]. The size of the PEG chain chosen took into account the size of the PEG used in Doxil (PEG-2000) [83], as well as the impact PEGs of various sizes could have on our system specifically. Previous studies suggested that increased circulation times can be achieved with increasing PEG chain lengths up to PEG-5000 [77, 84, 85]. However, we chose not to utilize PEG larger than 2000 Da for three reasons. First, it has been shown that rigid liposomes composed of DSPC (as is the case here) exhibit a drop off in circulation times when PEG greater than 2000 Da is incorporated due to chain entanglement and lipid phase separation resulting in increased opsonization [85–88]. Second, previous work using membranes containing a mixture of the α1(IV)1263–1277 PA and PEGs of various sizes resulted in binding of M14#5 human melanoma cells when PEG-120, PEG-750, or PEG-2000 were used, but not with PEG-5000 [89]. Neutron reflectivity data revealed head group lengths of 8.8, 9.0, and 16.8 nm for α1(IV)1263–1277 PA, DSPE-PEG-2000, and DSPE-PEG-5000, respectively [89]. The lack of binding observed with PEG-5000 was thus attributed to the complete masking of the α1(IV)1263–1277 PA by the PEG, thereby minimizing ligand accessibility. Third, the presence or absence of 5% PEG-2000 in α1(IV)1263–1277 PA/DMPC (1 : 19) liposomes had little effect on the delivery of Texas Red to CD44-positive fibroblasts [62].

In the present study, cells were directly exposed to each liposomal system and free DOX and incubated at 37°C. In this environment, free DOX can be taken up by cells more rapidly than liposome encapsulated DOX. However, free DOX was not as efficacious as CD44 targeted liposome encapsulated DOX towards M14#5 melanoma cells (Figure 5). Thus, the targeting strategy promoted more efficient DOX delivery *in vitro*. Further supporting this conclusion was the observed correlation between the cytotoxic effect of DOX-loaded targeted liposomes and CD44/CSPG content for M14#5 and BJ cell lines.

Eliaz and Szoka Jr. developed CD44-targeted liposomes using HA fragments (see Section 1) [20]. Following a 3 h treatment of B16F10 mouse melanoma cells with DOX encapsulated HA liposomes, IC_{50} values of 0.78–3.62 μM were observed [20]. The IC_{50} value for our CD44-targeted liposome is slightly higher (approximately 9-10 μM), but we have examined activity against a highly aggressive human melanoma cell line. In addition, as discussed earlier, using HA as a targeting moiety suffers from reduced selectivity as

(a) the cell surface receptor RHAMM binds to HA just as avidly as CD44 [28, 29] and (b) HA binding to CD44 is not sensitive to distinct glycosylation patterns of this receptor, while α1(IV)1263–1277 PA binding is [41]. Eliaz and Szoka Jr. reported an IC_{50} value for nontargeted PEG liposomes of >172.4 μM, similar to what we observed for nontargeted PEG liposomes with M14#5 melanoma cells (117.6 μM; Figure 5).

Potential DOX delivery *in vivo*, however, is quite different than *in vitro* when one considers circulation times. Unlike DOX encapsulated within PEGylated liposomes, free DOX is rapidly cleared from circulation, and therefore exposure to tumor cells is limited. In fact, it has previously been reported that free DOX is cleared 450-times faster than DOX encapsulated within PEGylated liposomes [90, 91]. Furthermore, extravasated PEGylated liposomes experience enhanced retention within the tumor site, which has been attributed to a lack of functional lymphatic drainage in tumors [51, 92]. In the B16F10 mouse melanoma model, DOX incorporated within nontargeted liposomes showed little effect in reducing tumor size, while targeted liposomes significantly reduced tumor size (Figure 8). The improved activity was due to the selective uptake of targeted liposomes by CD44-expressing cells rather than DOX released from disintegrated liposomes, as the targeted liposomes were more effective than the nontargeted liposomes (Figure 8), while both liposome types were of similar stability (Figures 2–4). The liposomal formulation utilized here has been noted previously as being highly stable compared with other liposomal compositions [63].

Several prior studies have examined the efficacy of DOX encapsulated, targeted liposomes on mouse tumor models [22, 24, 93]. Most relevant to the present study, Peer and Margalit compared DOX encapsulated HA liposomes, DOX encapsulated liposomes, and saline [22]. Mice were injected with C-26 colorectal tumor cells and treated at 4, 12, and 19 days with 10 mg/kg DOX. At day 31, tumor sizes were ~100, ~400, and ~1250 mm^3 for the HA liposome, liposome, and saline treatments. Thus, CD44 targeting via HA appeared to be effective. The relative reduction in tumor size by the HA liposomes compared with saline (~12.5-fold) was greater than seen here (~2-fold; Figure 8), but the DOX dose in the prior study was twice that of our treatments (10 mg/kg versus 5 mg/kg) and the tumor type was different (colorectal versus melanoma). It should be noted that the B16F10 tumor is highly aggressive, with a doubling time of less than 24 h. Interestingly, the difference in activity for the HA liposomes and liposomes (~4-fold) [22] was comparable to that observed here for the CD44-targeted and nontargeted liposomes (~3-fold; Figure 8).

Goren et al. utilized folate-targeted liposomes for treatment following injection of M109R-HiFR lung tumor cells into mice [93]. Tumor cells were pretreated with liposomes ([DOX] = 10 μM) and injected. The tumor weights after 35 days were 381 mg for untreated mice, 397 mg for mice treated with PEG liposomes (Doxil), and 57 mg for mice treated with folate-targeted liposomes. The relative reduction in tumor size by the folate-targeted liposomes compared with untreated mice (~6.7-fold) was also greater than that observed here. However, a significant difference between our study and that of Goren et al. is the injection of the tumor cells after pretreatment with liposomes in the latter case. One would anticipate that the liposomes would have a greater effect on tumor growth if they interacted with the tumor cells prior to the initiation of the tumor *in vivo*.

An apparent anomalous result from our study was the increased tumor size following nontargeted liposome treatment compared with saline control (Figure 8). Prior studies have typically reported the opposite result. For example, Charrois and Allen compared DOX encapsulated Stealth (PEG) liposomes with saline control for treatment of 4T1 mouse mammary carcinoma [70]. Saline or 6 mg/kg DOX encapsulated liposome was administered at day 4. At day 23, the tumor sizes were ~500 mm^3 for the saline treated mice and ~80 mm^3 for the liposome treated mice. In similar fashion, Han et al. compared DOX encapsulated PEG liposomes, DOX encapsulated comb-like polymer-incorporated liposomes, and PBS control for treatment of B16F10 inoculated mice [94]. Mice were treated at day 6 with 6 mg/kg DOX. At day 13, the tumor sizes were 300 mm^3 for PBS control and 50 mm^3 for the PEG liposomes and comb-like polymer liposomes. It is worth noting that, in our study, the differences between nontargeted liposomes and saline control were small at day 7 (Figure 8), which is similar to the result of Goren et al. reported above [93]. Also, the result at day 9 for the saline control is skewed lower due to one mouse treatment in which the tumor size decreased compared to day 7.

The nanoDDS described in the present study possesses several features to enhance drug selectivity and availability. The targeting capabilities rely upon a ligand that is uniquely selective for the CSPG-modified form of CD44 [41]. Although modeled after a collagen-derived sequence, α1(IV)1263–1277 PA is not recognized by the collagen-binding integrins found in melanoma ($\alpha1\beta1$, $\alpha2\beta1$, and $\alpha3\beta1$). Thus, promiscuous receptor binding is avoided, unlike the use of HA for targeting CD44. The triple-helical nature of the ligand renders it reasonably stable to proteolysis, especially compared to other targeting molecules. The nanoDDS can also incorporate PEG to improve circulation time while minimally compromising cytotoxic activity. In principle, multitargeting can be achieved by straightforward incorporation of additional PA ligands. Multitargeting may be especially advantageous for imaging and/or therapy of cancer stem cells, where targeting of only one cell surface biomarker may not encompass the full population [16]. Thus, PA targeted liposomes may represent the "next generation" of liposomal nanoDDSs [3, 51] that have potential to enhance selectivity and targeting of chemotherapeutic treatments against metastatic melanoma in the human body. Information from these initial *in vivo* studies can guide us to improve the design of the targeted delivery vehicles.

Conflict of Interests

G. B. Fields has a direct financial relationship with EMD Biosciences. Gregg B. Fields and coauthors have no direct financial relationships with any other commercial suppliers mentioned in the paper.

Acknowledgments

The authors gratefully acknowledge the support of this work by the National Institutes of Health (CA 77402 and EB 000289 to G. B. Fields). They thank Loice Ojwang for performing the light scattering studies.

References

[1] R. R. C. New, "Characterization of liposomes," in *Liposomes: A Practical Approach*, R. R. C. New, Ed., pp. 105–161, IRL Press, Oxford, UK, 1990.

[2] Y. S. Tarahovsky, "'Smart' liposomal nanocontainers in biology and medicine," *Biochemistry*, vol. 75, no. 7, pp. 811–824, 2010.

[3] V. P. Torchilin, "Recent advances with liposomes as pharmaceutical carriers," *Nature Reviews Drug Discovery*, vol. 4, no. 2, pp. 145–160, 2005.

[4] D. Naor, S. Nedvetzki, I. Golan, L. Melnik, and Y. Faitelson, "CD44 in cancer," *Critical Reviews in Clinical Laboratory Sciences*, vol. 39, no. 6, pp. 527–579, 2002.

[5] M. Zöller, "CD44: can a cancer-initiating cell profit from an abundantly expressed molecule?" *Nature Reviews Cancer*, vol. 11, no. 4, pp. 254–267, 2011.

[6] L. Thomas, T. Etoh, I. Stamenkovic, M. C. Mihm, and H. R. Byers, "Migration of human melanoma cells on hyaluronate is related to CD44 expression," *Journal of Investigative Dermatology*, vol. 100, no. 2, pp. 115–120, 1993.

[7] M. Goebeler, D. Kaufmann, E. B. Bröcker, and C. E. Klein, "Migration of highly aggressive melanoma cells on hyaluronic acid is associated with functional changes, increased turnover and shedding of CD44 receptors," *Journal of Cell Science*, vol. 109, no. 7, pp. 1957–1964, 1996.

[8] S. Misra, S. Ghatak, and B. P. Toole, "Regulation of MDR1 expression and drug resistance by a positive feedback loop involving hyaluronan, phosphoinositide 3-kinase, and ErbB2," *Journal of Biological Chemistry*, vol. 280, no. 21, pp. 20310–20315, 2005.

[9] L. Y. W. Bourguignon, K. Peyrollier, W. Xia, and E. Gilad, "Hyaluronan-CD44 interaction activates stem cell marker nanog, stat-3-mediated MDR1 gene expression, and ankyrin-regulated multidrug efflux in breast and ovarian tumor cells," *Journal of Biological Chemistry*, vol. 283, no. 25, pp. 17635–17651, 2008.

[10] L. Y. W. Bourguignon, C. C. Spevak, G. Wong, W. Xia, and E. Gilad, "Hyaluronan-CD44 interaction with protein kinase Cε promotes oncogenic signaling by the stem cell marker nanog and the production of microRNA-21, leading to down-regulation of the tumor suppressor protein PDCD4, anti-apoptosis, and chemotherapy resistance in breast tumor cells," *Journal of Biological Chemistry*, vol. 284, no. 39, pp. 26533–26546, 2009.

[11] P. Dalerba, R. W. Cho, and M. F. Clarke, "Cancer stem cells: models and concepts," *Annual Review of Medicine*, vol. 58, pp. 267–284, 2007.

[12] M. E. Prince, R. Sivanandan, A. Kaczorowski et al., "Identification of a subpopulation of cells with cancer stem cell properties in head and neck squamous cell carcinoma," *Proceedings of the National Academy of Sciences of the United States of America*, vol. 104, no. 3, pp. 973–978, 2007.

[13] M. P. Ponnusamy and S. K. Batra, "Ovarian cancer: emerging concept on cancer stem cells," *Journal of Ovarian Research*, vol. 1, no. 4, 2008.

[14] L. Du, H. Wang, L. He et al., "CD44 is of functional importance for colorectal cancer stem cells," *Clinical Cancer Research*, vol. 14, no. 21, pp. 6751–6760, 2008.

[15] E. M. Hurt, B. T. Kawasaki, G. J. Klarmann, S. B. Thomas, and W. L. Farrar, "$CD44^{+}CD24^{-}$ prostate cells are early cancer progenitor/stem cells that provide a model for patients with poor prognosis," *British Journal of Cancer*, vol. 98, no. 4, pp. 756–765, 2008.

[16] C. H. Stuelten, S. D. Mertins, J. I. Busch et al., "Complex display of putative tumor stem cell markers in the NCI60 tumor cell line panel," *Stem Cells*, vol. 28, no. 4, pp. 649–660, 2010.

[17] H. Clevers, "The cancer stem cell: premises, promises and challenges," *Nature Medicine*, vol. 17, no. 3, pp. 313–319, 2011.

[18] R. Tammi, K. Rilla, J. P. Pienimäki et al., "Hyaluronan enters keratinocytes by a novel endocytic route for catabolism," *Journal of Biological Chemistry*, vol. 276, no. 37, pp. 35111–35122, 2001.

[19] H. Jiang, R. S. Peterson, W. Wang, E. Bartnik, C. B. Knudson, and W. Knudson, "A requirement for the CD44 cytoplasmic domain for hyaluronan binding, pericellular matrix assembly, and receptor-mediated endocytosis in COS-7 cells," *Journal of Biological Chemistry*, vol. 277, no. 12, pp. 10531–10538, 2002.

[20] R. E. Eliaz and F. C. Szoka Jr., "Liposome-encapsulated doxorubicin targeted to CD44: a strategy to kill CD44 overexpressing tumor cells," *Cancer Research*, vol. 61, no. 6, pp. 2592–2601, 2001.

[21] R. E. Eliaz, S. Nir, C. Marty, and F. C. Szoka Jr., "Determination and modeling of kinetics of cancer cell killing by doxorubicin and doxorubicin encapsulated in targeted liposomes," *Cancer Research*, vol. 64, no. 2, pp. 711–718, 2004.

[22] D. Peer and R. Margalit, "Tumor-targeted hyaluronan nanoliposomes increase the antitumor activity of liposomal doxorubicin in syngeneic and human xenograft mouse tumor models," *Neoplasia*, vol. 6, no. 4, pp. 343–353, 2004.

[23] E. M. Rezler, D. R. Khan, J. Lauer-Fields, M. Cudic, D. Baronas-Lowell, and G. B. Fields, "Targeted drug delivery utilizing protein-like molecular architecture," *Journal of the American Chemical Society*, vol. 129, no. 16, pp. 4961–4972, 2007.

[24] V. M. Platt and F. C. Szoka Jr., "Anticancer therapeutics: targeting macromolecules and nanocarriers to hyaluronan or CD44, a hyaluronan receptor," *Molecular Pharmaceutics*, vol. 5, no. 4, pp. 474–486, 2008.

[25] D. Peer and R. Margalit, "Loading mitomycin C inside long circulating hyaluronan targeted nano-liposomes increases its antitumor activity in three mice tumor models," *International Journal of Cancer*, vol. 108, no. 5, pp. 780–789, 2004.

[26] S. Taetz, A. Bochot, C. Surace et al., "Hyaluronic acid-modified DOTAP/DOPE liposomes for the targeted delivery of anti-telomerase siRNA to CD44-expressing lung cancer cells," *Oligonucleotides*, vol. 19, no. 2, pp. 103–116, 2009.

[27] K. Akima, H. Ito, Y. Iwata et al., "Evaluation of antitumor activities of hyaluronate binding antitumor drugs: synthesis, characterization and antitumor activity," *Journal of Drug Targeting*, vol. 4, no. 1, pp. 1–8, 1996.

[28] Q. Chen, S. Cai, K. G. Shadrach, G. D. Prestwich, and J. G. Hollyfield, "Spacrcan binding to hyaluronan and other glycosaminoglycans: molecular and biochemical studies," *Journal of Biological Chemistry*, vol. 279, no. 22, pp. 23142–23150, 2004.

[29] V. B. Lokeshwar and M. G. Selzer, "Differences in hyaluronic acid-mediated functions and signaling in arterial, microvessel,

and vein-derived human endothelial cells," *Journal of Biological Chemistry*, vol. 275, no. 36, pp. 27641–27649, 2000.

[30] Y. Glucksam-Galnoy, T. Zor, and R. Margalit, "Hyaluronan-modified and regular multilamellar liposomes provide subcellular targeting to macrophages, without eliciting a pro-inflammatory response," *Journal of Controlled Release*, vol. 160, no. 2, pp. 388–393, 2012.

[31] B. Ruffell and P. Johnson, "Chondroitin sulfate addition to CD44H negatively regulates hyaluronan binding," *Biochemical and Biophysical Research Communications*, vol. 334, no. 2, pp. 306–312, 2005.

[32] B. Ruffell, G. F. T. Poon, S. S. M. Lee et al., "Differential use of chondroitin sulfate to regulate hyaluronan binding by receptor CD44 in inflammatory and interleukin 4-activated macrophages," *Journal of Biological Chemistry*, vol. 286, no. 22, pp. 19179–19190, 2011.

[33] J. Bajorath, B. Greenfield, S. B. Munro, A. J. Day, and A. Aruffo, "Identification of CD44 residues important for hyaluronan binding and delineation of the binding site," *Journal of Biological Chemistry*, vol. 273, no. 1, pp. 338–343, 1998.

[34] P. Teriete, S. Banerji, M. Noble et al., "Structure of the regulatory hyaluronan binding domain in the inflammatory leukocyte homing receptor CD44," *Molecular Cell*, vol. 13, no. 4, pp. 483–496, 2004.

[35] S. Banerji, A. J. Wright, M. Noble et al., "Structures of the Cd44-hyaluronan complex provide insight into a fundamental carbohydrate-protein interaction," *Nature Structural and Molecular Biology*, vol. 14, no. 3, pp. 234–239, 2007.

[36] J. Bajorath, "Molecular organization, structural features, and ligand binding characteristics of CD44, a highly variable cell surface glycoprotein with multiple functions," *Proteins*, vol. 39, no. 2, pp. 103–111, 2000.

[37] T. Ehnis, W. Dieterich, M. Bauer, B. Von Lampe, and D. Schuppan, "A chondroitin/dermatan sulfate form of CD44 is a receptor for collagen XIV (Undulin)," *Experimental Cell Research*, vol. 229, no. 2, pp. 388–397, 1996.

[38] R. A. F. Clark, F. Lin, D. Greiling, J. An, and J. R. Couchman, "Fibroblast invasive migration into fibronectin/fibrin gels requires a previously uncharacterized dermatan sulfate-CD44 proteoglycan," *Journal of Investigative Dermatology*, vol. 122, no. 2, pp. 266–277, 2004.

[39] R. Singh, B. J. Campbell, L. G. Yu et al., "Cell surface-expressed Thomsen-Friedenreich antigen in colon cancer is predominantly carried on high molecular weight splice variants of CD44," *Glycobiology*, vol. 11, no. 7, pp. 587–592, 2001.

[40] W. M. Lin, U. Karsten, S. Goletz, R. C. Cheng, and Y. Cao, "Expression of CD176 (Thomsen-Friedenreich antigen) on lung, breast and liver cancer-initiating cells," *International Journal of Experimental Pathology*, vol. 92, no. 2, pp. 97–105, 2011.

[41] J. L. Lauer-Fields, N. B. Malkar, G. Richet, K. Drauz, and G. B. Fields, "Melanoma cell CD44 interaction with the α1(IV)1263–1277 region from basement membrane collagen is modulated by ligand glycosylation," *Journal of Biological Chemistry*, vol. 278, no. 16, pp. 14321–14330, 2003.

[42] A. E. Faassen, D. L. Mooradian, R. T. Tranquillo et al., "Cell surface CD44-related chondroitin sulfate proteoglycan is required for transforming growth factor-β-stimulated mouse melanoma cell motility and invasive behavior on type I collagen," *Journal of Cell Science*, vol. 105, no. 2, pp. 501–511, 1993.

[43] A. E. Faassen, J. A. Schrager, D. J. Klein, T. R. Oegema, J. R. Couchman, and J. B. Mccarthy, "A cell surface chondroitin sulfate proteoglycan, immunologically related to CD44, is involved in type I collagen-mediated melanoma cell motility and invasion," *Journal of Cell Biology*, vol. 116, no. 2, pp. 521–531, 1992.

[44] J. R. Knutson, J. Iida, G. B. Fields, and J. B. Mccarthy, "CD44/chondroitin sulfate proteoglycan and $\alpha 2\beta 1$ integrin mediate human melanoma cell migration on type IV collagen and invasion of basement membranes," *Molecular Biology of the Cell*, vol. 7, no. 3, pp. 383–396, 1996.

[45] M. K. Chelberg, J. B. Mccarthy, A. P. N. Skubitz, L. T. Furcht, and E. C. Tsilibary, "Characterization of a synthetic peptide from type IV collagen that promotes melanoma cell adhesion, spreading, and motility," *Journal of Cell Biology*, vol. 111, no. 1, pp. 261–270, 1990.

[46] N. B. Malkar, J. L. Lauer-Fields, J. A. Borgia, and G. B. Fields, "Modulation of triple-helical stability and subsequent melanoma cellular responses by single-site substitution of fluoroproline derivatives," *Biochemistry*, vol. 41, no. 19, pp. 6054–6064, 2002.

[47] Y.-C. Yu, P. Berndt, M. Tirrell, and G. B. Fields, "Self-assembling amphiphiles for construction of protein molecular architecture," *Journal of the American Chemical Society*, vol. 118, no. 50, pp. 12515–12520, 1996.

[48] Y. C. Yu, M. Tirrell, and G. B. Fields, "Minimal lipidation stabilizes protein-like molecular architecture," *Journal of the American Chemical Society*, vol. 120, no. 39, pp. 9979–9987, 1998.

[49] Y.-C. Yu, V. Roontga, V. A. Daragan, K. H. Mayo, M. Tirrell, and G. B. Fields, "Structure and dynamics of peptide-amphiphiles incorporating triple- helical proteinlike molecular architecture," *Biochemistry*, vol. 38, no. 5, pp. 1659–1668, 1999.

[50] G. B. Fields, J. L. Lauer, Y. Dori, P. Forns, Y.-C. Yu, and M. Tirrell, "Protein like molecular architecture: biomaterial applications for inducing cellular receptor binding and signal transduction," *Biopolymers*, vol. 47, no. 2, pp. 143–151, 1998.

[51] A. A. Gabizon, "Pegylated liposomal doxorubicin: metamorphosis of an old drug into a new form of chemotherapy," *Cancer Investigation*, vol. 19, no. 4, pp. 424–436, 2001.

[52] M. L. Hwang, R. K. Prud'homme, J. Kohn, and J. L. Thomas, "Stabilization of phosphatidylserine/phosphatidylethanolamine liposomes with hydrophilic polymers having multiple "sticky feet"," *Langmuir*, vol. 17, no. 25, pp. 7713–7716, 2001.

[53] J. Jamil, S. Sheikh, and I. Ahmad, "Liposomes: the next generation," *Modern Drug Discovery*, vol. 7, no. 1, pp. 36–39, 2004.

[54] M. W. Ndinguri, R. Solipuram, R. P. Gambrell, S. Aggarwal, and R. P. Hammer, "Peptide targeting of platinum anti-cancer drugs," *Bioconjugate Chemistry*, vol. 20, no. 10, pp. 1869–1878, 2009.

[55] S. Amselem, A. Gabizon, and Y. Barenholz, "Optimization and upscaling of doxorubicin-containing liposomes for clinical use," *Journal of Pharmaceutical Sciences*, vol. 79, no. 12, pp. 1045–1052, 1990.

[56] V. P. Torchilin and V. Weissig, *Liposomes: A Practical Approach*, Oxford University Press, 2nd edition, 2003.

[57] J. C. M. Stewart, "Colorimetric determination of phospholipids with ammonium ferrothiocyanate," *Analytical Biochemistry*, vol. 104, no. 1, pp. 10–14, 1980.

[58] N. J. Zuidam, R. de Vrueh, and D. J. A. Crommelin, "Characterization of liposomes,," in *Liposomes: A Practical Approach*, V. P. Torchilin and V. Weissig, Eds., pp. 31–78, Oxford University Press, 2nd edition, 2003.

[59] M. V. Backer, T. I. Gaynutdinov, V. Patel, B. T. Jehning, E. Myshkin, and J. M. Backer, "Adapter protein for site-specific conjugation of payloads for targeted drug delivery," *Bioconjugate Chemistry*, vol. 15, no. 5, pp. 1021–1029, 2004.

[60] A. C. Hirbe, E. A. Morgan, M. C. Eagleton et al., "Granulocyte colony-stimulating factor enhances bone tumor growth in mice in an osteoclast-dependent manner," *Blood*, vol. 109, no. 8, pp. 3424–3431, 2007.

[61] M. M. Tomayko and C. P. Reynolds, "Determination of subcutaneous tumor size in athymic (nude) mice," *Cancer Chemotherapy and Pharmacology*, vol. 24, no. 3, pp. 148–154, 1989.

[62] E. M. Rezler, D. R. Khan, R. Tu, M. Tirrell, and G. B. Fields, "Peptide-mediated targeting of liposomes to tumor cells," *Methods in Molecular Biology*, vol. 386, pp. 269–298, 2007.

[63] D. R. Khan, E. M. Rezler, J. Lauer-Fields, and G. B. Fields, "Effects of drug hydrophobicity on liposomal stability," *Chemical Biology and Drug Design*, vol. 71, no. 1, pp. 3–7, 2008.

[64] H. Hojo, T. Kojima, K. Yamauchi, and M. Kinoshita, "Synthesis and liposome-formation of a thermostable lipid bearing cell adhesion peptide sequence," *Tetrahedron Letters*, vol. 37, no. 41, pp. 7391–7394, 1996.

[65] M. García, M. A. Alsina, F. Reig, and I. Haro, "Liposomes as vehicles for the presentation of a synthetic peptide containing an epitope of hepatitis A virus," *Vaccine*, vol. 18, no. 3-4, pp. 276–283, 1999.

[66] M. R. Jaafari and M. Foldvari, "Targeting of liposomes to melanoma cells with high levels of ICAM-1 expression through adhesive peptides from immunoglobulin domains," *Journal of Pharmaceutical Sciences*, vol. 91, no. 2, pp. 396–404, 2002.

[67] D. Simberg, T. Duza, J. H. Park et al., "Biomimetic amplification of nanoparticle homing to tumors," *Proceedings of the National Academy of Sciences of the United States of America*, vol. 104, no. 3, pp. 932–936, 2007.

[68] D. C. Drummond, O. Meyer, K. Hong, D. B. Kirpotin, and D. Papahadjopoulos, "Optimizing liposomes for delivery of chemotherapeutic agents to solid tumors," *Pharmacological Reviews*, vol. 51, no. 4, pp. 691–744, 1999.

[69] A. Nagayasu, K. Uchiyama, and H. Kiwada, "The size of liposomes: a factor which affects their targeting efficiency to tumors and therapeutic activity of liposomal antitumor drugs," *Advanced Drug Delivery Reviews*, vol. 40, no. 1-2, pp. 75–87, 1999.

[70] G. J. R. Charrois and T. M. Allen, "Rate of biodistribution of STEALTH liposomes to tumor and skin: influence of liposome diameter and implications for toxicity and therapeutic activity," *Biochimica et Biophysica Acta*, vol. 1609, no. 1, pp. 102–108, 2003.

[71] C.-Y. Fan, C.-C. Huang, W.-C. Chiu et al., "Production of multivalent protein binders using a self-trimerizing collagen-like peptide scaffold," *FASEB Journal*, vol. 22, no. 11, pp. 3795–3804, 2008.

[72] D. W. Siegmann, "Stimulation of quiescent 3T3 cells by phosphatidic acid-containing liposomes," *Biochemical and Biophysical Research Communications*, vol. 145, no. 1, pp. 228–233, 1987.

[73] D. A. Scott, A. D. Richardson, F. V. Filipp et al., "Comparative metabolic flux profiling of melanoma cell lines: beyond the Warburg effect," *Journal of Biological Chemistry*, vol. 286, no. 49, pp. 42626–42634, 2011.

[74] Promega, "Celltiter-Glo luminescent cell viability assay," Technical Bulletin, Promega Corporation, Madison, Wis, USA, 2011.

[75] J. Dou, M. Pan, P. Wen et al., "Isolation and identification of cancer stem-like cells from murine melanoma cell lines," *Cellular & Molecular Immunology*, vol. 4, no. 6, pp. 467–472, 2007.

[76] A. L. Klibanov, K. Maruyama, V. P. Torchilin, and L. Huang, "Amphipathic polyethyleneglycols effectively prolong the circulation time of liposomes," *FEBS Letters*, vol. 268, no. 1, pp. 235–237, 1990.

[77] T. M. Allen and C. Hansen, "Pharmacokinetics of stealth versus conventional liposomes: effect of dose," *Biochimica et Biophysica Acta*, vol. 1068, no. 2, pp. 133–141, 1991.

[78] T. M. Allen, C. Hansen, F. Martin, C. Redemann, and A. F. Yau-Young, "Liposomes containing synthetic lipid derivatives of poly(ethylene glycol) show prolonged circulation half-lives in vivo," *Biochimica et Biophysica Acta*, vol. 1066, no. 1, pp. 29–36, 1991.

[79] K. Maruyama, O. Ishida, T. Takizawa, and K. Moribe, "Possibility of active targeting to tumor tissues with liposomes," *Advanced Drug Delivery Reviews*, vol. 40, no. 1-2, pp. 89–102, 1999.

[80] N. Oku, "Anticancer therapy using glucuronate modified long-circulating liposomes," *Advanced Drug Delivery Reviews*, vol. 40, no. 1-2, pp. 63–73, 1999.

[81] N. Düzgüneş and S. Nir, "Mechanisms and kinetics of liposome-cell interactions," *Advanced Drug Delivery Reviews*, vol. 40, no. 1-2, pp. 3–18, 1999.

[82] K. R. Whiteman, V. Subr, K. Ulbrich, and V. P. Torchilin, "Poly(HPMA)-coated liposomes demonstrate prolonged circulation in mice," *Journal of Liposome Research*, vol. 11, no. 2-3, pp. 153–164, 2001.

[83] D. Lasic, "Doxorubicin in sterically stabilized," *Nature*, vol. 380, no. 6574, pp. 561–562, 1996.

[84] A. Mori, A. L. Klibanov, V. P. Torchilin, and L. Huang, "Influence of the steric barrier activity of amphipathic poly (ethyleneglycol) and ganglioside GM1 on the circulation time of liposomes and on the target binding of immunoliposomes in vivo," *FEBS Letters*, vol. 284, no. 2, pp. 263–266, 1991.

[85] K. Maruyama, T. Yuda, A. Okamoto, C. Ishikura, S. Kojima, and M. Iwatsuru, "Effect of molecular weight in amphipathic polyethyleneglycol on prolonging the circulation time of large unilamellar liposomes," *Chemical and Pharmaceutical Bulletin*, vol. 39, no. 6, pp. 1620–1622, 1991.

[86] K. Maruyama, T. Yuda, A. Okamoto, S. Kojima, A. Suginaka, and M. Iwatsuru, "Prolonged circulation time in vivo of large unilamellar liposomes composed of distearoyl phosphatidylcholine and cholesterol containing amphipathic poly(ethylene glycol)," *Biochimica et Biophysica Acta*, vol. 1128, no. 1, pp. 44–49, 1992.

[87] F. K. Bedu-Addo, P. Tang, Y. Xu, and L. Huang, "Effects of polyethyleneglycol chain length and phospholipid acyl chain composition on the Interaction of polyethyleneglycol-phospholipid conjugates with phospholipid: implications in liposomal drug delivery," *Pharmaceutical Research*, vol. 13, no. 5, pp. 710–717, 1996.

[88] P. J. Photos, L. Bacakova, B. Discher, F. S. Bates, and D. E. Discher, "Polymer vesicles in vivo: correlations with PEG molecular weight," *Journal of Controlled Release*, vol. 90, no. 3, pp. 323–334, 2003.

[89] Y. Dori, H. Bianco-Peled, S. K. Satija, G. B. Fields, J. B. Mccarthy, and M. Tirrell, "Ligand accessibility as means to control cell response to bioactive bilayer membranes," *Journal of Biomedical Materials Research*, vol. 50, no. 1, pp. 75–81, 2000.

[90] A. Gabizon, R. Catane, B. Uziely et al., "Prolonged circulation time and enhanced accumulation in malignant exudates of doxorubicin encapsulated in polyethylene-glycol coated liposomes," *Cancer Research*, vol. 54, no. 4, pp. 987–992, 1994.

[91] R. J. Lee and P. S. Low, "Folate-mediated tumor cell targeting of liposome-entrapped doxorubicin in vitro," *Biochimica et Biophysica Acta*, vol. 1233, no. 2, pp. 134–144, 1995.

[92] E. Roux, M. Lafleur, E. Lataste, P. Moreau, and J.-C. Leroux, "On the characterization of pH-sensitive liposome/polymer complexes," *Biomacromolecules*, vol. 4, no. 2, pp. 240–248, 2003.

[93] D. Goren, A. T. Horowitz, D. Tzemach, M. Tarshish, S. Zalipsky, and A. Gabizon, "Nuclear delivery of doxorubicin via folate-targeted liposomes with bypass of multidrug-resistance efflux pump," *Clinical Cancer Research*, vol. 6, no. 5, pp. 1949–1957, 2000.

[94] H. D. Han, A. Lee, T. Hwang et al., "Enhanced circulation time and antitumor activity of doxorubicin by comblike polymer-incorporated liposomes," *Journal of Controlled Release*, vol. 120, no. 3, pp. 161–168, 2007.